Fall 10-2021

Empirical Modeling of Tilt-Rotor Aerodynamic Performance

Michael C. Stratton
Old Dominion University, mike.stratton1@gmail.com

EMPIRICAL MODELING OF TILT-ROTOR AERODYNAMIC PERFORMANCE

by

Michael Cristian Stratton
B.S. December 2019, Old Dominion University

A Thesis Submitted to the Faculty of
Old Dominion University in Partial Fulfillment of the
Requirements for the Degree of

MASTER OF SCIENCE

AEROSPACE ENGINEERING

OLD DOMINION UNIVERSITY
October 2021

Approved By:

Dr. Drew Landman (Director)

Dr. Colin Britcher (Member)

Dr. Thomas Alberts (Member)

ABSTRACT

EMPIRICAL MODELING OF TILT-ROTOR AERODYNAMIC PERFORMANCE

Michael C. Stratton

Old Dominion University, 2021

Advisor: Dr. Drew Landman

There has been increasing interest into the performance of electric vertical takeoff and landing (eVTOL) aircraft. The propellers used for the eVTOL propulsion systems experience a broad range of aerodynamic conditions, not typically experienced by propellers in forward flight, that includes large incidence angles relative to the oncoming airflow. Formal experiment design and analysis techniques featuring response surface methods were applied to a subscale, tilt-rotor wind tunnel test for three, four, five, and six blade, 16-inch diameter, propeller configurations in support of development of the NASA LA-8 aircraft. Investigation of low-speed performance included a maximum speed of 12 m/s and a maximum RPM of 6800 tested over a range of incidence angles from 0° to 100°. High-speed testing achieved a maximum speed of 30 m/s and maximum RPM of 6000 while incidence angle was varied from 0° to 20°. Results were compared for each propeller configuration using nondimensional aerodynamic coefficients, including performance of off-axis forces and moments. The outcome of this research describes important behavior of propellers operating in conditions experienced by eVTOL vehicles as well as provides a general testing approach to performance characterization that includes empirical model building with uncertainty estimates.

ACKNOWLEDGMENTS

The support of NASA Langley was invaluable during this project. I would like to thank my NIFS mentor David North, supporting engineer Benjamin Simmons and everyone else at NASA LaRC for their valuable contributions which aided in the completion of this project. I would also like to thank my advisor Dr. Drew Landman for his unwavering support and encouragement.

NOMENCLATURE

A	Area
C_{F_x}, C_{F_y}, C_{F_z}	Propeller Force Coefficients
C_{M_x}, C_{M_y}, C_{M_z}	Propeller Moment Coefficients
C_P	Propeller Power Coefficient
$C_{P,rotor}$	Rotor Power Coefficient
C_{P_i}	Rotor Ideal Power Coefficient
C_T	Rotor Thrust Coefficient
D	Diameter
F_x, F_y, F_z	Propeller Forces
J	Advance Ratio
M	Figure of Merit
MS_{Error}	Error Mean Square
$MS_{Treatments}$	Treatment Mean Square
M_x, M_y, M_z	Propeller Moments
n	Revolutions/Second
P	Propeller Actual Power
P_i	Propeller Ideal Power
$P_{i,hover}$	Rotor Ideal Power
R	Radius
R^2	Coefficient of Determination
SS_{Error}	Error Sum of Squares
SS_{Total}	Total Sum of Squares
$SS_{Treatments}$	Treatment Sum of Squares
V	Velocity

V'	Velocity at Incidence
w	Induced Velocity
$\boldsymbol{X}$	Model Matrix
x	Factor Term
y	Model Response
α_i	Angle of Incidence
β	Regression Coefficient
$\hat{\beta}$	Regression Coefficient Estimate
ϵ	Random Error
η	Propeller Efficiency
μ	Mean
ρ	Air Density
σ	Standard Deviation
τ	Treatment Effect
ω	Rotational Velocity, Radians/Second
ANOVA	Analysis of Variance
AOI	Angle of Incidence
CCD	Central Composite Design
CFD	Computational Fluid Dynamics
CRD	Completely Randomized Design
DOE	Design of Experiments
DX	Design Expert™
ETC	Easy-To-Change
eVTOL	Electric Vertical Takeoff and Landing
FDS	Fraction of Design Space

HTC	Hard-To-Change
OLS	Ordinary Least Squares
OFAT	One-Factor-at-A-Time
REML	Restricted Estimated Maximum Likelihood
RPM	Revolutions Per Minute
RSM	Response Surface Methodology
SP	Sub-Plot
UAM	Urban Air Mobility
VIF	Variance Inflation Factor
V/STOL	Vertical/Short Takeoff and Landing
VTOL	Vertical Takeoff and Landing
WP	Whole-Plot

TABLE OF CONTENTS

Page

CHAPTER Page

LIST OF TABLES

Table Page

LIST OF FIGURES

Figure Page

1. INTRODUCTION

In recent years, there has been a surge of interest into the capabilities and performance of electric vertical takeoff and landing (eVTOL) vehicles as they pertain to the field of Urban Air Mobility (UAM). UAM is the emerging aviation market that seeks to use these vehicles to establish public and commercial transportation primarily within metropolitan areas. These vehicles have the potential to drastically reduce both ground and air traffic congestion, travel times, and emissions all of which are factors that end up costing commuters and nations billions of dollars. The United States alone is projected to have congestion costs of up to $200 billion by 2025 [1]. The use of electric propulsion systems in place of conventional power plants also decreases mechanical complexity which can allow more freedom in vehicle design thus affecting thrust distribution and increasing aerodynamic efficiency.

Major progress has been made in making this technology a practical reality and there are currently over 100 vectored thrust eVTOL configurations in the design or prototype phase according to the Vertical Flight Society [2]. In 2020, the US Air Force started an initiative called Agility Prime to boost eVTOL aircraft and technologies that are designed for civilian aviation but suitable for military missions such as cargo delivery or air medical evacuation. Collaborating companies include Joby Aviation and Sabrewing Aircraft Company which have prototypes for air-taxi and cargo aircraft, respectively. The program has a 2023 target date to begin fielding these aircraft [3, 4]. In addition, NASA has played a large part in contributing research into eVTOL technologies with research on vehicle aerodynamics of different designs, electric propulsion concepts, and acoustic and aerodynamic performance of various propeller configurations. The work done in this project was to support a new technology testbed for Advanced Air Mobility (what NASA sometimes calls UAM) at NASA Langley, the

Langley Aerodrome 8 (LA-8), see Figure 1. The LA-8 is a distributed electric propulsion eVTOL aircraft and the methods used in its testing provide a rapid means of analysis for aerodynamic, acoustic, and flight dynamics performance that can be used on new or future eVTOL designs.

Serious research into VTOL (not just electric) capabilities began in the 1950's and 60's and has since seen numerous configurations considered, either strictly in theory or through actual application and development. One example of the former was a design for a tilt-rotor aircraft by American engineer Haviland Hull Platt of the Platt-LePage Aircraft Company (Figure 2) [5]. The patent was approved but the design was never developed.

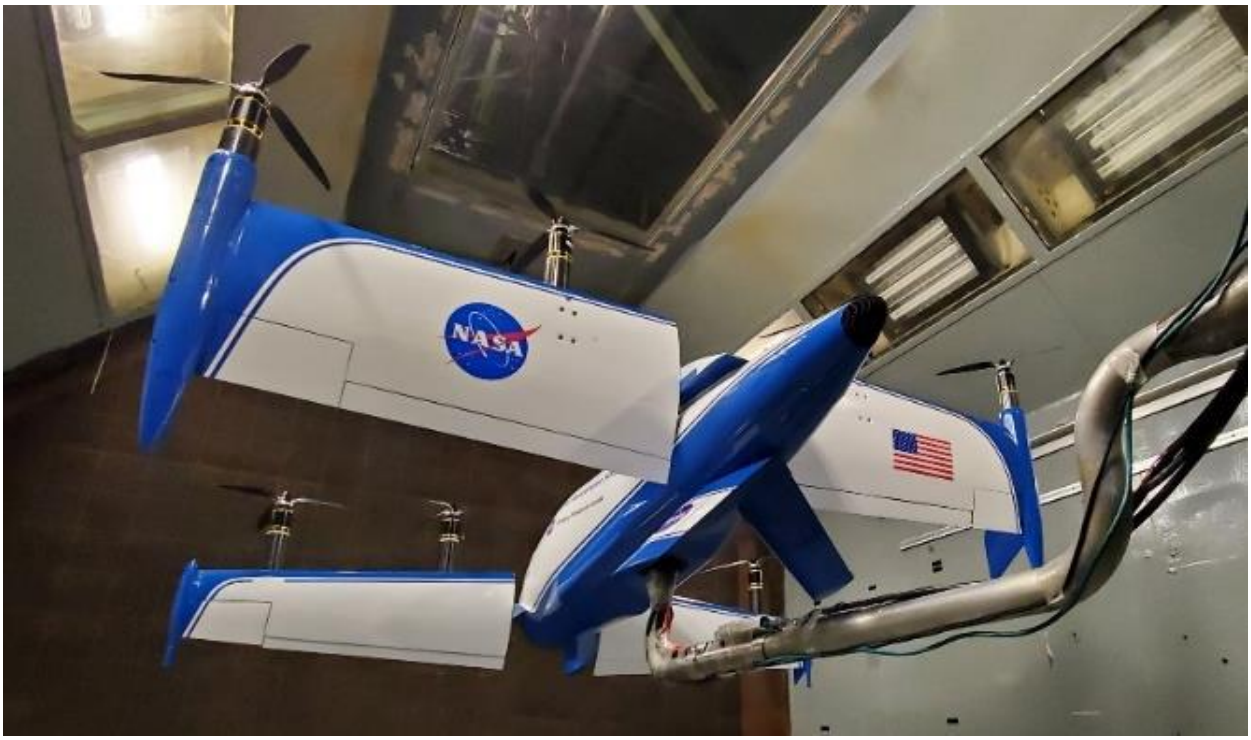

Figure 1. LA-8 Prototype undergoing testing at NASA Langley 12-foot Low Speed Wind Tunnel.

United States Patent Office

2,702,168
Patented Feb. 15, 1955

2,702,168

CONVERTIBLE AIRCRAFT

Haviland H. Platt, New York, N. Y.

Application July 7, 1950, Serial No. 172,507

15 Claims. (Cl. 244–7)

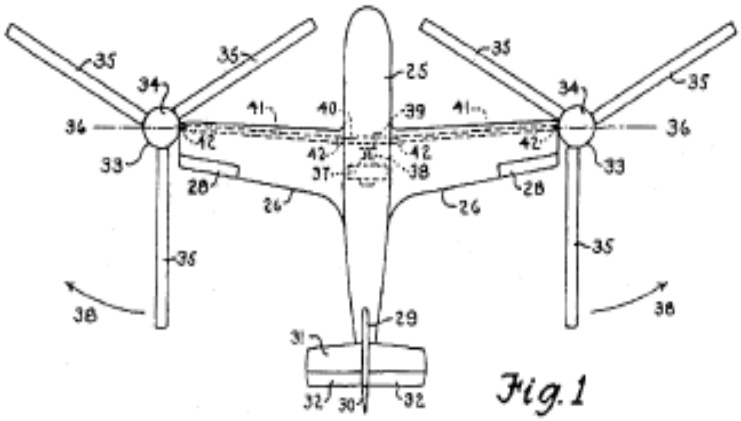

Fig. 1

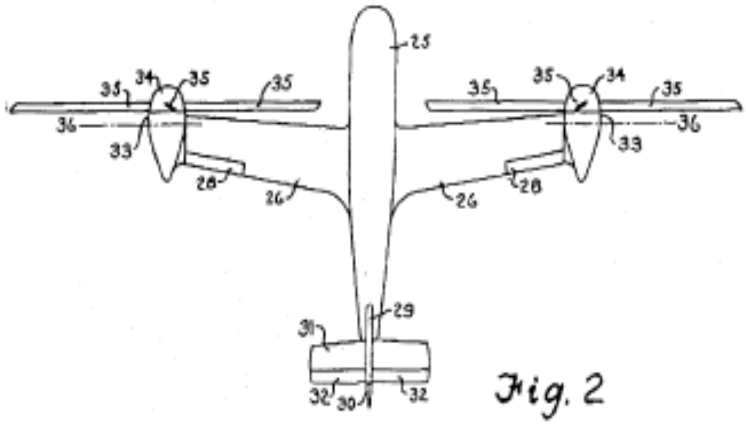

Fig. 2

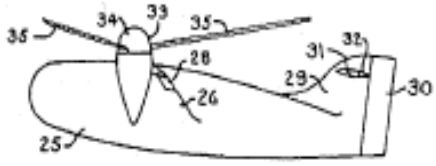

Fig. 3

INVENTOR.
HAVILAND H. PLATT
BY Howard L. Kalish
ATTORNEY.

Figure 2. Haviland Platt tilt-rotor patent [5].

Figure 3. AV-8B Harrier II Jet.

While VTOL operation has been achieved through various means of propulsion such as the deflected jet used in the McDonnell Douglas/British Aerospace Harrier (Figure 3), the primary focus of this project is on tilt-rotor dynamics, like the LA-8.

Some tilt-rotor aircraft can tilt just the rotors, which would be placed at the wingtips like the V-22 Osprey or the Platt-LePage design while others would tilt the entire wing. While in hover mode tilt-rotor aircraft achieve similar performance to that of the helicopter but do not suffer from the typical blade retreat problem once in forward flight [6]. In the tilt-wing method the entire wing and propeller system is tilted through approximately 90° as one piece like the LA-8. Early experiments with tilt-wing concepts like the Vertol VZ-2 would show that the lift of the wing is augmented by the propeller slipstream which comes with its own set of complications, in particular stalling of the wing at high incidence angle [7].

Figure 4. Greased Lightning 10 (GL-10) [31].

However, distributed propulsion systems such as those used on the GL-10 have been shown to provide advantageous solutions to these difficulties (Figure 4) [8].

The implications of this technology to largely replace some traditional modes of transportation places particular importance on being able to accurately and efficiently model the aerodynamics associated with their operation. One aspect of this entails performing wind tunnel experiments to gather data on performance characteristics of propeller configurations such as force and moment coefficients and efficiency. The various flight modes a tilt-rotor aircraft will go through, from hover, transition, and into forward flight can make setting up an adequate experiment to capture sufficient data a daunting task. This makes the use of more formal statistical engineering methods an attractive choice when often factors of interest must be constrained or held constant to avoid excessive costs in time and resources. The goal of this project was to add to the existing work on tilt-rotor characterization by providing a general testing approach that includes empirical model building with uncertainty estimates.

2. BACKGROUND

2.1 TILT-ROTOR OPERATIONAL ENVELOPE

A point should be made about the terms propeller and rotor since both can be used somewhat interchangeably. Typically, rotors are thought of as being used for hover like that of a conventional helicopter and propellers being used for cruise or forward flight like that of an airplane. The actual difference becomes a matter of size and hence disk loading since both could be used for hover operation, with rotors usually being much larger in diameter than propellers. The term “proprotor” has been used throughout literature on the subject as well [7].

For eVTOL aircraft, like the LA-8, the wing and propeller are operated at a nominal angle of incidence (α_i) range of zero to 90° from the horizontal. The hovering condition which includes taking off and landing vertically would be achieved with α_i being around 80° to 90° while forward flight would be at much lower angles closer to zero. Figure 5 shows the typical flight modes and velocities that an eVTOL aircraft would go through during operation. The

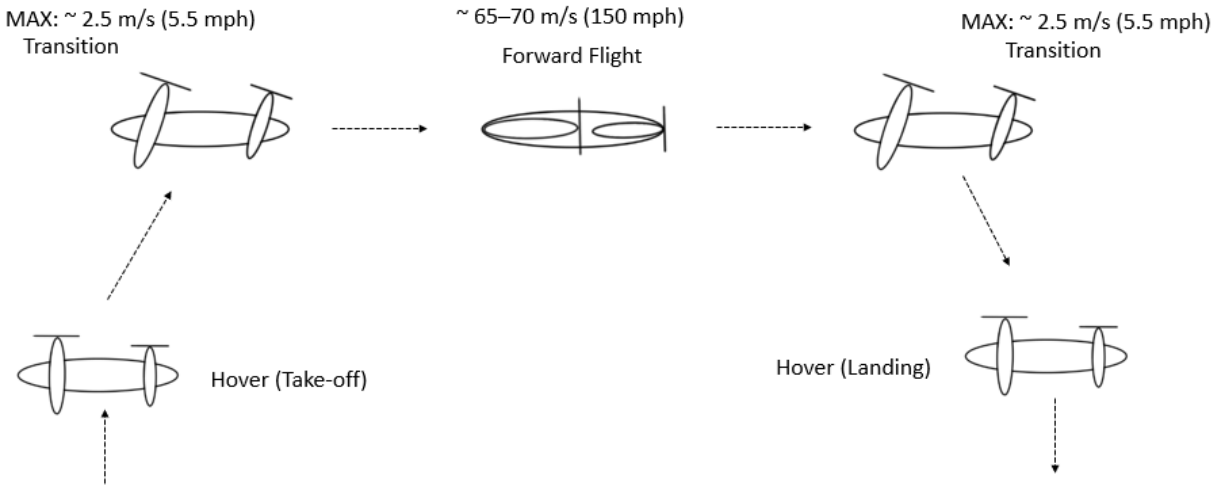

Figure 5. Operational flight modes for eVTOL aircraft.

transition and cruise speeds shown in the figure are taken from the UBER Elevate mission statement and would be the desired speed ranges for passenger carrying vehicles to ensure overall passenger comfort [9]. These speeds, however, are what would be typical of this particular application. Larger, more powerful VTOL aircraft, like the V-22 Osprey operate at much higher airspeeds. During the transition phase of flight, the interaction of the propeller system and the wing involve complicated modeling with recent and ongoing research consisting of using databases for aerodynamic coefficients, corrected airfoil data, and interpolating wind-tunnel data or applying simplifications to momentum theory [10]. These interactions were beyond the scope of this project.

2.2 PROPELLER PERFORMANCE MEASUREMENT AND METRICS

Performance characteristics of propellers are best examined using non-dimensional coefficients. Eliminating the units allows easy plotting of results and direct comparison of different propellers. It also allows the results obtained from a small-scale wind tunnel test to be used in the performance prediction of full-scale models. The most common non-dimensional performance characteristics are thrust, torque, power, and efficiency. Since these parameters depend on the incoming free stream velocity as well as the propeller tip speed the coefficients are usually evaluated at a range of advance ratios. The forces and moments used in defining these non-dimensional coefficients follow a sign convention commonly used for aircraft (Figure 6). The x-axis is aligned with the propeller motor axis and the y- and z-axes lie on the propeller plane. The z-axis is pointed down and the y-axis is pointed to the right if viewing the propeller disk from behind, facing the free stream velocity. The propeller incidence angle is measured between the x-axis and the free stream velocity (more on this topic in later sections).

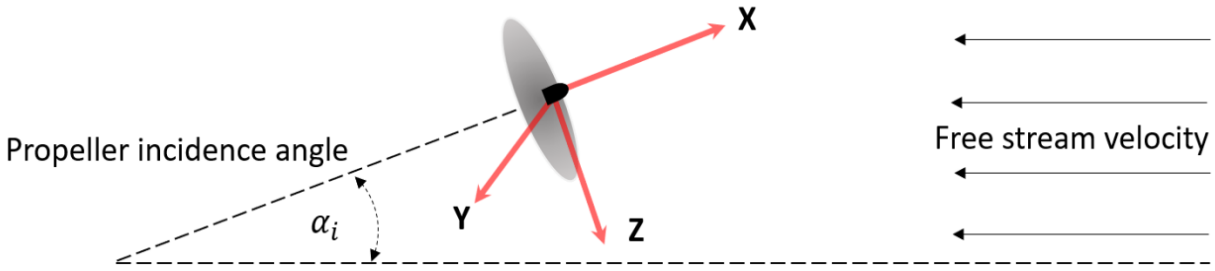

Figure 6. Convention of propeller incidence angle and axes relative to free stream velocity.

The non-dimensional coefficients are defined as follows:

Thrust coefficient $$C_{F_x} = \frac{F_x}{\rho n^2 D^4} \quad (1)$$

Torque coefficient $$C_{M_x} = \frac{M_x}{\rho n^2 D^5} \quad (2)$$

Power coefficient $$C_P = \frac{P}{\rho n^3 D^5} \quad (3)$$

Where the propeller power is defined as

$$P = 2\pi n M_x \quad (4)$$

Advance ratio $$J = \frac{V}{nD} \quad (5)$$

Efficiency
(Forward flight, $\alpha_i = 0$) $$\eta = \frac{F_x V}{P} \quad (6)$$

Efficiency is a measure of the useful power ($F_x V$) divided by the propeller input, or actual power from (4). In terms of C_{F_x}, C_P, and J efficiency can also be defined as

$$\eta = J\frac{C_{F_x}}{C_P} \tag{7}$$

Some typical performance plots are shown in Figure 7. These results are from experiments using an Aero-Naut CAM carbon 9×6 folding propeller [11]. The figures show curves where data was taken at a constant RPM over a range of velocity (or J). These plots allow easy interpretation of results and comparison of different propellers. This advantage can be seen in the plot of efficiency (Figure 7c), which combines thrust and power (or torque) coefficient as well as RPM and velocity into one graph.

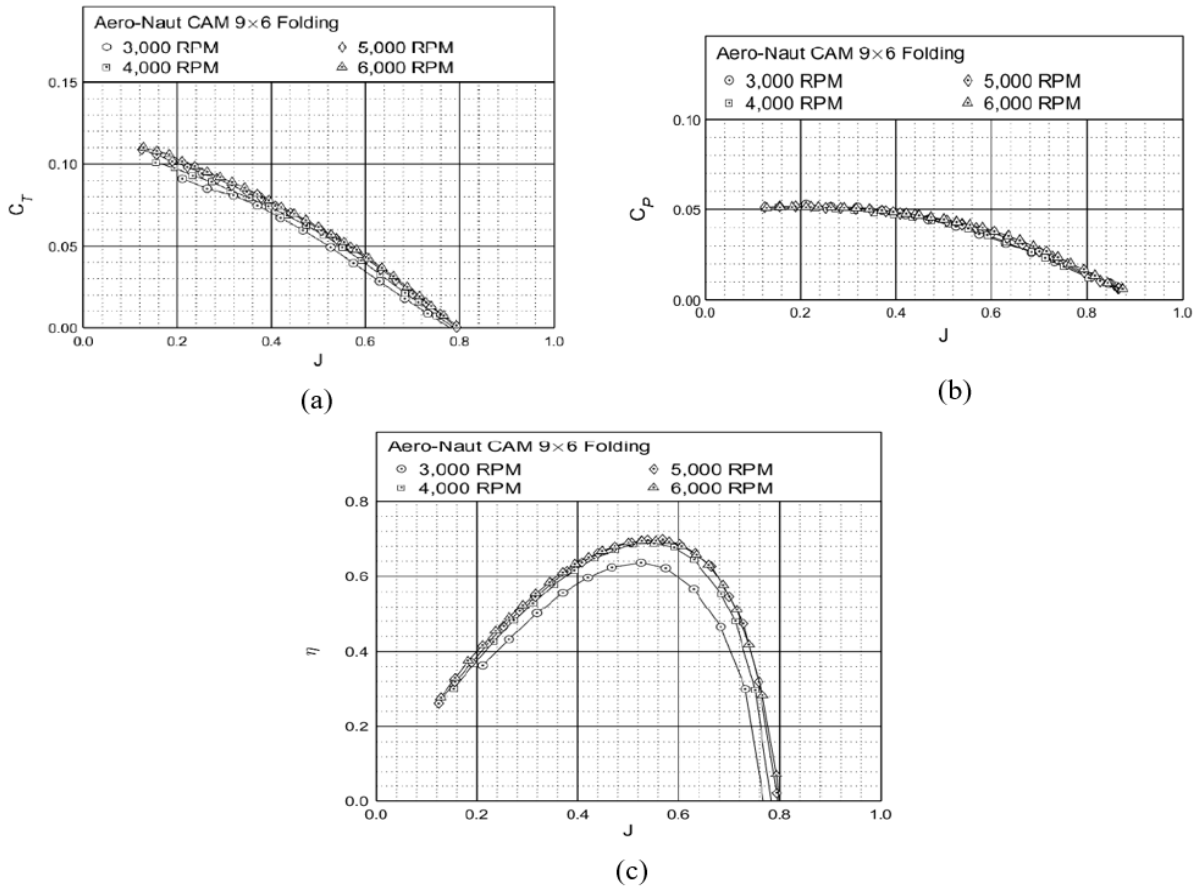

Figure 7. Typical non-dimensional coefficients: (a) thrust coefficient, (b) power coefficient, (c) efficiency [11].

2.3 ROTOR PERFORMANCE MEASUREMENT AND METRICS

During hover VTOL aircraft operate like helicopters, in other words the 'propellers' are acting as rotors. From momentum theory the ideal power [6] required during hover is defined as

$$P_{i,hover} = Tw = \frac{T^{3/2}}{\sqrt{2\rho A}} \tag{8}$$

Where w is the induced velocity at the propeller disk and A is the area of the propeller disk. It is important to note as the ideal power makes up most of the power consumed during hover.

Rotor performance is also analyzed in much of the same way propellers are, through the use of non-dimensional coefficients [12]. Thrust and power coefficients for the rotor are given as

$$C_T = \frac{T}{\rho A(\omega R)^2} \tag{9}$$

$$C_P = \frac{P}{\rho A(\omega R)^3} \tag{10}$$

where the power used in Eq. (10) is the actual total power required by the rotor which is defined the same as Eq. (4). The quantity ωR is the tip velocity where ω is the rotational velocity (rad/s) and R is the radius of the propeller disk. Using the ideal power in Eq. (8) the thrust and ideal power can be related in terms of coefficients which would be

$$C_{P_i} = \frac{C_T^{3/2}}{\sqrt{2}} \tag{11}$$

During hover ($V = 0$) no useful work is performed so efficiency would be zero. Instead, a parameter called the figure of merit is used to evaluate performance of hovering rotors which is defined as

$$M = \frac{P_{i,hover}}{P} \tag{12}$$

The figure of merit is the ratio of ideal power to actual power required by the rotor. To avoid misleading results when comparing rotor efficiencies, comparisons must be made at constant disk loading (T/A) [12].

2.4 TILT-ROTOR PERFORMANCE MEASUREMENT AND METRICS

The metrics discussed so far are concerned with modeling the axial airflow conditions ($\alpha_i = 0$) where thrust and torque are dominant, and the off-axis forces and moments are not as significant. At high α_i this is not always the case [10] and so the propeller side force F_y, normal force F_z, pitching moment M_y, and yawing moment M_z are presented similarly to thrust F_x and torque M_x, with non-dimensional coefficients defined as

$$C_{F_y} = \frac{F_y}{\rho n^2 D^4}, C_{F_z} = \frac{F_z}{\rho n^2 D^4}, C_{M_y} = \frac{M_y}{\rho n^2 D^5}, C_{M_z} = \frac{M_z}{\rho n^2 D^5} \quad (13)$$

These force and moment coefficients follow the sign convention described in Figure 6 and are consistent with Figure 8, where the y-axis points into the page.

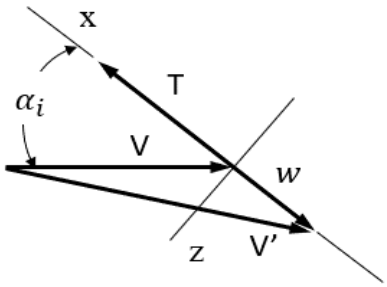

Figure 8. Propeller at angle of incidence (T = F_x).

As noted in Eq. (6) for efficiency this is correct for the forward flight case when the incidence angle of the propeller axis is equal to zero. At higher α_i a component of the velocity V' must be accounted for which makes use of this formulation insufficient (Figure 8).

McCormick describes a method according to Glauert's hypothesis for finding the component of velocity needed to calculate an approximation of efficiency for a propeller at a high angle of incidence [6]. A velocity w is induced at the propeller disk which leads to thrust given as

$$T = 2\rho A V' w \tag{14}$$

where $$V' = [(V\cos\alpha_i + w^2)^2 + (V\sin\alpha_i)^2]^{1/2} \tag{15}$$

This leads to $$w^4 + w^3 2V\cos\alpha_i + w^2V^2 = \left(\frac{T}{2\rho A}\right)^2 \tag{16}$$

Which given T and V, can be solved numerically for w and V' that then allows efficiency to be calculated as the ratio of an ideal power, defined as the product of the thrust and the velocity normal to the disk given by

$$P_i = T(V\cos\alpha_i + w) \tag{17}$$

to the actual power, Eq. (4). In addition, experiments done with propellers at varying incidence angles demonstrated that using the normal component of advance ratio, $J\cos\alpha_i$, could be effective in describing propeller performance metrics [10, 13].

3. LITERATURE SEARCH

3.1 EXPERIMENTAL WORK

Research into tilt-rotor aircraft over the decades has been an iterative process with many successes and failures but nonetheless the work has contributed to the understanding and development of this technology. In both academia and industry work has consisted of experiments that sought to characterize the performance of tilt-rotors both separately and in combination with wings at high incidence angles [10, 13-16]. Experiments designed to simply study the propeller usually implement a test stand where the propeller is mounted to a streamlined, rigid support which can be rotated through different angles. If the wing is to be included in the experiment, then semi-span wings and scaled or full-sized models would be used. Many involved the use of wind tunnels to replicate the flow conditions that the propellers or models would be subjected to during actual operation. Yaggy et al. [13] tested three different full-scale 3-bladed propellers, varying tunnel velocity, RPM, blade angle and propeller incidence angle from 0° to 85°. The three propellers showed similar forces and moment variations with incidence angle and $J \cos \alpha_i$. Kuhn and Draper [14] studied isolated propellers and propeller-wing interactions at incidence angles up to 90° and noted differences in performance due to the wing. Simmons and Hatke [17] and Stratton and Landman [18] are recent examples of research into the effects of the auxiliary forces and moments induced by propellers at high incidence angles. These studies had the advantage of using the same propeller geometry so direct comparisons could be made. Overall, the results showed similar trends and magnitudes of the aerodynamic coefficients. In addition to studying the off-axis forces and moments, Busan et al. [19] demonstrated the advantages of using DOE testing for wind tunnel experiments.

Figure 9. Bell 25-ft. diameter proprotor on semi-span wing in NASA Ames 40×80-ft. wind tunnel [5].

A rather famous example of tilt-rotor research was the NASA/Army joint project XV-15 aircraft which laid the foundation for the Bell-Boeing V-22 Osprey which is still in active service today. Before further development of the XV-15 took place, extensive wind tunnel tests were conducted with both small-scale and full-scale proprotors. Figure 9 shows a 25-ft diameter proprotor on a semi-span wing made by Bell Helicopter Company being tested in the NASA Ames 40 x 80-foot wind tunnel. This rotor was actually built for a previous aircraft, the Bell Model 300 but was used for testing of a full-scale rotor to better represent the structural and aerodynamic characteristics of the XV-15. The results of the wind tunnel tests were shown to agree with the theory on rotor dynamics and stability, which at the time was being developed into a standard by Dr. Wayne Johnson [5]. The tests also revealed that propulsive efficiencies in both the hover and cruise modes needed improvement. This led to design considerations that sought to find an optimum that included increased blade twist for better forward flight performance and larger rotor diameter (lower disk loading) for improved hover performance. Wind tunnel testing included the full range of axial flow conditions from hover to forward flight and flow speeds up to the tunnel capability of 170 knot, or about 195 mph.

In addition to testing of the proprotors, the entire XV-15 was tested in the Ames 40 x 80-ft wind tunnel (Figure 10). Although, these tests were less about the performance of the proprotors and more about collecting overall aerodynamic data of the XV-15. Force and moment data were collected, and testing covered a range of nacelle angles and airspeeds. Testing would show that the empennage experienced high loads at 60 and 90 degrees (hover mode) caused by strong vortices from the nacelle/wing interaction and proprotor tips which led to eventual structural improvements. Once actual flight testing took place, however, the loads were found to be less severe than were found during wind tunnel tests.

Figure 10. The XV-15 in the NASA Ames 40×80-ft. wind tunnel [5].

The work of Theys was a close representation of what was done during this project which studied the aerodynamic performance of an isolated 9 x 5 propeller at high incidence angles [20]. A small-scale test rig was mounted on a turntable inside a 6.5 ft x 5 ft x 16.5 ft (width x height x length) subsonic wind tunnel and tested over a range of airspeeds up to 9 m/s. The turntable allowed the test rig to be turned through incidence angles of 0° to 180° during testing (Figure 11). The propeller was driven by a brushless electric motor and force and moment data were measured with a load cell. Testing included taking measurements for a range of RPM and analyzing data through the use of the propeller performance metrics discussed in previous sections. Figure 12 and Figure 13 show a sample of force and moment data, respectively, presented as aerodynamic coefficients over a range of RPM. These figures are representative of the magnitudes of forces and moments seen in a small-scale propeller test of this kind.

Figure 11. Theys test rig mounted on turntable inside wind tunnel [20].

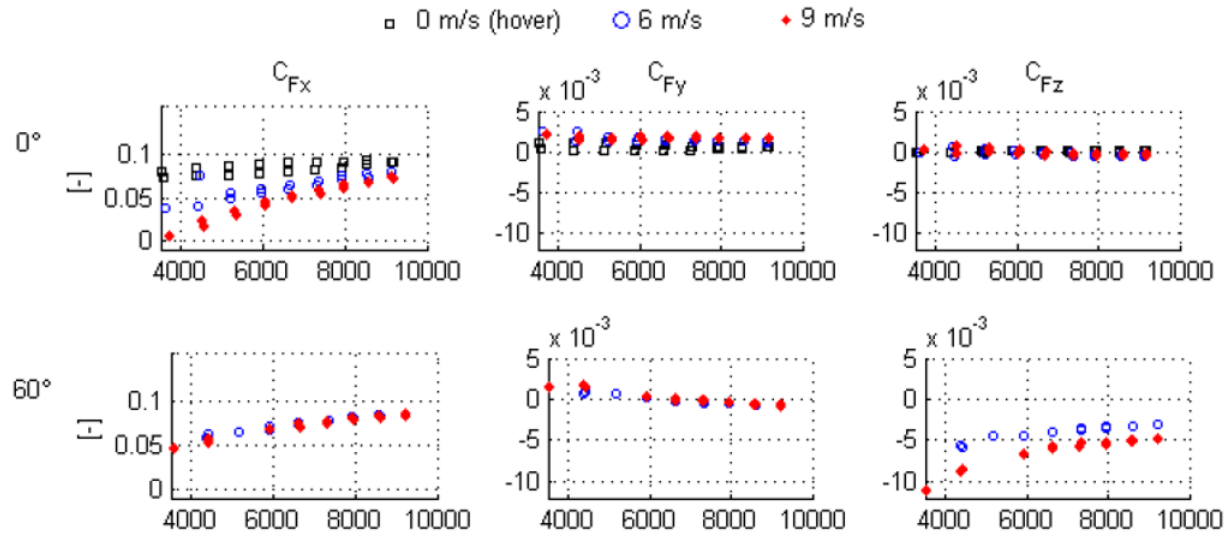

Figure 12. Force coefficients versus RPM for airspeeds tested at 0° and 60° [20].

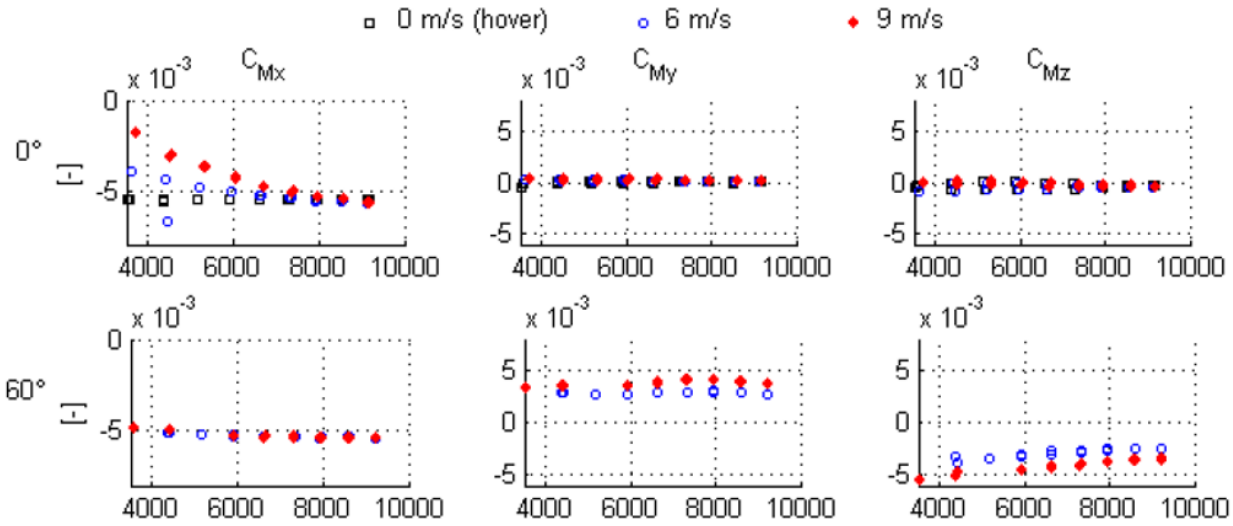

Figure 13. Moment coefficients versus RPM for airspeeds tested at 0° and 60° [20].

3.2 LITERATURE RELATED TO TILT-ROTOR THEORY

Of course, the extensive experimental research into tilt-rotor aircraft is guided by the theoretical work of countless others. The tilt-rotor flight envelope covers operating conditions described by conventional propeller and helicopter theory; Johnson describes all aspects of helicopter flight [12]. McCormick's text introduces various V/STOL concepts and their operational modes [6]. Performance analysis is given for flow augmentation devices, such as powered and unpowered flaps. Generalized cases of momentum, blade element and vortex theory are also presented as it applies to the design and analysis of helicopter rotors and propellers.

Of particular importance to this project and to the analysis of tilt-rotor performance in general is McCormick's chapter pertaining to wings and propellers in combination and separately at high angles of incidence. Some of the details were given in Chapter 2 for the approximation of efficiency based on the component of velocity that arises from a propeller being at an angle of incidence. Initial examination begins with assuming a propeller is far enough ahead of the wing to neglect any interactions. This would essentially be the case in an experiment with just the propeller, such as a wind tunnel test. Numerical solutions are then presented as separate figures showing the variation of induced velocity and required ideal power with speed for constant thrust and the variation of induced velocity and available thrust with speed for constant ideal power all for fixed angles of incidence. Figure 14 is taken from the text and shows the variation of available thrust with speed for constant ideal power.

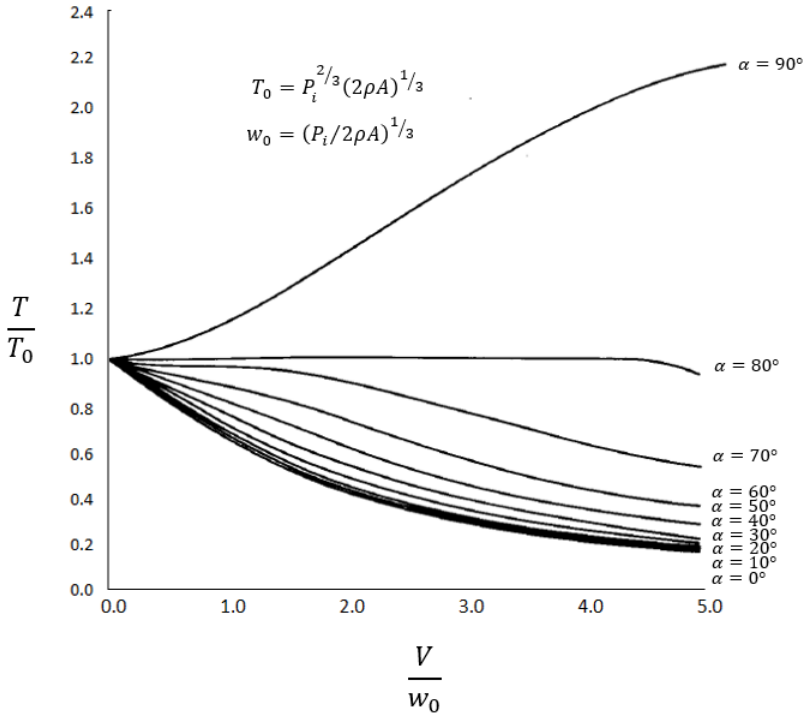

Figure 14. Variation of available thrust with speed for constant ideal power [6].

Figure 14 is interesting in that for a tilt-rotor vehicle it captures the entire flight envelope for a given power which would be hover (acting as a rotor) at high α_i, through transition, and finally into forward flight (acting as a propeller) at low α_i. Inspection of Figure 14 shows that thrust and velocity are taken with respect to reference parameters, T_0 and w_0. Since these relations are all derived from Eq. (16) which has velocity terms, the parameters are used to avoid difficulties when analyzing cases during hover when the velocity is zero. The numerical solutions of this section were also compared to similar experiments done during the 1950's at NASA (then NACA) Langley [14]. The results compared variation of power with forward speed for various α_i and were shown to have favorable overall agreement to the experimental data.

3.3 WORK USING COMPUTATIONAL FLUID DYNAMICS

Little time was spent investigating how CFD could be used during this experiment since it was beyond the scope of the project. It is evident, however, that the computational power used in CFD is a clear advantage in being able to accurately model the complicated interactions involved during the flight phases of tilt-rotor aircraft thus leading to optimized performance [21-23]. A more recent example of this was the HiPerTilt project by Leonardo Helicopters (LH) which partnered with the University of Bristol and the University of Glasgow [24]. The motivation for the project came from the development of LH's own tilt-rotor aircraft and the desire to have more design flexibility and overall design efficiency by taking advantage of the progress being made with CFD methods.

The work was split between improving prediction and optimization of the aerodynamics of the airframe as well as the aerodynamics of the rotors alone. Validation results were compared for CFD solvers being used at the time in order to optimize their methods. This included improving the predictions of drag along the airframe and the onset of stall along the wings of the tilt-rotor model being tested. Among the software being used was Fluent, and the Helicopter Multi Block (HMB) CFD solvers, both of which have been used extensively in industry. Wind tunnel tests were also conducted for comparison with the results obtained from the CFD analysis and were shown to be in close agreement.

Rotor optimization consisted of again validating currently used methods to demonstrate the use of CFD to simulate both rotors and propellers. It should come as no surprise that the rotor used as a reference was that of the XV-15. This was based on the amount of data that was freely available in literature; data from rotors of the S-76 helicopter were also used. The results were used with the goal of improving the figure of merit in hover and the propeller efficiency. Figure

15 shows the improvements made in both cases on the XV-15 rotor which were simulated with the HMB CFD solver.

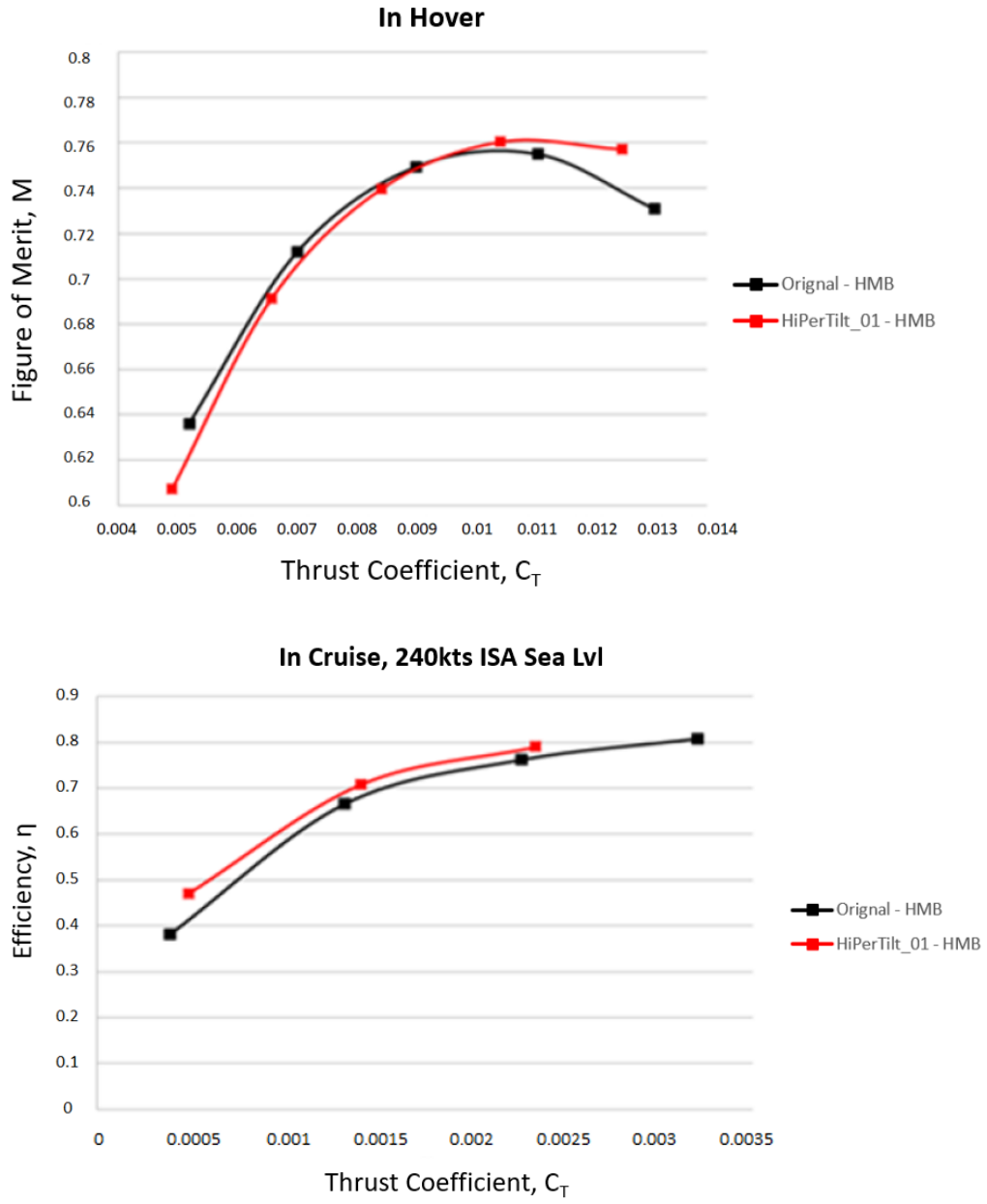

Figure 15. Comparison of the figure of merit and propeller efficiency for the original and optimized XV-15 rotor [24].

4. EXPERIMENT DESIGN USING STATISTICAL ENGINEERING METHODS

Focus has been placed on being able to provide accurate performance models that describe the operational envelope of the propellers in question and to do so efficiently. Therefore, it is important to provide some background information on common statistical methods used in experiment design and how they are used to arrive at meaningful conclusions when analyzing results.

4.1 EXPERIMENT DESIGNS

4.1.1 FACTORIAL DESIGN

The factorial design is one in which all factors of an experiment are varied simultaneously to include all possible combinations of factor levels. The change in a response due to the change in a factor level is a factor effect and when the difference in response between levels of one factor is not the same at all levels of another factor it is known as a factor interaction. If two levels, typically a high (+) and low (-) level, for each factor are used then a first order model that includes interaction can be developed. This is usually written as a 2^k design where k is the number of factors. The corresponding regression model would look like that of Eq. (18). Here, y is the response, the β's are the regression coefficients, and the x_i's are the factor terms. More on regression modeling will be given in a later section.

$$y = \beta_0 + \sum_i \beta_i x_i + \sum \sum_{i \neq j} \beta_{ij} x_i x_j + \cdots + \varepsilon, \quad i = 1,2,\ldots,k \tag{18}$$

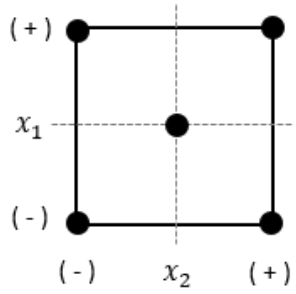

Figure 16. Full factorial design in two-factor space.

Accounting for possible interaction in an experiment is a major advantage over the extensively used one-factor-at-a-time (OFAT) approach which does not consider any possible interaction between factors. This generally makes factorial designs the most efficient when the effects of two or more factors are of interest [25]. Figure 16 shows a full-factorial design in two factor space with an added point known as a center. Center points are added to a design to allow testing for potential model augmentation that could support quadratic terms.

4.1.2 CENTRAL COMPOSITE DESIGN

When a model does require the addition of quadratic terms then the aforementioned factorial augmentation results in a design with points added to the axes through the origin of the design space (Figure 17). The reasoning behind adding the axial points is that when quadratic terms are found to be significant then the unknown parameters of the second-order model cannot be estimated with simply the full factorial design and center points. The central composite design, however, allows a complete second-order model to be fit (Eq. 19). The CCD has been used extensively with great success and is considered one of the most important designs when fitting second-order models [26].

$$y = \beta_0 + \sum_i \beta_i x_i + \sum \sum_{i \neq j} \beta_{ij} x_i x_j + \sum_i \beta_{ii} x_i^2 + \varepsilon, \quad i = 1,2,\dots,k \tag{19}$$

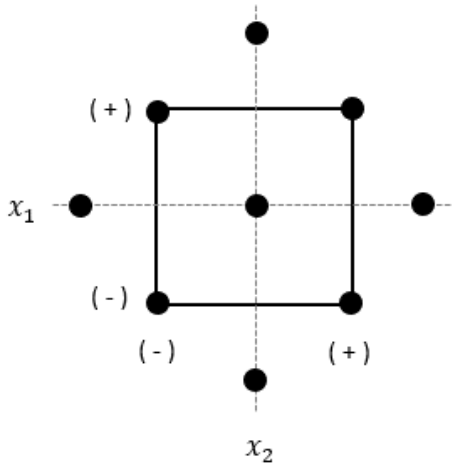

Figure 17. Central composite design in two-factor space.

4.1.3 OPTIMAL DESIGNS

The previous designs have properties that place them in the category of optimal designs. A design is usually considered an optimal design if it fits criterion that minimizes variance in some way. D-optimal designs minimize the variance of model regression coefficients (β_i's). This is done by making the determinant of $\boldsymbol{X'X}$ as large as possible. $\boldsymbol{X}$ is the model matrix containing the effects coding for the design; for a 2^2 design this is the combination of the intercepts, high (+1) and low (-1) levels of factors, as well as their interactions [26]. G-optimal designs seek to minimize the maximum variance of the predicted response at a point of interest in the design space which also depends on the variance of the regression coefficients. If instead multiple points of interest in the design space are to be examined, an average can be computed in an I-optimal design that seeks to minimize the prediction variance by integrating the variance function over the design space and dividing by the total area of the region. The I-optimal design is particularly useful when response predictions are needed. Many statistical programs, such as

Design Expert™, use algorithms for finding the optimal designs and Design Expert™ was used to generate an I-optimal design in this project [27].

4.1.4 SPLIT-PLOT DESIGNS

Randomization is a crucial principle in statistically designed experiments in that it makes true the assumption that observations or errors must be independently distributed random variables. Complete randomization of test runs is the ideal approach, although this is sometimes not achievable because of the excessive costs of time and resources [28, 29]. In addition, the feasibility, or restriction of implementing randomization with hard-to-change (HTC) factors can force test planning that requires some factors to be held constant. The split-plot design assigns run groups, called whole-plots (WP), where the HTC factors are held constant while sub-plots (SP) are groups of runs conducted within a WP where the randomization of easy-to-change (ETC) factors is more practical. The run order of WPs is also randomized. The consequences of the split-plot design are that there are now two types of variance estimates, one for the SP factors and one for the WP factors; the error associated with the SPs is usually less than that of the WPs because of increased homogeneity in the SPs. For this reason, significance testing is done in commercial software using Restricted Estimated Maximum Likelihood (REML) routines which is a high-level statistical method whose exact algorithms are not revealed by the vendor.

4.2 ANALYSIS

4.2.1 REGRESSION MODELING

As stated previously Eqs (18) and (19) were the regression equations for the first and second order models, respectively, of the 2^k design. These equations, or regression models, form the basis for expressing the results of an experiment quantitatively. With the goal of obtaining a value for the response y which depends on k independent variables (factors), shown in Eqs (18)

and (19) as the experiment factor terms or x_i's, and are either set before the experiment or chosen afterwards such as in the prediction of a future value, only the regression coefficients, β's, need to be determined. This is typically done using the method of ordinary least squares which seeks to find β's that minimize the sum of the squares of errors for the i^{th} observation. Since most experiments deal with multiple factors the regression model is best suited for matrix form, $\boldsymbol{y} = \boldsymbol{X\beta} + \boldsymbol{\epsilon}$, where $\boldsymbol{\epsilon}$ is a vector of random error. The least squares function then in matrix form is given as

$$L = (\boldsymbol{y} - \boldsymbol{X\beta})'(\boldsymbol{y} - \boldsymbol{X\beta}) \tag{20}$$

Equation (20) is differentiated with respect to $\boldsymbol{\beta}$ (or $\beta_0, \beta_1, \ldots, \beta_k$) and is set equal to zero. This leads to a set of equations called the normal equations which when solved for the matrix of regression coefficients is given as

$$\widehat{\boldsymbol{\beta}} = (\boldsymbol{X}'\,\boldsymbol{X})^{-1}\boldsymbol{X}'\boldsymbol{y} \tag{21}$$

Here, the hat notation used on $\boldsymbol{\beta}$ implies that it is an estimate of the regression coefficient. The reason Eq. (21) can be used to estimate the regression coefficients is because the variance can be expressed using the variance operator as $\boldsymbol{V} = \boldsymbol{\sigma I}$, where $\boldsymbol{I}$ is the identity matrix [26]. If, in the case of the split-plot design, Eq. (21) would be replaced by the General Linear Model instead which is expressed as $\widehat{\boldsymbol{\beta}} = (\boldsymbol{X'V^{-1}}\,\boldsymbol{X})^{-1}\boldsymbol{X'V^{-1}y}$ which gives what is called a generalized least square estimator. However, since there are two estimates of variance associated with the split-plot which are both unknown, this straightforward approach cannot be used. Instead, REML is relied on to estimate the variance components needed. The maximum likelihood estimation approach used in REML is a method that estimates parameters of a normal probability distribution with mean μ and standard deviation σ. Values of μ and σ are sought that maximize

the probability distribution function. The details are not presented here as the process is complex and automated in engineering design software. The basic steps are minimization of the natural log of the distribution function which involves differentiation with respect to the mean or standard deviation, setting the expression to zero and solving for the parameter. This can be done to give an estimate of both μ and σ. However, unlike the ordinary least squares (OLS) method which provides unbiased estimators ($\mu = 0$), maximum likelihood provides a biased estimate of the variance. If the log-likelihood function contains no information about the mean, then it can be optimized in terms of the variance components and provide an unbiased estimate. The log-likelihood function, which would then contain the variance-covariance matrix of split-plot error, would then be minimized numerically with respect to the two variance components and result in estimates. This is what is used in the background to build models in software like Design Expert™.

4.2.2 ANALYSIS OF VARIANCE

In many experiments more than two levels (sometimes called treatments) of a factor need to be compared. For simplicity, if the experiment containing a single factor is expressed as a model, as was done in previous sections, then the observations can be described as

$$y_{ij} = \mu + \tau_i + \epsilon_{ij} \begin{cases} i = 1, 2, \dots, a \\ j = 1, 2, \dots, n \end{cases} \quad (22)$$

where y_{ij} is the ijth observation (i is the factor level and j is the replicate at that factor level), μ is the overall mean, τ_i is the ith treatment effect, and ϵ_{ij} is a random error component that includes sources of variability such as measurement error, uncontrolled factors, and general background noise (e.g. variability over time or environmental variables). The objective for comparison then is to test a hypothesis about the equality of the a treatment means; that is, to see

how the effects are seen to vary from the overall mean. The model just described is what is known as the fixed-effects case in which conclusions apply only to the factor levels explicitly tested.

Analysis of variance is derived from the partitioning of total variability into its component parts where the measure of overall variability in the data is called the total sum of squares which is given as

$$SS_{Total} = \sum_{i=1}^{a}\sum_{j=1}^{n}\left(y_{ij} - \bar{y}_{..}\right)^2 \tag{23}$$

The "dot" notation subscript means summation over the subscript it replaces and $\bar{y}_{..}$ is defined as the grand mean of all observations. If Eq. (23) is expanded and simplified the partitioning leads to

$$SS_{Total} = n\sum_{i=1}^{a}(\bar{y}_{i.} - \bar{y}_{..}) + \sum_{i=1}^{a}\sum_{j=1}^{n}\left(y_{ij} - \bar{y}_{i.}\right)^2 \tag{24}$$

Which is more easily expressed in symbolic form as

$$SS_{Total} = SS_{Treatments} + SS_{Error} \tag{25}$$

Here $SS_{Treatments}$ is defined as the sum of squares of the differences between treatment means and the grand mean which accounts for the variability *between* treatment means, where as SS_{Error} is defined as the sum of squares of the differences of observations within treatments from the treatment mean which accounts for the variability *within* treatments. Obviously, a large value of $SS_{Treatments}$ indicates large differences in treatment means and a small value would suggest no difference in treatment means. Thus, the formal hypothesis test in terms of the factor effects model is given as

$$\begin{aligned} H_0&: \tau_1 = \tau_2 = \cdots \tau_a = 0 \\ H_1&: \quad at\ least\ one\ \tau_i \neq 0 \end{aligned} \tag{26}$$

So, if the null hypothesis is true, changing the levels of the factor has no effect on the mean response.

While the sums of squares cannot be compared directly because of the lack of independence due to Eq. (25), a new quantity called the mean squares can be used to test the hypothesis of equal treatment means. The mean square is a sum of squares divided by its degrees of freedom, given as

$$MS_{Treatments} = \frac{SS_{Treatments}}{a-1} \tag{27}$$

$$MS_{Error} = \frac{SS_{Error}}{a(n-1)} \tag{28}$$

These values would be used to compute a test statistic for the hypothesis of no differences in treatment means which is a ratio of the mean squares given by

$$F_0 = \frac{MS_{Treatments}}{MS_{Error}} \tag{29}$$

The test statistic is then compared to a table (or function if computer software is being used) of values with an F-distribution based on the degrees of freedom of the numerator and denominator and if the test statistic is greater than the critical F-value ($F_0 > F_{\alpha,a-1,a(n-1)}$) then H_0 is rejected and it is concluded that there are in fact differences in the treatment means. This analysis of variance (or ANOVA) is often summarized in table format for easy record keeping (Table. 1). P-values, based on a chosen level of significance, are often computed and included in the ANOVA table. This gives the decision maker an idea of just how significant the test statistic is; the test statistic could be just inside the critical region or much further away from the critical value.

Source of Variation	Sum of Squares	Degrees of Freedom	Mean Square	F_0
Between treatments	$SS_{Treatments}$	$a - 1$	$MS_{Treatments}$	$\frac{MS_{Treatments}}{MS_{Error}}$
Error (within treatments)	SS_{Error}	$a(n - 1)$	MS_{Error}	
Total	SS_{Total}	$an - 1$		

Table 1. ANOVA table for the single-factor, fixed effects model.

The analysis of variance can be extended to include more factors. The SS_{Total} is further partitioned to allow mean square estimates for each of the factors. Model adequacy testing is of interest and functions by comparing a model-dependent estimated variance to a model-independent estimated variance (pure error), which requires replicates for estimating pure error. This error is partitioned such that

$$SS_E = SS_{PE} + SS_{LoF} \tag{30}$$

where SS_{PE} is the sum of the squared deviations of the responses from the mean response in each set of replicates and SS_{LoF} is a weighted sum of squared deviations between the mean response at each level and the fitted value. The test statistic for lack of fit is then given by

$$F_0 = \frac{MS_{LoF}}{MS_{PE}} = \frac{SS_{LoF}/(m-p)}{SS_{PE}/(n-m)} \tag{31}$$

where m is the number of unique design points, n is the number of experiments, and p is the number of parameters in the model which includes the intercept. Then, if $F_0 > F_{\alpha,m-p,n-m}$ lack of fit is significant, and a more appropriate regression equation should be found.

4.2.3 SIGNIFICANCE TESTING: CRD AND SPD APPROACH

In the previous section the single-factor ANOVA model was an example of a completely randomized design (CRD). That is, the experiment would be performed in random order so that the experimental units are as uniform as possible. This can also be extended to experiments with multiple factors. The model would then follow that of Eq. (22) except now it would include multiple factors as well as their interactions. Similarly, the sum of squares would be partitioned into contributions from each factor, their interactions, and random error. In symbolic form this can be shown by

$$SS_{Total} = SS_A + SS_B + \cdots + SS_{AB} + SS_{AC} + \cdots + SS_{ABC} + \cdots + SS_{AB\cdots k} + SS_E \quad (32)$$

The sum of squares terms for the factors and their interactions would all be tested versus the mean square for error. A test statistic, F_0, could then be computed and compared to the critical F-value to determine if a factor or interaction is significant in the model. Obviously, inherent to CRDs is that the variance can be estimated by computing the mean squares. It is the comparison of these variance estimators that allows a formal test of significance for determining which factors or interactions are significant to the model being analyzed.

In designs where there is a restriction to randomization estimating the variance can be more difficult; the split-plot is an example of one of these designs. As mentioned in a previous section there are two types of error associated with the split-plot design, one coming from the randomization of WPs and the other from the randomization of the SPs. Consequently, there are two variance components associated with these errors. In the ANOVA procedure WP factors and the WP interactions are tested against the WP error, while SP factors and all other interactions are tested against the SP error. Using Design Expert™, REML, as outlined previously, must be

used to get explicit variance estimates in order to test which terms and interactions are significant.

5. EXPERIMENTAL DETAILS

5.1 THE OLD DOMINION UNIVERSITY LOW-SPEED WIND TUNNEL

Experiments were conducted in the Low-Speed Wind Tunnel at Old Dominion University. The wind tunnel is closed circuit and is driven by a 125-horsepower motor and turbulence levels for the low-speed and high-speed sections are reported as being 0.8 % and 0.2 %, respectively. The turbulence level, or turbulence intensity, is often given since flow "quality" is of particular importance in wind tunnel experiments and represents as a percentage how much the flow velocity fluctuates from the mean wind speed [30]. The 7 ft x 8 ft low-speed section is 7 ft long and can achieve a maximum free stream velocity of 12 m/s. The high-speed is 3 ft x 4 ft x 8 ft and can achieve a maximum free stream velocity of 55 m/s. Data was collected in both sections in order to build a complete operational envelope for the propellers studied. A layout of the wind tunnel and the 4 and 5- blade propeller configurations are shown in Figure 18.

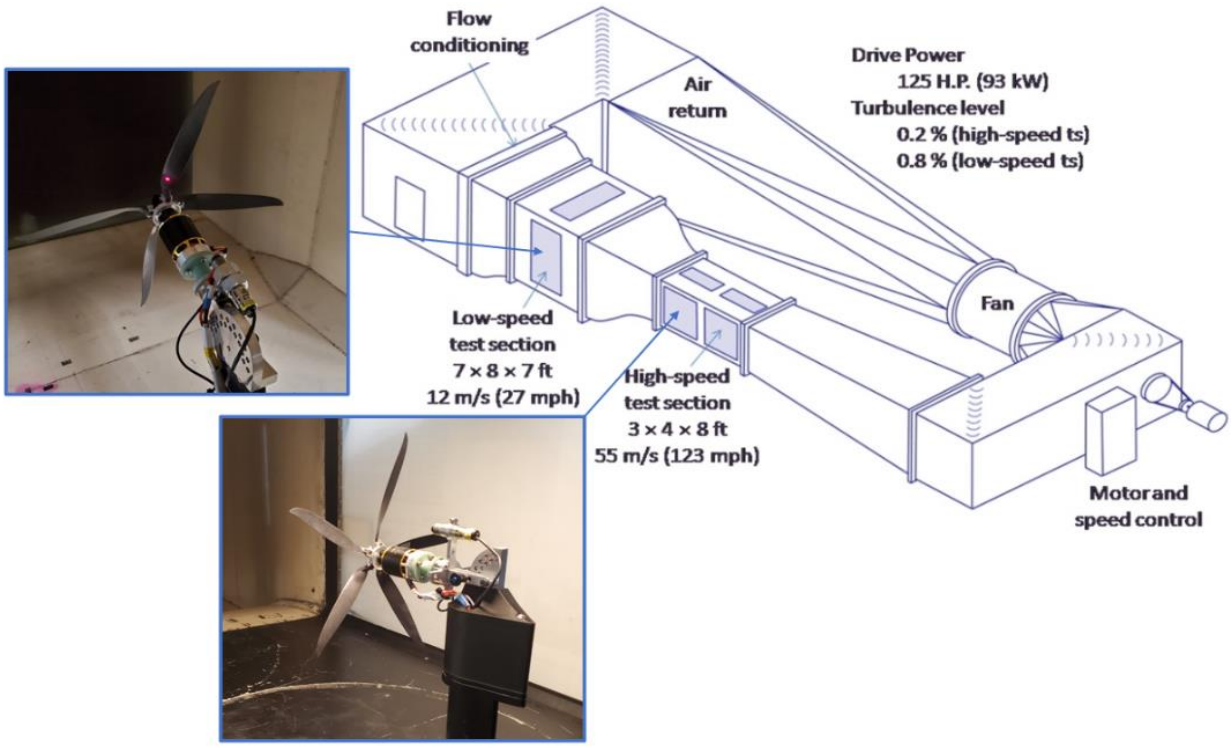

Figure 18. ODU Low-Speed Wind Tunnel and tilt-rotor supports.

5.2 TILT-ROTOR TEST STAND AND INSTRUMENTATION

5.2.1 LOW-SPEED TEST STAND

Custom mounting components were designed to provide a robust support system to replace the original test stand that utilized an electric servo motor to change angle of incidence (AOI). Previous experiments found that there were problems at high propeller pitch moments that caused the servo to “search” for the selected angle which led to a reassessment of the design. The new design featured a single aluminum sector with holes staggered and spaced every 10 degrees which allowed an AOI range from 0° to 180°, as seen in Figure 19. An aluminum lever arm, located on tunnel centerline, allowed the assembly to be rotated through the desired AOI range and held in place with a quick-release guide pin.

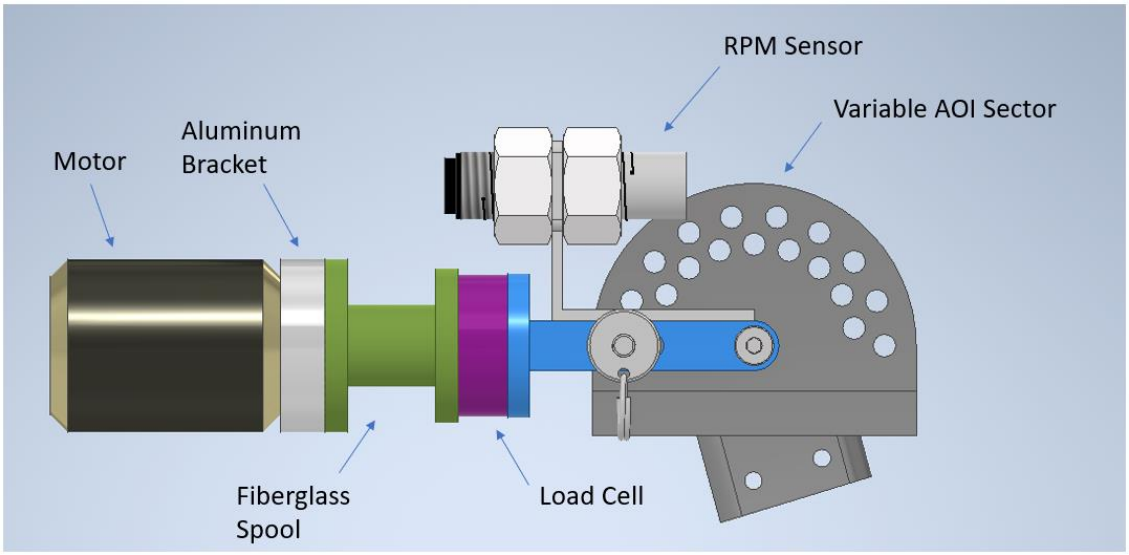

Figure 19. Low-speed test stand assembly.

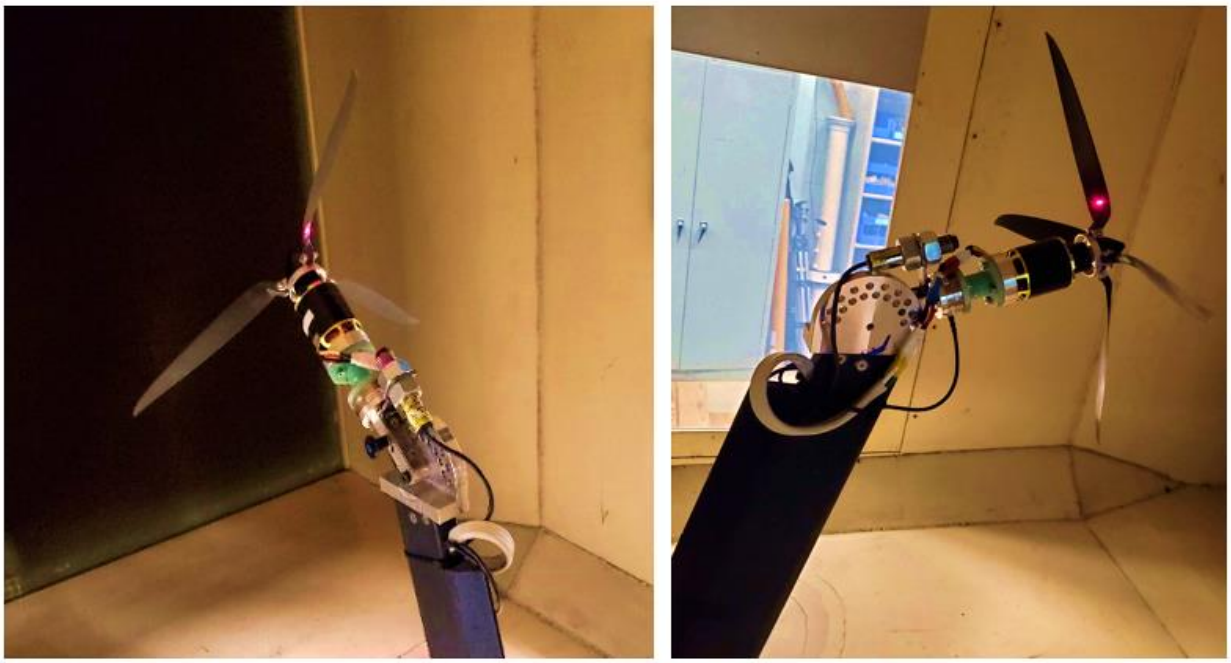

Figure 20. 3 and 4-blade propeller configurations in low-speed section.

An RPM sensor, which used a retroreflective laser diode unit, was attached to the lever arm and aimed at reflective tape placed on one of the propeller blades. This ensured accurate readings could be taken at any of the desired angles. The load cell was mounted to the face of the lever arm and the other side mounted to a spool-shaped fiberglass interface that helped thermally isolate the load cell which is important to maintain its accuracy. An aluminum bracket allowed the motor to be mounted to the other end of the fiberglass interface. The entire assembly was mounted to a streamlined strut that attached to the floor of the wind tunnel centerline to help minimize any unwanted aerodynamic interference (Figure 20).

The motor used, which was the same as that being used on the LA-8, was a Scorpion SII-4035-450KV brushless electric motor. The motor was powered by a Sorensen DCS55 – 55E DC power supply, rated for 55 volts with a capacity of 55 amps. A Castle Creations 100-amp ESC controlled the motor from outside the wind tunnel using a Mini-Maestro control board that connected to the computer using via USB [31]. Placing the ESC outside the wind tunnel also allowed it to be cooled with a fan to avoid overheating. Nominal voltage was set to 32 volts and current limited to 50 amps. Force and moment data were measured by an ATI Mini-40 load cell with respect to a coordinate system with origin at the face of the propeller plane as shown in Figure 21. A full layout of the testing equipment can be seen in APPENDIX A. The same setup was used for both the low-speed and high-speed sections. Placement of the load cell required a moment transfer to obtain the corrected values at the propeller plane coordinate system which was done using MATLAB (see APPENDIX B).

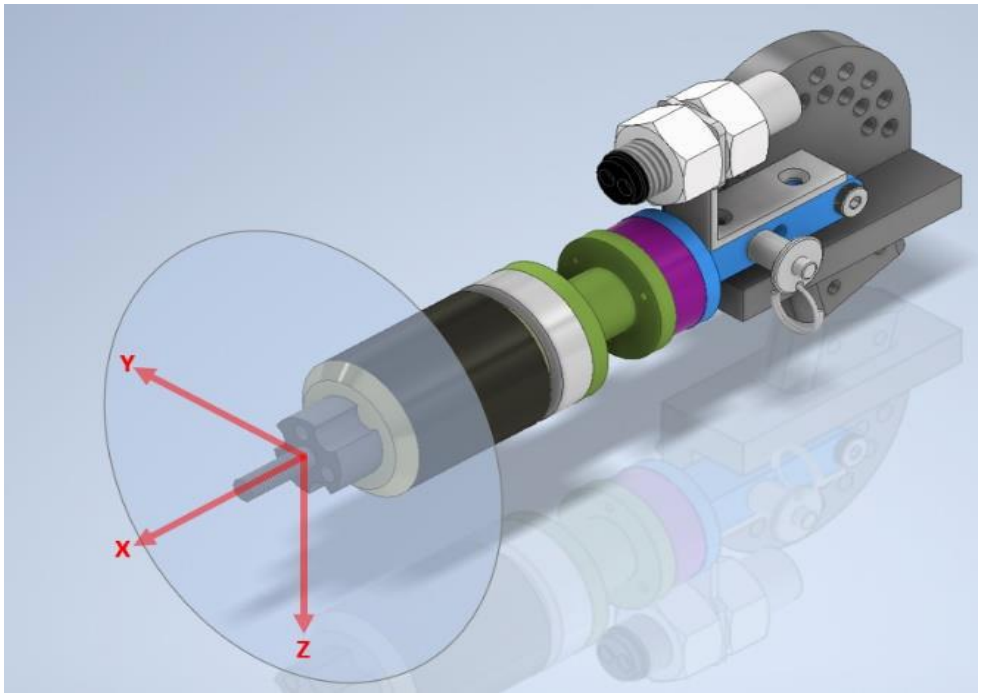

Figure 21. Propeller assembly coordinate system.

Propellers used during testing were three, four, five, and six blade configurations. The propeller blades used were Aeronaut CAM Carbon 16 x 8 folding propellers (Figure 22). These were identical to the blades being used on the LA-8 and also readily available commercially.

Figure 22. Aeronaut CAM Carbon blades in 5-blade propeller configuration.

5.2.2 HIGH-SPEED TEST STAND

A slightly redesigned test stand was developed for use in the 3ft x 4ft high-speed test section. New components needed for this section were designed around a pre-existing streamlined strut to reduce overall fabrication time and material cost. Mounting of the primary components such as the motor and load cell remained unchanged to facilitate a modular assembly that can be easily interchanged between both test sections. Material was cut away from the upper section of the strut to achieve a more streamlined shape. An aluminum base plate was attached to the strut that would accommodate the now lengthened variable AOI sector which would place the lever arm on the wind tunnel centerline. The same staggered hole design was used for adjusting AOI in 10-degree increments, however, the reduced wind tunnel cross sectional area limited AOI to a maximum of 20 degrees based on wall interference concerns.

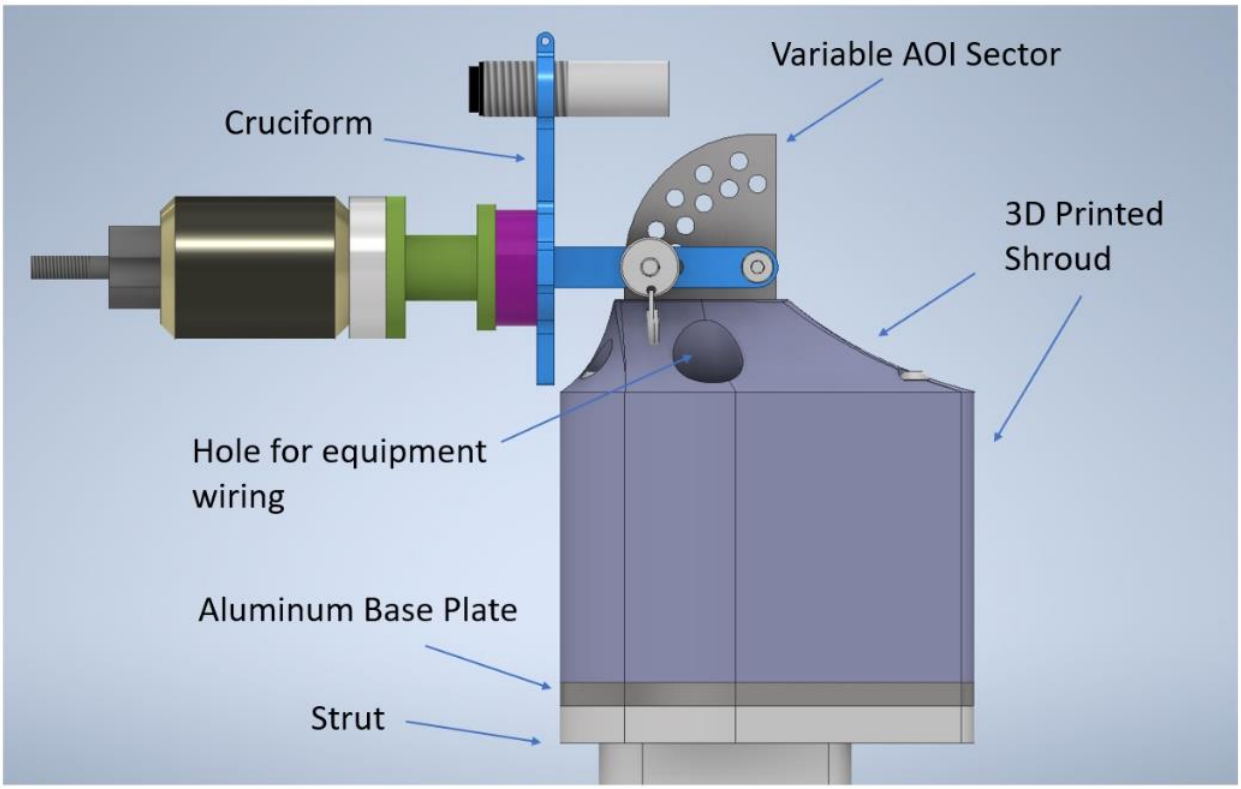

Figure 23. High-speed test stand assembly.

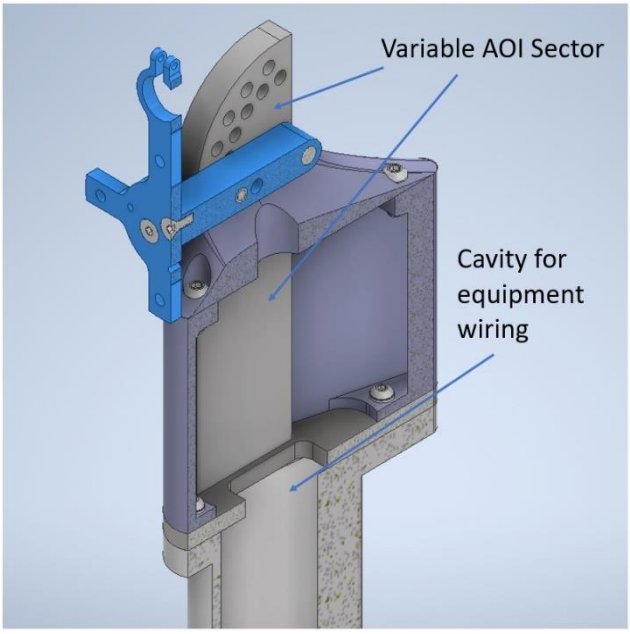

Figure 24. Cross-section view of high-speed test stand assembly.

A streamlined shroud was 3D printed and used to provide an aerodynamic cover of the larger AOI sector and to cover equipment wiring that needed to run to the motor and load cell which can be seen in Figure 23 and 24. The lever arm used a cruciform design, originally designed for a 3D printed nacelle which incorporated NACA ducts and a frontal air inlet to aid in motor cooling as well as to reduce the drag of the overall assembly behind the propeller (see APPENDIX C for figure). However, after separate testing that included the nacelle, it was found that the nacelle had a considerable impact on the measured forces and moments as well as contributing to motor overheating that resulted in undesirable data. For this reason, it was not used for testing during this experiment. With nothing else to aid in cooling of the motor it was decided to simply use an infrared thermometer (Figure 25) to ensure the temperature of the motor never exceeded ≈ 55°C in between experiment runs. Eventually a thermocouple (Figure 26) was introduced to the test rig that allowed temperature to be monitored from the computer outside the wind tunnel. The thermocouple was affixed using metal tape to the outside of the motor. Erroneous readings, reasoned to be from poor quality thermocouples, led to their use being abandoned.

Figure 25. Infrared thermometer.

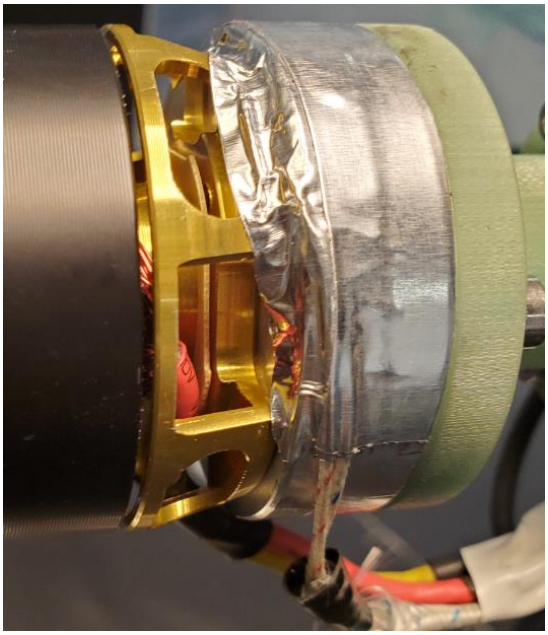

Figure 26. Thermocouple attached to motor.

5.2.3 LABVIEW SOFTWARE

LabVIEW is a visual programming software that uses graphical user interfaces (front panels) and visual programming in the form of block diagrams (back panels) for applications in

data acquisition, instrument control, or automation. The wind tunnel was controlled, and conditions were monitored by a custom LabVIEW program that in large part had already been programmed from past experiments. Figure 27 shows the current front panel that was used during testing. A user can designate a file location for the data to be saved as well as set the number of samples taken per run. Live plots of dynamic pressure and RPM ensured relatively stable conditions were achieved before taking data. This was important to minimize the variance between data points in a particular run. Force and moment values were displayed in real time as well as performance characteristics such as advance ratio and efficiency. An additional code file or VI (virtual instrument) could also be accessed that allowed the load cell to be biased or set back to zero when needed. This was done after changing blade configurations or AOI when the use of tools on the test rig induced loads on the load cell.

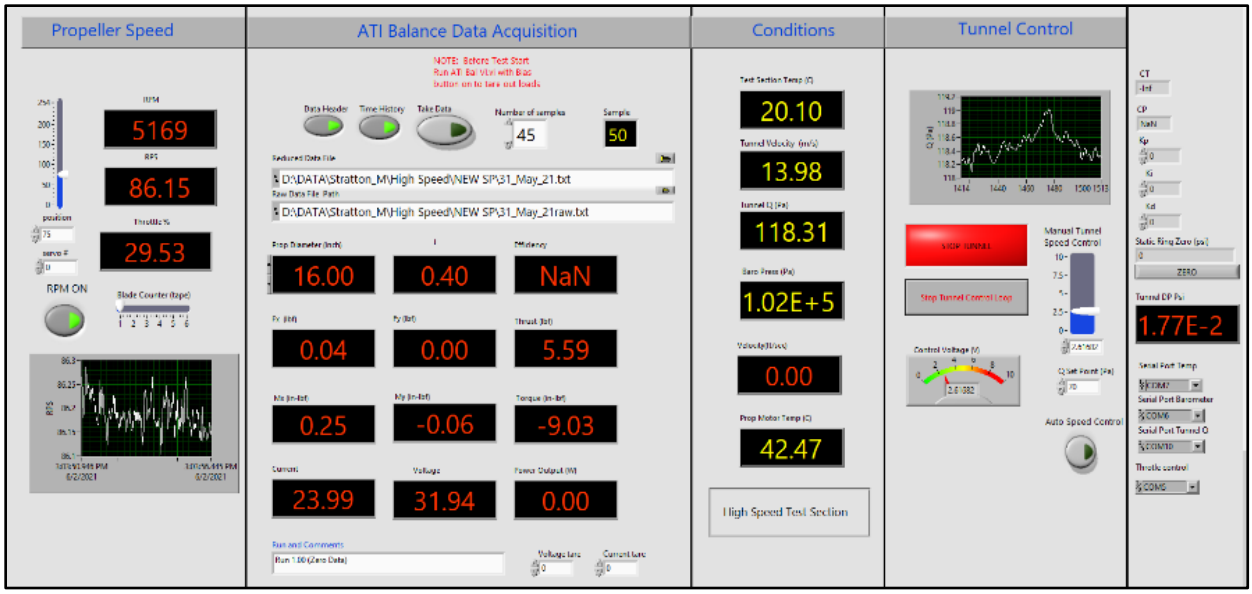

Figure 27. LabVIEW front panel.

5.3 SPLIT-PLOT EXPERIMENT DESIGN FOR WIND TUNNEL TESTING

5.3.1 DESIGN SPACE EXPLORATION FOR LOW-SPEED TESTING

Initial testing began with running a traditional OFAT test using a 3-blade propeller. This was done to facilitate exploration of the design space and for corroboration with existing data that was completed at the NASA LaRC 12-ft wind tunnel. Three factors were chosen: tunnel velocity, angle of incidence, and motor RPM. One factor, RPM, was varied while the other factors were held constant. Factor levels for tunnel velocity were 0 m/s, 6 m/s, and 12 m/s and AOI from 0° to 100° in increments of 20°. A sample of the test matrix for one case of AOI is shown in Table 2.

Velocity, (m/s)	AOI, (°)	RPM
0	0	4000
0	0	5500
0	0	7000
6	0	4000
6	0	5500
6	0	7000
12	0	4000
12	0	5500
12	0	7000

Table 2. Sample from OFAT test matrix.

Figure 28 shows the NASA comparison data as thrust and torque coefficients at incidence angles of 0°, 60°, and 80° over the range of tunnel velocities tested at each facility [17]. The data shows good comparison in general. The NASA data was tested over a wider range of RPM which can be seen from the data points that extend past that of the ODU data group. The complete OFAT test matrix and responses are given in APPENDIX D.

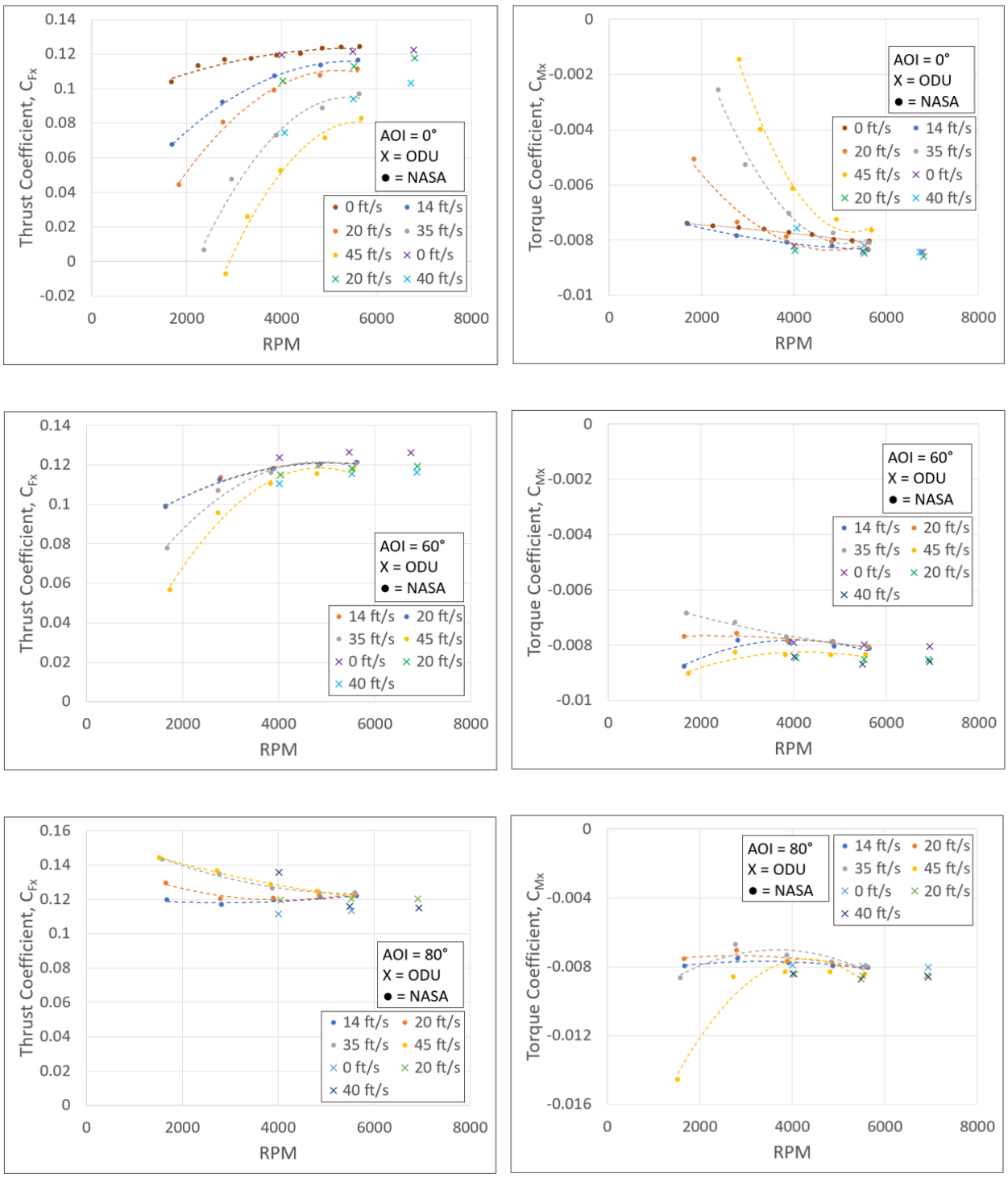

Figure 28. Comparison of NASA and ODU OFAT data at 0°, 60°, and 80° AOI.

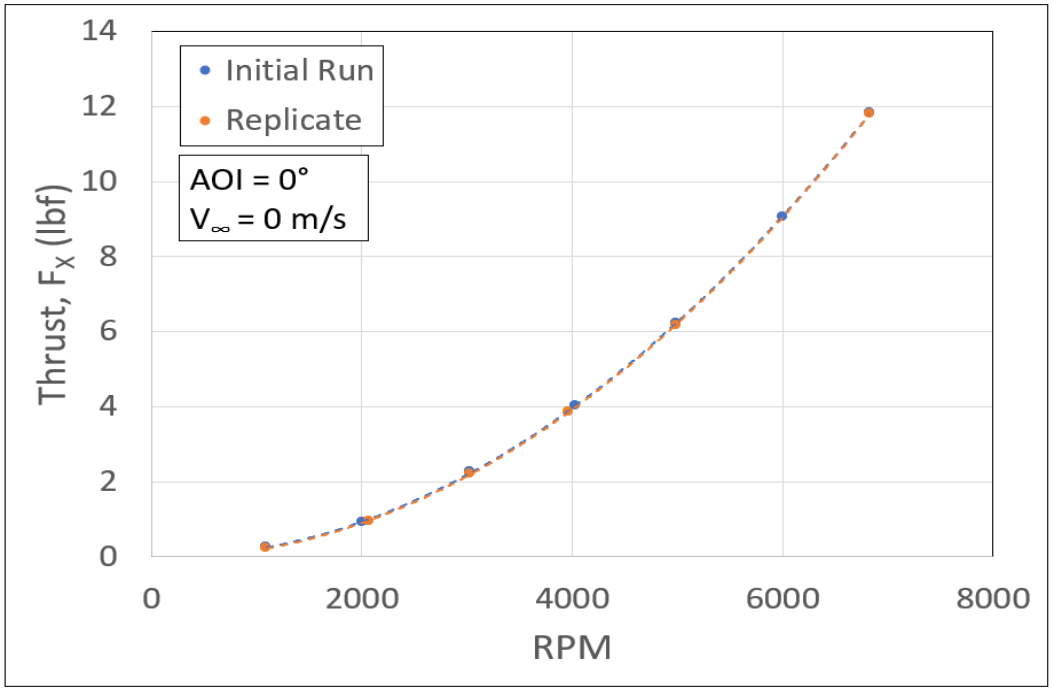

Figure 29. Static thrust comparison data.

A similar testing approach was used to record static thrust data where tunnel velocity was kept at 0 m/s (flow off), AOI at 0°, and motor speed varied from 1000 RPM to 6800 RPM. A replicate test run was also compared during the static thrust experiment to examine short term repeatability (Figure 29). These tests allowed the system as a whole to be evaluated and assessment of the RPM limits. Data was also taken to test the system for hysteresis. This ensured there were no unwanted time dependent variables in the measurements. Loose joints or connections, for example, would be seen as increasing variability or error in the data over time. The results provided confidence that components of the test rig were adequately secured. Motor speed was increased from 2000 RPM to 7000 RPM and then decreased from 7000 RPM back to 2000 RPM in a continuous sequence. This was repeated for tunnel velocities of 0 m/s, 6 m/s, and 12 m/s and for an AOI of 0° and 100°. No hysteresis in either thrust or torque coefficients was identified. Since no hysteresis was suspected in either coefficient, a completely randomized RPM

schedule could be implemented in subsequent experiments. The trial was not repeated for flow-on conditions although this would be a nice addition in the future.

5.3.2 INITIAL SPLIT-PLOT DESIGN: 4-BLADE

The split plot design process begins with understanding the factors and levels and the desired model order. Initially, implementing a split-plot design for the 3-blade configuration was not of interest since data had already been obtained from previous testing at NASA Langley. This led to the 4-blade configuration being used in the initial split-plot design. Factors and levels originally chosen were velocity from 0 m/s to 12 m/s, AOI from 0° to 100°, and motor speed from 4000 RPM to 6500 RPM. Next, factors are divided into HTC and ETC categories. AOI is a HTC factor and RPM and tunnel velocity are ETC. An I-optimal design was specified to minimize the error of prediction over the design space. Design runs are automatically chosen by the I-optimal routine in Design Expert™ software. The 4-blade propeller configuration was used to test the initial split-plot design. The design specified enough degrees of freedom to support a fifth order model but with the goal of using a fourth order model. This was done to provide a better internal estimate of error by allocating degrees of freedom from terms not chosen in the model, thus improving precision for significance testing. Once the design was generated in Design Expert™ some values had to be changed manually based on the constraints of the test rig. For example, if a value of 23.5° was generated by the I-Optimal routine this was changed to 20° as that was the next closest available increment.

The inclusion of the velocity range minimum 0 m/s was found to be problematic once testing began. At high angles of incidence and zero wind tunnel velocity, recirculation was suspected due to the close proximity of the wind tunnel floor to the propeller wake flow. This resulted in the removal of eight design points from the 4-blade experiment. There were also

limitations of the power supply that lowered the upper RPM limit from 6800 RPM to 6500 RPM. The constraints of the power supply became more limited as the blade number was increased. This resulted in further lowering of the upper RPM limit in each case. The 5-blade upper RPM limit was 5800 RPM while the 6-blade limit was 5500 RPM. The initial RPM range for the 6-blade was considered too limited so the minimum RPM was lowered to 3000 RPM.

5.3.3 SPLIT-PLOT DESIGN FOR LOW-SPEED TESTING

The lessons learned from the initial 4-blade split-plot experiment led to changes being made when setting levels of the next design to be generated in DX. The low velocity range limit was increased to 2 m/s to avoid the risk of recirculation at high incidence angles. The I-Optimal design routine was again implemented, and degrees of freedom specified for a fifth order model. Figures 30 and 31show three-dimensional and two-dimensional representations, respectively, of the design space and the design points used. The design points are colored based on run order. APPENDIX E shows the complete test matrices and responses for all low-speed experiments.

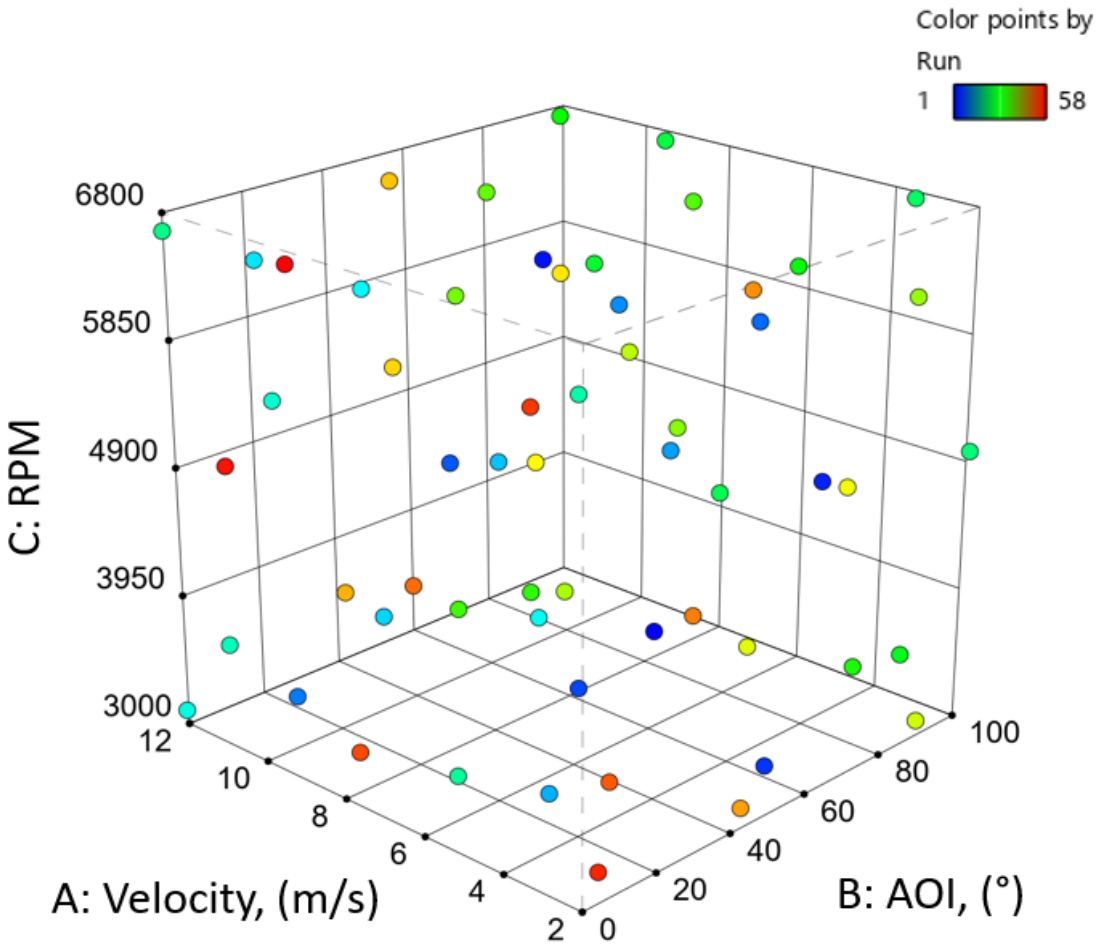

Figure 30. I-Optimal split-plot design for 3-blade propeller (3-factor space).

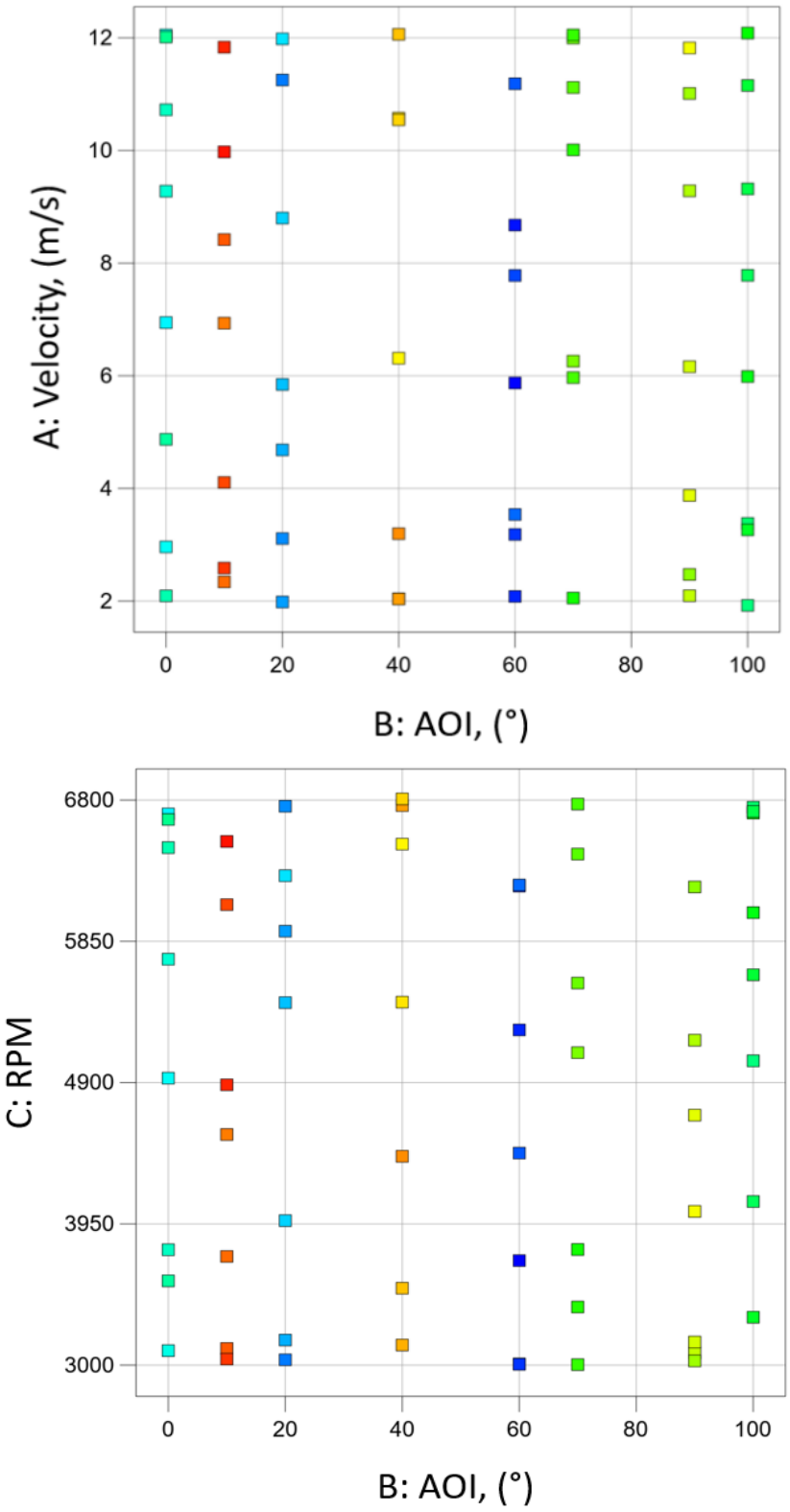

Figure 31. I-Optimal split-plot design for 3-blade propeller (3-factor space).

Split-plot model degrees of freedom for the 3-blade experiment are shown in Table 3. The degrees of freedom allocated to the model in either the WP or SP is what is used to estimate model terms. This left three degrees of freedom for estimating error associated with the WP terms and twenty degrees of freedom for estimating error associated with the SP terms (Table 4a). Any insignificant terms not included in the model of a response would then be added to the number of degrees of freedom being used to test for lack of model fit. The table also shows the variance inflation factor (VIF) for each term. VIF is a measure of the dependencies between a factor (or term) in question on the other factors in the model. Terms were shown to have some mild correlation with a single term maximum of approximately 30. Typically, higher order polynomial models have larger VIF values. Power (β) is also given for each term which provides the probability (1- β) of failing to include a significant term in the model. Power is typically lower for WP terms since these factors are not being changed as often compared to the SP factors. The design metrics for each blade configuration are given in Table 4 and 5.

	Source	df
	Whole-plot	
	Model	4
	Corr Total	7
	Subplot	
	Model	30
	Corr Total	50

Table 3. Split-plot degrees of freedom for the 3-blade propeller.

(a)

Term	Standard Error*	Error df†	VIF	Restricted‡ VIF	Power
Whole-Plot					
b	1.74	3	17.5783	10.2953	7.0 %
b^2	4.37	3	29.1117	18.445	5.3 %
b^3	2.05	3	12.5921	9.60409	6.5 %
b^4	4.00	3	23.3699	17.581	5.4 %
Subplot					
A	0.7547	20	17.4729	17.317	24.3 %
C	0.7409	20	16.7145	15.5712	25.1 %
Ab	1.27	20	24.17	24.7949	11.7 %
AC	1.27	20	26.6613	26.2165	11.7 %
bC	1.31	20	25.8202	23.4083	11.3 %
A^2	1.68	20	22.4469	21.9684	8.7 %
C^2	1.84	20	24.8992	25.3059	8.1 %
AbC	0.4231	20	1.3901	1.4486	61.4 %
A^2b	0.5457	20	3.68334	1.47673	41.5 %
A^2C	0.5448	20	3.80266	3.79234	41.6 %
Ab^2	0.5468	20	3.46383	3.63319	41.3 %
AC^2	0.5435	20	3.77467	3.73483	41.8 %
b^2C	0.5719	20	3.70083	3.47985	38.4 %
bC^2	0.5827	20	3.94631	1.56624	37.2 %
A^3	0.7668	20	12.6383	12.3918	23.7 %
C^3	0.8076	20	12.2398	11.7999	21.8 %
A^2b^2	1.06	20	5.96786	3.81957	14.7 %
A^2bC	0.7721	20	3.98686	3.80506	23.4 %
A^2C^2	1.07	20	6.32098	6.26703	14.4 %
Ab^2C	0.7580	20	3.747	3.66221	24.2 %
AbC^2	0.7645	20	3.86099	3.79131	23.8 %
b^2C^2	1.09	20	5.8868	3.68679	14.2 %
A^3b	1.09	20	12.8828	12.7953	14.0 %
A^3C	1.10	20	13.6767	13.744	14.0 %
Ab^3	1.08	20	11.4153	12.4752	14.3 %
AC^3	1.14	20	12.8244	14.273	13.2 %
b^3C	1.11	20	12.7889	11.539	13.8 %
bC^3	1.20	20	13.2625	12.1769	12.5 %
A^4	1.44	20	18.6641	18.5434	10.2 %
C^4	1.57	20	19.9038	20.09	9.3 %

(b)

Term	Standard Error*	Error df†	VIF	Restricted‡ VIF	Power
Whole-Plot					
b	1.71	3	18.5092	10.3333	7.1 %
b^2	4.09	3	21.2498	14.4242	5.4 %
b^3	2.04	3	12.2565	9.46592	6.5 %
b^4	3.70	3	17.3277	13.9403	5.4 %
Subplot					
A	0.8516	12	20.8466	20.7823	19.1 %
C	0.8395	12	19.1126	17.9746	19.5 %
Ab	1.58	12	38.1043	38.6592	9.0 %
AC	1.87	12	41.1258	55.4587	7.8 %
bC	1.59	12	33.6795	33.127	8.9 %
A^2	2.21	12	35.9815	35.5704	7.0 %
C^2	2.05	12	24.7141	25.7702	7.4 %
AbC	0.4176	12	1.45961	1.46014	59.5 %
A^2b	0.5726	12	4.09875	1.65998	36.2 %
A^2C	0.5757	12	4.34539	4.32323	35.9 %
Ab^2	0.6175	12	4.47332	4.49408	32.0 %
AC^2	0.5925	12	4.36105	4.50656	34.2 %
b^2C	0.6501	12	4.33619	4.24579	29.4 %
bC^2	0.6623	12	4.59179	1.86261	28.5 %
A^3	0.8493	12	15.8344	15.8354	19.2 %
C^3	0.8944	12	14.1483	13.773	17.8 %
A^2b^2	1.24	12	7.88059	5.03031	11.5 %
A^2bC	0.8324	12	5.06579	4.71074	19.8 %
A^2C^2	1.34	12	9.10382	9.7301	10.6 %
Ab^2C	0.9369	12	5.56715	5.48505	16.6 %
AbC^2	0.8961	12	5.40594	5.32087	17.7 %
b^2C^2	1.45	12	8.05959	5.58801	9.7 %
A^3b	1.27	12	19.27	19.2082	11.2 %
A^3C	1.58	12	20.6172	30.4781	9.0 %
Ab^3	1.24	12	14.4066	15.5095	11.5 %
AC^3	1.30	12	15.7752	17.994	11.0 %
b^3C	1.26	12	13.6353	13.7807	11.3 %
bC^3	1.32	12	15.3777	15.2244	10.7 %
A^4	1.84	12	29.8517	29.3134	7.9 %
C^4	2.05	12	24.6075	28.1781	7.3 %

Table 4. Design metrics table for (a) 3-blade and (b) 4-blade split plot design.

(a)

Term	Standard Error*	Error df†	VIF	Restricted‡ VIF	Power
Whole-Plot					
b	1.76	3	19.7474	10.5584	7.0 %
b^2	4.37	3	29.4997	18.4251	5.3 %
b^3	2.06	3	13.4433	9.69434	6.4 %
b^4	4.00	3	23.8016	17.6295	5.4 %
Subplot					
A	0.7534	20	17.0475	17.1126	24.4 %
C	0.8014	20	18.4431	17.2704	22.1 %
Ab	1.27	20	24.6085	24.3708	11.6 %
AC	1.31	20	27.0817	26.952	11.2 %
bC	1.44	20	28.3194	27.9457	10.1 %
A^2	1.77	20	24.5627	25.7042	8.4 %
C^2	2.02	20	28.1307	28.6209	7.6 %
AbC	0.4354	20	1.47619	1.44593	58.9 %
A^2b	0.5576	20	3.7457	1.53319	40.0 %
A^2C	0.5581	20	3.86511	3.78571	40.0 %
Ab^2	0.5517	20	3.44949	3.63109	40.7 %
AC^2	0.5692	20	3.81971	3.86949	38.7 %
b^2C	0.6295	20	4.15616	4.08034	32.8 %
bC^2	0.6138	20	3.81304	1.63931	34.2 %
A^3	0.7487	20	12.3651	12.131	24.6 %
C^3	0.8767	20	12.6457	12.4249	19.2 %
A^2b^2	1.03	20	5.78569	3.59528	15.3 %
A^2bC	0.8072	20	3.97527	3.75439	21.9 %
A^2C^2	1.16	20	6.87268	7.35525	13.1 %
Ab^2C	0.7798	20	3.71277	3.64104	23.1 %
AbC^2	0.8625	20	4.32603	4.26942	19.7 %
b^2C^2	1.16	20	5.96784	3.98727	13.0 %
A^3b	1.10	20	12.7636	12.6307	13.9 %
A^3C	1.06	20	13.1631	13.3213	14.6 %
Ab^3	1.08	20	12.3001	12.3969	14.3 %
AC^3	1.25	20	14.8832	15.211	11.9 %
b^3C	1.14	20	11.5549	11.5578	13.3 %
bC^3	1.33	20	14.2952	14.1921	11.0 %
A^4	1.52	20	21.8663	22.1652	9.6 %
C^4	1.82	20	22.8418	23.5696	8.2 %

(b)

Term	Standard Error*	Error df†	VIF	Restricted‡ VIF	Power
Whole-Plot					
b	1.74	3	16.6618	10.2905	7.0 %
b^2	4.41	3	30.6216	18.7081	5.3 %
b^3	2.06	3	12.0365	9.63961	6.4 %
b^4	4.03	3	24.6174	17.8309	5.4 %
Subplot					
A	0.7132	20	15.4348	15.5527	26.7 %
C	0.7293	20	15.8349	14.5622	25.7 %
Ab	1.32	20	25.6861	25.0808	11.2 %
AC	1.21	20	25.2109	24.837	12.4 %
bC	1.35	20	25.6888	25.1243	10.9 %
A^2	1.70	20	23.5078	23.593	8.7 %
C^2	1.92	20	25.7992	25.569	7.9 %
AbC	0.3793	20	1.24721	1.21417	70.8 %
A^2b	0.5489	20	3.68277	1.56335	41.1 %
A^2C	0.5308	20	3.77737	3.64185	43.4 %
Ab^2	0.5731	20	3.76115	3.56925	38.3 %
AC^2	0.5782	20	4.02956	4.00284	37.7 %
b^2C	0.5780	20	3.43279	3.59926	37.7 %
bC^2	0.6252	20	4.26029	1.68943	33.1 %
A^3	0.7648	20	12.8442	12.7372	23.8 %
C^3	0.8286	20	12.9046	11.726	21.0 %
A^2b^2	1.08	20	6.02167	4.1582	14.3 %
A^2bC	0.7601	20	4.20395	4.20255	24.0 %
A^2C^2	1.11	20	7.29926	7.42683	13.8 %
Ab^2C	0.8343	20	4.52289	4.48405	20.8 %
AbC^2	0.9898	20	5.2567	5.59998	16.1 %
b^2C^2	1.22	20	7.15888	4.31275	12.2 %
A^3b	1.19	20	13.6062	14.808	12.6 %
A^3C	1.06	20	14.4285	14.4135	14.6 %
Ab^3	1.18	20	13.8324	12.9108	12.8 %
AC^3	1.15	20	14.8367	14.5154	13.2 %
b^3C	1.22	20	13.3946	14.2117	12.2 %
bC^3	1.22	20	13.2652	12.6304	12.3 %
A^4	1.47	20	20.8177	21.18	10.0 %
C^4	1.82	20	23.2383	23.772	8.2 %

Table 5. Design metrics table for (a) 5-blade and (b) 6-blade split-plot design.

While power is generally a good metric when determining if a model can estimate significant terms, it is not entirely adequate in the context of response surface designs where more emphasis is placed on predicting an outcome, as is the case with characterization. Since the response surface is created by predicting the mean outcome (the response) as a function of inputs over the region of experimentation (the factor inputs and their levels), a better metric would be to

look at the standard error of the predicted mean response. Figure 32 shows a graph of this standard error over a fraction of the design space (FDS) for all the low-speed split-plot designs. The plot shows that for each experiment roughly 80% of the design space has a standard error of approximately 1.1 or less at 95% confidence ($\alpha = 0.05$). This corresponds to overall stability of variance throughout the design space.

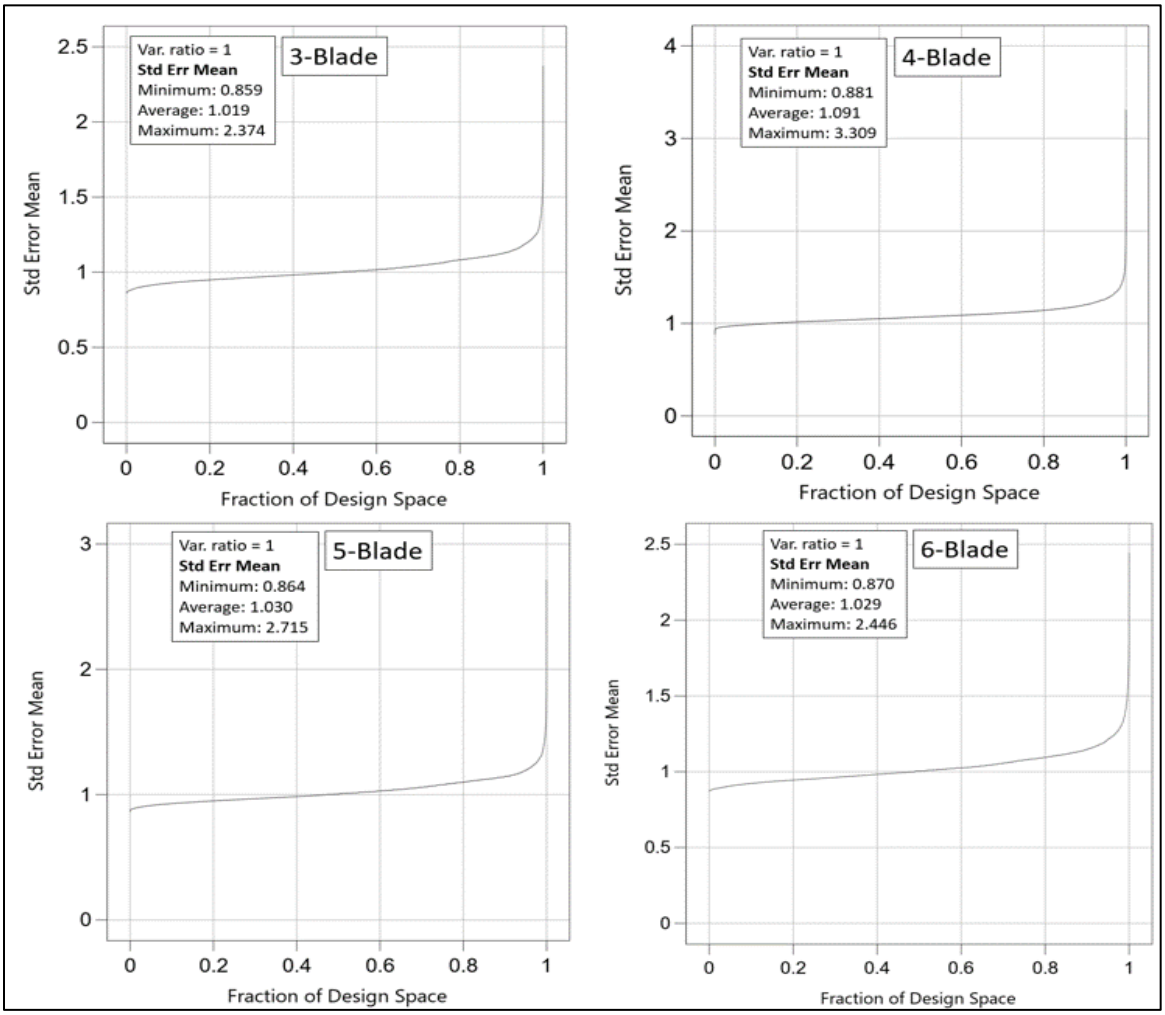

Figure 32. FDS graph for low-speed split-plot designs.

Figures 33 and 34 shows the standard error of the mean responses or prediction variance as contour plots for all factor combinations for all low-speed split-plot designs assuming a WP/SP variance ratio of 1. The contour plots show a relatively uniform distribution overall where larger values seen at the edge of the design space were to be expected.

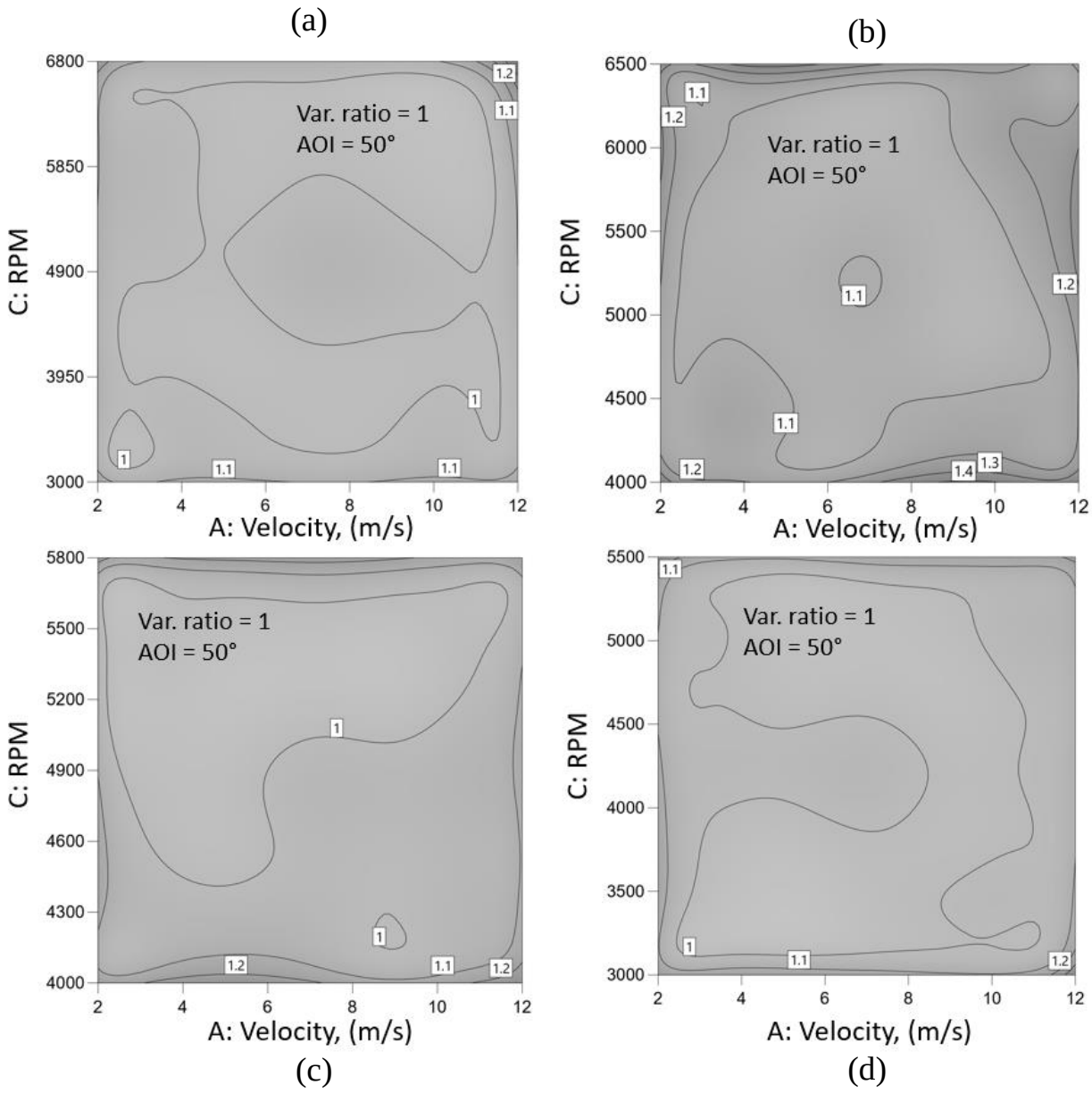

Figure 33. Contour plots of prediction variance (RPM vs. Velocity) for (a) 3-blade, (b) 4-blade, (c) 5-blade, and (d) 6-blade split-plot designs.

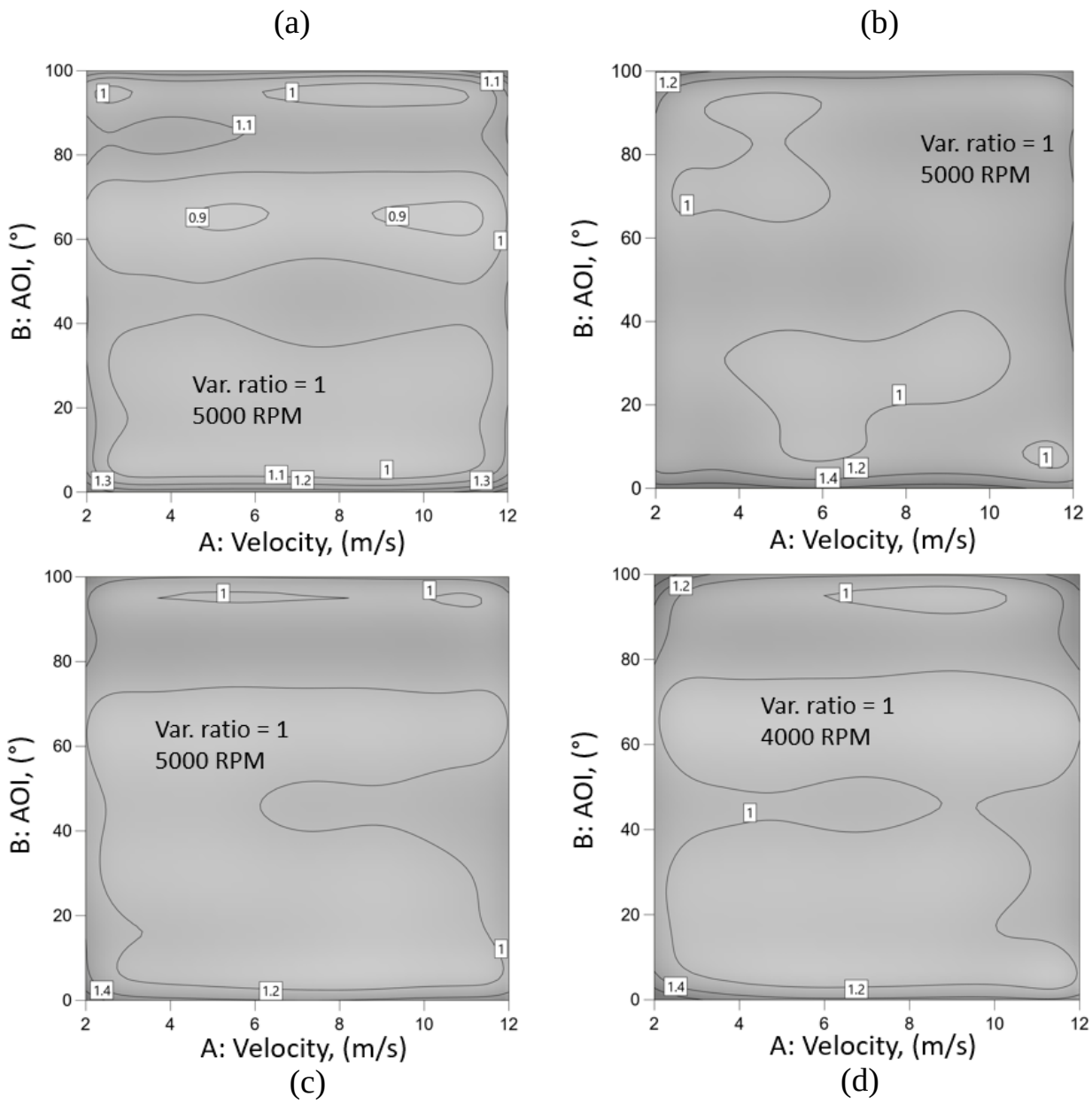

Figure 34. Contour plots of prediction variance (AOI vs. Velocity) for (a) 3-blade, (b) 4-blade, (c) 5-blade, and (d) 6-blade split-plot designs.

5.3.4 DESIGN SPACE EXPLORATION FOR HIGH-SPEED TESTING

Before implementing the split-plot design in the high-speed section exploratory testing was done to determine if there would be any limits in RPM at the increased tunnel velocities. This was done to develop an operational envelope in which a zero thrust case could be avoided since this would be of no interest. An OFAT test was carried out on each propeller configuration where AOI and RPM would be held constant while tunnel velocity would be varied. Factor levels for angle of incidence were 0°, 10°, and 20° and motor speed at 4000 RPM, 5000 RPM, and 6000 RPM. A sample of the test matrix for the 4000 RPM case is shown in Table 6.

Velocity (m/s)	AOI (°)	RPM
12	0	4000
15	0	4000
20	0	4000
25	0	4000
30	0	4000
12	10	4000
15	10	4000
20	10	4000
25	10	4000
30	10	4000
12	20	4000
15	20	4000
20	20	4000
25	20	4000
30	20	4000

Table 6. Sample of high-speed OFAT test matrix.

The OFAT tests revealed that a windmill condition imposed a limit on the airspeed that could be achieved. Windmilling occurs when the freestream velocity reaches a speed that overpowers the motor causing the propeller to rotate solely due to the aerodynamic lift generated by the blades [32]. This would be seen as the propeller producing negative thrust. Figure 35 shows data from the 3-blade OFAT test as thrust against airspeed for the three levels of RPM.

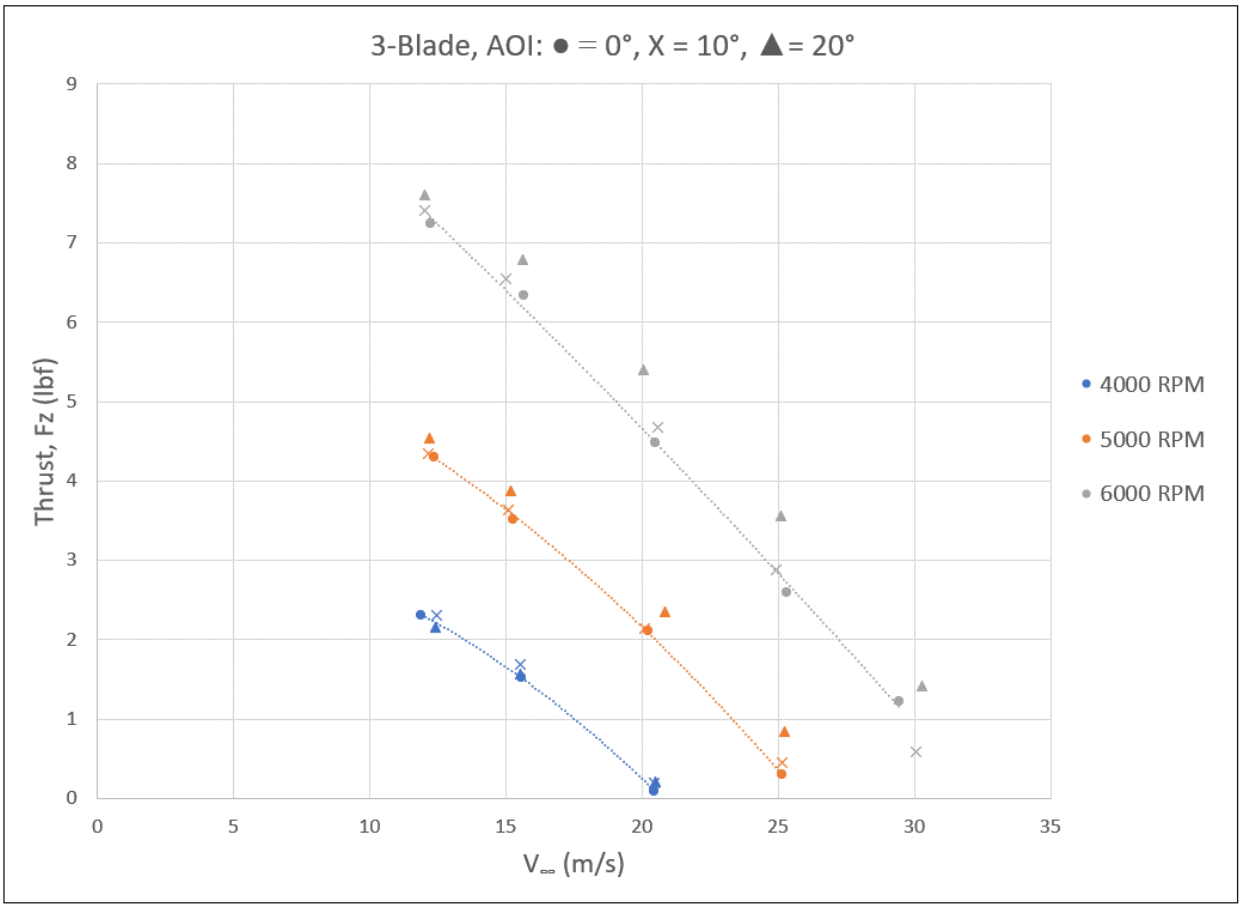

Figure 35. Effect of airspeed on thrust at three levels of RPM for 3-blade OFAT test.

This windmill condition led to constraints on the design space in both RPM and velocity. To prevent software from extrapolating when building the design, a linear equation must be used to describe the constraints. In this case, the equation was defined as

$$1 \leq \frac{HL_A - A}{HL_A - CP_A} + \frac{C - LL_C}{CP_C - LL_C} \tag{33}$$

Here, HL_A is the high-level of factor A (velocity), LL_C is the low-level of factor C (RPM), and CP_A and CP_C are the constraint points of factor A and C, respectively. Figure 36 shows a visual representation of the region of operability and the equation used to describe the constraints on the design space.

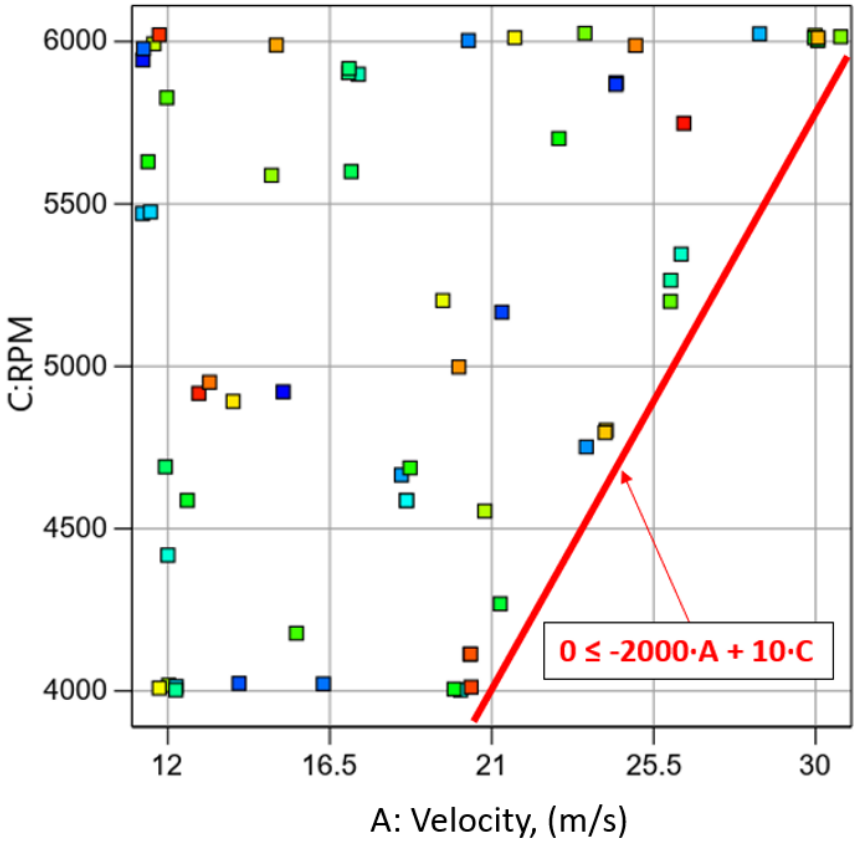

Figure 36. Region of operability and design space constraints in high-speed section.

5.3.5 SPLIT-PLOT DESIGN FOR HIGH-SPEED TESTING

Once the factor limits were known and the constraint equation was calculated for the design space a final design could be generated in DX. The I-Optimal routine was implemented once again but degrees of freedom were specified for a third order model instead of the fifth order model of the low-speed tests. Results from the preliminary OFAT tests suggested that a third order model would be sufficient. Degrees of freedom were limited with respect to angle of incidence since the number of levels were reduced. As a result, no terms could be included in the model that had angle of incidence higher than second order. The limited degrees of freedom for angle of incidence was in part due to the fear of increased wall interference effects at high incidence angles in the smaller wind tunnel section and also because lower incidences at high-speed would be more representative of the transition flight mode.

Factor levels chosen were the same as those from the OFAT experiments, velocity from 12 m/s to 30 m/s, angle of incidence at 0°, 10°, and 20°, and motor speed from 4000 RPM to 6000 RPM, with blade number being added as a categorical factor. This increased run efficiency of the experiment since all blade configurations could be tested in one design. Changing propeller configuration, however, required the wind tunnel to be stopped which made this a HTC factor, similar to adjusting angle of incidence. The complete split-plot design and responses are shown in Table 7. Note some of the factor values for velocity are below the minimum level of 12 m/s; this is addressed in a later section.

			ETC	HTC	ETC	HTC						
	Group	Run	Factor 1 A:Velocity, m/s	Factor 2 B:AOI, °	Factor 3 C:RPM	Factor 4 D:Blades	Response 1 CF_x	Response 2 CF_y	Response 3 CF_z	Response 4 CM_x	Response 5 CM_y	Response 6 CM_z
Whole Plot	1	1	15.21	10	4921	6	0.10117	0.00043	-0.00493	-0.01151	0.00011	-0.00239
	1	2	11.30	10	5943	6	0.14442	0.00045	-0.00376	-0.01369	0.00027	-0.00197
	1	3	24.46	10	5874	6	0.05078	0.00052	-0.00508	-0.00747	0.00050	-0.00259
	1	4	24.45	10	5868	6	0.05054	0.00056	-0.00507	-0.00746	0.00050	-0.00261
Whole Plot	2	5	21.28	10	5167	4	0.03962	0.00035	-0.00439	-0.00542	0.00034	-0.00197
	2	6	13.98	10	4023	4	0.06313	0.00072	-0.00365	-0.00733	0.00014	-0.00196
	2	7	11.32	10	5978	4	0.11100	-0.00010	-0.00176	-0.00963	0.00056	-0.00122
Whole Plot	3	8	16.32	20	4022	3	0.04929	-0.00003	-0.00692	-0.00593	0.00042	-0.00308
	3	9	20.35	20	6004	3	0.06572	0.00021	-0.00455	-0.00679	0.00131	-0.00288
	3	10	23.63	20	4752	3	0.01915	0.00047	-0.00923	-0.00333	0.00032	-0.00370
Whole Plot	4	11	18.49	20	4665	6	0.07466	0.00117	-0.00985	-0.00941	0.00110	-0.00490
	4	12	28.44	20	6024	6	0.03389	0.00161	-0.01182	-0.00587	0.00111	-0.00514
	4	13	11.30	20	5470	6	0.14316	-0.00021	-0.00526	-0.01344	0.00161	-0.00285
Whole Plot	5	14	11.52	0	5475	3	0.09261	0.00003	-0.00063	-0.00812	-0.00035	-0.00032
	5	15	12.23	0	4014	3	0.06599	0.00056	-0.00155	-0.00717	-0.00066	-0.00059
	5	16	18.63	0	4588	3	0.03798	-0.00011	-0.00170	-0.00516	-0.00066	-0.00045
	5	17	18.63	0	4587	3	0.03788	-0.00019	-0.00165	-0.00515	-0.00064	-0.00042
Whole Plot	6	18	20.14	20	4003	6	0.02616	0.00253	-0.01403	-0.00483	0.00038	-0.00643
	6	19	12.00	20	4418	6	0.12736	0.00035	-0.00693	-0.01283	0.00120	-0.00353
	6	20	26.26	20	5345	6	0.02905	0.00128	-0.01315	-0.00520	0.00079	-0.00530
	6	21	17.29	20	5899	6	0.11628	-0.00013	-0.00717	-0.01192	0.00195	-0.00350
Whole Plot	7	22	25.97	10	5265	5	0.01106	0.00053	-0.00654	-0.00340	0.00005	-0.00274
	7	23	12.22	10	4003	5	0.09216	0.00052	-0.00332	-0.01015	0.00011	-0.00208
	7	24	17.02	10	5904	5	0.09755	0.00049	-0.00351	-0.01033	0.00038	-0.00222
	7	25	17.03	10	5917	5	0.09733	0.00067	-0.00369	-0.01035	0.00032	-0.00231
Whole Plot	8	26	11.93	10	4690	4	0.09392	-0.00006	-0.00297	-0.00905	0.00025	-0.00146
	8	27	17.10	10	5600	4	0.07661	-0.00015	-0.00336	-0.00804	0.00036	-0.00161
	8	28	30.06	10	6003	4	-0.00131	0.00029	-0.00607	-0.00169	0.00015	-0.00211
	8	29	21.24	10	4269	4	0.00030	-0.00023	-0.00682	-0.00176	-0.00031	-0.00230
Whole Plot	9	30	12.54	0	4587	3	0.07658	-0.00020	-0.00042	-0.00757	-0.00024	-0.00015
	9	31	19.96	0	4006	3	0.00570	-0.00035	-0.00121	-0.00222	-0.00038	-0.00027
	9	32	22.87	0	5701	3	0.03895	-0.00042	-0.00080	-0.00503	-0.00027	-0.00018
Whole Plot	10	33	11.45	0	5630	5	0.12722	0.00012	-0.00062	-0.01189	-0.00037	-0.00038
	10	34	18.73	0	4687	5	0.05050	0.00003	-0.00100	-0.00724	-0.00044	-0.00054
	10	35	29.97	0	6012	5	0.00161	-0.00041	-0.00108	-0.00249	-0.00029	-0.00029
Whole Plot	11	36	15.57	0	4178	4	0.05275	-0.00152	-0.00137	-0.00646	-0.00053	0.00012
	11	37	11.97	0	5827	4	0.10594	-0.00053	-0.00063	-0.00944	-0.00032	-0.00011
	11	38	25.97	0	5200	4	-0.00271	-0.00108	-0.00126	-0.00155	-0.00037	-0.00007
	11	39	23.59	0	6026	4	0.04242	-0.00081	-0.00086	-0.00554	-0.00028	-0.00012
Whole Plot	12	40	30.70	0	6015	6	-0.00707	-0.00107	-0.00062	-0.00198	-0.00025	-0.00013
	12	41	14.88	0	5588	6	0.11343	-0.00062	-0.00028	-0.01201	-0.00034	-0.00033
	12	42	12.02	0	4018	6	0.10093	-0.00044	-0.00006	-0.01179	-0.00050	-0.00048
	12	43	20.81	0	4554	6	0.02594	-0.00065	-0.00061	-0.00536	-0.00035	-0.00021
Whole Plot	13	44	11.61	20	5993	5	0.13766	-0.00150	-0.00327	-0.01171	0.00208	-0.00190
	13	45	29.98	20	6019	5	0.01911	0.00137	-0.01105	-0.00400	0.00115	-0.00481
	13	46	19.64	20	5203	5	0.07789	-0.00116	-0.00703	-0.00842	0.00162	-0.00324
	13	47	11.76	20	4009	5	0.11188	-0.00293	-0.00423	-0.01051	0.00183	-0.00190
Whole Plot	14	48	21.64	20	6012	4	0.06309	0.00041	-0.00637	-0.00710	0.00126	-0.00319
	14	49	13.81	20	4892	4	0.08791	0.00021	-0.00474	-0.00870	0.00098	-0.00288
	14	50	24.18	20	4803	4	0.01001	0.00167	-0.01040	-0.00286	0.00064	-0.00458
	14	51	24.15	20	4796	4	0.01008	0.00151	-0.01047	-0.00285	0.00063	-0.00452
Whole Plot	15	52	30.10	10	6012	3	0.00778	-0.00026	-0.00495	-0.00210	0.00202	-0.00161
	15	53	14.39	10	5989	3	0.08825	-0.00076	-0.00184	-0.00787	0.00118	-0.00125
	15	54	19.91	10	4998	3	0.04191	0.00025	-0.00419	-0.00528	0.00152	-0.00147
Whole Plot	16	55	25.00	10	5988	5	0.04589	0.00009	-0.00481	-0.00639	0.00038	-0.00225
	16	56	13.16	10	4951	5	0.10693	-0.00030	-0.00252	-0.01072	0.00041	-0.00185
	16	57	20.39	10	4114	5	0.00730	0.00052	-0.00666	-0.00293	-0.00017	-0.00304
	16	58	20.41	10	4114	5	0.00744	0.00039	-0.00654	-0.00291	-0.00012	-0.00301
Whole Plot	17	59	20.43	20	4012	3	0.01451	-0.00012	-0.00968	-0.00302	0.00017	-0.00388
	17	60	11.76	20	6021	3	0.10043	-0.00104	-0.00294	-0.00825	0.00106	-0.00170
	17	61	12.86	20	4917	3	0.08593	-0.00133	-0.00375	-0.00779	0.00086	-0.00198
	17	62	26.34	20	5748	3	0.03113	-0.00046	-0.00790	-0.00424	0.00067	-0.00301

Table 7. Complete high-speed split-plot design.

As before split-plot degrees of freedom are shown in Table 8. Note the WP degrees of freedom for the model have increased since there were two HTC factors instead of one as in the low-speed experiment. This left five degrees of freedom to estimate the WP error which was an improvement from the low-speed design, the result is higher values of power. The design metrics table also shows fewer degrees of freedom left for SP error in comparison but more than adequate (Table 9). The numbers in the brackets refer to the different terms of the categoric factor (blade number). There are four levels of blade number and there can only be one less term than there are levels of the categoric factor, thus the highest term shown is three.

	Source	df
	Whole-plot	
	Model	11
	Corr Total	16
	Subplot	
	Model	37
	Corr Total	45

Table 8. Split-plot degrees of freedom for the high-speed experiment.

Term	Standard Error*	Error df†	VIF	Restricted‡ VIF	Power
Whole-Plot					
b	0.5211	5	6.31796	2.32246	34.4 %
d[1]	1.11	5			8.7 %
d[2]	0.9315	5			
d[3]	0.8908	5			
bd[1]	0.6028	5			13.5 %
bd[2]	0.7255	5			
bd[3]	0.7631	5			
b^2	0.7915	5	4.21827	1.9041	17.9 %
b^2d[1]	1.21	5			7.9 %
b^2d[2]	1.07	5			
b^2d[3]	1.13	5			
Subplot					
A	1.04	8	21.9615	24.0924	13.7 %
C	1.44	8	61.9669	63.7792	9.4 %
Ab	0.6922	8	7.79178	7.2776	24.7 %
AC	2.06	8	45.2874	65.8692	7.1 %
Ad[1]	0.7705	8			10.4 %
Ad[2]	0.7557	8			
Ad[3]	0.9388	8			
bC	0.5024	8	5.49176	5.06082	41.8 %
Cd[1]	0.6000	8			11.9 %
Cd[2]	0.6161	8			
Cd[3]	0.8852	8			
A^2	2.00	8	22.0439	29.7621	7.3 %
C^2	0.7158	8	4.10729	4.84029	23.4 %
AbC	0.7435	8	5.72374	5.38872	22.1 %
Abd[1]	0.8260	8			14.7 %
Abd[2]	0.7385	8			
Abd[3]	0.5712	8			
ACd[1]	0.8389	8			8.7 %
ACd[2]	0.9367	8			
ACd[3]	1.21	8			
bCd[1]	0.5917	8			11.4 %
bCd[2]	1.04	8			
bCd[3]	0.8594	8			
A^2b	1.36	8	22.3712	11.6639	10.0 %
A^2C	2.49	8	47.0592	68.1987	6.5 %
A^2d[1]	1.12	8			8.6 %
A^2d[2]	1.16	8			
A^2d[3]	1.26	8			
Ab^2	0.9516	8	11.7842	13.6165	15.3 %
AC^2	1.33	8	20.005	23.384	10.2 %
b^2C	1.21	8	29.0212	29.5117	11.3 %
bC^2	0.8151	8	11.7546	5.82706	19.2 %
C^2d[1]	0.7765	8			10.6 %
C^2d[2]	1.08	8			
C^2d[3]	0.9112	8			
A^3	2.05	8	40.9238	59.479	7.2 %
C^3	1.29	8	37.9151	40.533	10.5 %

Table 9. Design metrics table for high-speed split-plot design.

Figure 37 shows the FDS graph for the high-speed design. The standard error was shown to be higher with roughly 80% of the design space having a value of approximately 1.5 or less. This can be attributed to the higher correlation between terms compared to the low-speed experiments and the greater number of factor levels and categoric factors. This was to be expected since the factor constraints led to asymmetry in the design space which is typical of multicollinearity. The contour plots of prediction variance, shown as an average of the blade numbers used, for the factor combinations is presented in Figure 38. Again, the effect of multicollinearity can be seen in the wider distribution of prediction variance.

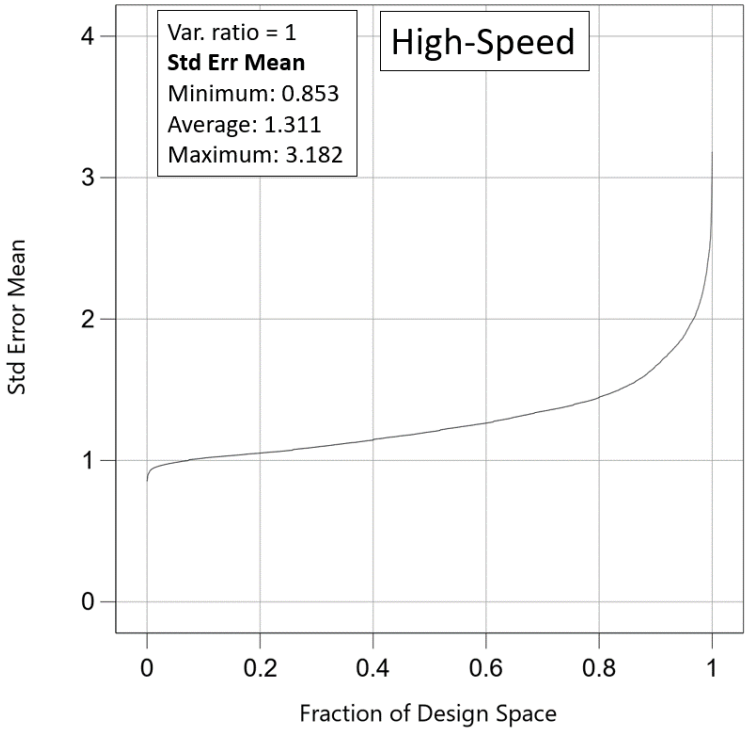

Figure 37. FDS graph for high-speed split-plot design.

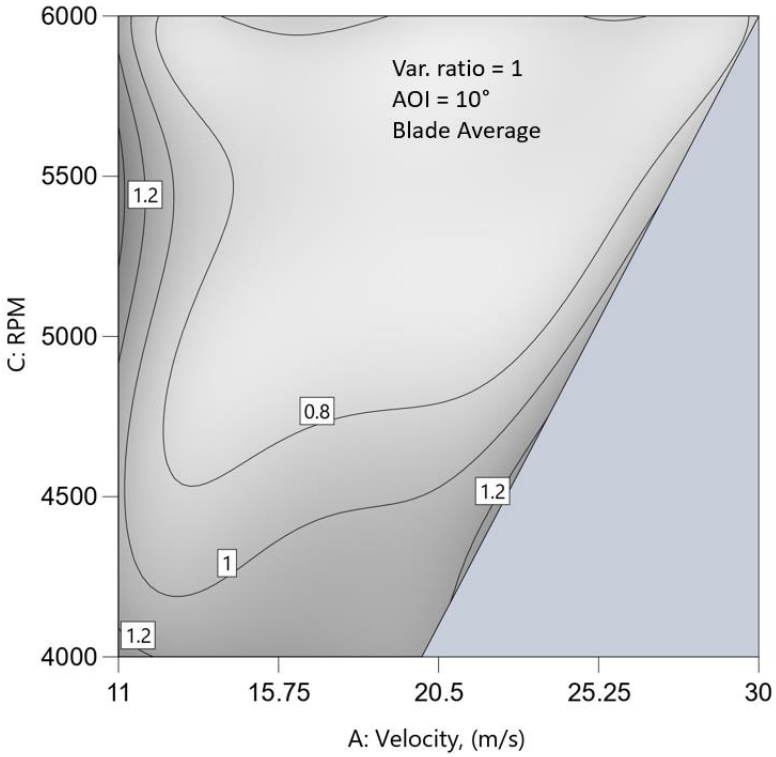

(a)

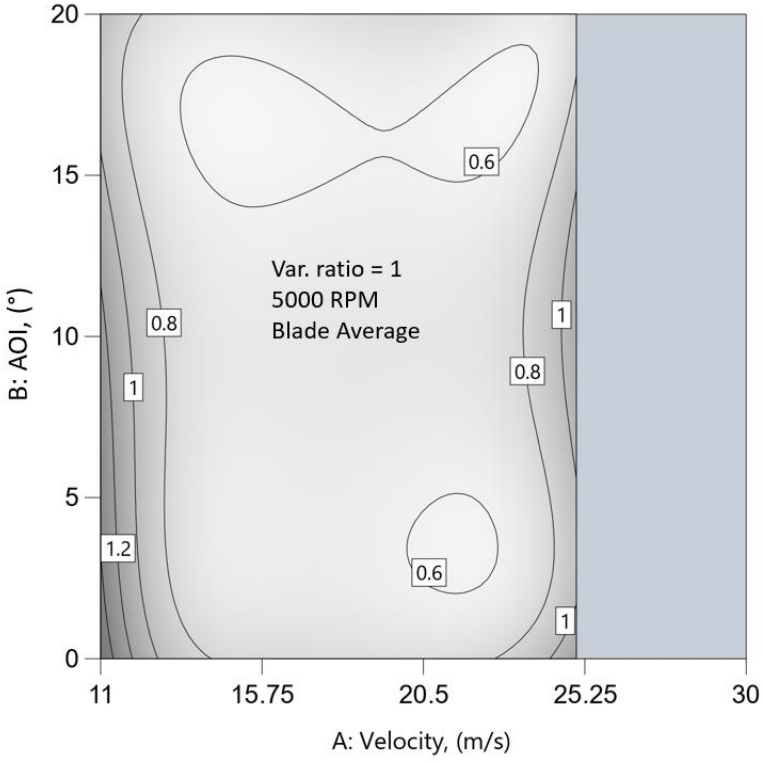

(b)

Figure 38. Contour plots of average prediction variance for (a) velocity vs. RPM, (b) velocity vs. AOI.

5.3.6 BOUNDARY CORRECTIONS IN HIGH-SPEED TEST SECTION

Inspection of the data for velocity in Table 7 shows that some values are below the velocity range minimum of 12 m/s. After data was collected, corrections were made to velocity that accounted for solid blockage of the test stand as well as the propeller in a closed wall test section. As a result, the corrected velocities put some values well below the chosen factor level, so the low limit of velocity was simply changed to 11 m/s in DX.

Velocity corrections made for the solid blockage effects are given as

$$\frac{\Delta V_{sb}}{V_u} = \epsilon_{sb} = \frac{K \cdot (model\ volume)}{C^{3/2}} \tag{34}$$

where ϵ_{sb} is the ratio of the change in velocity due to the blockage to the uncorrected velocity, K is the body shape factor (approximated as 1.2), the model volume is the overall volume of the test stand, and C is the cross-sectional area of the high-speed test section of the wind tunnel [31]. This led to the approximation of $\epsilon_{sb} = 0.0011490$.

Corrections made to velocity for the effects of the wall interference on the propeller slipstream were computed using Glauert's method according to AGARD [33]. Thrust was calculated from the uncorrected velocity to determine the quantity τ which was used to approximate V/V_C , the ratio of uncorrected and corrected stream velocities in a solid wall wind tunnel (Fig. 39). The quantity A_P/C is the ratio of the cross-sectional areas of the propeller disk to the wind tunnel test section. APPENDIX F shows the equations used for plotting the curves of Fig. 39. The uncorrected and corrected velocity ratios for both the propeller stream and solid blockage were added to solve for the final corrected velocity. Table 10 shows a sample of the values computed for the first four runs of the split-plot design. While this method was developed

for propeller at zero incidence, it was used to understand the magnitude of corrections assuming small incidence angles.

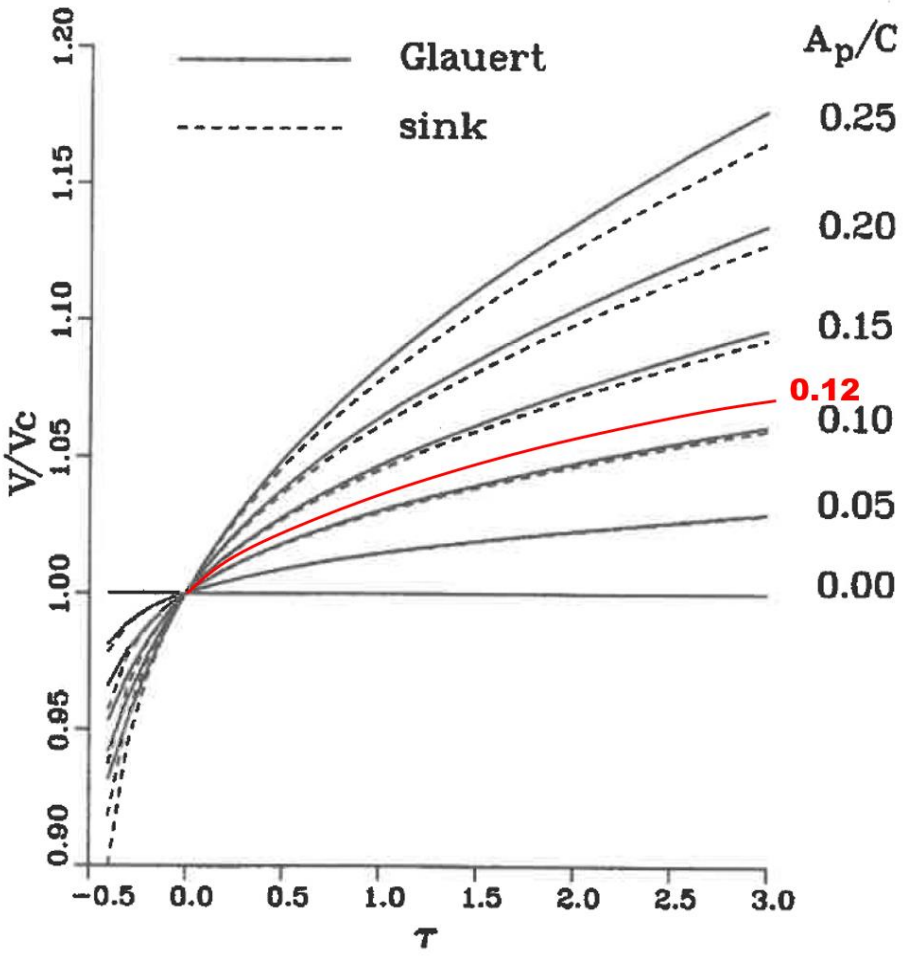

Figure 39. Ratio of uncorrected and corrected stream velocities in a solid wall wind tunnel (red curve approximated for use as a guide).

$V_\infty (m/s)$	$T = C_T \rho n^2 D^4$	$\tau = \frac{T}{\rho A_p V^2}$	V/V_C	$\sum V_C/V$	V_C
15.57	22.18	0.6	1.03	0.98	15.21
12.08	46.18	2.0	1.07	0.94	11.30
24.68	15.85	0.2	1.01	0.99	24.46
24.67	15.74	0.2	1.01	0.99	24.45

Table 10. Sample data for velocity corrections using Glauert's method.

Design Expert™ was used to generate interaction plots to compare the results of the low-speed and high-speed experiments. The split-plot designs and responses of the low-speed experiments were used to create a historical model that would be analyzed as a fully randomized experiment. While not mathematically rigorously justified, this allowed all the blade configurations to be examined at once. Figures 40 and 41 show comparisons at 5000 RPM and 4000 RPM, respectively, for an incidence angle of 0°. The comparisons show that the boundary corrections provided good overall agreement to the low-speed data for the same conditions. The minor exception being for the 5-blade configuration. The results were also agreeable at incidence angles of 10° and 20°, although these comparisons were not shown for brevity since the overall trend changed very little.

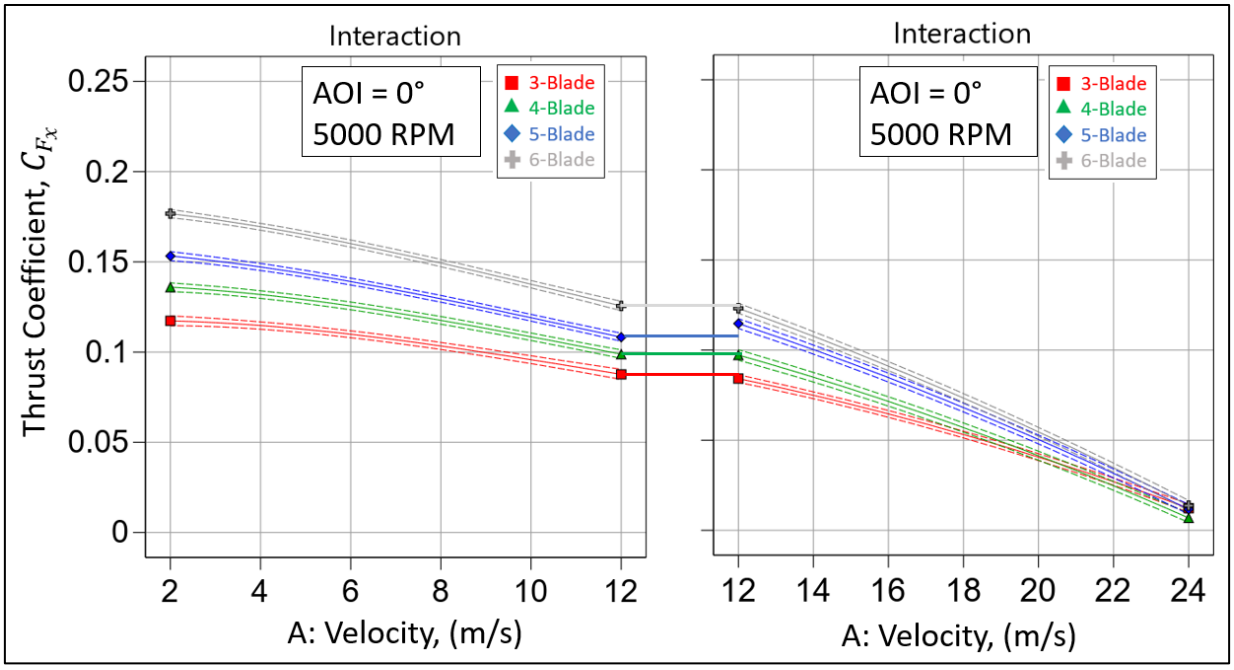

Figure 40. Low-speed and high-speed comparison at AOI = 0° and 5000 RPM.

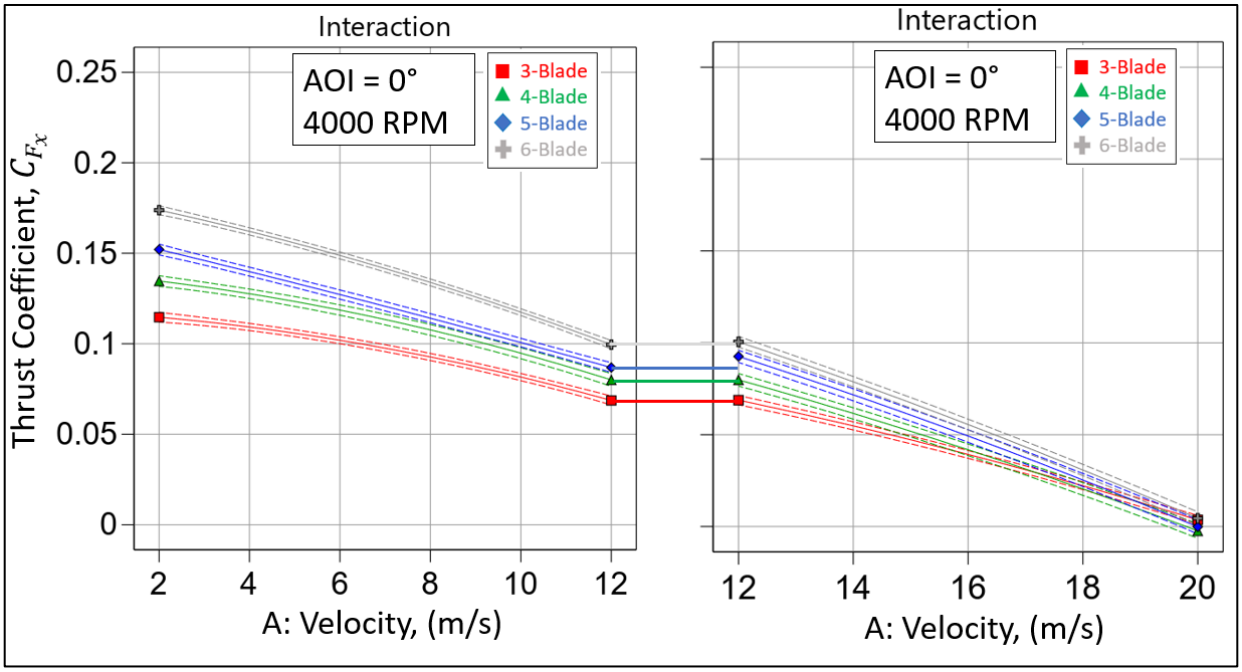

Figure 41. Low-speed and high-speed comparison at AOI = 0° and 4000 RPM.

6. RESULTS

6.1 ANALYSIS METHODS

The experiments were analyzed in DX using analysis of aariance with REML at a significance level of five percent ($\alpha = 0.05$) or 95% confidence [26]. The ANOVA tables identified significant terms in the models, both main effects and interactions. Design Expert™ also provided estimates of the WP and SP variance components. In some cases, WP error was found to be less than the SP error. This was contrary to the information stated in previous sections regarding WP error typically being greater than SP error. This was reasoned to be from the repeatability of the WP factor, AOI. The accuracy with which incidence angle could be set during the experiments drastically reduced the error associated with the WPs. Design Expert™ calls the source of WP error "Group" and SP error "Residual", the variance components from both the low and high-speed experiments are shown in Table 11 and 12, respectively.

Low-Speed						
3-Blade						
Source	C_{Fx}	C_{Fy}	C_{Fz}	C_{Mx}	C_{My}	C_{Mz}
Group	3.58E-07	4.27E-08	1.59E-06	2.42E-09	2.07E-07	3.02E-09
Residual	2.07E-06	7.02E-08	6.54E-07	1.56E-08	1.23E-07	2.38E-08
4-Blade						
Source	C_{Fx}	C_{Fy}	C_{Fz}	C_{Mx}	C_{My}	C_{Mz}
Group	8.35E-07	7.57E-07	1.46E-06	4.94E-09	4.23E-07	5.62E-07
Residual	7.53E-07	1.06E-07	1.61E-07	7.28E-09	3.53E-08	1.57E-07
5-Blade						
Source	C_{Fx}	C_{Fy}	C_{Fz}	C_{Mx}	C_{My}	C_{Mz}
Group	3.49E-06	1.04E-06	1.40E-06	1.17E-08	2.51E-07	1.49E-07
Residual	2.18E-06	2.53E-07	3.36E-07	1.03E-08	9.24E-08	5.07E-08
6-Blade						
Source	C_{Fx}	C_{Fy}	C_{Fz}	C_{Mx}	C_{My}	C_{Mz}
Group	0	6.31E-07	9.61E-09	0	1.50E-07	1.04E-07
Residual	2.22E-06	4.79E-07	8.10E-07	3.18E-08	1.18E-07	9.31E-08

Table 11. Low-speed split-plot variance components.

High-Speed						
Source	C_{Fx}	C_{Fy}	C_{Fz}	C_{Mx}	C_{My}	C_{Mz}
Group	6.31E-07	7.70E-08	1.02E-07	5.64E-09	2.42E-09	4.31E-08
Residual	1.58E-06	8.40E-08	4.07E-08	7.28E-10	2.23E-08	5.20E-09

Table 12. High-speed split-plot variance components.

Residuals, or the error between the fitted and observed values, were analyzed for each response. This was done to test the underlying statistical assumptions of normal, independently distributed error with constant variance. Figure 42 shows representative residual plots for the thrust coefficient from the high-speed experiment. Frequently called the “fat-pencil” test, the normal probability plot uses a transformed Y-axis to show that the underlying error distribution is normal. If so, the plot will resemble a straight line; more emphasis is placed on central values than on the extremes. The residuals versus the predicted (fitted) values demonstrates constant variance which shows that the residuals should be structureless. Residuals versus factors (not shown) showed variance was also constant across all factors. Residuals versus run shows that error is independent of time since there is no visible trend. The residuals shown in the plots are externally studentized residuals, which are scaled using the standard deviation and location in the design space. Red error bars above and below the data are also shown in the plots which are bounds that the data should lie within. Any points positioned close to the boundary lines are considered potential outliers and could warrant closer inspection. APPENDIX G provides a report of all residual diagnostics for all experiments performed.

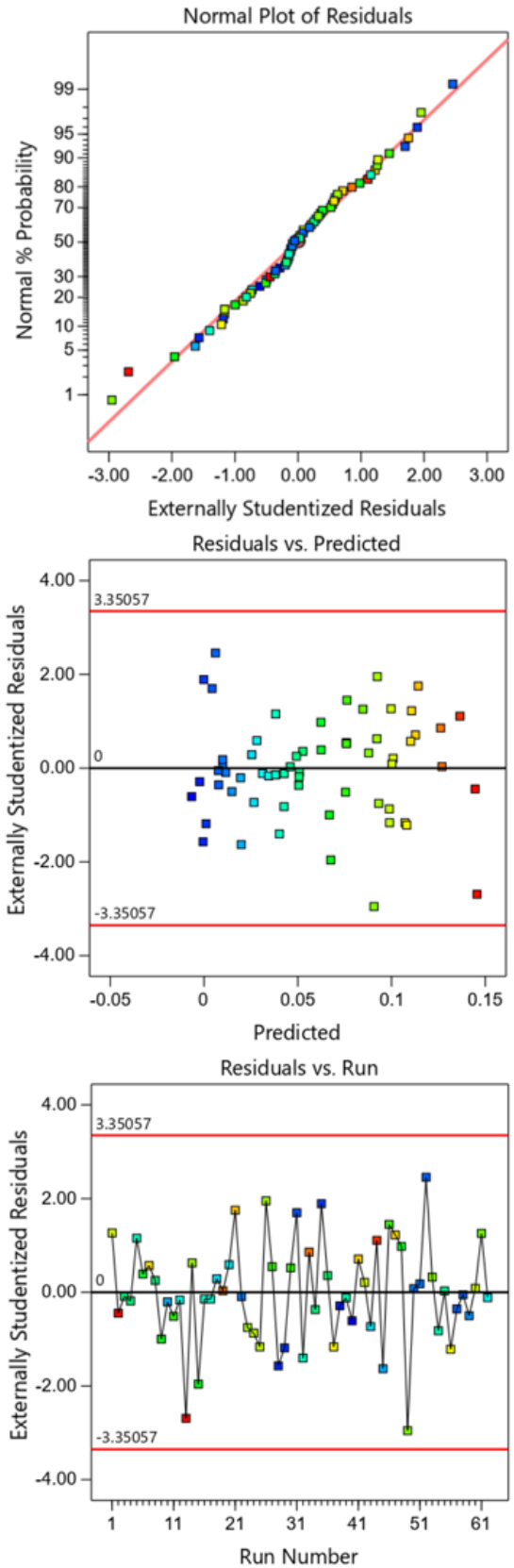

Figure 42. Residual plots for high-speed thrust coefficient, C_{F_x}.

To ensure that the fitted models were an appropriate representation of the experimental data, it was necessary to examine the proportion of variability explained by the models which is best expressed using the R^2 family of statistics. Table 13 and 14 show R^2 statistics from the low-speed and high-speed data, respectively. Thrust ($\boldsymbol{C_{F_x}}$) and torque ($\boldsymbol{C_{M_x}}$) show excellent model fit with R^2 of approximately 98% and a minimum value of 93% seen in the adjusted R^2 from the 4-blade test. The adjusted R^2 reflects the number of terms included in the model. Any difference seen between the R^2 value and the adjusted R^2 values may suggest a simpler model would suffice for future experiments. The lower R^2 and adjusted R^2 values, seen for instance in the side force coefficient $\boldsymbol{C_{F_y}}$, were reasoned to be from the very small forces being measured which would be more susceptible to error. This would result in more "noise" or unexplained variability in the data which was seen in DX as a very large coefficient of variation (C.V.) percentage, which is expressed as a noise to signal ratio.

Low-Speed				
	3-Blade		4-Blade	
	R^2	Adjusted R^2	R^2	Adjusted R^2
CFx	0.9958	0.9924	0.9977	0.9951
CFy	0.9545	0.9189	0.9675	0.9276
CFz	0.9852	0.9765	0.9957	0.9931
CMx	0.9703	0.9502	0.9642	0.9373
CMy	0.9604	0.9389	0.9965	0.9940
CMz	0.9982	0.9972	0.9721	0.9573

	5-Blade		6-Blade	
	R^2	Adjusted R^2	R^2	Adjusted R^2
CFx	0.9958	0.9928	0.9985	0.9968
CFy	0.8588	0.8128	0.9169	0.8753
CFz	0.9912	0.9869	0.9908	0.9825
CMx	0.9720	0.9620	0.9859	0.9748
CMy	0.9939	0.9916	0.9956	0.9922
CMz	0.9970	0.9948	0.9960	0.9942

Table 13. R^2 values for low-speed dimensionless force and moment coefficients in X, Y, & Z.

High-Speed		
	R^2	Adjusted R^2
C_{Fx}	0.9995	0.9989
C_{Fy}	0.9153	0.8675
C_{Fz}	0.9983	0.9953
C_{Mx}	1.0000	0.9999
C_{My}	0.9771	0.9550
C_{Mz}	0.9991	0.9967

Table 14. R^2 values for high-speed dimensionless force and moment coefficients in X, Y, & Z.

Once the residuals had been adequately assessed and there was confidence in the models ability to accurately explain the variability in the experiments, the regression models could be used for prediction. Regression model coefficients for all blade configurations from the high-speed experiment are shown in Table 15 and 16. Values for the six predicted responses can be obtained directly from these tables. Equation 35 shows the thrust coefficient equation for the 3-blade configuration. Factor values at points of interest would be used in the appropriate terms and a response would be obtained. The regression equations, however, must still only be used within the factor levels, that is extrapolation from the design space should be avoided. Full regression models for the low-speed experiments are given in APPENDIX H.

$$C_{F_x} = 0.0819 - 0.0237 \cdot V - 0.00137 \cdot AoA + 6.30 \times 10^{-5} \cdot RPM + 3.50 \times 10^{-5} \cdot V \cdot AoA + \cdots \quad (35)$$

Coded regression models avoid potential problems with non-orthogonal regression coefficients and are recommended for prediction models. These models are also included in APPENDIX H.

	3-Blade						4-Blade					
	CFx	CFy	CFz	CMx	CMy	CMz	CFx	CFy	CFz	CMx	CMy	CMz
Intercept	8.19E-02	7.94E-03	-5.48E-03	-2.48E-02	4.88E-03	-5.22E-03	9.97E-02	2.51E-03	-1.77E-03	-3.15E-02	4.26E-03	1.62E-03
Velocity	-2.37E-02	-4.70E-05	-8.68E-04	2.21E-03	-6.26E-04	-6.70E-05	-2.83E-02	-4.70E-05	-1.05E-03	2.66E-03	-5.69E-04	-1.10E-05
AOI	-1.37E-03	2.43E-04	-2.57E-04	-5.60E-05	2.12E-04	-7.20E-05	-1.36E-03	6.77E-04	-1.44E-04	-1.44E-04	-4.40E-05	-1.89E-04
RPM	6.30E-05	-2.74E-06	3.91E-06	4.93E-06	-4.56E-07	1.85E-06	7.60E-05	-1.85E-06	3.25E-06	5.79E-06	-3.84E-07	-7.42E-07
Blades	-	-	-	-	-	-	-	-	-	-	-	-
Velocity*AOI	3.50E-05	8.15E-06	-3.60E-05	-8.55E-06	4.71E-06	-1.90E-05	3.50E-05	8.15E-06	-3.60E-05	-1.30E-05	4.71E-06	-1.80E-05
Velocity*RPM	9.28E-06	-	9.95E-09	-1.04E-06	2.73E-08	-1.99E-08	9.87E-06	-	5.06E-08	-1.14E-06	2.73E-08	-4.17E-09
Velocity*Blades	-	-	-	-	-	-	-	-	-	-	-	-
AOI*RPM	9.17E-08	-5.72E-08	1.06E-08	1.19E-07	1.67E-08	1.91E-09	9.17E-08	-1.23E-07	-1.92E-08	1.51E-07	1.67E-08	1.30E-08
AOI*Blades	-	-	-	-	-	-	-	-	-	-	-	-
RPM*Blades	-	-	-	-	-	-	-	-	-	-	-	-
Velocity^2	-4.43E-04	-	3.80E-05	6.00E-05	2.30E-05	4.81E-06	-4.43E-04	-	3.60E-05	6.70E-05	2.10E-05	4.68E-07
AOI^2	1.13E-04	-2.00E-05	2.60E-05	-1.60E-05	-1.30E-05	1.00E-05	1.13E-04	-2.00E-05	2.60E-05	-1.60E-05	6.94E-07	1.00E-05
RPM^2	-2.25E-08	2.48E-10	-3.74E-10	3.60E-11	-	-5.05E-11	-2.46E-08	2.48E-10	-3.74E-10	6.68E-11	-	1.65E-10
Velocity*AOI*RPM	-	-	8.86E-09	6.59E-10	-	3.02E-09	-	-	8.86E-09	6.59E-10	-	3.02E-09
Velocity*AOI*Blades	-	-	-	-	-	-	-	-	-	-	-	-
Velocity*RPM*Blades	-	-	-	-	-	-	-	-	-	-	-	-
AOI*RPM*Blades	-	-	-	-	-	-	-	-	-	-	-	-
Velocity^2*AOI	-	-	-8.23E-07	2.64E-07	-1.94E-07	-1.11E-07	-	-	-8.23E-07	2.64E-07	-1.94E-07	-1.11E-07
Velocity^2*RPM	6.08E-08	-	-	-1.22E-08	-	3.96E-09	6.08E-08	-	-	-1.22E-08	-	3.96E-09
Velocity^2*Blades	-	-	-	-	-	-	-	-	-	-	-	-
Velocity*AOI^2	-	-	-	-3.61E-07	-	-	-	-	-	-3.61E-07	-	-
Velocity*RPM^2	-9.45E-10	-	-	1.23E-10	-	-1.30E-11	-9.45E-10	-	-	1.23E-10	-	-1.30E-11
AOI^2*RPM	-1.53E-08	2.76E-09	-4.36E-09	4.00E-09	-	-1.54E-09	-1.53E-08	2.76E-09	-4.36E-09	4.00E-09	-	-1.54E-09
AOI^2*Blades	-	-	-	-	-	-	-	-	-	-	-	-
AOI*RPM^2	-	-	-	-2.03E-11	-	-	-	-	-	-2.03E-11	-	-
RPM^2*Blades	-	-	-	-	-	-	-	-	-	-	-	-
Velocity^3	-	-	-5.57E-07	3.36E-07	-3.34E-07	-3.66E-07	-	-	-5.57E-07	3.36E-07	-3.34E-07	-3.66E-07
AOI^3	-	-	-	-	-	-	-	-	-	-	-	-
RPM^3	2.24E-12	-	-	-8.11E-14	-	-	2.24E-12	-	-	-8.11E-14	-	-

Table 15. Regression model coefficients for high-speed 3 and 4-blade dimensionless force and moment coefficients in X, Y, and Z.

	5-Blade						6-Blade					
	CFx	CFy	CFz	CMx	CMy	CMz	CFx	CFy	CFz	CMx	CMy	CMz
Intercept	7.25E-02	9.47E-03	2.41E-03	-3.36E-02	4.32E-03	-7.62E-03	1.15E-01	5.62E-03	2.76E-03	-2.78E-02	1.89E-03	-8.89E-03
Velocity	-3.07E-02	-4.70E-05	-1.18E-03	2.77E-03	-5.37E-04	-9.90E-05	-3.04E-02	-4.70E-05	-1.08E-03	2.98E-03	-4.04E-04	-1.21E-04
AOI	-1.02E-03	-1.57E-04	-3.50E-04	9.70E-05	-8.80E-05	7.50E-05	-9.54E-04	5.68E-04	-5.70E-04	-4.70E-05	-1.01E-04	-2.54E-04
RPM	1.00E-04	-2.91E-06	2.73E-06	5.16E-06	-4.41E-07	2.65E-06	8.50E-05	-2.34E-06	1.95E-06	1.86E-06	-1.88E-07	3.61E-06
Blades	-	-	-	-	-	-	-	-	-	-	-	-
Velocity*AOI	3.50E-05	8.15E-06	-4.00E-05	-1.20E-05	4.71E-06	-2.20E-05	3.50E-05	8.15E-06	-4.10E-05	-1.20E-05	4.71E-06	-2.20E-05
Velocity*RPM	1.00E-05	8.36E-09	3.56E-08	-1.13E-06	2.73E-08	-1.18E-08	9.99E-06	-1.05E-07	1.02E-07	-1.18E-06	2.73E-08	1.86E-08
Velocity*Blades	-	-	-	-	-	-	-	-	-	-	-	-
AOI*RPM	9.17E-08	-	3.34E-08	1.03E-07	1.67E-08	-1.72E-08	9.17E-08	-	5.22E-08	1.25E-07	1.67E-08	3.06E-08
AOI*Blades	-	-	-	-	-	-	-	-	-	-	-	-
RPM*Blades	-	-	-	-	-	-	-	-	-	-	-	-
Velocity^2	-4.43E-04	-	4.20E-05	6.40E-05	2.00E-05	4.18E-06	-4.43E-04	-	3.10E-05	6.70E-05	1.70E-05	6.26E-07
AOI^2	1.13E-04	-2.00E-05	2.60E-05	-1.60E-05	4.45E-06	1.00E-05	1.13E-04	-2.00E-05	2.60E-05	-1.60E-05	3.84E-06	1.00E-05
RPM^2	-2.70E-08	2.48E-10	-3.74E-10	1.16E-10	-	-1.30E-10	-2.51E-08	2.48E-10	-3.74E-10	4.82E-10	-	-2.96E-10
Velocity*AOI*RPM	-	-	8.86E-09	6.59E-10	-	3.02E-09	-	-	8.86E-09	6.59E-10	-	3.02E-09
Velocity*AOI*Blades	-	-	-	-	-	-	-	-	-	-	-	-
Velocity*RPM*Blades	-	-	-	-	-	-	-	-	-	-	-	-
AOI*RPM*Blades	-	-	-	-	-	-	-	-	-	-	-	-
Velocity^2*AOI	-	-	-8.23E-07	2.64E-07	-1.94E-07	-1.11E-07	-	-	-8.23E-07	2.64E-07	-1.94E-07	-1.11E-07
Velocity^2*RPM	6.08E-08	-	-4.36E-09	-1.22E-08	-	3.96E-09	6.08E-08	2.76E-09	-	-1.22E-08	-	3.96E-09
Velocity^2*Blades	-	-	-	-	-	-	-	-	-	-	-	-
Velocity*AOI^2	-	-	-	-3.61E-07	-	-	-	-	-	-3.61E-07	-	-
Velocity*RPM^2	-9.45E-10	-	-	1.23E-10	-	-1.30E-11	-9.45E-10	-	-	1.23E-10	-	-1.30E-11
AOI^2*RPM	-1.53E-08	2.76E-09	-	4.00E-09	-	-1.54E-09	-1.53E-08	-	-4.36E-09	4.00E-09	-	-1.54E-09
AOI^2*Blades	-	-	-	-	-	-	-	-	-	-	-	-
AOI*RPM^2	-	-	-	-2.03E-11	-	-	-	-	-	-2.03E-11	-	-
RPM^2*Blades	-	-	-	-	-	-	-	-	-	-	-	-
Velocity^3	-	-	-5.57E-07	3.36E-07	-3.34E-07	-3.66E-07	-	-	-5.57E-07	3.36E-07	-3.34E-07	-3.66E-07
AOI^3	-	-	-	-	-	-	-	-	-	-	-	-
RPM^3	2.24E-12	-	-	-8.11E-14	-	-	2.24E-12	-	-	-8.11E-14	-	-

Table 16. Regression model coefficients for high-speed 5 and 6-blade dimensionless force and moment coefficients in X, Y, and Z.

6.2 PREDICTION TOOL IN MATLAB

The regression models were used to write a code using MATLAB that would compute responses in the form of the aerodynamic coefficients based on the user defined input. The regression model coefficients from each experiment, low-speed and high-speed, were transferred from DX to an external spreadsheet using Microsoft Excel so that the data could be imported into MATLAB. All the required regression information as well as the spreadsheet containing factor input and responses were then stored in a folder that the program would reference throughout the code. The coded regression equations were used for all computations within the code. Working with coded variables is typical when performing regression analysis and model fitting which is done so the magnitudes of the regression coefficients can be compared directly for relative importance and bias from non-orthogonal coefficients is avoided. Using the coded regression equations meant that the factor input had to be transformed into coded variables. The transformation equation is given by

$$x = \frac{\zeta - \frac{(\zeta_{low} + \zeta_{high})}{2}}{\frac{(\zeta_{high} - \zeta_{low})}{2}} \tag{36}$$

Where x is the coded variable and ζ is the variable in its natural units. The subscripts “low” and “high” indicate the low and high levels of the factor being transformed. The aerodynamic responses based on the coded factor input and regression equations were then written to an external spreadsheet, again using Microsoft Excel, and the program would end. The external spreadsheet approach was chosen so that the results could be easily transferrable, to other software for example. Tables 17 and 18 show a representation of what the user defined factor input and response output would look like for both low-speed and high-speed, respectively. Factor input could be either a single point or multiple points, as seen in the tables. It was

expected that the program would be most useful when multiple points could be analyzed at once. The low-speed factor input was split between blade configurations since this reflects how the experiments were carried out, as individual regression models. The high-speed points of interest, being all part of one model, will be computed for any blade configuration entered (3, 4, 5, or 6). While both low-speed and high-speed factor inputs must be kept within the constraints of the model design space. The initial development of the program included prediction intervals for each response. It was realized that the upper and lower bounds of the prediction intervals, which were calculated using the ordinary least squares method, were narrower than that of the prediction intervals given in Design Expert™ which used the generalized least squares method for variance estimation. For this reason, the prediction intervals were not included. The full MATLAB script is given in APPENDIX I.

Low-Speed

3-Blade			4-Blade			5-Blade			6-Blade		
x_1 - Velocity (m/s)	x_2 - AOI	x_3 - RPM	x_1 - Velocity (m/s)	x_2 - AOI	x_3 - RPM	x_1 - Velocity (m/s)	x_2 - AOI	x_3 - RPM	x_1 - Velocity (m/s)	x_2 - AOI	x_3 - RPM
6.3	84	5207	6.3	84	5207	6.3	84	5207	6.3	84	5207
6.3	58	5201	6.3	58	5201	6.3	58	5201	6.3	58	5201
8.8	51	4149	8.8	51	4149	8.8	51	4149	8.8	51	4149
10.8	40	4092	10.8	40	4092	10.8	40	4092	10.8	40	4092
.	.	.	.	.	.	.	.	.	.	.	.
.	.	.	.	.	.	.	.	.	.	.	.
.	.	.	.	.	.	.	.	.	.	.	.

Responses

3-Blade						4-Blade					
C_{Fx}	C_{Fy}	C_{Fz}	C_{Mx}	C_{My}	C_{Mz}	C_{Fx}	C_{Fy}	C_{Fz}	C_{Mx}	C_{My}	C_{Mz}
0.120784	-0.001825	-0.006750	-0.008381	0.002923	-0.005040	0.138043	-0.002067	-0.008760	-0.010091	0.003847	-0.004502
0.116458	-0.001655	-0.004758	-0.008239	0.002220	-0.003380	0.135069	-0.002257	-0.006809	-0.010014	0.002316	-0.003645
0.107207	-0.000499	-0.007120	-0.008222	0.002563	-0.004749	0.123757	-0.001476	-0.009722	-0.010023	0.002780	-0.004941
0.093456	-0.000037	-0.006432	-0.008004	0.002315	-0.004360	0.109168	-0.000364	-0.008685	-0.009660	0.002328	-0.004694
.	.	.	.	.	.	.	.	.	.	.	.
.	.	.	.	.	.	.	.	.	.	.	.
.	.	.	.	.	.	.	.	.	.	.	.

5-Blade						6-Blade					
C_{Fx}	C_{Fy}	C_{Fz}	C_{Mx}	C_{My}	C_{Mz}	C_{Fx}	C_{Fy}	C_{Fz}	C_{Mx}	C_{My}	C_{Mz}
0.156110	-0.000605	-0.007487	-0.011589	0.005484	-0.006185	0.178301	-0.001422	-0.009956	-0.014315	0.005379	-0.006564
0.152008	-0.000479	-0.005325	-0.011583	0.003780	-0.004608	0.176964	-0.001244	-0.006907	-0.014336	0.003725	-0.004847
0.139559	0.000263	-0.008837	-0.011583	0.004728	-0.006563	0.162988	-0.001064	-0.011835	-0.014380	0.004601	-0.007281
0.124568	0.000471	-0.008855	-0.011318	0.003925	-0.006020	0.145317	-0.000481	-0.011318	-0.013924	0.003744	-0.006903
.	.	.	.	.	.	.	.	.	.	.	.
.	.	.	.	.	.	.	.	.	.	.	.
.	.	.	.	.	.	.	.	.	.	.	.

Table 17. Low-speed factor input and corresponding aerodynamic responses from MATLAB prediction tool.

High-Speed

x_1 - Velocity (m/s)	x_2 - AOI	x_3 - RPM	x_4 - Blades
14.0	26	3935	3
16.5	16	4013	3
18.8	12	4127	3
18.8	8	4147	3
14.0	26	3935	4
16.5	16	4013	4
.	.	.	.
.	.	.	.

Responses

Blade #	C_{Fx}	C_{Fy}	C_{Fz}	C_{Mx}	C_{My}	C_{Mz}
3	0.053422	-0.000308	-0.003792	-0.005994	-0.000400	-0.002151
3	0.027004	0.000105	-0.003767	-0.003042	0.000728	-0.001407
3	0.015075	0.000198	-0.003935	-0.002034	0.000775	-0.001214
3	0.013006	0.000072	-0.003122	-0.001955	0.000617	-0.000802
4	0.059188	-0.000308	-0.004851	-0.006125	0.000370	-0.002192
4	0.031089	0.000105	-0.004346	-0.003924	0.000522	-0.001950
.	.	.	.	.	.	.
.	.	.	.	.	.	.

Table 18. High-speed factor input and corresponding aerodynamic responses from MATLAB prediction tool.

7. DISCUSSION

7.1 APPLICATION OF THE MATLAB PREDICTION TOOL

The obvious advantage of the MATLAB prediction tool is that one would not need to use Design Expert™ to analyze the responses and obtain regression models, the statistical legwork is inherent to the code itself. In addition, the responses obtained from the program use models that are based on empirical data and optimized in the sense that the models reflect the most appropriate fit for the factors and levels chosen and prediction error has been minimized. For practical applications, the prediction tool could be used with a simulation where optimization of a particular response is desired, or comparison of the blade configurations is needed. This would be useful when time or resources do not permit performing an actual wind-tunnel experiment. An example where the prediction tool could be of use is the work done at NASA Langley to develop an algorithm for Rapid Aero Modeling (RAM) intended for UAM applications [34]. The testing process incorporates DOE and RSM theory that guides an experimenter through the modeling process based on the user defined input and test facility chosen. If the test facility were a simulation the test points generated by the RAM process could be used in the prediction tool to obtain the aerodynamic responses needed for performance evaluation.

The prediction tool was used to plot the efficiency and thrust coefficient of trim data for the LA-8 from testing completed at the NASA Langley 12 ft wind tunnel using the 3-blade propeller configuration. The data points represent conditions of the full flight envelope, that is from high incidence angles near hover, through transition, into forward flight (see Table 19). The data was given for conditions of both wings which is shown in Table 19, but this was not taken into consideration, so analysis is shown as if it were for only one wing. The wing angle corresponds to the AOI since the thrust line is the airfoil zero lift line. The single-trim point for a

LA-8 Trim Points			
V_∞, (m/s)	Wing	Wing Angle, (AOI)	RPM
6.25	1	84	5207
6.25	2	58	5201
8.84	1 & 2	51	4149
10.83	1 & 2	40	4092
13.98	1 & 2	26	3935
16.54	1 & 2	16	4013
18.75	1	12	4127
18.75	2	8	4147

Table 19. LA-8 trim data.

wing angle of 26° was also omitted since this was an extrapolation of the high-speed model which had a maximum level of 20° for incidence angle.

Figure 43 shows efficiency plotted versus advance ratio where advance ratio has been calculated using the velocity component V' (red curve) that was introduced in Section 2.4. For comparison, the normal component of advance ratio (blue curve), $J\cos\alpha_i$, was also used. Simmons and Hatke [17] suggest the importance of using both the normal ($J\cos\alpha_i$) and tangential ($J\sin\alpha_i$) component of advance ratio in aerodynamic database development. This led to the consideration of advance ratio that would account for both components of free-stream velocity using Eq. (15). Efficiency was calculated using the ideal power P_i as defined in Eq. (17) and the actual power P_{actual} defined in Eq. (4). The calculations to obtain P_i followed that of [6]. The thrust for a given trim point is solved for from the thrust coefficient predicted by the regression model at that point. This is then used in Eq. (16) to solve for the induced velocity which then allowed the velocity component V' to be calculated. This procedure was done iteratively using MATLAB. This efficiency metric allows comparison of efficiency as a function of AOI as shown in Figure 43. The incidence angle of the corresponding trim point is indicated next to each point in the figure.

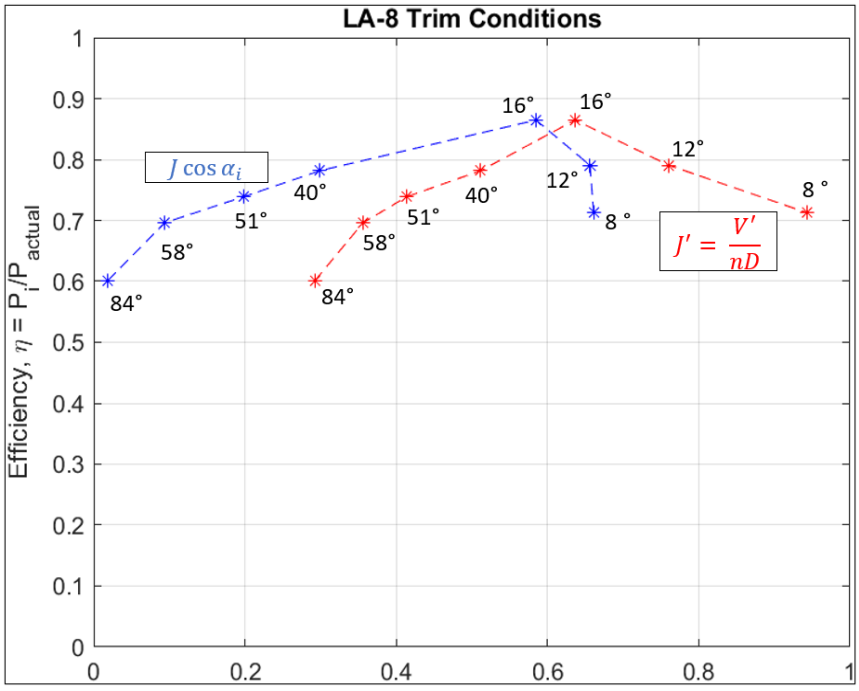

Figure 43. Efficiency vs. advance ratio using velocity component V'(red curve) and efficiency vs. normal component of advance ratio (blue curve).

Thrust coefficient was also compared for the 3-blade configuration at the trimmed data points (Figure 44). The figure again compares the use of the modified advance ratio using V' (red curve) and the use of $J \cos \alpha_i$ (blue curve). While both variations of advance ratio show the same overall trend for the performance metric being analyzed, J'(red curve) displays larger advance ratio values. Using the normal component of advance ratio (blue curve) both Figures 43 and 44 match trends seen in the literature [10, 13, 17]. The use of V' in calculating advance ratio may suggest a better approximation when examining performance metrics since Eq. (15) considers the two components of free stream velocity as well as the induced velocity.

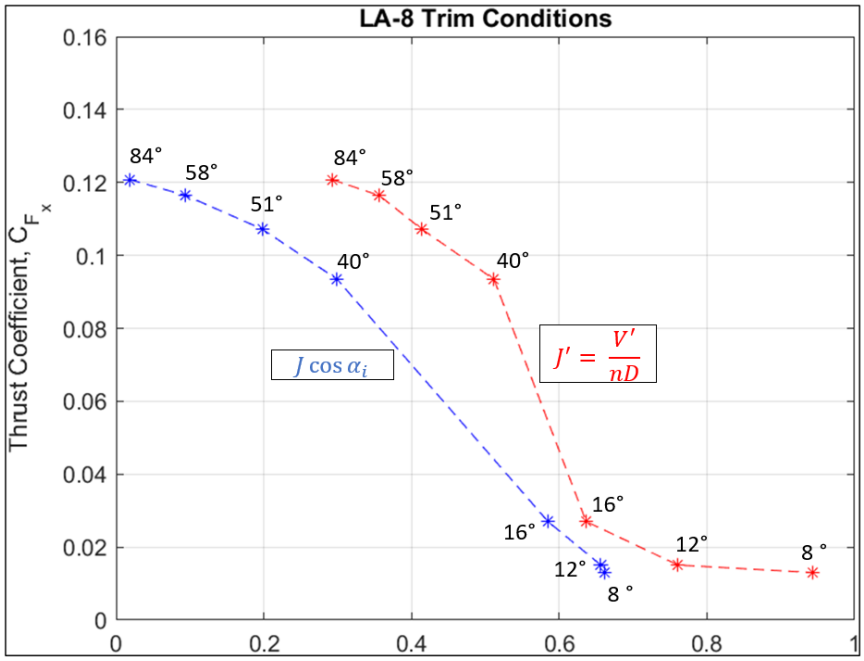

Figure 44. 3-blade thrust coefficient vs. advance ratio using velocity component V' (red curve) and 3-blade thrust coefficient vs. normal component of advance ratio (blue curve).

7.2 DESCRIPTION OF FORCE AND MOMENT COEFFICIENT RESPONSES

7.2.1 LOW-SPEED

While the advantages of having a powerful analysis tool like Design Expert™ is obvious, this can lead to a saturation of information in terms of analyzing the responses. The ambition of this section is to present the overall description of the aerodynamic responses to provide a concise and informative presentation of the trends seen in the data.

Figure 45 shows the effect of RPM, both high and low levels from each experiment, on thrust coefficient for all blade configurations at 0° incidence over the range of velocity. Overall similar trends can be seen for each blade configuration. Higher thrust is observed at lower tunnel velocity before decreasing as tunnel velocity is increased due to an increase in advance ratio. This effect is greater at lower RPM. This is explained by considering the local angle of attack the

propeller blade makes with its relative airflow. In general, the local angle of attack increases as RPM is increased for a given velocity. This creates more lift on the blade and thus translates into more thrust, seen as a higher thrust coefficient. As expected, an increase in blade number was shown to have higher thrust coefficient values – more blades mean more lift force created [35]. This also requires more torque for a given RPM which leads to higher thrust. Confidence intervals at 95% are shown as dashed lines; green dots are actual experimental design points (not shown on all graphs). At AOI of 45° similar trends are seen for all blade configurations but with different slopes (Figure 46). Notably, the decrease in thrust coefficient at increased tunnel velocity is not as severe at an increased incidence angle. The 5-blade propeller also shows the least separation between levels of RPM due to the reduced RPM range.

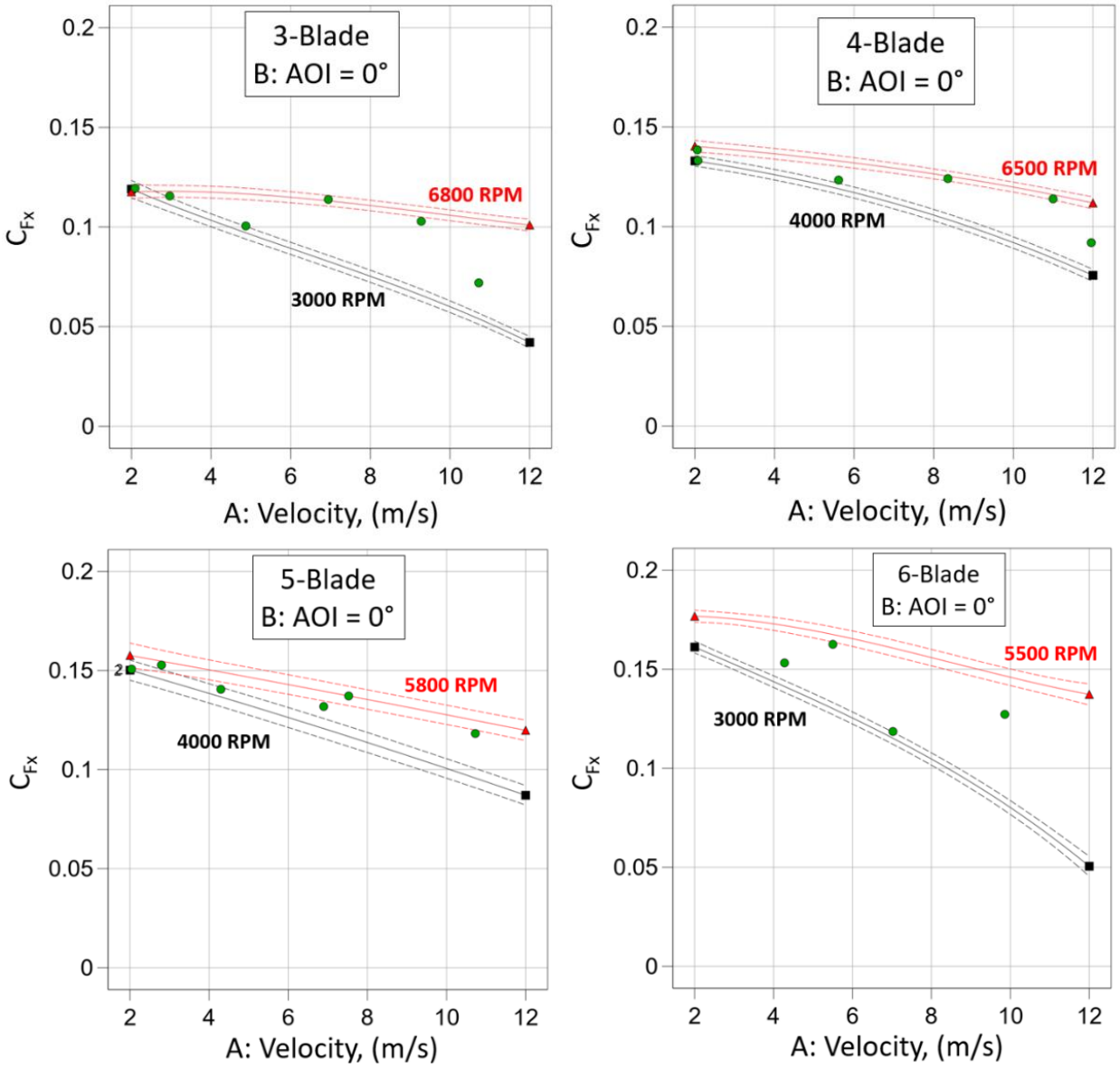

Figure 45. Effect of RPM on thrust coefficient for 3, 4, 5, and 6-blade propellers at 0° incidence over velocity range.

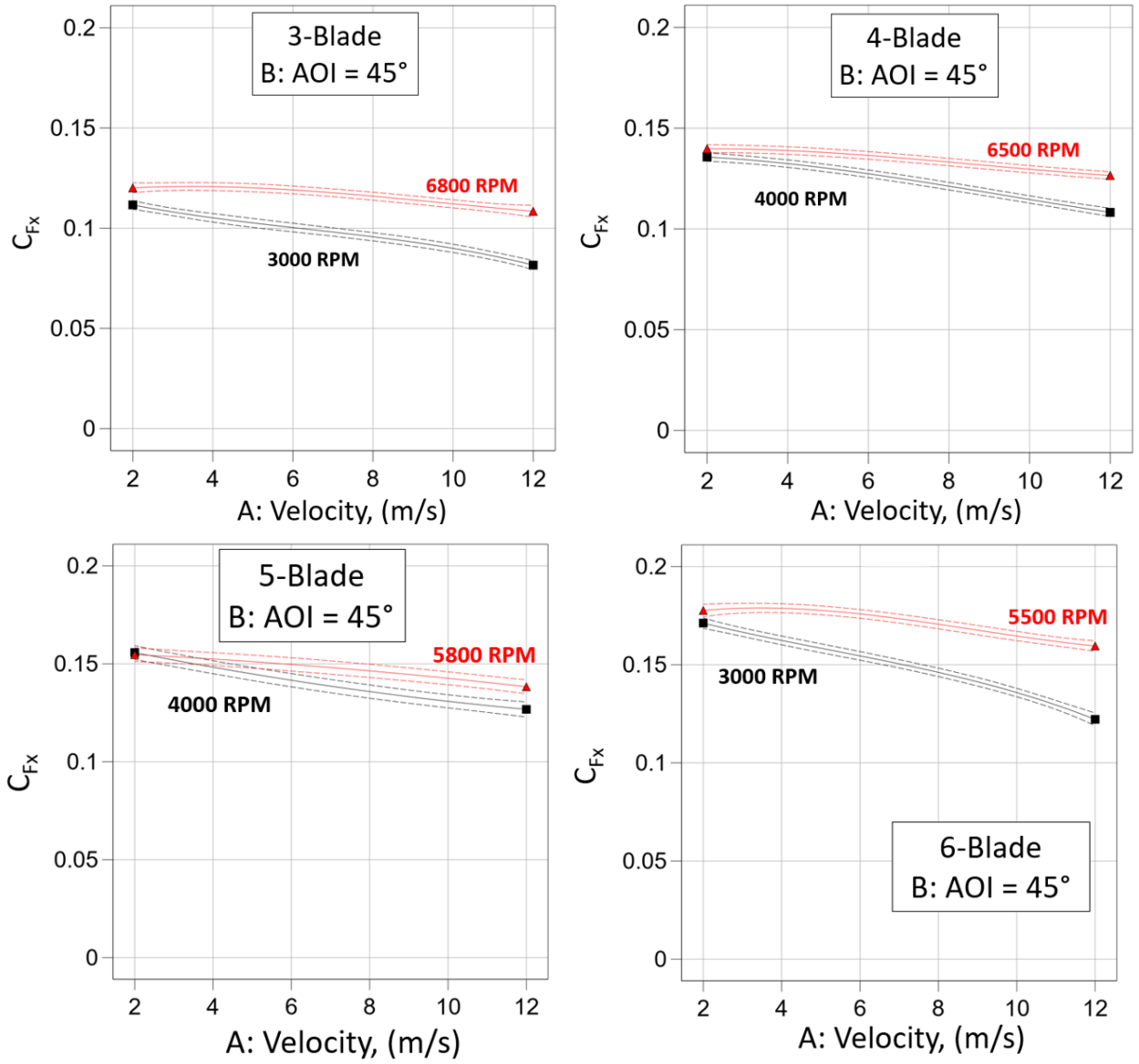

Figure 46. Effect of RPM on thrust coefficient for 3, 4, 5, and 6-blade propellers at 45° incidence over velocity range.

The separation in RPM levels diminishes at increased angle of incidence and mostly disappears at 60° which can be seen in Figure 47**.** At 90° incidence the thrust coefficient trend reverses which shows lower RPM producing higher thrust coefficient at increased tunnel velocities (Figure 48). These trends were similar to results seen in literature [17, 20].

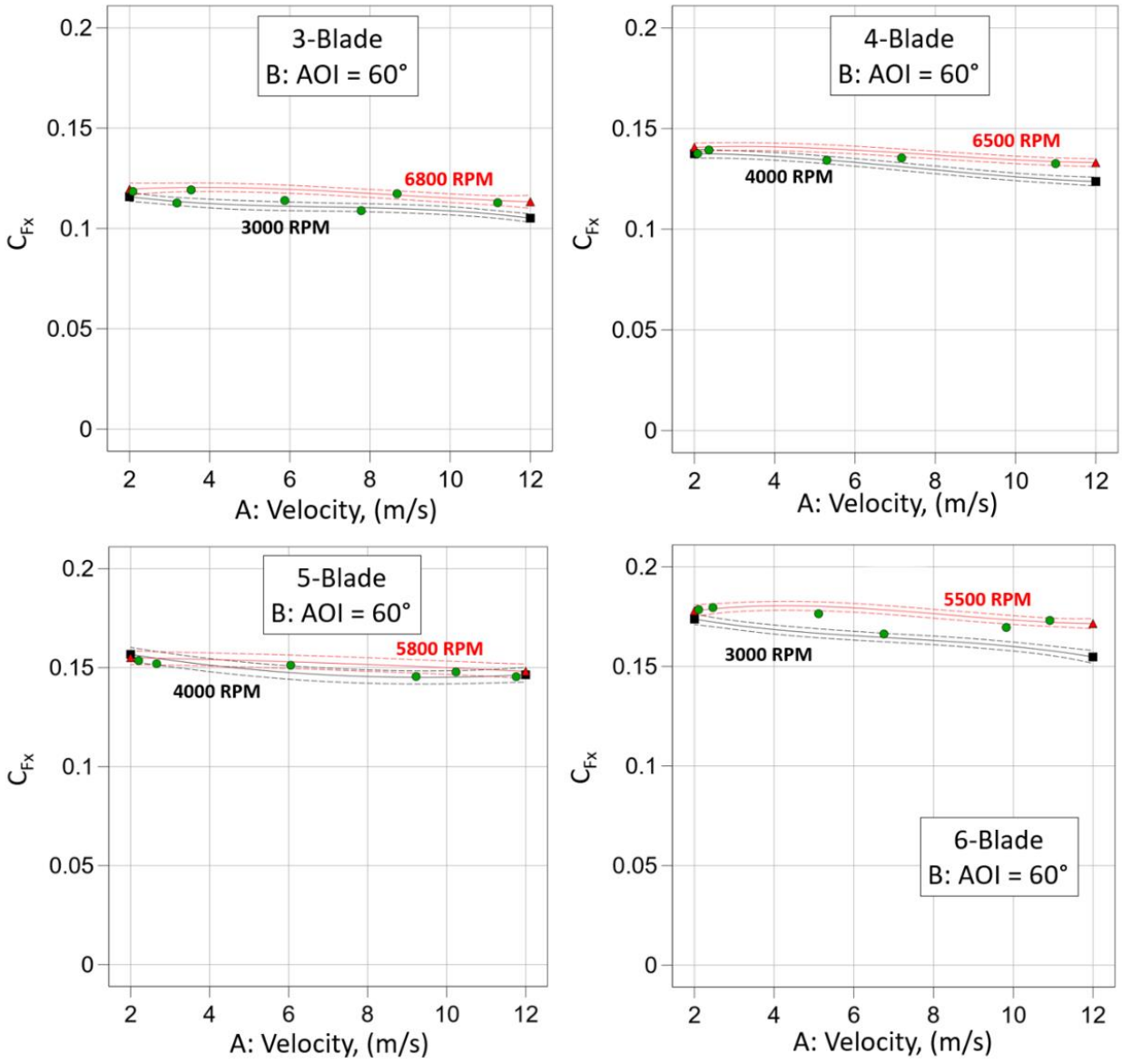

Figure 47. Effect of RPM on thrust coefficient for 3, 4, 5, and 6-blade propellers at 60° incidence over velocity range.

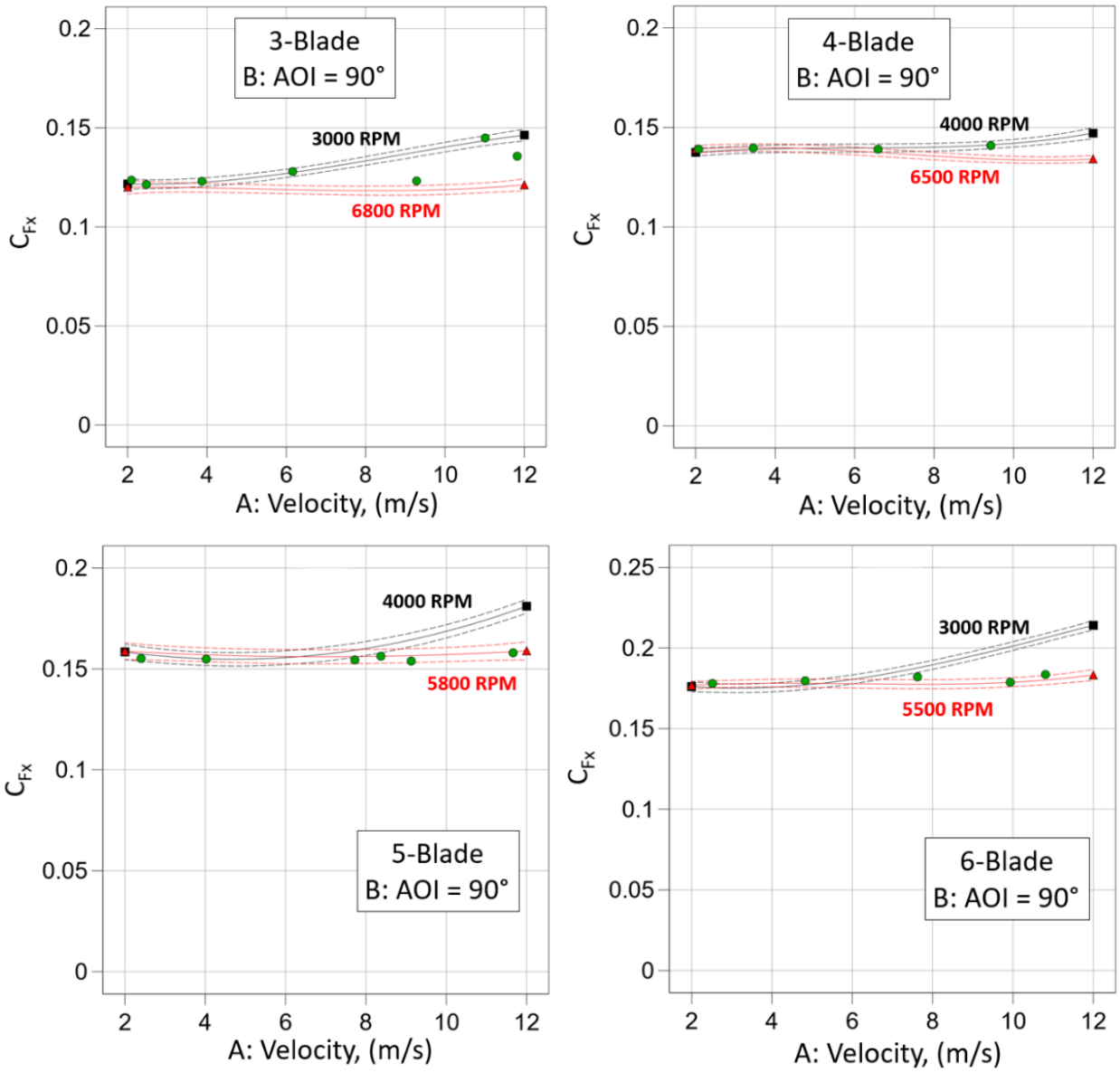

Figure 48. Effect of RPM on thrust coefficient for 3, 4, 5, and 6-blade propellers at 90° incidence over velocity range.

The effect of RPM on torque coefficient is shown for 0° incidence for each blade configuration in Fig. 49. Only one case of incidence is shown since the trend in torque coefficient was directly related to the trends seen in the thrust coefficient, that is if thrust coefficient was seen to decrease (or increase) for a given case then torque coefficient would decrease (or increase) as well, as expected.

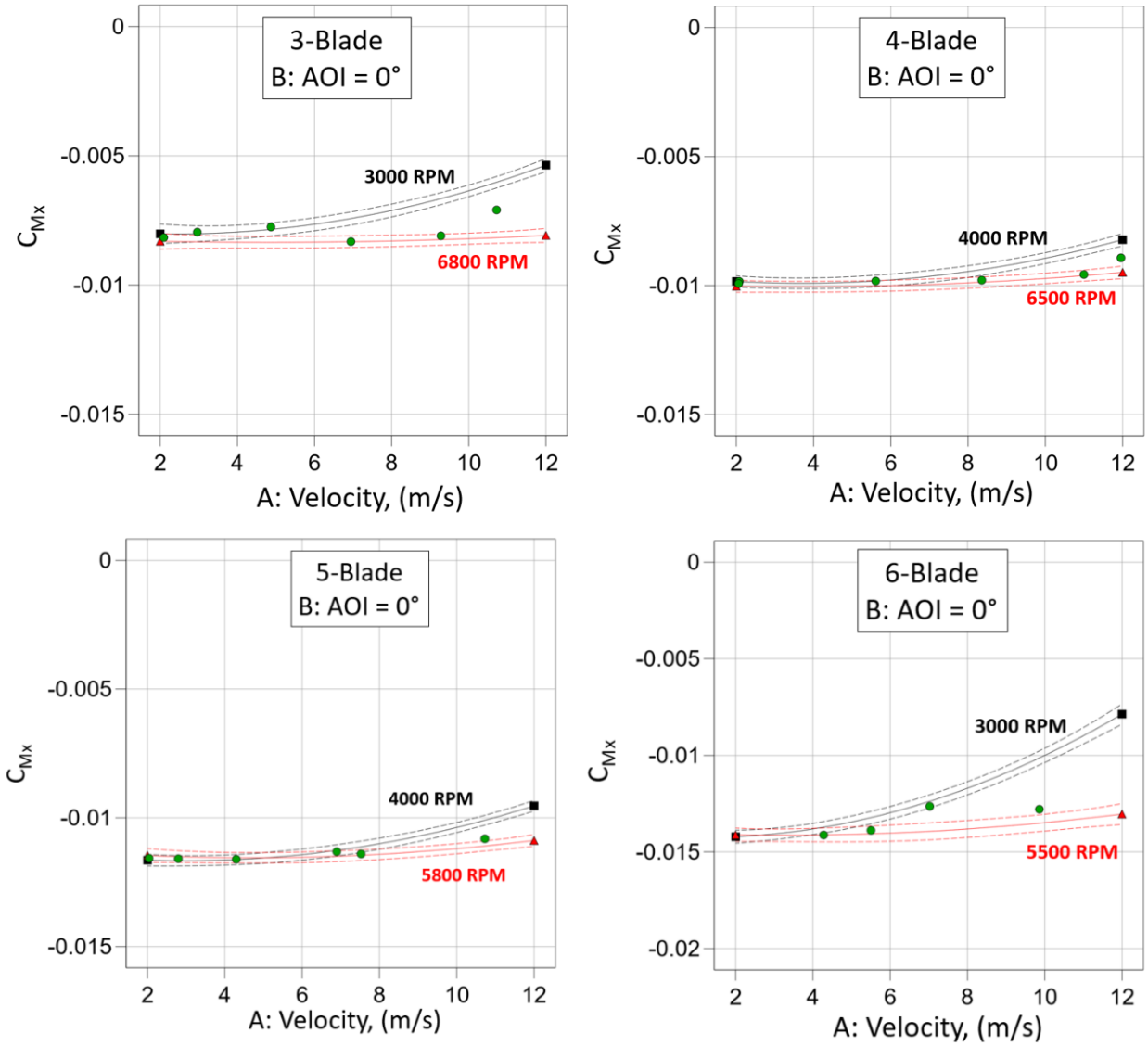

Figure 49. Effect of RPM on torque coefficient for 3, 4, 5, and 6-blade propellers at 0° incidence over velocity range.

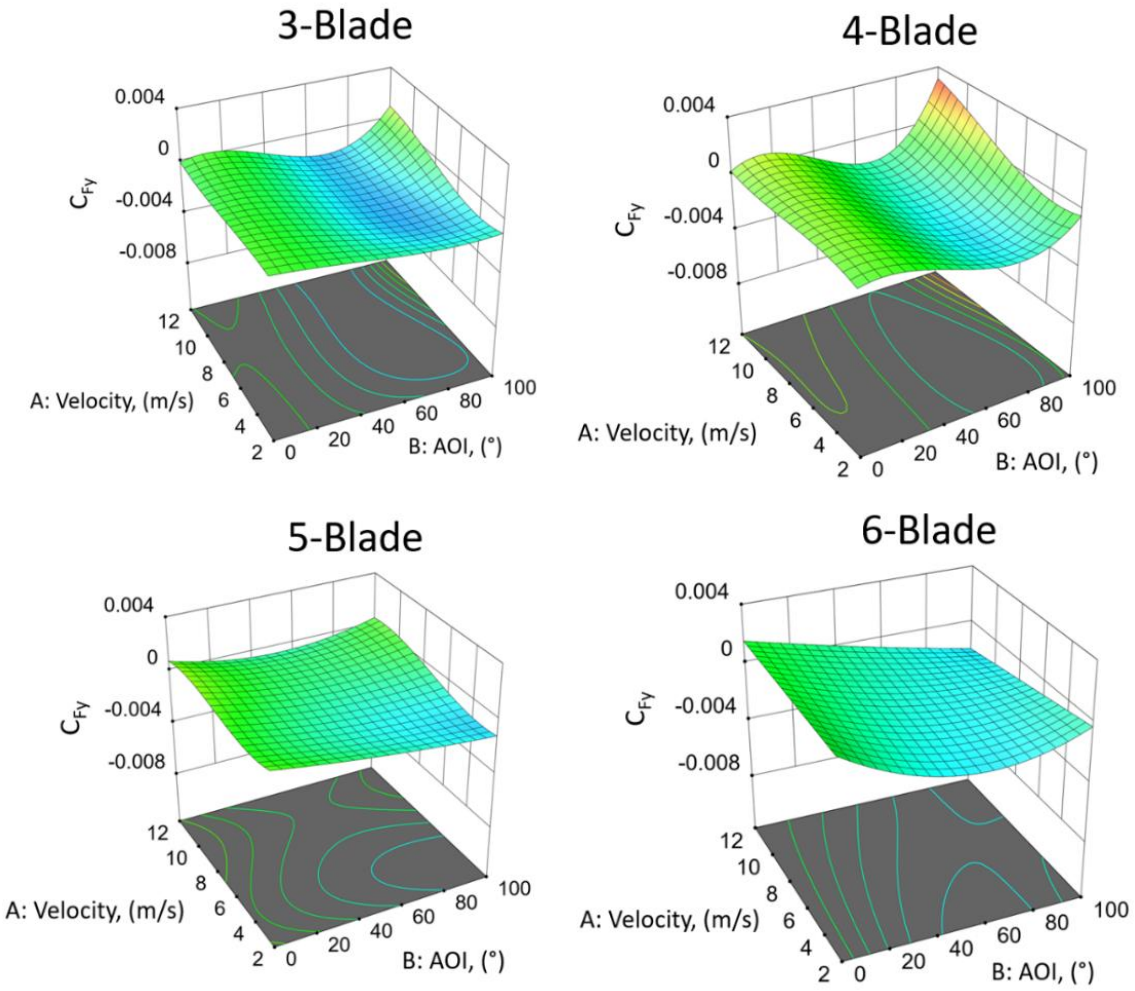

Figure 50. Surface plots of side force coefficient for 3, 4, 5, and 6-blade propellers at 5000 RPM.

Surface plots were chosen to display the responses of the auxiliary forces and moments to better represent the trends through the entire range of incidence angles. A common factor level of 5000 RPM was chosen for comparison between blade configurations. In general, the two auxiliary force coefficients are small compared to the thrust coefficient. Figure 50 shows the side force coefficient was essentially negligible for all incidence angles. The normal force coefficient (Figure 51) is shown to be more significant at nonzero incident angles, increasing in magnitude

at higher tunnel velocities. This force represents a drag force when negative which is essentially the entire range of incidence angles except those very close to zero. Overall, the trends are similar between blade configurations. The minor variations in the side force coefficients could be reasoned to be from the increased noise-to-signal ratio due to the small magnitude of the measured forces.

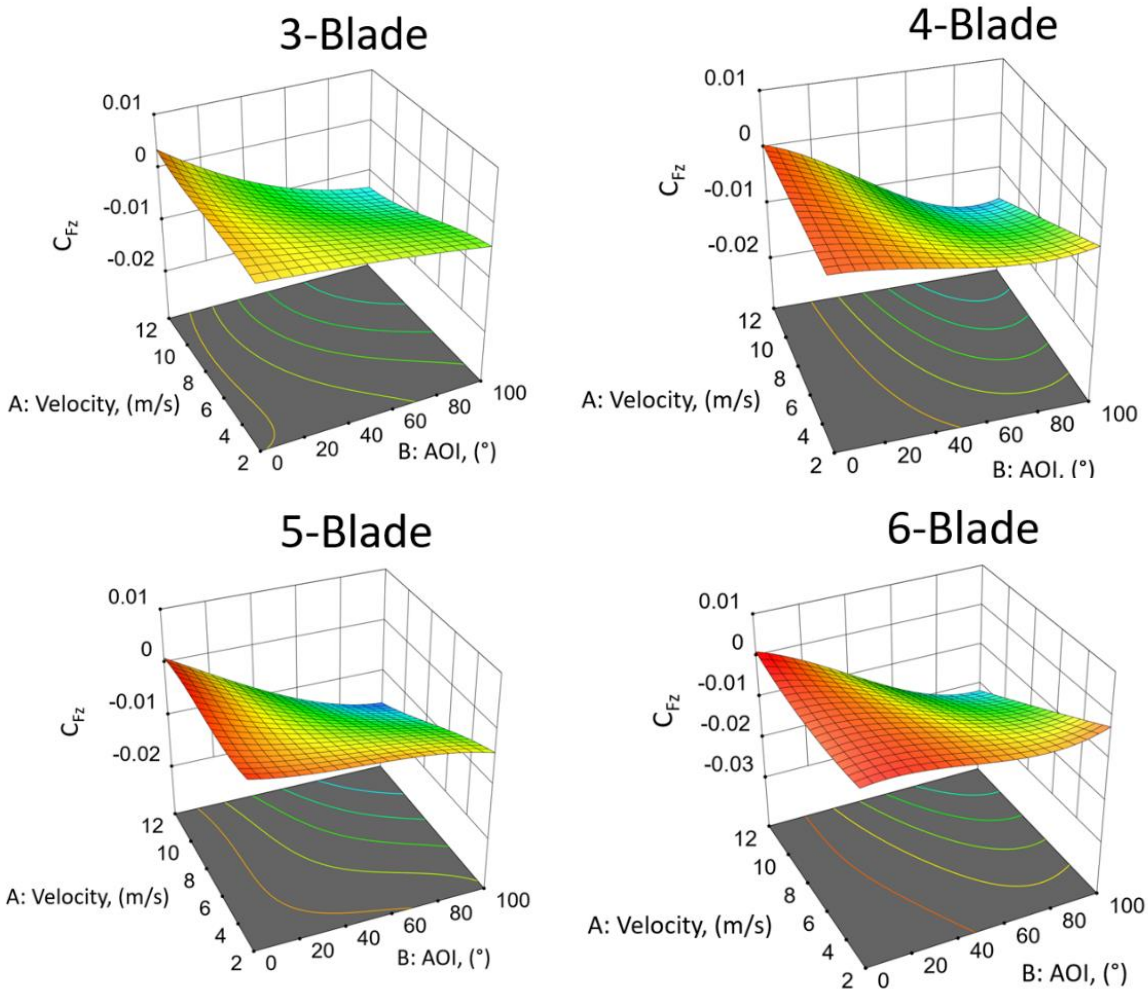

Figure 51. Surface plots of normal force coefficient for 3, 4, 5, and 6-blade propellers at 5000 RPM.

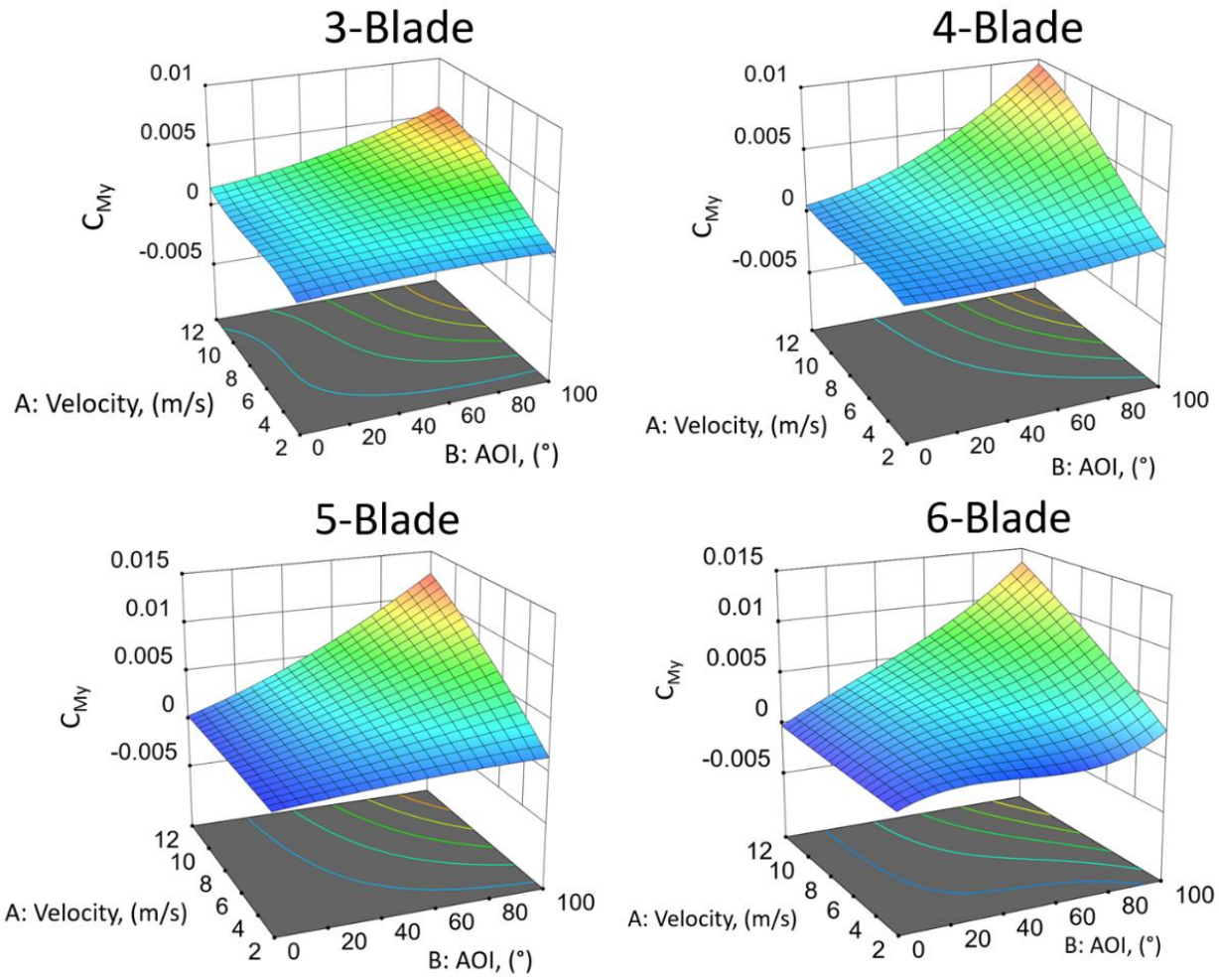

Figure 52. Surface plots of pitching moment coefficient for 3, 4, 5, and 6-blade propellers at 5000 RPM.

The pitching and yawing moment coefficients were found to be of the same order of magnitude as the torque coefficient results at high incidence angles and tunnel velocities for all blade configurations, which can be seen in Figures 52 and 53, respectively. The increase in pitching moment is closer to 90° due to a greater difference in flow velocities through the propeller disk at these angles. The yawing moment coefficients display the same increase in magnitude at high tunnel velocities and incidence angles close to 90°, however, this moment is a result of the uneven lift forces from the advancing and retreating blades [35].

The trends seen in the results of the low-speed experiements matched closely the results described in [17, 20]. A direct comparison of the 3- and 4-blade results are given in [18].

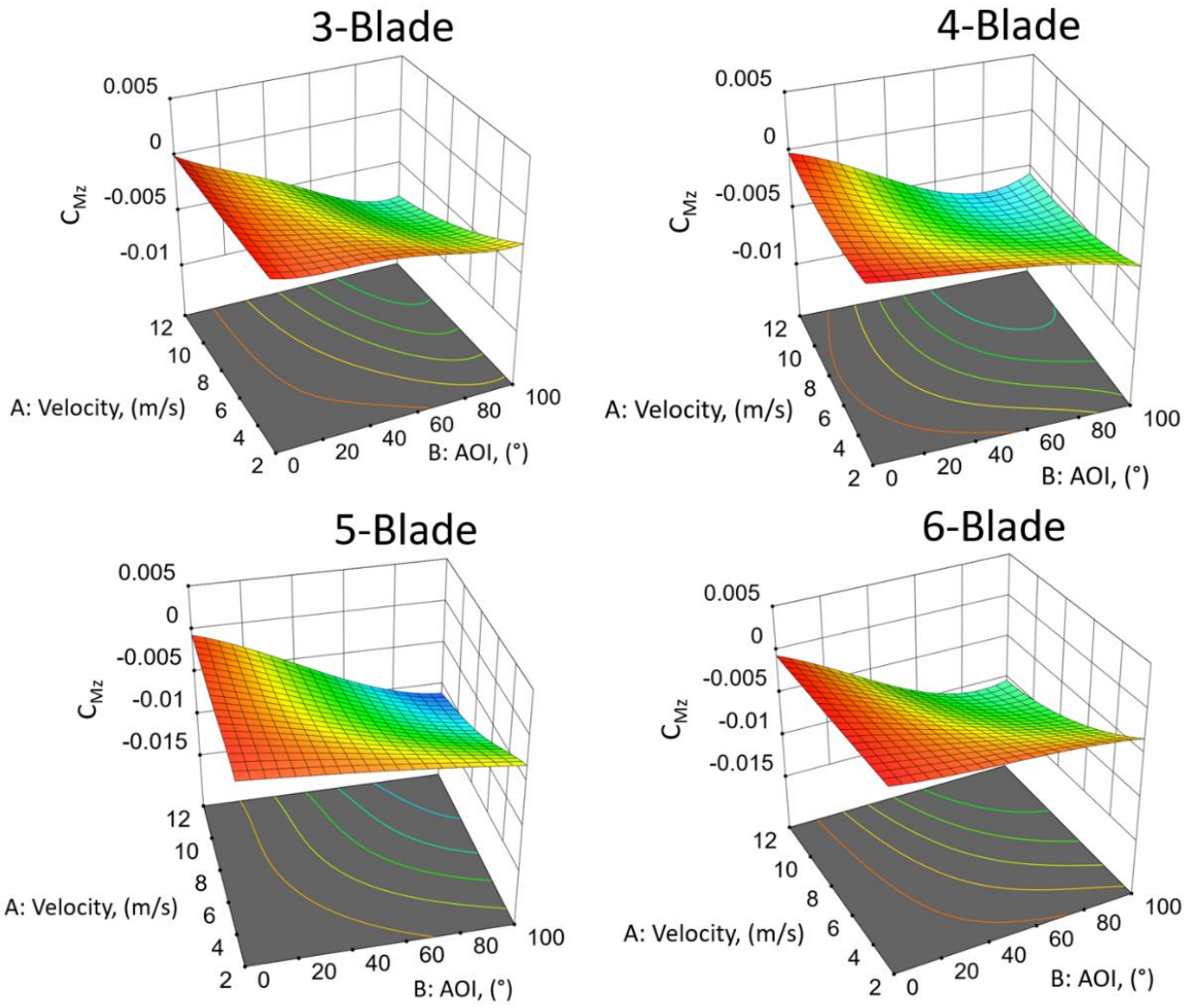

Figure 53. Surface plots of yawing moment coefficient for 3, 4, 5, and 6-blade propellers at 5000 RPM.

7.2.2 HIGH-SPEED

Similar trends were observed for the thrust coefficient in the results of the high-speed experiment. The effect of blade number on the thrust coefficient at 6000 RPM over the range of velocity for incidence angles of 0° and 20° is shown in Figure. 54. Thrust coefficient decreases for all blade configurations as tunnel velocity is increased. This is again because of an increase in advance ratio. Minor increases in thrust coefficient were observed at 20°, particularly for the 5- and 6-blade configuration. At high tunnel velocities close to 30 m/s the difference in thrust coefficient between blade configurations decreases while the 3-blade configuration shows an unexplained minor increase compared to the 4-blade. A low blade loading condition on the folding blades may be to blame. Figure 55 shows the torque coefficient at the same conditions over the range of velocity. Similar to the low-speed experiments, the trends represent a direct relation to the thrust coefficient. The decrease in magnitude of the torque coefficients represent a decrease in the thrust coefficient for each blade configuration.

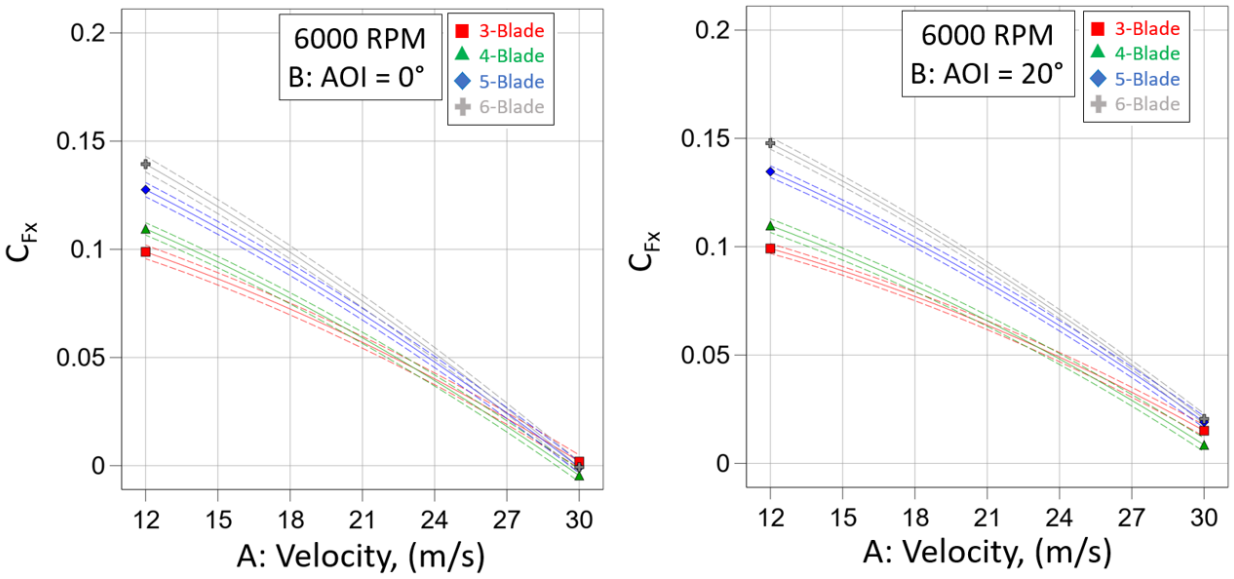

Figure 54. Thrust coefficient for 3, 4, 5, and 6-blade propellers at 6000 RPM and at 0° and 20° incidence over velocity range.

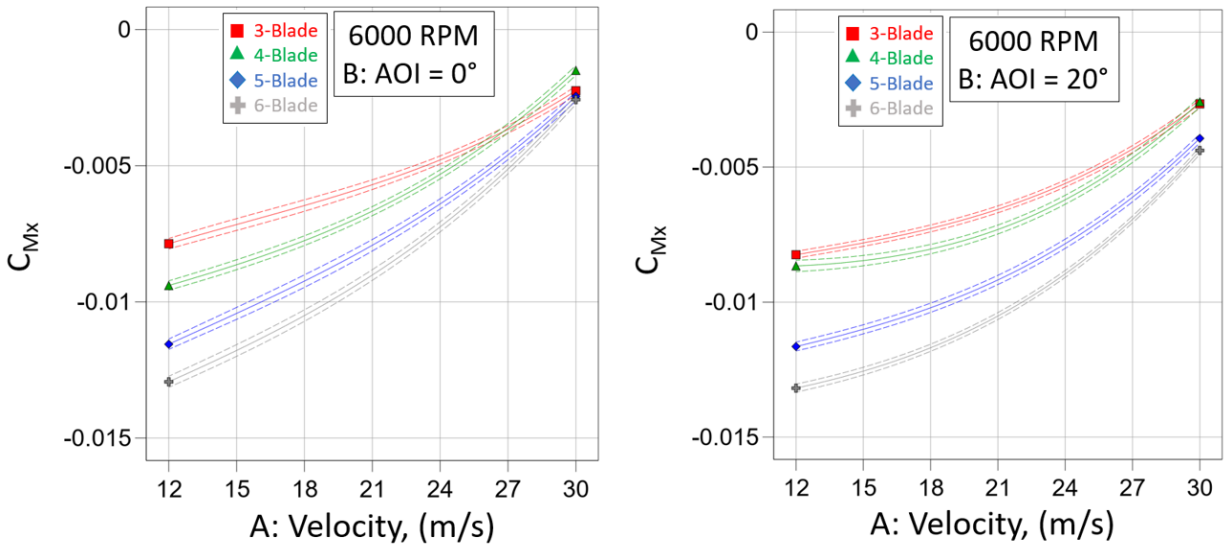

Figure 55. Torque coefficient for 3, 4, 5, and 6-blade propellers at 6000 RPM and at 0° and 20° incidence over velocity range.

Surface plots were again chosen to display the entire range of incidence angle. A factor level of 6000 RPM was chosen so that the complete range of velocity could be examined for each blade configuration; recall the constraints of the design space. Similar to the low-speed responses, the side force coefficient (Figure 56) was essentially negligible compared to the thrust coefficient for all blade configurations. The 5- and 6-blade side force coefficient showed an unexplained opposite sign change with increasing incidence angle compared to the low-speed 5- and 6-blade surface plots. Simmons and Hatke [17] mention a cyclic blade flapping effect due to the folding design of the propellers. The inconsistency in trend could be attributed to the blade flapping and the phenomena could be compounded by increasing the number of blades. The overall responses also are more uniform compared to the low-speed results, which could be reasoned to come from the lower range of incidence angles. The normal force coefficient (Figure 57) is again significant at nonzero angles of incidence. This increase in magnitude, while similar

to the response of the low-speed results, occurs at lower incidence angles. This would suggest the drag force is more significant at higher airspeeds.

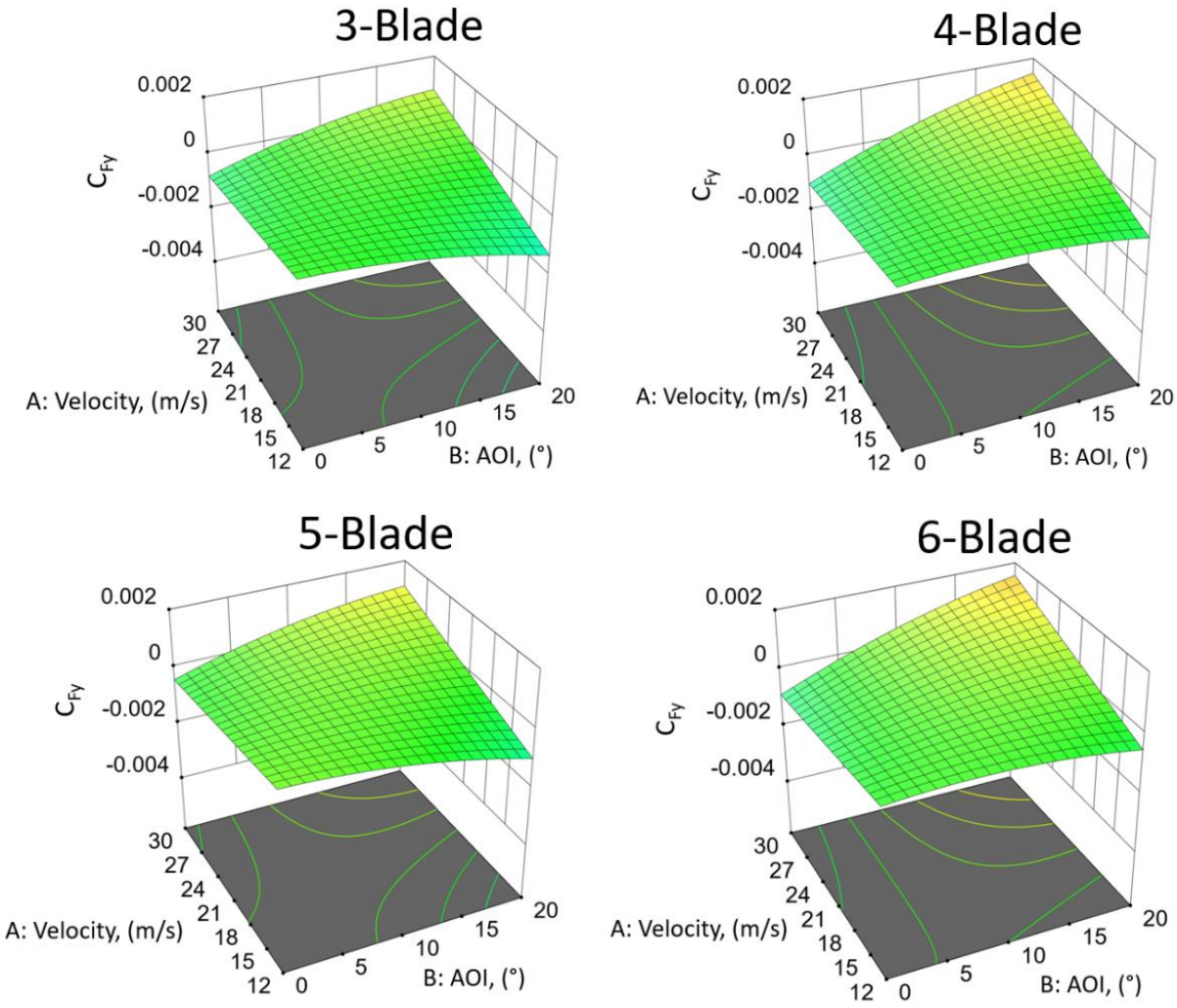

Figure 56. Surface plots of side force coefficient for 3, 4, 5, and 6-blade propellers at 6000 RPM.

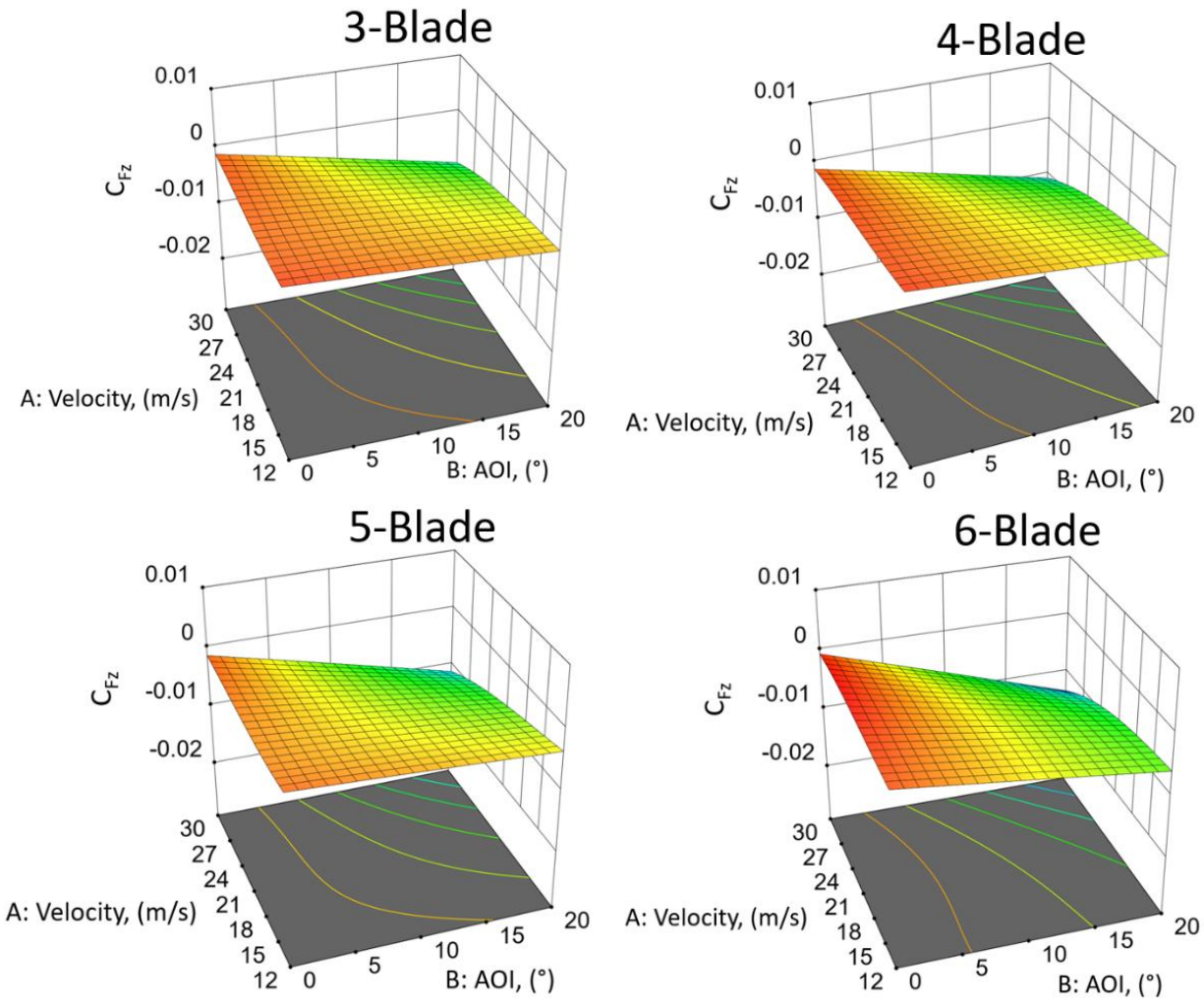

Figure 57. Surface plots of normal force coefficient for 3, 4, 5, and 6-blade propellers at 6000 RPM.

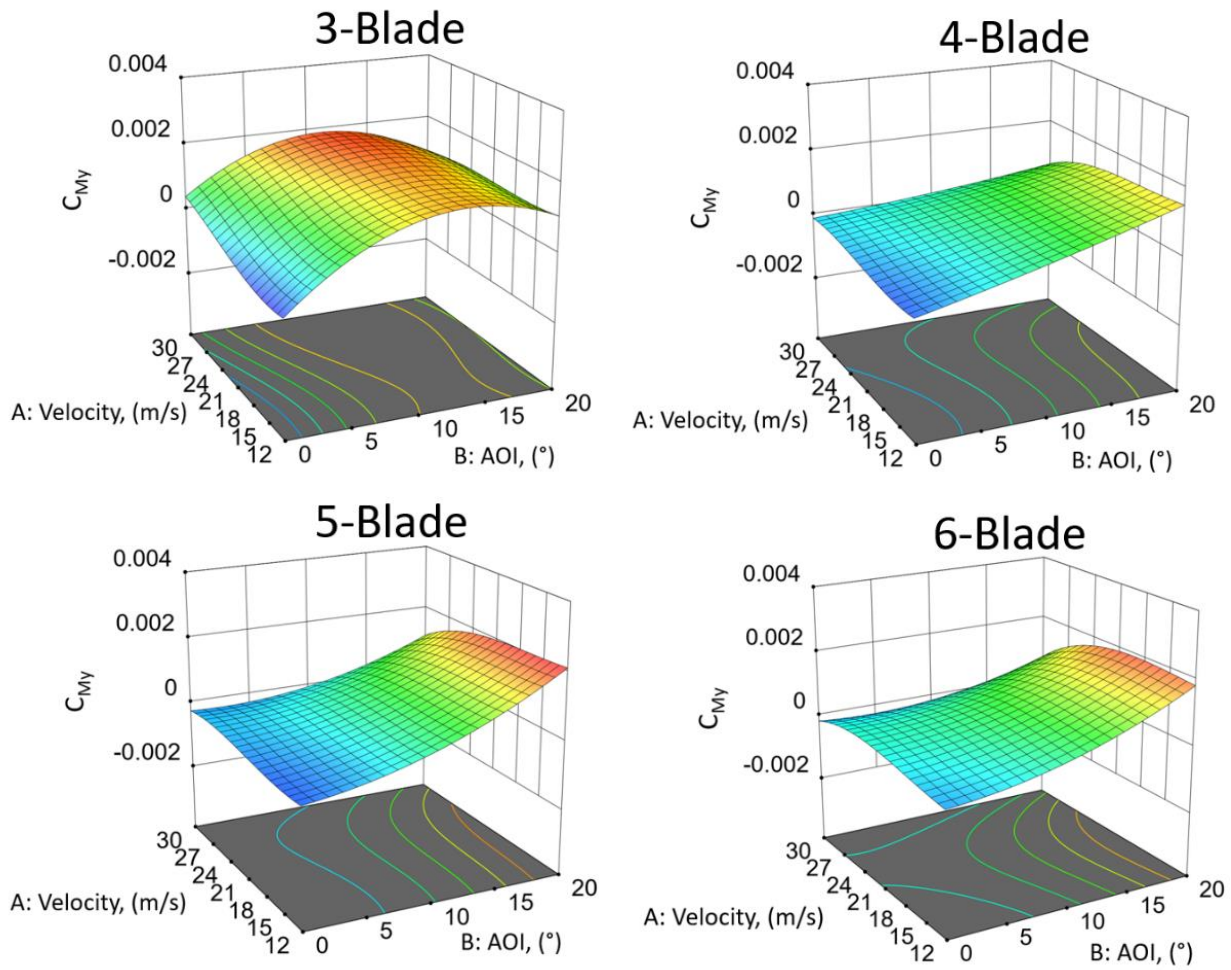

Figure 58. Surface plots of pitching moment coefficient for 3, 4, 5, and 6-blade propellers at 6000 RPM.

Similar to the low-speed responses, the pitching and yawing moment coefficients were shown to be on the same order of magnitude as the torque coefficient at increased tunnel velocities and incidence angles, as seen in Figures 58 and 59, respectively. The pitching moment showed an increase in response at lower incidence angles due to the increased speed, and thus an increased difference in flow velocity through the propeller disk. The 3-blade pitching moment shows a noticeable difference in trend compared to the other blade configurations.

This again could be reasoned to be from an increased noise-to-signal ratio with measuring very small forces. The yawing moment coefficient was shown to be more uniform for all blade configurations. The increase in magnitude follows the same trend as that for the high-speed results which can again be explained by the uneven lift forces from the advancing and retreating blades, though not as large in magnitude due to the lower incidence angles.

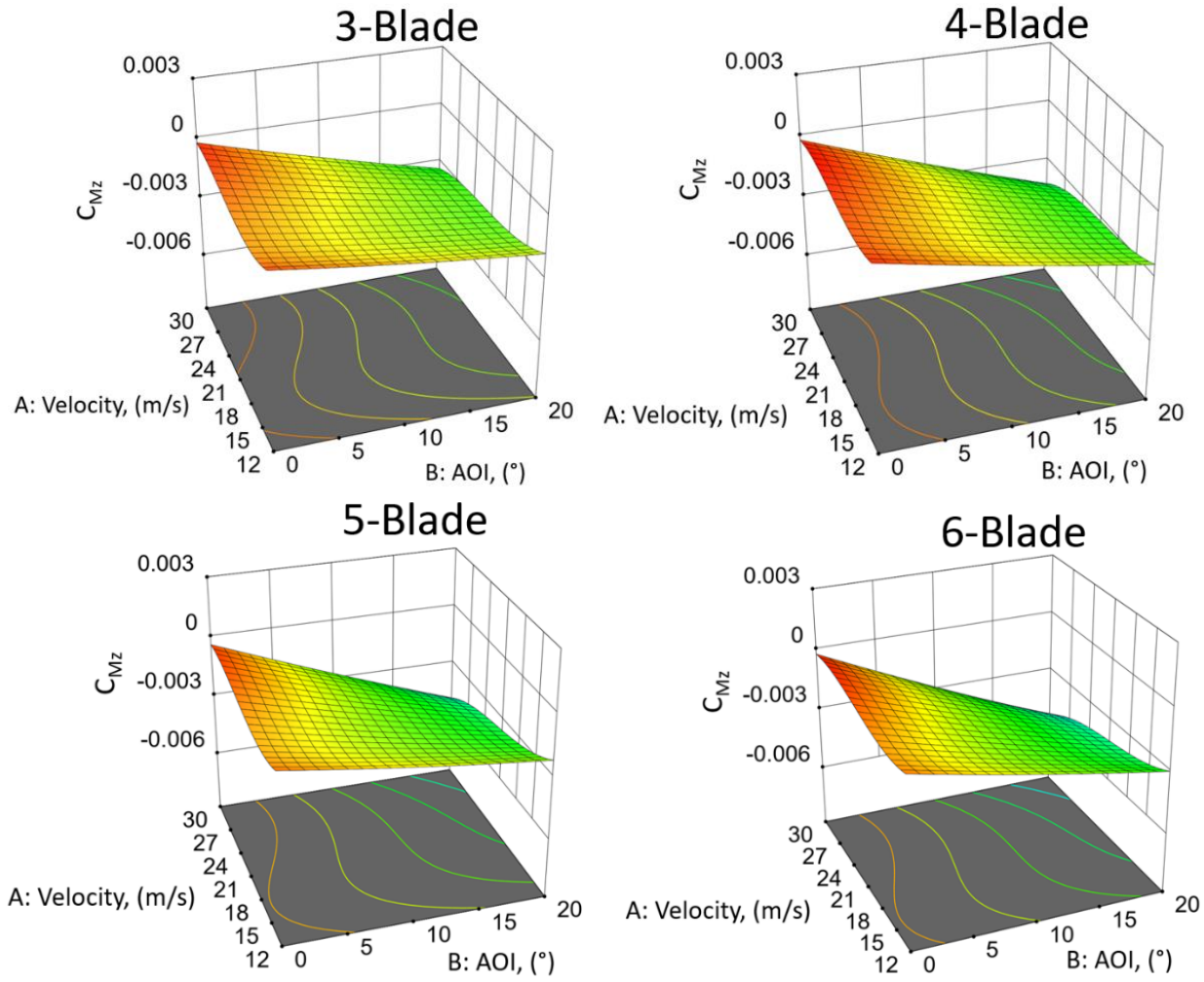

Figure 59. Surface plots of yawing moment coefficient for 3, 4, 5, and 6-blade propellers at 6000 RPM.

8. CONCLUSIONS AND FUTURE WORK

The use of statistical engineering methods has proven to provide adequate models for characterization of the propellers tested at angles of incidence. Using techniques from DOE, experimental efficiency was obtained while still incorporating necessary randomization on constrained factors and minimizing variance. This allowed significant model terms to be estimated with 95% confidence. A re-designed, robust test rig for both the low- and high-speed test sections ensured accurate measurements could be recorded, including proper thermal isolation of the load cell which was important for maintaining overall reliability of the data. The limitations of the power supply reduced the maximum achievable motor speeds, particularly as blade number was increased. The use of a higher rated power supply and motor in future experiments would allow a more consistent range of RPM for comparisons of blade configurations.

Results were compared for each blade configuration. As expected, the comparisons concluded that an increase in blade number increased the thrust coefficient for a given RPM over the velocity range for both low- and high-speed data. While an increase in tunnel velocity decreased thrust coefficient for both high and low levels of RPM, this effect was attenuated as incidence angle was increased. At incidence angles near 90° (low-speed), lower RPM was shown to improve thrust coefficient. Auxiliary forces and moments were compared using surface plots to cover the full range of incidence angles. The side and normal force coefficients were smaller in magnitude compared to the thrust coefficient, while the normal force proved to be more significant than the side force, which was essentially negligible. The pitching and yawing moments were of the same order of magnitude in both low- and high-speed results, overall

showing more significance at higher incidence angles and tunnel velocities. The high-speed responses generally showed the same trends as seen in the low-speed data.

Using the obtained regression models a program was written using MATLAB that provided a tool that could be used externally to statistical analysis software like Design Expert™. The prediction tool affords the user with responses, in the form of aerodynamic coefficients, for the 4-blade configurations tested that can be used for performance evaluation at points of interest. This would afford a user results based on actual empirical data which could be used, for example, in a simulation that has a goal of optimizing performance of a UAM vehicle in particular modes of flight.

Comparative performance analysis could benefit greatly by expanding the lower range of tested RPM's. One scenario is noise reduction. If the LA-8 were fitted with 6-blade propellers, the RPM could be greatly reduced versus the current 3-blade propellers which would lower tip speed and presumably noise. Unfortunately, reviewing the trim points shows required thrust is achieved by the 6-blade propellers well below the tested RPM limits.

While analyzing propellers alone, particularly at high incidence angles, provides great insight into the dynamics of VTOL flight, this is just one aspect of the problem. Further investigation of the complicated interactions of the propellers and wings together are inevitable if a complete understanding is to be obtained. The reliability and effectiveness of using DOE methods in wind tunnel experimentation has proven to be a valuable tool when constraints on factors can significantly increase time and resources needed to collect data. Future experiments involving variation of wing angle or propeller location relative to the wing could take advantage of the techniques used in this project to build a more complete model of responses in the various modes of flight.

REFERENCES

1. Schrank, D., B. Eisele, T. Lomax, *2019 URBAN MOBILITY REPORT*. The Texas A&M Transportation Institute.
2. *Electric VTOL NEWS*, URL: https://evtol.news/aircraft.
3. *Agile Change in Air Force "Agility Prime" Launch Pays Off,* URL: https://evtol.news/news/agile-change-in-air-force-agility-prime-launch-pays-off.
4. *AFWERX Agility Prime Announces "flying car" Military Airworthiness, Infrastructure Milestones*. Air Force Research Laboratory Public Affairs, URL: https://www.af.mil/News/Article-Display/Article/2452683/afwerx-agility-prime-announces-flying-car-military-airworthiness-infrastructure.
5. Maisel, M.D., D.J. Giulianetti, D.C. Dugan, *The History of The XV-15 Tilt Rotor Research Aircraft From Concept to Flight*. The NASA History Series, National Aeronautics and Space Administration, Office of Policy and Plans, NASA History Division, Washington, D.C., 2000.
6. McCormick, Jr., B.W., *Aerodynamics of V/STOL Flight*. 1967, New York: Academic Press, Inc.
7. Harris, F. D., *Introduction to Autogyros, Helicopters, and Other V/STOL Aircraft*. Volume III: Other V/STOL Aircraft. 2015: National Aeronautics and Space Administration.
8. Rothhaar, P.M., P.C. Murphy, B.J. Bacon, I.M. Gregory, J.A. Grauer, R.C. Busan, M.A. Croom, *NASA Langley Distributed Propulsion VTOL Tilt-Wing Aircraft Testing, Modeling, Simulation, Control, and Flight Test Development.* AIAA, 2014 DOI: 10.2514/6.2014-2999.

9. *Uber Air Vehicle Requirements and Missions*. 2020, URL: https://s3.amazonaws.com/uber-static/elevate/Summary+Mission+and+Requirements.pdf.
10. Simmons, B.M., *System Identification for Propellers at High Incidence Angles*. AIAA, 2021 DOI: 10.2514/6.2021-1190.
11. Dantsker, O.D., M. Caccamo, R.W. Deters, M.S. Selig, *Performance Testing of Aero-Naut CAM Folding Propellers*. AIAA, 2020 DOI: 10.2514/6.2020-2762.
12. Johnson, W. *Helicopter Theory*. 1980, New York: Dover Publications, Inc.
13. Yaggy, P.F., V.L. Rogallo, *A Wind-Tunnel Investigation of Three Propellers Through an Angle-Of-Attack Range From 0° to 85°*. Technical Note D-318. 1960: National Aeronautics and Space Administration.
14. Kuhn, R.E., J.W. Draper, *Investigation of the Aerodynamic Characteristics of a Model Wing-Propeller Combination and of the Wing and Propeller Separately at Angles of Attack up to 90°*. Report 1263. 1956: National Advisory Committee for Aeronautics.
15. Felker, F.F., J.S. Light, *Rotor/Wing Aerodynamics Interactions in Hover*. Technical Memorandum 88255. 1986: National Aeronautics and Space Administration.
16. Abrego, A.I., L.E. Olson, E.A. Romander, D.A. Barrows, A.W. Burner, *Blade Displacement Measurement Technique Applied to a Full-Scale Rotor Test*. 2012.
17. Simmons, B.M., D.B. Hatke, *Investigation of High Incidence Angle Propeller Aerodynamics for Subscale eVTOL Aircraft*. TM-20210014010. 2021: National Aeronautics and Space Administration.
18. Stratton, M., D. Landman, *Wind Tunnel Test and Empirical Modeling of Tilt-Rotor Performance for eVTOL Applications*. AIAA, 2021 DOI: 10.2514/6.2021-0834.

19. Busan, R.C., P.C. Murphy, D.B. Hatke, B.M. Simmons, *Wind Tunnel Testing Techniques for a Tandem Tilt-Wing, Distributed Electric Propulsion VTOL Aircraft,* AIAA, 2021 DOI: 10.2514/6.2021-1189.

20. Theys, B., G. Dimitriadis, T. Andrianne, P. Hendrick, J. De Shutter, *Wind Tunnel Testing of a VTOL MAV Propeller in Tilted Operating Mode*. ICUAS, 2014.

21. Furusawa, Y., K. Kitamura, *Unsteady Numerical Simulation on Angle-of-Attack Effects of Tractor-Propeller/Wing and Pusher-Propeller/Wing Interactions*. AIAA, 2020 DOI: 10.2514/6.2020-1030.

22. Koning, W.J.F., *Wind Tunnel Interference Effects on Tiltrotor Testing Using Computational Fluid Dynamics*. 2016: National Aeronautics and Space Administration.

23. Yeo, H., W. Johnson, *Performance and Design Investigation of Heavy Lift Tilt-Rotor with Aerodynamic Interference Effects.* Journal of Aircraft, 2009 DOI: 10.2514/1.40102.

24. Dehaeze, F., C.B. Allen, G.N. Barakos, *The Collaborative Development of New CFD Methods Adapted for Tilt Rotor Aircraft in the HiPerTilt Project*. AIAA, 2017 DOI: 10.2514/6.2017-3919.

25. Montgomery, D., *Design and Analysis of Experiments*. 9th ed. 2017: John Wiley & Sons, Inc.

26. Myers, R.H., D.C. Montgomery, C.M. Anderson-Cook, Response Surface Methodology. 3rd ed. 2009: John Wiley & Sons, Inc.

27. *DesignExpert*. 2021. URL: https://www.statease.com/software/design-expert/.

28. Landman, D, D. Yoder, *Wind Tunnel Balance Calibration with Temperature Using Design Experiments*. AIAA Journal of Aircraft, Vol. 51, No. 3, pp 841-848, 2014, DOI: 10.2514/1.C032416.

29. Landman, D., *Statistical Engineering for Wind Tunnel Testing of Mars Parachute Designs*. AIAA Journal of Aircraft, 2020, https://doi.org/10.2514/1.C035913.

30. Barlow, J.B., W.H. Rae, Jr., A. Pope, *Low-Speed Wind Tunnel Testing*. 3rd ed. 1999: John Wiley & Sons, Inc.

31. Duvall, B.E., *Development and Implementation of a Propeller Test Capability for Gl-10 "Greased Lightning" Propeller Design*. 2016, Old Dominion University.

32. Gudmundsson, S., *General Aviation Aircraft Design*. 1st ed. 2014: Elsevier Inc.

33. Ewald, B.F.R., *Wind Tunnel Wall Correction*. AGARD-AG-336. AGARD, 1998.

34. Murphy, P.C., B.M. Simmons, D.B. Hatke, R.C. Busan, *Rapid Aero Modeling for Urban Air Mobility Aircraft in Wind-Tunnel Tests*. AIAA, 2021 DOI: 10.2514/6.2021-1644.

35. Kermode, A.C., *Mechanics of Flight*. 11th ed. 2006: Pearson Education Limited, Inc.

A: DIAGRAM OF EQUIPMENT LAYOUT

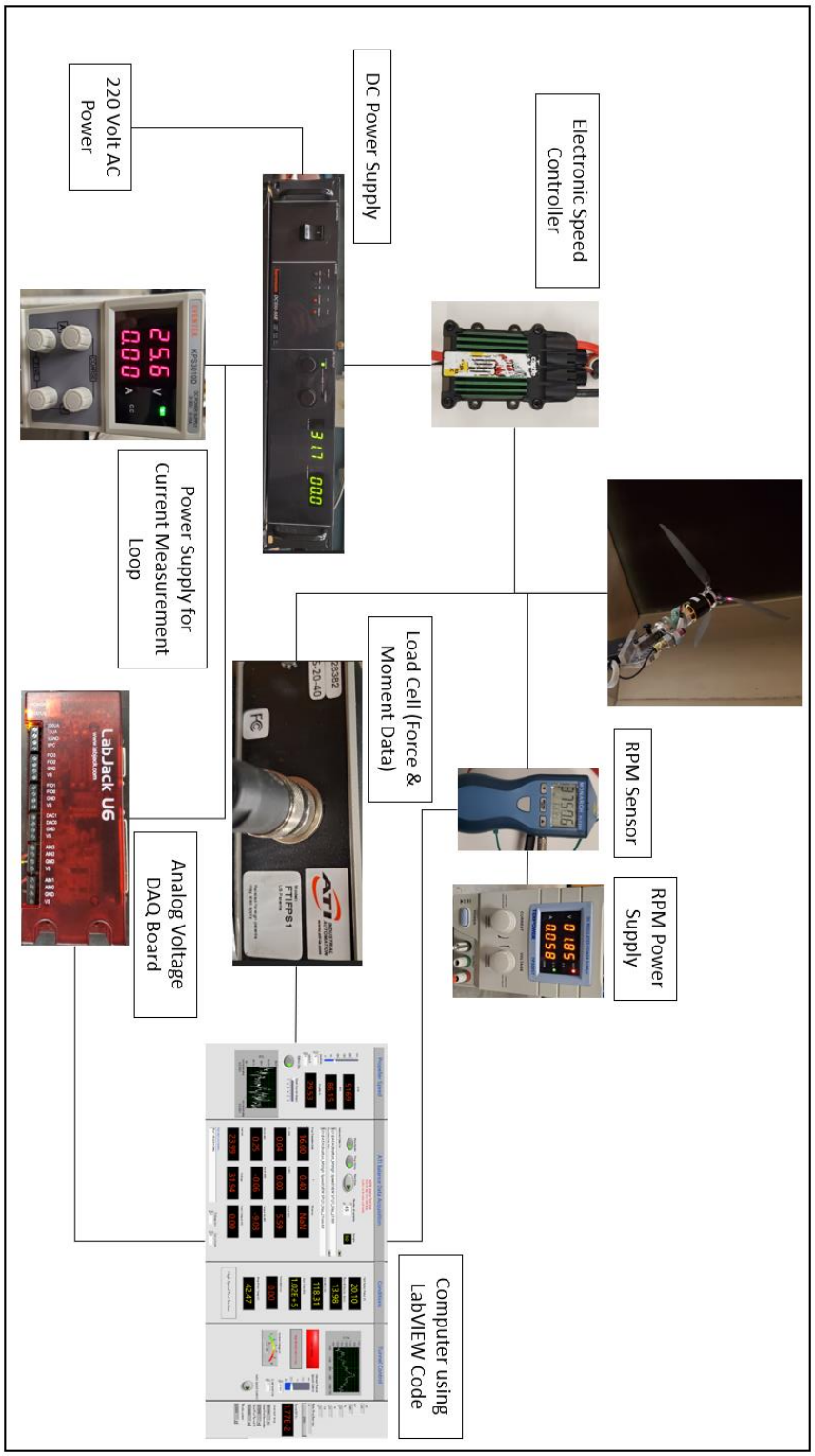

Figure 60. ODU LSWT data acquisition system and equipment layout.

B: MOMENT TRANSFER PROGRAM

```
% Moment Transfer Program
% Michael Stratton
% Fall 2020

clear, clc
format long g

% Importing raw force and moment data
filename = 'C:\Users\mikes\Documents\Academia\Propeller
 Characterization\Tilt Rotor\Test Plans\High Speed\OFAT
 Exploration.xlsx';
F = readmatrix(filename,'Sheet','LabVIEW
 Data','Range','B263:D280')'; % lbf
M = readmatrix(filename,'Sheet','LabVIEW
 Data','Range','E263:G280')'; % in-lb

% Moment arm distance from face of load cell to propeller plane
r12 = [0,0,5.625]'; % in
r_12 = repmat(r12,1,length(F));

% Moment transfer calculation
M_ = M - cross(r_12,F); % in-lb
M_ = M_';

% Writing corrected data to Excel file
writematrix(M_,'C:\Users\mikes\Documents\Academia\Propeller
 Characterization\Tilt Rotor\Test Plans\High Speed\OFAT
 Exploration.xlsx','Sheet','LabVIEW Data','Range','AB263:AD280');
```

Published with MATLAB® R2020b

C: 3-D PRINTED NACELLE

Figure 61. High-speed test rig with 3D-printed nacelle.

D: OFAT TEST MATRIX AND RESPONSES FOR 3-BLADE EXPERIMENT

	Velocity, m/s	RPM	AoA, °	CFx	CFy	CFz	CMx	CMy	CMz
	0.12	4002	0	0.11947	0.00003	0.00004	-0.00822	0.00001	-0.00010
	0.27	5503	0	0.12151	-0.00012	-0.00023	-0.00840	-0.00011	-0.00004
	0.46	6786	0	0.12251	-0.00010	-0.00019	-0.00844	-0.00010	-0.00004
	5.95	4028	0	0.10458	-0.00019	-0.00004	-0.00838	-0.00010	-0.00002
	5.96	5519	0	0.11313	-0.00017	-0.00006	-0.00848	-0.00012	-0.00004
	5.98	6810	0	0.11769	-0.00018	-0.00005	-0.00858	-0.00013	-0.00004
	11.94	4059	0	0.07449	-0.00045	0.00057	-0.00757	0.00010	0.00019
	11.95	5519	0	0.09409	-0.00036	0.00023	-0.00821	-0.00003	0.00009
	11.96	6727	0	0.10333	-0.00033	0.00014	-0.00844	-0.00008	0.00007
	6.01	4013	0	0.10309	-0.00020	0.00015	-0.00832	-0.00007	0.00002
	6.02	5485	0	0.11311	-0.00025	0.00006	-0.00852	-0.00010	0.00001
replicates	6.04	6763	0	0.11684	-0.00024	0.00010	-0.00854	-0.00008	0.00000
	11.94	4044	0	0.07311	-0.00080	0.00093	-0.00753	0.00021	0.00032
	11.95	5485	0	0.09382	-0.00062	0.00044	-0.00826	0.00004	0.00019
	11.96	6902	0	0.10349	-0.00033	0.00033	-0.00842	-0.00001	0.00007
	0.03	3970	20	0.11935	0.00089	0.00003	-0.00828	-0.00004	0.00031
	0.06	5540	20	0.12069	0.00080	0.00004	-0.00836	-0.00007	0.00010
	0.06	6712	20	0.12344	0.00072	0.00030	-0.00856	-0.00024	0.00014
	5.95	4030	20	0.10549	-0.00013	-0.00145	-0.00836	0.00099	-0.00154
	5.96	5502	20	0.11419	-0.00033	-0.00145	-0.00852	0.00085	-0.00120
	5.96	6875	20	0.11771	-0.00058	-0.00149	-0.00852	0.00075	-0.00090
	12.12	4084	20	0.07732	0.00003	-0.00304	-0.00768	0.00112	-0.00247
	12.11	5483	20	0.09596	-0.00047	-0.00234	-0.00828	0.00140	-0.00189
	12.10	6850	20	0.10457	-0.00065	-0.00219	-0.00841	0.00141	-0.00137
	0.00	3936	40	0.12455	0.00049	-0.00131	-0.00877	0.00031	0.00044
	0.01	5476	40	0.12477	0.00048	-0.00159	-0.00881	0.00035	0.00027
	0.01	6781	40	0.12527	0.00046	-0.00194	-0.00888	0.00022	0.00040
	6.01	4062	40	0.11212	-0.00141	-0.00593	-0.00858	0.00101	-0.00282
	6.00	5475	40	0.11717	-0.00126	-0.00431	-0.00854	0.00121	-0.00216
	5.96	6831	40	0.11942	-0.00114	-0.00348	-0.00853	0.00121	-0.00172
	12.01	4045	40	0.09363	-0.00100	-0.00932	-0.00845	0.00150	-0.00484
	11.98	5523	40	0.10676	-0.00177	-0.00693	-0.00861	0.00224	-0.00334
	11.93	6911	40	0.11195	-0.00196	-0.00606	-0.00859	0.00232	-0.00237
	0.01	4012	60	0.12385	0.00046	0.00018	-0.00870	0.00013	0.00006
	0.07	5464	60	0.12658	0.00053	-0.00130	-0.00886	-0.00030	0.00020
	0.15	6756	60	0.12627	0.00065	-0.00036	-0.00883	-0.00018	0.00027
	6.10	4032	60	0.11492	-0.00134	-0.00512	-0.00831	0.00305	-0.00423
	6.07	5526	60	0.11834	-0.00185	-0.00450	-0.00835	0.00230	-0.00312
	6.03	6881	60	0.11931	-0.00187	-0.00388	-0.00836	0.00203	-0.00239
	12.14	4017	60	0.11063	-0.00062	-0.00919	-0.00862	0.00480	-0.00701
	12.10	5526	60	0.11544	-0.00196	-0.00900	-0.00851	0.00417	-0.00478
	12.05	6876	60	0.11634	-0.00253	-0.00823	-0.00845	0.00379	-0.00349
	0.00	3998	80	0.11163	0.00103	0.00096	-0.00791	0.00032	-0.00015
	0.02	5527	80	0.11345	0.00059	-0.00009	-0.00797	-0.00014	-0.00014
	0.12	6932	80	0.11509	0.00056	-0.00011	-0.00804	-0.00027	-0.00010
	6.08	4044	80	0.11983	-0.00050	-0.00654	-0.00844	0.00360	-0.00577
	6.05	5521	80	0.12036	-0.00142	-0.00604	-0.00852	0.00268	-0.00422
	6.03	6913	80	0.12028	-0.00170	-0.00524	-0.00850	0.00232	-0.00328
	12.08	4009	80	0.13573	-0.00040	-0.01405	-0.00841	0.00495	-0.00925
	12.01	5492	80	0.11594	-0.00071	-0.01317	-0.00870	0.00574	-0.00544
	11.98	6936	80	0.11492	-0.00136	-0.01131	-0.00858	0.00513	-0.00391
	0.02	3981	100	0.11578	0.00136	0.00144	-0.00817	0.00035	-0.00008
	0.03	5494	100	0.11851	0.00040	0.00050	-0.00827	-0.00007	0.00009
	0.06	6924	100	0.11882	0.00047	0.00023	-0.00829	-0.00019	0.00016
	5.97	4014	100	0.11852	0.00117	-0.00738	-0.00882	0.00550	-0.00612
	5.94	5501	100	0.11769	-0.00054	-0.00644	-0.00868	0.00395	-0.00412
	5.92	6839	100	0.11881	-0.00141	-0.00582	-0.00861	0.00301	-0.00320
	12.02	4039	100	0.14171	0.00244	-0.00916	-0.01054	0.00723	-0.00670
	11.97	5478	100	0.12439	0.00175	-0.01148	-0.00980	0.00760	-0.00421
	11.93	6720	100	0.11445	0.00084	-0.01160	-0.00923	0.00753	-0.00325

E: LOW-SPEED TEST MATRICES AND RESPONSES

3-Blade Test Matrix and Responses

			ETC	HTC	ETC						
	Group	Run	Factor 1 A:Velocity, m/s	Factor 2 B:AOI, °	Factor 3 C:RPM	Response 1 CF_x	Response 2 CF_y	Response 3 CF_z	Response 4 CM_x	Response 5 CM_y	Response 6 CM_z
Whole Plot	1	1	5.87	60	3704	0.11396	-0.00040	-0.00651	-0.00814	0.00228	-0.00446
	1	2	8.68	60	6222	0.11730	-0.00177	-0.00646	-0.00826	0.00264	-0.00391
	1	3	2.08	60	5254	0.11845	-0.00072	-0.00158	-0.00805	0.00053	-0.00128
	1	4	3.18	60	3006	0.11268	-0.00013	-0.00429	-0.00814	0.00148	-0.00312
	1	5	7.78	60	3009	0.10888	0.00178	-0.01046	-0.00842	0.00234	-0.00686
	1	6	11.19	60	4426	0.11283	-0.00039	-0.01010	-0.00835	0.00356	-0.00642
	1	7	3.54	60	6229	0.11925	-0.00119	-0.00240	-0.00821	0.00095	-0.00184
Whole Plot	2	8	11.25	20	3037	0.05514	0.00101	-0.00407	-0.00648	0.00078	-0.00304
	2	9	3.11	20	6759	0.11909	-0.00025	-0.00019	-0.00828	0.00051	-0.00062
	2	10	1.98	20	5918	0.11806	-0.00008	0.00055	-0.00809	0.00055	-0.00049
	2	11	4.68	20	3169	0.09734	0.00079	0.00306	-0.00788	0.00227	-0.00159
	2	12	5.85	20	5438	0.11140	0.00000	-0.00021	-0.00819	0.00121	-0.00122
	2	13	8.80	20	3972	0.08839	0.00061	0.00021	-0.00781	0.00181	-0.00216
	2	14	11.98	20	6292	0.10019	-0.00003	-0.00151	-0.00816	0.00163	-0.00171
Whole Plot	3	15	6.95	0	6707	0.11383	0.00009	0.00045	-0.00832	0.00013	-0.00012
	3	16	2.96	0	4930	0.11560	0.00019	0.00216	-0.00795	0.00067	-0.00010
	3	17	12.05	0	3098	0.04563	0.00027	0.00649	-0.00540	0.00227	0.00009
	3	18	9.28	0	5730	0.10285	-0.00005	0.00186	-0.00810	0.00062	-0.00003
	3	19	10.72	0	3777	0.07196	-0.00031	0.00516	-0.00710	0.00179	0.00016
	3	20	2.09	0	6481	0.11950	-0.00007	0.00153	-0.00816	0.00048	0.00000
	3	21	4.87	0	3567	0.10054	-0.00016	0.00597	-0.00775	0.00201	0.00011
	3	22	12.01	0	6670	0.10035	-0.00001	0.00156	-0.00808	0.00052	-0.00004
Whole Plot	4	23	1.92	100	5046	0.11851	-0.00086	-0.00269	-0.00810	0.00096	-0.00230
	4	24	3.38	100	6752	0.12015	-0.00109	-0.00344	-0.00829	0.00141	-0.00251
	4	25	7.78	100	4101	0.12673	0.00097	-0.00988	-0.00901	0.00506	-0.00746
	4	26	9.32	100	6724	0.11730	-0.00105	-0.00948	-0.00863	0.00504	-0.00523
	4	27	11.16	100	5625	0.12700	0.00023	-0.01084	-0.00934	0.00592	-0.00674
	4	28	3.27	100	3323	0.11882	-0.00104	-0.00625	-0.00837	0.00214	-0.00457
	4	29	5.99	100	6043	0.11933	-0.00146	-0.00662	-0.00857	0.00298	-0.00448
	4	30	12.08	100	6713	0.12190	-0.00036	-0.01102	-0.00912	0.00611	-0.00559
Whole Plot	5	31	2.05	70	3778	0.11803	-0.00079	-0.00247	-0.00803	0.00074	-0.00208
	5	32	10.01	70	3391	0.12037	0.00007	-0.01324	-0.00838	0.00361	-0.00869
	5	33	12.05	70	3004	0.12146	0.00083	-0.01736	-0.00872	0.00364	-0.01112
	5	34	5.97	70	6774	0.11882	-0.00200	-0.00435	-0.00827	0.00196	-0.00302
	5	35	11.12	70	6437	0.11740	-0.00261	-0.00861	-0.00824	0.00373	-0.00498
	5	36	12.00	70	5570	0.11792	-0.00267	-0.01007	-0.00822	0.00424	-0.00610
	5	37	6.26	70	5102	0.11640	-0.00244	-0.00483	-0.00813	0.00280	-0.00395
Whole Plot	6	38	2.47	90	6216	0.12141	-0.00108	-0.00332	-0.00828	0.00071	-0.00218
	6	39	11.01	90	3029	0.14485	0.00280	-0.01997	-0.00933	0.00311	-0.01249
	6	40	9.29	90	5185	0.12320	-0.00094	-0.01177	-0.00875	0.00443	-0.00721
	6	41	2.10	90	3083	0.12357	-0.00092	-0.00722	-0.00827	-0.00018	-0.00340
	6	42	6.16	90	3156	0.12795	0.00083	-0.01374	-0.00862	0.00278	-0.00830
	6	43	3.88	90	4681	0.12304	-0.00109	-0.00636	-0.00845	0.00131	-0.00386
	6	44	11.82	90	4034	0.13567	0.00091	-0.01610	-0.00910	0.00434	-0.01026
Whole Plot	7	45	6.31	40	6504	0.11719	-0.00094	-0.00304	-0.00837	0.00151	-0.00196
	7	46	10.57	40	5441	0.10625	-0.00097	-0.00503	-0.00829	0.00259	-0.00331
	7	47	10.54	40	6808	0.11032	-0.00125	-0.00457	-0.00824	0.00240	-0.00252
	7	48	12.06	40	3518	0.07955	0.00037	-0.00671	-0.00776	0.00231	-0.00532
	7	49	2.04	40	3136	0.11069	-0.00094	0.00144	-0.00790	0.00192	-0.00091
	7	50	2.04	40	6763	0.11957	-0.00046	-0.00035	-0.00821	0.00060	-0.00062
	7	51	3.20	40	4405	0.11375	-0.00063	-0.00032	-0.00798	0.00155	-0.00139
Whole Plot	8	52	6.93	10	4551	0.10264	0.00034	-0.00116	-0.00814	0.00036	-0.00097
	8	53	2.34	10	3731	0.11394	0.00030	-0.00065	-0.00806	0.00009	-0.00058
	8	54	8.42	10	3112	0.07533	0.00078	-0.00198	-0.00757	0.00011	-0.00145
	8	55	4.11	10	6097	0.11745	-0.00005	-0.00055	-0.00829	0.00023	-0.00050
	8	56	2.58	10	3041	0.10912	-0.00011	0.00015	-0.00803	0.00048	-0.00054
	8	57	11.83	10	4886	0.08596	0.00017	-0.00099	-0.00776	0.00071	-0.00114
	8	58	9.98	10	6522	0.10581	-0.00008	-0.00074	-0.00826	0.00070	-0.00076

4-Blade Test Matrix and Responses

			ETC	HTC	ETC						
			Factor 1	Factor 2	Factor 3	Response 1	Response 2	Response 3	Response 4	Response 5	Response 6
	Group	Run	A:Velocity, m/s	B: AOI, °	C: RPM	CF_x	CF_y	CF_z	CM_x	CM_y	CM_z
Whole Plot	1	1	8.05	40	4971	0.12628	-0.00102	-0.00510	-0.01002	0.00258	-0.00333
	1	2	9.22	40	4048	0.11454	-0.00053	-0.00653	-0.00984	0.00262	-0.00447
	1	3	2.68	40	3979	0.13338	-0.00127	-0.00194	-0.00986	0.00113	-0.00142
	1	4	12.00	40	6468	0.12423	-0.00126	-0.00606	-0.00993	0.00325	-0.00330
	1	5	3.20	40	5761	0.13649	-0.00103	-0.00195	-0.00984	0.00101	-0.00128
	1	6	6.73	40	6296	0.13279	-0.00105	-0.00375	-0.00997	0.00214	-0.00227
Whole Plot	2	7	9.43	90	4725	0.14087	-0.00001	-0.01280	-0.01024	0.00679	-0.00819
	2	8	3.45	90	6271	0.13969	-0.00146	-0.00385	-0.00992	0.00170	-0.00292
	2	9	12.10	90	6368	0.13726	-0.00014	-0.01353	-0.01016	0.00748	-0.00654
	2	10	2.08	90	5650	0.13906	-0.00093	-0.00300	-0.00977	0.00116	-0.00256
	2	11	6.59	90	6373	0.13903	-0.00139	-0.00725	-0.01008	0.00377	-0.00447
	2	12	12.13	90	6187	0.13696	-0.00009	-0.01393	-0.01019	0.00766	-0.00664
Whole Plot	3	13	5.30	60	4371	0.13429	-0.00109	-0.00633	-0.00994	0.00245	-0.00394
	3	14	11.00	60	5539	0.13258	-0.00112	-0.01067	-0.01002	0.00431	-0.00451
	3	15	12.07	60	4538	0.12934	-0.00017	-0.01320	-0.01019	0.00481	-0.00631
	3	16	7.16	60	6183	0.13541	-0.00177	-0.00614	-0.00990	0.00300	-0.00325
	3	17	2.08	60	5014	0.13757	-0.00059	-0.00193	-0.00983	0.00077	-0.00163
	3	18	2.36	60	6436	0.13932	-0.00096	-0.00204	-0.00987	0.00065	-0.00128
Whole Plot	4	19	11.07	20	4594	0.10162	0.00042	-0.00344	-0.00943	0.00119	-0.00255
	4	20	9.76	20	6144	0.12066	-0.00013	-0.00250	-0.00982	0.00139	-0.00163
	4	21	1.97	20	4300	0.13584	-0.00043	-0.00112	-0.00993	0.00022	-0.00066
	4	22	11.80	20	6540	0.11617	-0.00008	-0.00295	-0.00967	0.00150	-0.00172
	4	23	4.96	20	5150	0.12959	-0.00045	-0.00177	-0.00989	0.00079	-0.00119
	4	24	1.97	20	6418	0.13915	-0.00029	-0.00082	-0.00993	0.00014	-0.00050
	4	25	12.07	20	4070	0.08619	0.00053	-0.00407	-0.00885	0.00114	-0.00289
Whole Plot	5	26	11.40	80	4044	0.14043	-0.00148	-0.01991	-0.01042	0.00543	-0.00737
	5	27	10.18	80	6492	0.13493	-0.00223	-0.01274	-0.01015	0.00473	-0.00339
	5	28	1.99	80	4268	0.13983	-0.00448	-0.00623	-0.01011	-0.00090	-0.00125
	5	29	4.97	80	5293	0.13892	-0.00340	-0.00834	-0.01019	0.00175	-0.00289
	5	30	5.84	80	4014	0.13909	-0.00404	-0.01294	-0.01039	0.00219	-0.00414
Whole Plot	6	31	5.61	0	4507	0.12336	0.00049	0.00138	-0.00982	0.00061	-0.00029
	6	32	2.06	0	5803	0.13848	0.00053	0.00059	-0.00992	0.00023	-0.00027
	6	33	11.00	0	6193	0.11393	0.00045	0.00058	-0.00957	0.00025	-0.00024
	6	34	2.08	0	4055	0.13312	0.00052	0.00134	-0.00984	0.00049	-0.00027
	6	35	11.96	0	4659	0.09197	0.00039	0.00172	-0.00893	0.00075	-0.00017
	6	36	8.36	0	6476	0.12412	0.00025	0.00057	-0.00979	0.00024	-0.00019
Whole Plot	7	37	11.01	100	6423	0.12863	0.00170	-0.01325	-0.01015	0.00896	-0.00361
	7	38	9.02	100	4250	0.14030	0.00282	-0.01315	-0.01072	0.00886	-0.00568
	7	39	1.99	100	4032	0.13423	-0.00026	-0.00322	-0.00970	0.00183	-0.00307
	7	40	8.09	100	5762	0.13028	0.00086	-0.01111	-0.01007	0.00703	-0.00411
	7	41	11.75	100	5032	0.14234	0.00333	-0.01439	-0.01092	0.00992	-0.00454
	7	42	2.10	100	6482	0.13550	-0.00162	-0.00301	-0.00960	0.00140	-0.00244
	7	43	3.76	100	4770	0.13530	-0.00076	-0.00507	-0.00988	0.00312	-0.00368
Whole Plot	8	44	6.13	10	4141	0.11852	0.00012	-0.00126	-0.00981	0.00044	-0.00096
	8	45	12.08	10	5602	0.10536	0.00028	-0.00172	-0.00935	0.00065	-0.00112
	8	46	2.77	10	6459	0.13819	-0.00010	-0.00092	-0.00993	-0.00003	-0.00038
	8	47	5.47	10	6239	0.13205	-0.00019	-0.00098	-0.00992	0.00030	-0.00057
	8	48	8.87	10	5312	0.11571	-0.00026	-0.00148	-0.00969	0.00048	-0.00086
	8	49	10.72	10	4038	0.08998	-0.00017	-0.00205	-0.00899	0.00029	-0.00114
	8	50	2.10	10	4717	0.13643	-0.00059	-0.00075	-0.00993	-0.00004	-0.00019

5-Blade Test Matrix and Responses

			ETC	HTC	ETC						
	Group	Run	Factor 1 A:Velocity, m/s	Factor 2 B:AOI, °	Factor 3 C:RPM	Response 1 CF_x	Response 2 CF_y	Response 3 CF_z	Response 4 CM_x	Response 5 CM_y	Response 6 CM_z
Whole Plot	1	1	8.37	90	5348	0.15632	0.00003	-0.00993	-0.01171	0.00820	-0.00788
	1	2	11.67	90	5605	0.15797	0.00026	-0.01465	-0.01181	0.01056	-0.00964
	1	3	4.03	90	4515	0.15485	-0.00069	-0.00481	-0.01149	0.00415	-0.00473
	1	4	7.72	90	4016	0.15447	0.00176	-0.01042	-0.01156	0.00951	-0.00994
	1	5	2.40	90	5701	0.15517	-0.00028	-0.00258	-0.01150	0.00232	-0.00307
	1	6	9.13	90	5785	0.15388	0.00023	-0.01055	-0.01162	0.00836	-0.00767
	1	7	12.00	90	4654	0.16428	-0.00005	-0.01616	-0.01202	0.01152	-0.01133
Whole Plot	2	8	1.90	70	4006	0.15889	-0.00228	-0.00455	-0.01175	0.00006	-0.00184
	2	9	7.96	70	4319	0.15671	-0.00166	-0.01188	-0.01185	0.00501	-0.00719
	2	10	12.12	70	4052	0.16123	-0.00092	-0.01825	-0.01223	0.00737	-0.01039
	2	11	4.79	70	5656	0.15540	-0.00024	-0.00488	-0.01157	0.00275	-0.00414
	2	12	2.09	70	5402	0.15680	-0.00115	-0.00238	-0.01158	0.00091	-0.00168
	2	13	10.55	70	4852	0.15563	-0.00130	-0.01331	-0.01176	0.00655	-0.00811
	2	14	4.55	70	4094	0.15365	-0.00236	-0.00644	-0.01165	0.00319	-0.00439
Whole Plot	3	15	6.05	60	5129	0.15119	0.00064	-0.00471	-0.01150	0.00415	-0.00505
	3	16	11.76	60	4430	0.14544	0.00168	-0.01093	-0.01179	0.00739	-0.00889
	3	17	9.23	60	4009	0.14554	0.00194	-0.00878	-0.01175	0.00672	-0.00820
	3	18	10.24	60	5658	0.14781	0.00085	-0.00738	-0.01157	0.00656	-0.00650
	3	19	2.20	60	5770	0.15357	0.00164	-0.00013	-0.01143	0.00173	-0.00254
	3	20	12.06	60	5279	0.14505	0.00111	-0.00989	-0.01167	0.00741	-0.00770
	3	21	2.66	60	4782	0.15197	0.00058	-0.00009	-0.01136	0.00260	-0.00286
	4	22	3.37	100	5029	0.15635	-0.00087	-0.00548	-0.01161	0.00281	-0.00398
Whole Plot	4	23	6.99	100	4731	0.15644	-0.00007	-0.01125	-0.01175	0.00818	-0.00831
	4	24	5.59	100	5584	0.15715	-0.00078	-0.00799	-0.01174	0.00498	-0.00538
	4	25	11.12	100	5184	0.16383	0.00125	-0.01544	-0.01245	0.01185	-0.00990
	4	26	2.12	100	4559	0.15540	-0.00079	-0.00373	-0.01157	0.00234	-0.00327
	4	27	10.48	100	4251	0.17385	0.00169	-0.01458	-0.01286	0.01225	-0.01085
	4	28	3.23	100	4093	0.15799	-0.00146	-0.00555	-0.01172	0.00337	-0.00415
	4	29	12.02	100	3997	0.19118	0.00311	-0.01619	-0.01358	0.01263	-0.01182
	5	30	2.19	40	4198	0.15490	-0.00090	-0.00186	-0.01171	0.00092	-0.00132
Whole Plot	5	31	6.98	40	5690	0.14689	0.00132	-0.00397	-0.01166	0.00300	-0.00369
	5	32	9.21	40	5298	0.14062	-0.00054	-0.00613	-0.01167	0.00350	-0.00400
	5	33	12.05	40	5782	0.13491	0.00044	-0.00638	-0.01148	0.00434	-0.00472
	5	34	5.54	40	4559	0.14556	-0.00145	-0.00393	-0.01171	0.00269	-0.00269
	5	35	2.11	40	5114	0.15489	-0.00026	-0.00111	-0.01159	0.00091	-0.00123
	5	36	3.25	40	5577	0.15381	0.00019	-0.00103	-0.01159	0.00173	-0.00207
	6	37	12.11	0	4023	0.08795	0.00081	0.00161	-0.00956	0.00072	-0.00035
Whole Plot	6	38	4.30	0	4133	0.14053	0.00000	0.00063	-0.01161	0.00021	-0.00014
	6	39	7.53	0	5668	0.13716	0.00250	0.00121	-0.01140	0.00044	-0.00112
	6	40	2.04	0	4166	0.15074	0.00112	0.00170	-0.01157	0.00058	-0.00056
	6	41	10.73	0	5196	0.11823	0.00148	0.00161	-0.01081	0.00060	-0.00070
	6	42	2.80	0	5272	0.15278	0.00141	0.00129	-0.01159	0.00043	-0.00069
	6	43	6.90	0	4740	0.13185	0.00125	0.00192	-0.01132	0.00071	-0.00067
	6	44	12.05	0	5617	0.11529	0.00193	0.00137	-0.01072	0.00054	-0.00088
Whole Plot	7	45	9.02	10	4012	0.11051	-0.00065	-0.00154	-0.01086	0.00072	-0.00104
	7	46	10.75	10	4253	0.10372	0.00012	-0.00139	-0.01048	0.00090	-0.00139
	7	47	10.04	10	5743	0.12823	0.00128	-0.00023	-0.01119	0.00134	-0.00161
	7	48	7.43	10	5316	0.13701	-0.00039	-0.00166	-0.01151	0.00052	-0.00088
	7	49	4.56	10	5785	0.15021	0.00024	-0.00092	-0.01168	0.00038	-0.00083
	7	50	12.06	10	4844	0.10643	-0.00081	-0.00233	-0.01052	0.00054	-0.00105
	7	51	2.74	10	4544	0.15084	-0.00166	-0.00114	-0.01172	0.00003	0.00003
Whole Plot	8	52	1.99	20	5666	0.15398	0.00278	0.00144	-0.01155	0.00124	-0.00185
	8	53	4.48	20	5099	0.14757	0.00092	-0.00103	-0.01165	0.00131	-0.00183
	8	54	6.81	20	4169	0.12964	0.00105	-0.00221	-0.01147	0.00158	-0.00261
	8	55	11.49	20	5517	0.12249	0.00138	-0.00299	-0.01108	0.00203	-0.00293
	8	56	2.84	20	4055	0.14726	0.00050	-0.00060	-0.01172	0.00104	-0.00144
	8	57	11.65	20	4076	0.09840	0.00168	-0.00380	-0.01030	0.00162	-0.00362
	8	58	9.38	20	4750	0.12317	0.00045	-0.00250	-0.01122	0.00192	-0.00258

6-Blade Test Matrix and Responses

			ETC	HTC	ETC						
	Group	Run	Factor 1 A:Velocity, m/s	Factor 2 B:AOI, °	Factor 3 C:RPM	Response 1 CF_x	Response 2 CF_y	Response 3 CF_z	Response 4 CM_x	Response 5 CM_y	Response 6 CM_z
Whole Plot	1	1	7.05	10	4357	0.14852	0.00038	-0.00119	-0.01378	0.00086	-0.00145
	1	2	10.98	10	5435	0.14000	0.00013	-0.00257	-0.01326	0.00065	-0.00146
	1	3	1.95	10	3869	0.17119	-0.00034	-0.00130	-0.01410	-0.00013	-0.00047
	1	4	11.55	10	3056	0.06870	0.00085	-0.00493	-0.00937	0.00017	-0.00233
	1	5	10.01	10	3444	0.10633	0.00006	-0.00352	-0.01211	0.00018	-0.00171
	1	6	3.06	10	4590	0.17090	-0.00051	-0.00119	-0.01409	0.00013	-0.00054
	1	7	11.56	10	5010	0.12892	0.00056	-0.00160	-0.01287	0.00109	-0.00168
Whole Plot	2	8	9.13	100	4129	0.18880	-0.00125	-0.01845	-0.01540	0.01216	-0.01118
	2	9	12.10	100	5081	0.19060	-0.00283	-0.02243	-0.01576	0.01295	-0.00977
	2	10	7.33	100	3037	0.19162	0.00231	-0.01741	-0.01542	0.01108	-0.01234
	2	11	4.33	100	3488	0.17488	-0.00098	-0.00766	-0.01428	0.00707	-0.00726
	2	12	12.02	100	3032	0.23079	0.00828	-0.02229	-0.01802	0.01535	-0.01698
	2	13	2.88	100	5376	0.17785	-0.00058	-0.00447	-0.01405	0.00336	-0.00392
	2	14	5.91	100	4938	0.17716	-0.00039	-0.00984	-0.01425	0.00701	-0.00764
Whole Plot	3	15	10.91	100	3366	0.21447	0.00634	-0.01830	-0.01676	0.01541	-0.01482
	3	16	11.84	40	3251	0.12158	0.00140	-0.01522	-0.01308	0.00282	-0.00868
	3	17	9.31	40	3013	0.13317	0.00053	-0.01332	-0.01378	0.00222	-0.00747
	3	18	3.48	40	3917	0.17299	-0.00160	-0.00412	-0.01445	0.00184	-0.00235
	3	19	6.52	40	5442	0.16988	-0.00067	-0.00514	-0.01417	0.00310	-0.00338
	3	20	5.00	40	3112	0.15594	0.00054	-0.00658	-0.01438	0.00232	-0.00466
	3	21	9.11	40	4708	0.15686	-0.00035	-0.00778	-0.01405	0.00396	-0.00510
	4	22	2.04	40	3080	0.16974	-0.00097	-0.00287	-0.01435	0.00105	-0.00189
Whole Plot	4	23	6.75	60	3263	0.16629	0.00038	-0.01114	-0.01446	0.00547	-0.00793
	4	24	5.12	60	4990	0.17647	-0.00074	-0.00705	-0.01418	0.00282	-0.00490
	4	25	10.92	60	5384	0.17309	-0.00155	-0.01359	-0.01428	0.00614	-0.00742
	4	26	12.09	60	4830	0.17139	-0.00096	-0.01629	-0.01448	0.00691	-0.00882
	4	27	2.11	60	4547	0.17853	-0.00196	-0.00444	-0.01412	0.00029	-0.00202
	4	28	9.83	60	3899	0.16960	-0.00049	-0.01675	-0.01464	0.00566	-0.00916
	4	29	2.46	60	5464	0.17959	-0.00190	-0.00436	-0.01414	0.00033	-0.00197
	5	30	10.93	70	3051	0.17646	0.00099	-0.02718	-0.01529	0.00592	-0.01378
Whole Plot	5	31	12.09	70	3834	0.18082	-0.00012	-0.02234	-0.01487	0.00805	-0.01257
	5	32	2.62	70	5097	0.17928	-0.00208	-0.00405	-0.01419	0.00100	-0.00254
	5	33	3.49	70	3088	0.17322	-0.00464	-0.01111	-0.01456	0.00137	-0.00402
	5	34	12.08	70	5457	0.17643	-0.00238	-0.01674	-0.01451	0.00746	-0.00881
	5	35	8.12	70	5193	0.17692	-0.00309	-0.01218	-0.01441	0.00544	-0.00648
	5	36	2.32	70	3577	0.17489	-0.00397	-0.00618	-0.01425	0.00064	-0.00232
	6	37	5.40	70	4264	0.17605	-0.00350	-0.01034	-0.01433	0.00357	-0.00530
Whole Plot	6	38	1.85	90	5421	0.17769	-0.00223	-0.00465	-0.01404	0.00138	-0.00300
	6	39	2.52	90	4327	0.17803	-0.00078	-0.00475	-0.01405	0.00254	-0.00387
	6	40	4.83	90	5442	0.17968	-0.00139	-0.00750	-0.01427	0.00412	-0.00524
	6	41	7.62	90	3612	0.18214	0.00162	-0.01531	-0.01460	0.01023	-0.01187
	6	42	1.96	90	3061	0.17600	-0.00324	-0.00705	-0.01430	0.00133	-0.00299
	6	43	10.81	90	4714	0.18359	-0.00001	-0.01883	-0.01469	0.01173	-0.01185
	6	44	9.93	90	5424	0.17873	-0.00098	-0.01578	-0.01446	0.01001	-0.00948
Whole Plot	7	45	8.75	20	5269	0.15355	0.00055	-0.00339	-0.01397	0.00197	-0.00263
	7	46	3.77	20	5438	0.17400	-0.00001	-0.00145	-0.01430	0.00103	-0.00139
	7	47	6.67	20	3791	0.14502	0.00115	-0.00260	-0.01388	0.00187	-0.00305
	7	48	11.48	20	4260	0.12124	0.00160	-0.00443	-0.01279	0.00206	-0.00386
	7	49	2.76	20	3218	0.16116	-0.00009	-0.00018	-0.01439	0.00168	-0.00145
	7	50	2.01	20	5109	0.17678	0.00003	-0.00066	-0.01419	0.00059	-0.00092
	7	51	12.03	20	5400	0.13659	0.00066	-0.00372	-0.01327	0.00241	-0.00306
Whole Plot	8	52	12.06	0	3836	0.09753	0.00068	0.00002	-0.01141	0.00009	-0.00029
	8	53	4.28	0	3544	0.15322	0.00085	-0.00014	-0.01412	-0.00005	-0.00043
	8	54	1.98	0	3032	0.16264	0.00149	-0.00061	-0.01427	-0.00024	-0.00062
	8	55	5.50	0	5085	0.16258	0.00144	-0.00161	-0.01388	-0.00049	-0.00061
	8	56	1.95	0	5461	0.17644	0.00133	-0.00160	-0.01391	-0.00047	-0.00054
	8	57	9.86	0	4400	0.12726	0.00162	-0.00166	-0.01279	-0.00037	-0.00061
	8	58	7.03	0	3089	0.11858	0.00248	-0.00228	-0.01264	-0.00044	-0.00083

F: GLAUERT'S METHOD EQUATIONS FOR VELOCITY CORRECTIONS

Ratio of the uncorrected and corrected stream velocities $$\lambda = \frac{V}{V_c} \quad \text{(F.1)}$$

Blockage ratio $$\alpha = \frac{A_p}{C} \quad \text{(F.2)}$$

Thrust coefficient $$\tau = \frac{T}{\rho A_p V^2} \quad \text{(F.3)}$$

Ratio of streamtube area to propeller area $$\sigma = \frac{A_1}{A_p} \quad \text{(F.4)}$$

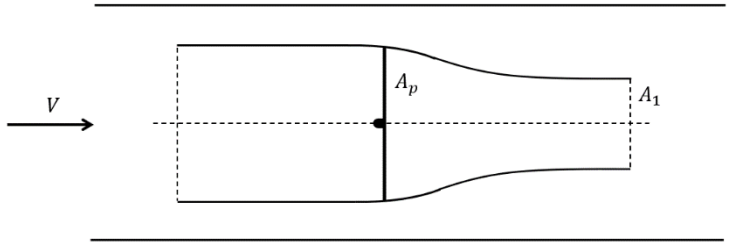

Figure 62. Cross-section of propeller slipstream in wind tunnel.

The interdependence of Eqns. (F.1 – F.4) is then described by the system of non-linear equations

$$f = \frac{(1-\sigma)(1-\alpha\sigma)}{\sigma(1-\alpha\sigma^2)^2} \quad \text{(F.5)}$$

$$x = \frac{1+f}{1-f} \quad \text{(F.6)}$$

$$\lambda = 1 + (x-1)\alpha\sigma^2 - \frac{(2\sigma-1)x-1}{2\sigma} \quad \text{(F.7)}$$

$$\tau = \frac{(x+1)(x-1)}{2\lambda^2} \quad \text{(F.8)}$$

Evaluate λ for a given α and τ by adjusting σ through successive sweeps of Eqns. (F.5 – F.8) until an appropriate value of τ is found.

G: RESIDUAL DIAGNOSTICS FOR LOW-SPEED EXPERIMENTS

Residual Diagnostics for 3-Blade Experiment

CFx										
Run Order	Actual Value	Predicted Value	Residual	Leverage	Internally Studentized Residuals	Externally Studentized Residuals	Cook's Distance	Cook's Random Distance	Influence on Fitted Value DFFITS	Standard Order
1	0.114	0.1133	0.0006	0.257	0.487	0.459	0.003	0.009	0.113	22
2	0.1173	0.1166	0.0007	0.254	0.55	0.546	0.005	0.006	0.146	19
3	0.1184	0.1181	0.0003	0.351	0.245	0.249	0.002	0.013	0.093	21
4	0.1127	0.1135	-0.0008	0.35	-0.672	-0.657	0.01	0.006	-0.227	20
5	0.1089	0.1104	-0.0016	0.362	-1.275	-1.26	0.037	0.021	-0.448	17
6	0.1128	0.1118	0.001	0.23	0.721	0.72	0.008	0.002	0.174	18
7	0.1193	0.1196	-0.0003	0.256	-0.261	-0.258	0.001	0.014	-0.069	23
8	0.0551	0.0572	-0.002	0.47	-1.812	-1.857	0.122	0.119	-0.862	49
9	0.1191	0.1203	-0.0012	0.411	-1.036	-1.002	0.028	0.001	-0.395	48
10	0.1181	0.1184	-0.0003	0.386	-0.255	-0.207	0.001	0.015	-0.053	51
11	0.0973	0.0962	0.0012	0.402	0.983	1.075	0.048	0.095	0.492	45
12	0.1114	0.1113	0.0001	0.22	0.062	0.083	0	0.015	0.037	47
13	0.0884	0.088	0.0004	0.233	0.3	0.316	0.002	0.014	0.097	50
14	0.1002	0.1001	0.0001	0.463	0.095	0.164	0.002	0.015	0.113	46
15	0.1138	0.1131	0.0007	0.561	0.73	0.817	0.045	0.003	0.509	10
16	0.1156	0.1171	-0.0015	0.494	-1.38	-1.274	0.06	0.035	-0.594	14
17	0.0456	0.0446	0.001	0.751	1.409	1.593	0.299	0.057	1.227	11
18	0.1028	0.1046	-0.0017	0.378	-1.498	-1.386	0.042	0.038	-0.489	15
19	0.072	0.0724	-0.0004	0.384	-0.382	-0.291	0.001	0.018	-0.072	9
20	0.1195	0.1182	0.0013	0.741	1.763	2.067	0.491	0.415	1.585	16
21	0.1005	0.1026	-0.002	0.525	-1.947	-2.022	0.178	0.239	-1.06	13
22	0.1003	0.1008	-0.0005	0.755	-0.633	-0.406	0.015	0.015	-0.252	12
23	0.1185	0.1204	-0.0019	0.703	-2.338	-2.363	0.479	0.325	-1.624	1
24	0.1202	0.1202	-3.84E-06	0.668	-0.004	0.226	0.01	0.012	0.227	2
25	0.1267	0.1273	-0.0005	0.441	-0.467	-0.358	0.002	0.025	-0.107	8
26	0.1173	0.1183	-0.001	0.572	-1.05	-0.784	0.02	0.005	-0.349	5
27	0.127	0.1257	0.0013	0.489	1.189	1.373	0.135	0.653	0.806	3
28	0.1188	0.1206	-0.0018	0.567	-1.83	-1.811	0.162	0.169	-0.986	7
29	0.1193	0.1185	0.0008	0.402	0.698	0.728	0.02	0	0.338	6
30	0.1219	0.1228	-0.0009	0.798	-1.408	-0.998	0.113	0.011	-0.699	4
31	0.118	0.1187	-0.0007	0.367	-0.53	-0.466	0.004	0.02	-0.131	27
32	0.1204	0.1208	-0.0004	0.291	-0.309	-0.24	0	0.017	-0.029	28
33	0.1215	0.1206	0.0009	0.515	0.841	1.018	0.068	0.109	0.608	29
34	0.1188	0.1195	-0.0007	0.425	-0.597	-0.507	0.005	0.021	-0.168	26
35	0.1174	0.1171	0.0003	0.434	0.265	0.353	0.007	0.011	0.206	30
36	0.1179	0.1184	-0.0004	0.455	-0.4	-0.272	0.001	0.017	-0.058	25
37	0.1164	0.119	-0.0026	0.214	-1.917	-1.924	0.037	0.103	-0.386	24
38	0.1214	0.12	0.0014	0.364	1.17	1.061	0.021	0.082	0.308	31
39	0.1448	0.1432	0.0016	0.587	1.617	1.3	0.06	0.011	0.592	37
40	0.1232	0.1242	-0.001	0.239	-0.777	-0.912	0.049	0.704	-0.358	33
41	0.1236	0.1215	0.002	0.558	1.934	1.833	0.147	0.159	0.921	35
42	0.1279	0.1268	0.0011	0.341	0.9	0.756	0.007	0.043	0.168	36
43	0.123	0.1203	0.0027	0.29	2.095	2.282	0.098	0.407	0.663	32
44	0.1357	0.1365	-0.0009	0.429	-0.761	-0.924	0.045	0.104	-0.493	34
45	0.1172	0.1176	-0.0004	0.301	-0.294	-0.29	0.002	0.014	-0.09	42
46	0.1062	0.105	0.0013	0.2	0.94	0.921	0.011	0.016	0.199	41
47	0.1103	0.11	0.0003	0.41	0.277	0.283	0.003	0.014	0.122	44
48	0.0796	0.0814	-0.0019	0.413	-1.567	-1.657	0.096	0.187	-0.722	43
49	0.1107	0.1108	-0.0001	0.447	-0.114	-0.111	0	0.015	-0.048	39
50	0.1196	0.1203	-0.0007	0.538	-0.652	-0.667	0.022	0.005	-0.356	40
51	0.1138	0.1125	0.0013	0.26	0.955	0.959	0.016	0.001	0.262	38
52	0.1026	0.101	0.0017	0.199	1.212	1.156	0.011	0.038	0.192	58
53	0.1139	0.1131	0.0009	0.314	0.692	0.581	0.003	0.023	0.115	57
54	0.0753	0.0736	0.0017	0.41	1.416	1.392	0.051	0.076	0.518	54
55	0.1174	0.1172	0.0003	0.254	0.199	0.11	0	0.018	-0.036	55
56	0.1091	0.1089	0.0002	0.546	0.198	-0.012	0.002	0.014	-0.104	56
57	0.086	0.0853	0.0006	0.523	0.589	0.413	0.003	0.018	0.126	52
58	0.1058	0.1059	-0.0001	0.341	-0.055	-0.18	0.005	0.029	-0.143	53

CFy										
Run Order	Actual Value	Predicted Value	Residual	Leverage	Internally Studentized Residuals	Externally Studentized Residuals	Cook's Distance	Cook's Random Distance	Influence on Fitted Value DFFITS	Standard Order
1	-0.0004	-0.0004	0	0.175	0.053	-0.08	0.005	0.017	-0.119	22
2	-0.0018	-0.0021	0.0003	0.218	0.982	0.79	0.001	0.026	0.053	19
3	-0.0007	-0.0008	0.0001	0.385	0.261	-0.1	0.016	0.014	-0.259	21
4	-0.0001	-0.0003	0.0002	0.324	0.708	0.411	0.001	0.014	-0.052	20
5	0.0018	0.0011	0.0007	0.396	2.694	2.606	0.125	0.305	0.819	17
6	-0.0004	-0.001	0.0006	0.26	2.207	2.177	0.058	0.177	0.453	18
7	-0.0012	-0.0013	0.0001	0.216	0.45	0.246	0.002	0.014	-0.08	23
8	0.001	0.0013	-0.0002	0.364	-0.948	-1.038	0.05	0.055	-0.451	49
9	-0.0003	-0.0002	-0.0001	0.32	-0.213	-0.263	0.004	0.009	-0.127	48
10	-0.0001	-0.0001	0	0.397	0.062	-0.018	0.001	0.015	-0.055	51
11	0.0008	0.0005	0.0003	0.317	0.989	0.906	0.018	0.001	0.263	45
12	4.55E-06	-0.0002	0.0002	0.255	0.725	0.644	0.006	0.007	0.142	47
13	0.0006	0.0004	0.0002	0.228	0.703	0.616	0.005	0.005	0.119	50
14	0	-0.0001	0	0.388	0.188	0.113	0	0.017	0	46
15	0.0001	0.0002	-0.0001	0.651	-0.363	-0.282	0.006	0.017	-0.162	10
16	0.0002	0.0003	-0.0001	0.496	-0.472	-0.374	0.006	0.012	-0.167	14
17	0.0003	0	0.0003	0.733	1.863	2.097	0.511	0.286	1.56	11
18	-0.0001	-0.0001	0.0001	0.43	0.308	0.3	0.005	0.011	0.152	15
19	-0.0003	-0.0001	-0.0003	0.378	-1.127	-0.919	0.026	0.002	-0.336	9
20	-0.0001	-0.0002	0.0001	0.715	0.618	0.709	0.068	0.002	0.534	16
21	-0.0002	0.0002	-0.0003	0.494	-1.565	-1.43	0.105	0.053	-0.703	13
22	-8.44E-06	-0.0001	0.0001	0.77	0.553	0.697	0.084	0.002	0.564	12
23	-0.0009	-0.0008	0	0.693	-0.23	-0.042	0	0.017	0.028	1
24	-0.0011	-0.0012	0.0001	0.621	0.433	0.565	0.038	0.003	0.411	2
25	0.001	0.0009	0.0001	0.458	0.391	0.449	0.018	0.02	0.265	8
26	-0.001	-0.0008	-0.0003	0.641	-1.494	-1.226	0.105	0.013	-0.714	5
27	0.0002	0.0002	0	0.415	-0.07	0.014	0.001	0.016	0.049	3
28	-0.001	-0.0007	-0.0003	0.535	-1.542	-1.386	0.111	0.032	-0.714	7
29	-0.0015	-0.0014	0	0.41	-0.181	-0.077	0	0.018	0.011	6
30	-0.0004	-0.0004	0.0001	0.802	0.481	0.793	0.13	0.002	0.688	4
31	-0.0008	-0.0009	0.0002	0.342	0.563	0.941	0.136[1]	1.099[1]	0.606	27
32	0.0001	0.0006	-0.0006	0.236	-2.06	-1.932	0.038	0.133	-0.355	28
33	0.0008	0.0011	-0.0002	0.552	-0.994	-0.487	0	0.017	-0.011	29
34	-0.002	-0.002	0	0.409	-0.05	0.345	0.036	0.067	0.374	26
35	-0.0026	-0.0024	-0.0002	0.35	-0.679	-0.354	0.001	0.015	0.062	30
36	-0.0027	-0.0022	-0.0005	0.397	-1.954	-1.655	0.045	0.035	-0.459	25
37	-0.0024	-0.0019	-0.0006	0.282	-2.149	-2.042	0.055	0.155	-0.458	24
38	-0.0011	-0.001	-0.0001	0.387	-0.235	-0.433	0.021	0.007	-0.288	31
39	0.0028	0.0027	0.0001	0.533	0.543	0.321	0	0.018	0.047	37
40	-0.0009	-0.001	0.0001	0.298	0.227	0.1	0.001	0.014	-0.055	33
41	-0.0009	-0.0012	0.0003	0.581	1.163	1.11	0.065	0.02	0.548	35
42	0.0008	0.0008	0	0.46	0.087	-0.138	0.008	0.011	-0.187	36
43	-0.0011	-0.0014	0.0003	0.327	1.264	1.207	0.032	0.009	0.34	32
44	0.0009	0.0007	0.0002	0.428	0.661	0.504	0.003	0.019	0.116	34
45	-0.0009	-0.001	0	0.222	0.127	0.21	0.005	0.006	0.12	42
46	-0.001	-0.001	0	0.253	0.13	0.234	0.007	0.011	0.144	41
47	-0.0012	-0.0011	-0.0002	0.399	-0.733	-0.556	0.003	0.013	-0.117	44
48	0.0004	0.0005	-0.0002	0.349	-0.668	-0.516	0.002	0.016	-0.089	43
49	-0.0009	-0.0004	-0.0005	0.415	-2.124	-2.148	0.132	0.227	-0.81	39
50	-0.0005	-0.0004	0	0.522	-0.207	0.072	0.007	0.014	0.178	40
51	-0.0006	-0.0005	-0.0001	0.297	-0.451	-0.318	0	0.017	-0.011	38
52	0.0003	0.0001	0.0002	0.274	0.688	0.682	0.011	0.001	0.191	58
53	0.0003	0	0.0003	0.334	1.162	1.179	0.035	0.017	0.393	57
54	0.0008	0.0008	0	0.506	-0.106	-0.174	0.003	0.015	-0.116	54
55	0	0.0001	-0.0001	0.278	-0.443	-0.48	0.009	0.006	-0.162	55
56	-0.0001	-0.0002	0.0001	0.515	0.257	0.249	0.003	0.016	0.112	56
57	0.0002	0.0003	-0.0001	0.482	-0.429	-0.553	0.022	0.004	-0.31	52
58	-0.0001	0.0001	-0.0002	0.292	-0.583	-0.611	0.012	0.002	-0.206	53

CFz										
Run Order	Actual Value	Predicted Value	Residual	Leverage	Internally Studentized Residuals	Externally Studentized Residuals	Cook's Distance	Cook's Random Distance	Influence on Fitted Value DFFITS	Standard Order
1	-0.0065	-0.0056	-0.0009	0.225	-0.719	-0.649	0.011	0.003	-0.117	22
2	-0.0065	-0.0064	-0.0001	0.216	-0.061	-0.003	0.002	0.011	0.042	19
3	-0.0016	-0.0014	-0.0001	0.29	-0.113	-0.037	0.001	0.014	0.043	21
4	-0.0043	-0.0037	-0.0006	0.364	-0.501	-0.447	0.006	0.008	-0.107	20
5	-0.0105	-0.0107	0.0002	0.227	0.19	0.241	0.008	0.002	0.103	17
6	-0.0101	-0.0099	-0.0002	0.266	-0.195	-0.125	0	0.015	0.015	18
7	-0.0024	-0.0019	-0.0005	0.268	-0.414	-0.346	0.002	0.013	-0.05	23
8	-0.0041	-0.0037	-0.0003	0.319	-0.252	-0.504	0.059	0.044	-0.314	49
9	-0.0002	-0.0006	0.0005	0.332	0.35	0.182	0.004	0.012	-0.079	48
10	0.0005	0.0003	0.0003	0.321	0.215	0.03	0.011	0.005	-0.129	51
11	0.0031	0.0007	0.0023	0.198	1.759	1.774	0.072	0.347	0.296	45
12	-0.0002	-0.0007	0.0005	0.172	0.366	0.263	0.001	0.012	-0.027	47
13	0.0002	-0.0012	0.0014	0.201	1.051	0.973	0.015	0.002	0.127	50
14	-0.0015	-0.002	0.0004	0.326	0.348	0.182	0.004	0.011	-0.078	46
15	0.0004	0.0003	0.0002	0.328	0.152	-0.082	0.017	0	-0.165	10
16	0.0022	0.0014	0.0007	0.397	0.727	0.378	0	0.016	-0.008	14
17	0.0065	0.0051	0.0014	0.638	1.489	1.206	0.135	0.007	0.55	11
18	0.0019	0.0013	0.0006	0.337	0.567	0.258	0.002	0.012	-0.051	15
19	0.0052	0.0049	0.0003	0.367	0.253	-0.029	0.017	0.003	-0.164	9
20	0.0015	0.0005	0.001	0.568	1.059	0.659	0.013	0.009	0.166	16
21	0.006	0.0039	0.002	0.354	1.969	1.564	0.119	0.157	0.437	13
22	0.0016	0.0013	0.0003	0.596	0.267	-0.282	0.079	0.005	-0.404	12
23	-0.0027	-0.0037	0.001	0.471	1.086	0.585	0.002	0.016	0.065	1
24	-0.0034	-0.0043	0.0008	0.652	0.939	0.304	0.003	0.014	-0.075	2
25	-0.0099	-0.0111	0.0012	0.319	1.202	0.739	0.007	0.016	0.092	8
26	-0.0095	-0.0104	0.0009	0.38	0.947	0.471	0	0.016	0.002	5
27	-0.0108	-0.0121	0.0013	0.383	1.345	0.826	0.012	0.009	0.143	3
28	-0.0063	-0.0076	0.0014	0.477	1.458	0.977	0.039	0.01	0.265	7
29	-0.0066	-0.0065	-0.0001	0.261	-0.142	-0.279	0.032	0.052	-0.203	6
30	-0.011	-0.0121	0.001	0.646	1.215	0.611	0.006	0.012	0.121	4
31	-0.0025	-0.0025	0	0.4	0.028	-0.111	0.009	0.009	-0.131	27
32	-0.0132	-0.0132	-0.0001	0.226	-0.056	-0.123	0.006	0.005	-0.081	28
33	-0.0174	-0.0179	0.0005	0.414	0.439	0.4	0.005	0.013	0.097	29
34	-0.0043	-0.0051	0.0007	0.254	0.556	0.511	0.007	0.007	0.091	26
35	-0.0086	-0.0088	0.0002	0.252	0.152	0.083	0.001	0.015	-0.03	30
36	-0.0101	-0.0101	-5.75E-07	0.301	0	-0.092	0.005	0.008	-0.091	25
37	-0.0048	-0.0059	0.001	0.184	0.783	0.729	0.014	0.001	0.112	24
38	-0.0033	-0.0024	-0.0009	0.34	-0.725	-0.337	0.017	0.009	0.155	31
39	-0.02	-0.0191	-0.0009	0.552	-0.755	-0.132	0.042	0.002	0.315	37
40	-0.0118	-0.0106	-0.0012	0.224	-0.961	-0.672	0.001	0.013	0.024	33
41	-0.0072	-0.0059	-0.0013	0.443	-1.082	-0.678	0	0.015	0.021	35
42	-0.0137	-0.0113	-0.0025	0.193	-1.978	-1.663	0.025	0.043	-0.18	36
43	-0.0064	-0.0051	-0.0013	0.258	-1.018	-0.717	0	0.015	0.012	32
44	-0.0161	-0.0143	-0.0018	0.429	-1.559	-1.255	0.026	0.005	-0.234	34
45	-0.003	-0.0028	-0.0003	0.169	-0.199	-0.28	0.02	0.028	-0.132	42
46	-0.005	-0.0057	0.0007	0.214	0.534	0.386	0	0.015	-0.007	41
47	-0.0046	-0.0052	0.0006	0.541	0.518	0.235	0.003	0.014	-0.08	44
48	-0.0067	-0.008	0.0013	0.437	1.057	0.999	0.047	0	0.295	43
49	0.0014	0	0.0014	0.374	1.156	1.1	0.046	0.011	0.287	39
50	-0.0003	-0.0014	0.001	0.532	0.867	0.738	0.018	0.009	0.203	40
51	-0.0003	-0.0009	0.0006	0.256	0.474	0.314	0.001	0.014	-0.029	38
52	-0.0012	0.0008	-0.002	0.175	-1.543	-1.205	0.001	0.017	-0.032	58
53	-0.0007	0.0022	-0.0028	0.378	-2.318	-2.156	0.099	0.092	-0.452	57
54	-0.002	0.0008	-0.0028	0.223	-2.17	-1.884	0.031	0.033	-0.201	54
55	-0.0005	0.0006	-0.0012	0.274	-0.936	-0.517	0.02	0.018	0.151	55
56	0.0002	0.0027	-0.0026	0.518	-2.2	-1.931	0.112	0.026	-0.524	56
57	-0.001	0.0008	-0.0018	0.371	-1.487	-1.063	0.001	0.017	-0.03	52
58	-0.0007	-0.0009	0.0001	0.22	0.115	0.442	0.141[1]	1.382[1]	0.362	53

CMx										
Run Order	Actual Value	Predicted Value	Residual	Leverage	Internally Studentized Residuals	Externally Studentized Residuals	Cook's Distance	Cook's Random Distance	Influence on Fitted Value DFFITS	Standard Order
1	-0.0081	-0.0082	0.0001	0.165	0.71	0.692	0.005	0.012	0.129	22
2	-0.0083	-0.0082	0	0.187	-0.166	-0.14	0	0.015	-0.008	19
3	-0.0081	-0.008	-5.57E-06	0.289	-0.05	-0.01	0	0.015	0.025	21
4	-0.0081	-0.0081	0	0.304	-0.442	-0.391	0.002	0.013	-0.091	20
5	-0.0084	-0.0083	-0.0002	0.303	-1.571	-1.552	0.041	0.047	-0.446	17
6	-0.0084	-0.0083	0	0.227	-0.307	-0.274	0.001	0.014	-0.043	18
7	-0.0082	-0.0082	-3.58E-06	0.217	-0.031	-0.001	0	0.015	0.022	23
8	-0.0065	-0.0068	0.0003	0.396	3.072	3.373	0.24	0.88	1.257	49
9	-0.0083	-0.0083	0	0.31	0.308	0.178	0	0.014	-0.028	48
10	-0.0081	-0.008	-0.0001	0.344	-0.487	-0.606	0.019	0.049	-0.296	51
11	-0.0079	-0.008	0.0001	0.25	0.933	0.848	0.007	0.058	0.161	45
12	-0.0082	-0.0082	0.0001	0.194	0.447	0.362	0	0.017	0.018	47
13	-0.0078	-0.0079	0.0001	0.175	0.696	0.613	0.001	0.03	0.062	50
14	-0.0082	-0.0082	0	0.391	0.405	0.239	0	0.015	-0.004	46
15	-0.0083	-0.0083	1.01E-06	0.583	0.012	-0.06	0.001	0.014	-0.065	10
16	-0.008	-0.008	0	0.497	0.245	0.18	0.001	0.016	0.063	14
17	-0.0054	-0.0055	0.0001	0.748	1.197	1.034	0.121	0.002	0.728	11
18	-0.0081	-0.0082	0.0001	0.313	0.761	0.695	0.009	0.018	0.205	15
19	-0.0071	-0.0069	-0.0002	0.345	-2.25	-2.24	0.127	0.557	-0.812	9
20	-0.0082	-0.0082	0	0.774[x]	0.542	0.4	0.019	0.012	0.277	16
21	-0.0078	-0.0079	0.0002	0.432	1.737	1.7	0.091	0.066	0.71	13
22	-0.0081	-0.0081	5.15E-06	0.811[x]	0.091	-0.066	0.002	0.016	-0.084	12
23	-0.0081	-0.0082	0.0001	0.635	1.229	1.215	0.117	0.017	0.772	1
24	-0.0083	-0.0083	-3.63E-06	0.707	-0.052	-0.073	0.001	0.015	-0.058	2
25	-0.009	-0.009	0	0.406	-0.449	-0.44	0.007	0.014	-0.186	8
26	-0.0086	-0.0088	0.0002	0.525	2.198	2.061	0.176	0.284	1.02	5
27	-0.0093	-0.0092	-0.0002	0.436	-1.931	-1.937	0.141	0.256	-0.872	3
28	-0.0084	-0.0084	0.0001	0.496	0.596	0.569	0.015	0.006	0.281	7
29	-0.0086	-0.0085	0	0.338	-0.406	-0.379	0.003	0.012	-0.131	6
30	-0.0091	-0.0091	0	0.790[x]	-0.557	-0.539	0.044	0.008	-0.419	4
31	-0.008	-0.008	0	0.323	0.126	0.056	0	0.015	-0.028	27
32	-0.0084	-0.0085	0.0001	0.175	0.977	0.916	0.006	0.008	0.139	28
33	-0.0087	-0.0086	-0.0002	0.488	-1.624	-1.773	0.148	0.253	-0.915	29
34	-0.0083	-0.0083	-8.37E-06	0.322	-0.077	-0.145	0.002	0.015	-0.095	26
35	-0.0082	-0.0082	6.49E-06	0.362	0.062	-0.011	0.001	0.014	-0.05	30
36	-0.0082	-0.0084	0.0002	0.359	1.597	1.534	0.05	0.029	0.508	25
37	-0.0081	-0.0083	0.0002	0.178	1.269	1.225	0.013	0.018	0.2	24
38	-0.0083	-0.0082	-0.0001	0.37	-0.637	-0.618	0.01	0.006	-0.22	31
39	-0.0093	-0.0094	0.0001	0.628	0.777	0.825	0.052	0.004	0.52	37
40	-0.0087	-0.0087	0	0.21	-0.4	-0.382	0.002	0.011	-0.073	33
41	-0.0083	-0.0082	-0.0001	0.57	-0.639	-0.629	0.024	0.006	-0.348	35
42	-0.0086	-0.0087	0	0.417	0.273	0.307	0.004	0.011	0.148	36
43	-0.0085	-0.0083	-0.0002	0.231	-1.338	-1.339	0.027	0.019	-0.314	32
44	-0.0091	-0.0092	0.0001	0.419	1.293	1.315	0.06	0.054	0.56	34
45	-0.0084	-0.0083	-0.0001	0.201	-0.818	-0.768	0.005	0.006	-0.138	42
46	-0.0083	-0.0082	0	0.179	-0.379	-0.343	0.001	0.014	-0.045	41
47	-0.0082	-0.0082	-0.0001	0.424	-0.859	-0.819	0.02	0.017	-0.323	44
48	-0.0078	-0.0076	-0.0001	0.398	-1.163	-1.153	0.039	0.008	-0.444	43
49	-0.0079	-0.0079	0	0.423	0.31	0.379	0.008	0.008	0.201	39
50	-0.0082	-0.0083	0.0001	0.502	0.85	1.013	0.068	0.09	0.583	40
51	-0.008	-0.008	0	0.24	0.308	0.338	0.003	0.014	0.111	38
52	-0.0081	-0.0081	0	0.203	-0.333	-0.256	0	0.015	0.001	58
53	-0.0081	-0.0079	-0.0002	0.33	-1.499	-1.386	0.029	0.034	-0.372	57
54	-0.0076	-0.0073	-0.0002	0.43	-2.174	-2.525	0.216	0.527	-1.105	54
55	-0.0083	-0.0082	-0.0001	0.17	-0.521	-0.465	0.001	0.021	-0.041	55
56	-0.008	-0.008	-0.0001	0.597	-0.595	-0.315	0.001	0.016	-0.065	56
57	-0.0078	-0.0077	0	0.493	-0.141	0.078	0.005	0.017	0.151	52
58	-0.0083	-0.0083	0	0.217	0.102	0.182	0.004	0.035	0.105	53

CMy										
Run Order	Actual Value	Predicted Value	Residual	Leverage	Internally Studentized Residuals	Externally Studentized Residuals	Cook's Distance	Cook's Random Distance	Influence on Fitted Value DFFITS	Standard Order
1	0.0023	0.0026	-0.0003	0.145	-0.573	-0.474	0.001	0.01	-0.04	22
2	0.0026	0.0028	-0.0001	0.184	-0.222	-0.155	0	0.014	0.012	19
3	0.0005	0.0008	-0.0003	0.262	-0.55	-0.47	0.003	0.011	-0.074	21
4	0.0015	0.0018	-0.0003	0.244	-0.624	-0.539	0.005	0.007	-0.086	20
5	0.0023	0.0026	-0.0003	0.265	-0.58	-0.497	0.004	0.009	-0.082	17
6	0.0036	0.0033	0.0002	0.197	0.442	0.487	0.021	0.007	0.155	18
7	0.001	0.001	-0.0001	0.165	-0.112	-0.055	0.001	0.012	0.029	23
8	0.0008	0.0013	-0.0005	0.257	-1.018	-1.199	0.098	0.299	-0.402	49
9	0.0005	0.0003	0.0002	0.263	0.477	0.423	0.002	0.012	0.061	48
10	0.0005	0.0004	0.0001	0.262	0.288	0.225	0	0.015	0.005	51
11	0.0023	0.0019	0.0004	0.321	0.786	0.801	0.024	0.004	0.213	45
12	0.0012	0.0011	0.0001	0.152	0.148	0.1	0	0.013	-0.019	47
13	0.0018	0.0014	0.0004	0.182	0.831	0.786	0.011	0.003	0.116	50
14	0.0016	0.0014	0.0003	0.29	0.56	0.523	0.006	0.008	0.102	46
15	0.0001	0.0002	0	0.473	-0.069	-0.478	0.089	0.046	-0.444	10
16	0.0007	0.0006	0.0001	0.302	0.13	-0.1	0.018	0.004	-0.174	14
17	0.0023	0.0016	0.0007	0.652	2.015	1.783	0.327	0.114	0.927	11
18	0.0006	0.0007	-0.0001	0.344	-0.241	-0.456	0.059	0.08	-0.324	15
19	0.0018	0.001	0.0008	0.29	1.943	1.471	0.052	0.047	0.309	9
20	0.0005	0	0.0005	0.567	1.446	1.054	0.06	0	0.383	16
21	0.002	0.0014	0.0006	0.413	1.473	1.093	0.04	0.009	0.288	13
22	0.0005	0.0003	0.0002	0.676[x]	0.608	-0.054	0.037	0.006	-0.298	12
23	0.001	0.0006	0.0004	0.515	1.109	0.698	0.014	0.013	0.18	1
24	0.0014	0.0012	0.0003	0.5	0.708	0.289	0.001	0.014	-0.04	2
25	0.0051	0.0044	0.0006	0.338	1.571	1.147	0.04	0.016	0.271	8
26	0.005	0.005	0.0001	0.517	0.256	-0.158	0.031	0.003	-0.276	5
27	0.0059	0.0059	0.0001	0.283	0.126	-0.067	0.011	0.003	-0.137	3
28	0.0021	0.0017	0.0005	0.405	1.277	0.874	0.022	0.008	0.211	7
29	0.003	0.0029	0.0001	0.346	0.332	0.056	0.007	0.006	-0.118	6
30	0.0061	0.0057	0.0004	0.774[x]	1.372	0.937	0.105	0.001	0.494	4
31	0.0007	0.0007	0	0.234	0.036	-0.087	0.01	0.004	-0.114	27
32	0.0036	0.0032	0.0004	0.24	0.901	0.816	0.011	0.009	0.126	28
33	0.0036	0.003	0.0006	0.485	1.319	1.445	0.128	0.035	0.582	29
34	0.002	0.0017	0.0003	0.266	0.52	0.402	0	0.015	0.017	26
35	0.0037	0.0038	0	0.205	-0.068	-0.169	0.01	0.001	-0.116	30
36	0.0042	0.004	0.0002	0.257	0.413	0.293	0	0.015	-0.014	25
37	0.0028	0.0026	0.0002	0.145	0.441	0.349	0	0.015	0	24
38	0.0007	0.001	-0.0003	0.339	-0.625	-0.26	0.015	0.009	0.163	31
39	0.0031	0.0039	-0.0008	0.403	-1.746	-1.489	0.046	0.007	-0.336	37
40	0.0044	0.0046	-0.0002	0.222	-0.453	-0.198	0.013	0.011	0.128	33
41	-0.0002	0.0005	-0.0007	0.533	-1.586	-1.391	0.075	0.018	-0.434	35
42	0.0028	0.0035	-0.0007	0.383	-1.455	-1.173	0.018	0.009	-0.199	36
43	0.0013	0.0018	-0.0005	0.246	-1.074	-0.806	0	0.016	-0.025	32
44	0.0043	0.0048	-0.0004	0.351	-0.928	-0.579	0.001	0.013	0.041	34
45	0.0015	0.0012	0.0003	0.179	0.617	0.481	0	0.015	0.016	42
46	0.0026	0.0024	0.0002	0.163	0.349	0.234	0.001	0.012	-0.029	41
47	0.0024	0.0019	0.0005	0.3	1.048	0.904	0.015	0.001	0.167	44
48	0.0023	0.0024	-0.0001	0.263	-0.254	-0.415	0.034	0.02	-0.232	43
49	0.0019	0.0009	0.001	0.359	2.086	2.297	0.215	0.553	0.732	39
50	0.0006	0.0007	-0.0001	0.47	-0.208	-0.632	0.107	0.046	-0.502	40
51	0.0016	0.0013	0.0002	0.196	0.505	0.374	0	0.015	-0.005	38
52	0.0004	0.0012	-0.0008	0.161	-1.68	-1.388	0.005	0.012	-0.076	58
53	0.0001	0.0009	-0.0008	0.309	-1.786	-1.449	0.014	0.011	-0.173	57
54	0.0001	0.0009	-0.0008	0.429	-1.641	-1.29	0.017	0.018	-0.196	54
55	0.0002	0.0005	-0.0002	0.285	-0.449	-0.03	0.057	0.127	0.284	55
56	0.0005	0.0013	-0.0009	0.418	-1.904	-1.555	0.033	0.007	-0.291	56
57	0.0007	0.0017	-0.001	0.298	-2.145	-1.96	0.062	0.049	-0.338	52
58	0.0007	0.0008	-0.0001	0.335	-0.16	0.358	0.13	0.387	0.466	53

CMz										
Run Order	Actual Value	Predicted Value	Residual	Leverage	Internally Studentized Residuals	Externally Studentized Residuals	Cook's Distance	Cook's Random Distance	Influence on Fitted Value DFFITS	Standard Order
1	-0.0045	-0.0044	0	0.151	-0.181	-0.135	0	0.014	0.011	22
2	-0.0039	-0.0039	0	0.166	-0.213	-0.161	0	0.014	0.009	19
3	-0.0013	-0.0012	-0.0001	0.301	-0.603	-0.503	0.002	0.018	-0.092	21
4	-0.0031	-0.003	-0.0001	0.284	-0.889	-0.772	0.006	0.014	-0.15	20
5	-0.0069	-0.0067	-0.0002	0.201	-1.084	-1.008	0.008	0.041	-0.159	17
6	-0.0064	-0.0063	-0.0001	0.253	-0.678	-0.653	0.007	0.051	-0.145	18
7	-0.0018	-0.0018	-0.0001	0.19	-0.379	-0.311	0	0.016	-0.018	23
8	-0.003	-0.0031	0	0.4	0.282	0.281	0.003	0.012	0.117	49
9	-0.0006	-0.0006	6.57E-06	0.369	0.052	0.056	0	0.014	0.024	48
10	-0.0005	-0.0006	0.0001	0.37	0.618	0.607	0.012	0.006	0.229	51
11	-0.0016	-0.0015	-0.0001	0.218	-0.374	-0.358	0.002	0.01	-0.076	45
12	-0.0012	-0.0013	0.0001	0.216	0.48	0.463	0.003	0.008	0.104	47
13	-0.0022	-0.0021	-0.0001	0.201	-0.725	-0.698	0.006	0.003	-0.143	50
14	-0.0017	-0.0017	-0.0001	0.355	-0.466	-0.456	0.006	0.008	-0.164	46
15	-0.0001	0	-0.0001	0.406	-0.795	-0.736	0.018	0.002	-0.295	10
16	-0.0001	0	-0.0001	0.505	-0.745	-0.701	0.025	0.003	-0.353	14
17	0.0001	0	0	0.636	0.53	0.499	0.021	0.007	0.311	11
18	0	-0.0001	0.0001	0.371	0.425	0.404	0.005	0.012	0.153	15
19	0.0002	0.0001	0.0001	0.353	0.597	0.558	0.009	0.006	0.2	9
20	-4.07E-06	-9.19E-08	-3.98E-06	0.624	-0.042	-0.032	0	0.015	-0.017	16
21	0.0001	0	0.0001	0.335	0.603	0.561	0.008	0.005	0.186	13
22	0	0	-0.0001	0.628	-0.967	-0.917	0.067	0.004	-0.566	12
23	-0.0023	-0.0021	-0.0002	0.653	-1.903	-1.958	0.332	0.124	-1.29	1
24	-0.0025	-0.0025	0	0.624	0.406	0.339	0.008	0.012	0.193	2
25	-0.0075	-0.0078	0.0003	0.382	2.442	2.529	0.162	0.357	0.959	8
26	-0.0052	-0.0051	-0.0001	0.361	-0.98	-0.934	0.024	0.003	-0.342	5
27	-0.0067	-0.0068	0	0.513	0.33	0.296	0.004	0.02	0.141	3
28	-0.0046	-0.0047	0.0001	0.435	1.135	1.059	0.04	0.005	0.446	7
29	-0.0045	-0.0044	-0.0001	0.297	-0.825	-0.77	0.014	0.011	-0.239	6
30	-0.0056	-0.0056	0	0.67	0.248	0.174	0.002	0.013	0.094	4
31	-0.0021	-0.002	-0.0001	0.334	-0.457	-0.667	0.048	0.558	-0.381	27
32	-0.0087	-0.0088	0.0001	0.144	0.411	0.351	0	0.017	0.016	28
33	-0.0111	-0.011	-0.0001	0.399	-0.678	-0.827	0.048	0.248	-0.436	29
34	-0.003	-0.0032	0.0002	0.272	1.507	1.481	0.037	0.164	0.365	26
35	-0.005	-0.0051	0.0002	0.358	1.224	1.026	0.013	0.012	0.246	30
36	-0.0061	-0.0061	0	0.362	0.347	0.215	0	0.015	0	25
37	-0.004	-0.0043	0.0003	0.181	2.287	2.494	0.067	0.398	0.46	24
38	-0.0022	-0.0023	0.0001	0.37	0.67	0.708	0.021	0.025	0.306	31
39	-0.0125	-0.0127	0.0002	0.472	1.543	1.632	0.144	0.275	0.835	37
40	-0.0072	-0.0069	-0.0003	0.254	-2.524	-2.627	0.092	0.386	-0.651	33
41	-0.0034	-0.0034	0	0.526	0.315	0.406	0.014	0.01	0.261	35
42	-0.0083	-0.0079	-0.0004	0.274	-2.646	-2.697	0.107	0.453	-0.714	36
43	-0.0039	-0.004	0.0001	0.292	0.929	0.944	0.03	0.109	0.329	32
44	-0.0103	-0.0102	0	0.436	-0.267	-0.188	0	0.016	-0.043	34
45	-0.002	-0.0019	-0.0001	0.155	-0.478	-0.463	0.003	0.01	-0.082	42
46	-0.0033	-0.0033	0	0.235	-0.14	-0.148	0.001	0.013	-0.046	41
47	-0.0025	-0.0026	0.0001	0.341	0.694	0.659	0.011	0.012	0.217	44
48	-0.0053	-0.0054	0.0001	0.32	0.738	0.696	0.01	0.004	0.212	43
49	-0.0009	-0.0011	0.0002	0.32	1.725	1.738	0.065	0.067	0.548	39
50	-0.0006	-0.0005	-0.0002	0.373	-1.295	-1.294	0.056	0.067	-0.503	40
51	-0.0014	-0.0013	0	0.253	-0.335	-0.337	0.003	0.01	-0.099	38
52	-0.001	-0.0009	0	0.214	-0.323	-0.315	0.002	0.011	-0.073	58
53	-0.0006	-0.0005	-0.0001	0.339	-0.857	-0.858	0.02	0.004	-0.298	57
54	-0.0015	-0.0014	-0.0001	0.271	-0.686	-0.681	0.011	0.011	-0.197	54
55	-0.0005	-0.0006	0.0002	0.2	1.041	1.02	0.014	0.003	0.205	55
56	-0.0005	-0.0006	0.0001	0.515	0.647	0.62	0.019	0.005	0.305	56
57	-0.0011	-0.0011	0	0.508	-0.381	-0.401	0.01	0.01	-0.214	52
58	-0.0008	-0.0009	0.0001	0.224	0.77	0.752	0.009	0.002	0.171	53

Residual Diagnostics for 4-Blade Experiment

CFx										
Run Order	Actual Value	Predicted Value	Residual	Leverage	Internally Studentized Residuals	Externally Studentized Residuals	Cook's Distance	Cook's Random Distance	Influence on Fitted Value DFFITS	Standard Order
1	0.1263	0.1252	0.001	0.294	1.037	1.029	0.034	0.024	0.318	25
2	0.1145	0.1145	0	0.433	0.022	-0.019	0	0.024	-0.032	23
3	0.1334	0.1338	-0.0004	0.599	-0.486	-0.705	0.053	0	-0.468	20
4	0.1242	0.124	0.0002	0.508	0.266	0.26	0.004	0.019	0.117	21
5	0.1365	0.1367	-0.0002	0.335	-0.204	-0.236	0.004	0.017	-0.106	22
6	0.1328	0.1329	-0.0001	0.301	-0.139	-0.161	0.002	0.019	-0.07	24
7	0.1409	0.1403	0.0006	0.427	0.599	-0.066	0.069	0.343	-0.421	12
8	0.1397	0.1387	0.001	0.299	1.009	0.646	0.001	0.021	-0.04	11
9	0.1373	0.1353	0.002	0.398	1.988	1.679	0.036	0.019	0.383	8
10	0.1391	0.1369	0.0022	0.536	2.31	2.335	0.179	0.214	0.926	13
11	0.139	0.1369	0.0022	0.492	2.226	2.269	0.163	0.175	0.84	10
12	0.137	0.1368	0.0001	0.367	0.126	-0.329	0.046	0.147	-0.409	9
13	0.1343	0.1357	-0.0014	0.29	-1.388	-1.13	0.012	0.017	-0.184	47
14	0.1326	0.1328	-0.0002	0.414	-0.262	0.146	0.026	0.038	0.297	46
15	0.1293	0.1297	-0.0003	0.511	-0.38	0.139	0.029	0.011	0.339	44
16	0.1354	0.1364	-0.001	0.248	-0.954	-0.692	0.001	0.028	-0.037	48
17	0.1376	0.1392	-0.0016	0.377	-1.638	-1.385	0.032	0.022	-0.344	49
18	0.1393	0.1406	-0.0013	0.593	-1.501	-1.146	0.04	0.018	-0.413	45
19	0.1016	0.102	-0.0004	0.314	-0.42	-0.498	0.018	0.014	-0.231	14
20	0.1207	0.1198	0.0009	0.294	0.891	0.788	0.014	0.001	0.194	17
21	0.1358	0.135	0.0009	0.394	0.925	0.851	0.023	0.002	0.285	18
22	0.1162	0.116	0.0002	0.539	0.219	0.05	0.001	0.024	-0.063	19
23	0.1296	0.1294	0.0002	0.346	0.229	0.123	0	0.024	-0.022	15
24	0.1391	0.1385	0.0007	0.529	0.752	0.714	0.026	0.008	0.314	16
25	0.0862	0.0864	-0.0002	0.603	-0.286	-0.629	0.059	0.001	-0.492	35
26	0.1404	0.1403	0.0001	0.698	0.097	0.057	0	0.025	0.018	36
27	0.1349	0.1362	-0.0012	0.434	-1.307	-1.634	0.185	0.508	-0.834	33
28	0.1398	0.1388	0.001	0.505	1.094	1.297	0.104	0.062	0.682	34
29	0.1389	0.1386	0.0003	0.357	0.33	0.319	0.004	0.015	0.113	37
30	0.1391	0.1388	0.0002	0.565	0.271	0.29	0.006	0.019	0.156	1
31	0.1234	0.1238	-0.0005	0.544	-0.685	-0.404	0.005	0.022	-0.134	4
32	0.1385	0.1393	-0.0008	0.77	-1.331	-1.237	0.231	0.034	-0.886	5
33	0.1139	0.1139	0.0001	0.579	0.09	0.31	0.019	0.007	0.277	6
34	0.1331	0.1333	-0.0001	0.826	-0.279	0.241	0.029	0.016	0.3	3
35	0.092	0.0916	0.0004	0.697	0.587	1.039	0.197	0.077	0.86	7
36	0.1241	0.1252	-0.0011	0.631	-1.659	-1.354	0.137	0.041	-0.769	2
37	0.1286	0.1284	0.0002	0.596	0.323	0.941	0.192	0.396	0.827	31
38	0.1403	0.1404	-0.0002	0.638	-0.239	0.42	0.062	0.006	0.5	32
39	0.1342	0.1354	-0.0012	0.848	-2.451	-1.581	0.378	0.031	-1.084	30
40	0.1303	0.1318	-0.0015	0.51	-2.115	-1.47	0.074	0.045	-0.556	27
41	0.1423	0.1433	-0.001	0.766	-1.702	-0.858	0.052	0.021	-0.42	26
42	0.1355	0.1366	-0.0011	0.832	-1.997	-1.378	0.336	0.116	-0.958	29
43	0.1353	0.1362	-0.0009	0.601	-1.319	-0.639	0.007	0.029	-0.163	28
44	0.1185	0.1181	0.0004	0.518	0.454	0.367	0.003	0.022	0.112	39
45	0.1054	0.1056	-0.0002	0.558	-0.259	-0.592	0.055	0.018	-0.453	40
46	0.1382	0.1377	0.0005	0.436	0.497	0.44	0.005	0.021	0.132	41
47	0.132	0.131	0.001	0.399	1.019	1.035	0.038	0.004	0.373	42
48	0.1157	0.1158	-0.0001	0.443	-0.084	-0.258	0.013	0.009	-0.207	38
49	0.09	0.0895	0.0004	0.532	0.474	0.412	0.006	0.017	0.148	43
50	0.1364	0.1364	5.28E-06	0.426	0.005	-0.143	0.007	0.014	-0.146	50

CFy										
Run Order	Actual Value	Predicted Value	Residual	Leverage	Internally Studentized Residuals	Externally Studentized Residuals	Cook's Distance	Cook's Random Distance	Influence on Fitted Value DFFITS	Standard Order
1	-0.001	-0.001	0	0.232	-0.023	-0.007	0	0.027	0.007	25
2	-0.0005	-0.0006	0.0001	0.362	0.113	0.146	0.006	0.017	0.074	23
3	-0.0013	-0.001	-0.0003	0.568	-0.37	-0.49	0.049	0	-0.27	20
4	-0.0013	-0.001	-0.0003	0.426	-0.398	-0.441	0.035	0.001	-0.193	21
5	-0.001	-0.001	-0.0001	0.385	-0.093	-0.074	0	0.027	-0.016	22
6	-0.0011	-0.0013	0.0003	0.295	0.399	0.402	0.027	0.013	0.146	24
7	0	-0.0001	0.0001	0.452	0.12	-0.062	0.022	0.008	-0.144	12
8	-0.0015	-0.0019	0.0004	0.313	0.592	0.528	0.013	0.001	0.113	11
9	-0.0001	-0.0003	0.0001	0.387	0.171	0.059	0.003	0.019	-0.058	8
10	-0.0009	-0.0011	0.0002	0.634	0.289	0.171	0	0.027	-0.012	13
11	-0.0014	-0.0015	0.0001	0.467	0.194	0.054	0.005	0.019	-0.077	10
12	-0.0001	-0.0004	0.0003	0.401	0.417	0.352	0.004	0.019	0.066	9
13	-0.0011	-0.0027	0.0016	0.297	2.189	1.798	0.078	0.279	0.265	47
14	-0.0011	-0.002	0.0009	0.44	1.325	0.725	0.006	0.014	-0.086	46
15	-0.0002	-0.0013	0.0011	0.505	1.595	1.059	0.006	0.026	0.085	44
16	-0.0018	-0.0022	0.0004	0.24	0.566	0.147	0.068	0.82	-0.203	48
17	-0.0006	-0.002	0.0014	0.38	2.048	1.65	0.072	0.095	0.283	49
18	-0.001	-0.0019	0.0009	0.552	1.331	0.643	0.015	0.01	-0.143	45
19	0.0004	0.0007	-0.0003	0.383	-0.372	-0.282	0.002	0.024	-0.048	14
20	-0.0001	-0.0002	0.0001	0.347	0.117	0.223	0.025	0.001	0.149	17
21	-0.0004	-0.0002	-0.0003	0.408	-0.38	-0.294	0.003	0.023	-0.057	18
22	-0.0001	0.0001	-0.0002	0.632	-0.262	-0.138	0	0.027	0.013	19
23	-0.0004	0	-0.0004	0.334	-0.601	-0.516	0.022	0	-0.132	15
24	-0.0003	-0.0001	-0.0001	0.582	-0.212	-0.066	0.003	0.025	0.059	16
25	0.0005	0.0007	-0.0001	0.663	-0.192	0.002	0.009	0.022	0.111	35
26	-0.0015	-0.0002	-0.0013	0.786	-1.936	-1.315	0.058	0.014	-0.308	36
27	-0.0022	-0.0014	-0.0008	0.521	-1.2	-0.115	0.328	0.846	0.528	33
28	-0.0045	-0.0028	-0.0017	0.584	-2.523	-2.545	0.397[1]	1.046[1]	-0.868	34
29	-0.0034	-0.0024	-0.001	0.296	-1.438	-0.804	0.012	0.016	0.086	37
30	-0.004	-0.0028	-0.0013	0.587	-1.871	-1.222	0.01	0.024	-0.121	1
31	0.0005	0.0001	0.0004	0.593	0.982	0.428	0.008	0.022	0.099	4
32	0.0005	0.0003	0.0002	0.799	0.601	-0.176	0.089	0.003	-0.346	5
33	0.0004	0	0.0004	0.547	0.932	0.374	0.003	0.025	0.057	6
34	0.0005	0	0.0005	0.814	1.236	0.849	0.176	0.003	0.497	3
35	0.0004	0.0001	0.0003	0.751	0.814	0.199	0.001	0.026	-0.044	7
36	0.0003	1.29E-06	0.0003	0.644	0.604	0.054	0.014	0.015	-0.139	2
37	0.0017	0.0015	0.0002	0.638	0.359	-0.012	0.014	0.014	-0.128	31
38	0.0028	0.0026	0.0002	0.695	0.599	0.208	0	0.028	0.022	32
39	-0.0003	-0.0009	0.0006	0.846	1.524	2.017	1.416[1]	1.184[1]	1.552	30
40	0.0009	0.0006	0.0003	0.515	0.631	0.253	0.001	0.026	0.036	27
41	0.0033	0.003	0.0003	0.776	0.798	0.458	0.04	0.01	0.228	26
42	-0.0016	-0.0018	0.0002	0.865	0.434	-0.239	0.103	0.016	-0.35	29
43	-0.0008	-0.0007	-0.0001	0.688	-0.191	-0.66	0.292	0.21	-0.601	28
44	0.0001	0.0006	-0.0005	0.463	-0.652	-0.513	0.004	0.023	-0.07	39
45	0.0003	0.0006	-0.0003	0.628	-0.435	-0.114	0.018	0.013	0.162	40
46	-0.0001	0.0003	-0.0004	0.499	-0.491	-0.281	0.002	0.024	0.047	41
47	-0.0002	0.0002	-0.0004	0.397	-0.505	-0.325	0.001	0.026	0.023	42
48	-0.0003	0.0003	-0.0005	0.371	-0.717	-0.586	0.008	0.015	-0.085	38
49	-0.0002	0.0003	-0.0005	0.542	-0.652	-0.533	0.008	0.02	-0.102	43
50	-0.0006	-0.0002	-0.0004	0.499	-0.483	-0.264	0.003	0.022	0.06	50

CFz										
Run Order	Actual Value	Predicted Value	Residual	Leverage	Internally Studentized Residuals	Externally Studentized Residuals	Cook's Distance	Cook's Random Distance	Influence on Fitted Value DFFITS	Standard Order
1	-0.0051	-0.0056	0.0005	0.17	0.475	0.276	0.004	0.007	-0.033	25
2	-0.0065	-0.0077	0.0011	0.254	1.154	0.876	0.031	0.014	0.118	23
3	-0.0019	-0.0032	0.0012	0.41	1.271	1.102	0.114	0.107	0.284	20
4	-0.0061	-0.0067	0.0006	0.354	0.608	0.347	0.003	0.015	-0.037	21
5	-0.002	-0.0024	0.0004	0.257	0.447	0.224	0.009	0.003	-0.062	22
6	-0.0038	-0.004	0.0003	0.162	0.3	0.14	0.009	0.003	-0.055	24
7	-0.0128	-0.0133	0.0005	0.295	0.497	0.232	0.036	0.007	-0.114	12
8	-0.0039	-0.005	0.0011	0.224	1.065	0.829	0.01	0.002	0.065	11
9	-0.0135	-0.0143	0.0008	0.243	0.77	0.542	0	0.019	-0.005	8
10	-0.003	-0.0036	0.0006	0.316	0.615	0.363	0.009	0.007	-0.068	13
11	-0.0072	-0.0082	0.001	0.118	0.94	0.7	0.001	0.013	0.017	10
12	-0.0139	-0.0149	0.001	0.237	0.937	0.705	0.003	0.013	0.036	9
13	-0.0063	-0.0071	0.0008	0.204	0.816	0.547	0.001	0.019	0.015	47
14	-0.0107	-0.0113	0.0007	0.281	0.692	0.427	0.001	0.018	-0.016	46
15	-0.0132	-0.0139	0.0007	0.339	0.707	0.432	0	0.018	-0.015	44
16	-0.0061	-0.007	0.0009	0.184	0.89	0.604	0.002	0.013	0.025	48
17	-0.0019	-0.003	0.0011	0.234	1.104	0.802	0.015	0.001	0.081	49
18	-0.002	-0.0024	0.0003	0.453	0.334	-0.045	0.094	0.032	-0.251	45
19	-0.0034	-0.0029	-0.0006	0.28	-0.576	-0.399	0.002	0.015	-0.032	14
20	-0.0025	-0.0024	-0.0001	0.222	-0.099	0.01	0.016	0.001	0.074	17
21	-0.0011	-0.0003	-0.0008	0.354	-0.826	-0.68	0.043	0.003	-0.15	18
22	-0.0029	-0.0026	-0.0003	0.457	-0.351	-0.15	0.006	0.013	0.066	19
23	-0.0018	-0.0012	-0.0006	0.178	-0.616	-0.427	0.002	0.013	-0.026	15
24	-0.0008	-0.0006	-0.0003	0.425	-0.276	-0.07	0.018	0.006	0.102	16
25	-0.0041	-0.0036	-0.0005	0.393	-0.531	-0.365	0.002	0.018	-0.032	35
26	-0.0199	-0.0182	-0.0017	0.508	-1.787	-1.097	0	0.019	-0.012	36
27	-0.0127	-0.0112	-0.0015	0.435	-1.593	-0.856	0.022	0.014	0.106	33
28	-0.0062	-0.0044	-0.0018	0.399	-1.893	-1.253	0.006	0.015	-0.065	34
29	-0.0083	-0.0071	-0.0013	0.233	-1.308	-0.701	0.036	0.058	0.101	37
30	-0.0129	-0.0107	-0.0023	0.312	-2.349	-1.717	0.048	0.089	-0.192	1
31	0.0014	0.0006	0.0008	0.322	1.341	0.548	0.006	0.009	0.06	4
32	0.0006	0.0001	0.0005	0.671	0.891	0.131	0.031	0.008	-0.151	5
33	0.0006	0.0003	0.0003	0.504	0.473	-0.05	0.065	0.007	-0.211	6
34	0.0013	0.0006	0.0008	0.679	1.338	0.596	0.036	0.01	0.17	3
35	0.0017	0.0007	0.001	0.625	1.826	1.091	0.284	0.095	0.472	7
36	0.0006	0.0002	0.0004	0.537	0.671	0.064	0.037	0.001	-0.161	2
37	-0.0132	-0.0129	-0.0003	0.545	-0.528	-0.458	0.124	0.026	-0.281	31
38	-0.0132	-0.0131	-0.0001	0.519	-0.137	-0.135	0.012	0.01	-0.089	32
39	-0.0032	-0.0037	0.0005	0.755[1]	0.844	1.027	0.66	0.19	0.758	30
40	-0.0111	-0.0106	-0.0005	0.454	-0.808	-0.585	0.153	0.132	-0.297	27
41	-0.0144	-0.0153	0.0009	0.435	1.504	0.912	0.264	0.982	0.391	26
42	-0.003	-0.0033	0.0003	0.735[1]	0.454	0.466	0.142	0	0.327	29
43	-0.0051	-0.0048	-0.0003	0.481	-0.513	-0.378	0.062	0.007	-0.201	28
44	-0.0013	-0.0003	-0.001	0.157	-0.955	-0.728	0.004	0.009	-0.032	39
45	-0.0017	-0.0011	-0.0006	0.292	-0.618	-0.391	0.004	0.011	0.046	40
46	-0.0009	-0.0003	-0.0006	0.378	-0.577	-0.312	0.014	0.006	0.09	41
47	-0.001	-0.0005	-0.0004	0.139	-0.414	-0.255	0.006	0	0.043	42
48	-0.0015	-0.0007	-0.0008	0.163	-0.742	-0.535	0	0.019	0.001	38
49	-0.0021	-0.0009	-0.0012	0.38	-1.141	-0.996	0.059	0.01	-0.189	43
50	-0.0007	0.0002	-0.0009	0.313	-0.905	-0.703	0.007	0.012	-0.059	50

CMx										
Run Order	Actual Value	Predicted Value	Residual	Leverage	Internally Studentized Residuals	Externally Studentized Residuals	Cook's Distance	Cook's Random Distance	Influence on Fitted Value DFFITS	Standard Order
1	-0.01	-0.0099	-0.0001	0.239	-0.887	-0.797	0.01	0.008	-0.161	25
2	-0.0098	-0.0098	0	0.293	-0.273	-0.182	0	0.02	-0.001	23
3	-0.0099	-0.0099	0	0.391	0.204	0.33	0.012	0.006	0.207	20
4	-0.0099	-0.0098	-0.0001	0.394	-1.286	-1.257	0.062	0.018	-0.461	21
5	-0.0098	-0.0099	0	0.262	0.226	0.286	0.006	0.009	0.132	22
6	-0.01	-0.01	-2.40E-07	0.228	-0.003	0.057	0.001	0.014	0.059	24
7	-0.0102	-0.0105	0.0003	0.275	2.677	3.101	0.258[1]	1.968[1]	0.89	12
8	-0.0099	-0.0099	-0.0001	0.204	-0.618	-0.657	0.017	0.024	-0.199	11
9	-0.0102	-0.0101	0	0.376	-0.152	-0.31	0.014	0.009	-0.215	8
10	-0.0098	-0.0098	0	0.384	0.396	0.256	0	0.02	0.008	13
11	-0.0101	-0.0101	0	0.436	-0.277	-0.536	0.043	0.028	-0.372	10
12	-0.0102	-0.0102	0.0001	0.341	0.592	0.463	0.002	0.018	0.078	9
13	-0.0099	-0.0101	0.0002	0.214	1.967	1.856	0.038	0.155	0.302	47
14	-0.01	-0.0101	0.0001	0.334	1.173	0.843	0.003	0.021	0.092	46
15	-0.0102	-0.0102	0	0.398	-0.387	-0.77	0.09	0.307	-0.546	44
16	-0.0099	-0.01	0.0001	0.201	1.156	0.924	0.003	0.032	0.071	48
17	-0.0098	-0.01	0.0001	0.356	1.725	1.471	0.035	0.055	0.344	49
18	-0.0099	-0.0099	0.0001	0.4	0.857	0.477	0	0.018	-0.029	45
19	-0.0094	-0.0095	0	0.265	0.301	0.329	0.006	0.012	0.126	14
20	-0.0098	-0.0098	0	0.214	-0.515	-0.452	0.003	0.014	-0.079	17
21	-0.0099	-0.0098	-0.0001	0.372	-0.97	-0.934	0.033	0.001	-0.33	18
22	-0.0097	-0.0097	0	0.529	0.488	0.657	0.042	0.006	0.408	19
23	-0.0099	-0.0099	0	0.233	-0.447	-0.385	0.002	0.016	-0.069	15
24	-0.0099	-0.0099	0	0.453	-0.579	-0.547	0.014	0.013	-0.219	16
25	-0.0088	-0.0089	0	0.537	0.416	0.582	0.035	0.006	0.373	35
26	-0.0104	-0.0104	0	0.652	-0.358	0.654	0.181	0.234	0.798	36
27	-0.0102	-0.0101	-0.0001	0.338	-0.621	-0.225	0.01	0.063	0.162	33
28	-0.0101	-0.01	-0.0001	0.448	-1.762	-1.469	0.047	0.113	-0.425	34
29	-0.0102	-0.01	-0.0002	0.272	-2.035	-1.895	0.045	0.166	-0.374	37
30	-0.0104	-0.0102	-0.0002	0.519	-1.943	-1.669	0.092	0.112	-0.613	1
31	-0.0098	-0.0099	0	0.462	0.391	0.31	0.005	0.015	0.13	4
32	-0.0099	-0.0099	0	0.611	0.338	0.278	0.007	0.016	0.155	5
33	-0.0096	-0.0095	-0.0001	0.484	-0.762	-0.698	0.034	0.008	-0.362	6
34	-0.0098	-0.0099	0	0.703	0.498	0.433	0.023	0.017	0.287	3
35	-0.0089	-0.0089	0	0.606	-0.805	-0.849	0.077	0.004	-0.548	7
36	-0.0098	-0.0099	0.0001	0.547	1.028	0.912	0.06	0.002	0.491	2
37	-0.0101	-0.0102	0	0.412	0.533	0.43	0.008	0.01	0.166	31
38	-0.0107	-0.0106	-0.0001	0.455	-1.74	-1.506	0.145	0.391	-0.721	32
39	-0.0097	-0.0097	0	0.753	0.51	0.476	0.036	0.038	0.343	30
40	-0.0101	-0.0101	0	0.392	0.648	0.522	0.011	0.009	0.196	27
41	-0.0109	-0.0109	0	0.641	-0.694	-0.75	0.067	0.026	-0.509	26
42	-0.0096	-0.0097	0.0001	0.732	1.148	1.251	0.291	0.247	0.938	29
43	-0.0099	-0.0099	0	0.372	0.456	0.353	0.004	0.017	0.12	28
44	-0.0098	-0.0098	9.01E-06	0.455	0.108	0.094	0	0.02	0.031	39
45	-0.0094	-0.0095	0.0001	0.438	1.309	1.502	0.15	0.26	0.716	40
46	-0.0099	-0.01	0	0.359	0.322	0.324	0.004	0.014	0.114	41
47	-0.0099	-0.0099	0	0.27	-0.29	-0.302	0.003	0.012	-0.097	42
48	-0.0097	-0.0096	-0.0001	0.237	-0.574	-0.58	0.01	0.002	-0.159	38
49	-0.009	-0.009	0	0.335	-0.2	-0.223	0.003	0.014	-0.091	43
50	-0.0099	-0.0099	0	0.367	-0.193	-0.232	0.004	0.015	-0.106	50

CMy										
Run Order	Actual Value	Predicted Value	Residual	Leverage	Internally Studentized Residuals	Externally Studentized Residuals	Cook's Distance	Cook's Random Distance	Influence on Fitted Value DFFITS	Standard Order
1	0.0026	0.002	0.0006	0.214	1.138	0.836	0.006	0.009	0.04	25
2	0.0026	0.002	0.0006	0.291	1.062	0.768	0.003	0.018	0.033	23
3	0.0011	0.0005	0.0007	0.51	1.239	1.042	0.064	0.002	0.207	20
4	0.0033	0.0027	0.0005	0.39	1.015	0.714	0.001	0.02	0.023	21
5	0.001	0.0008	0.0003	0.302	0.475	0.155	0.069	0.137	-0.168	22
6	0.0021	0.0016	0.0005	0.179	0.967	0.676	0	0.021	0.001	24
7	0.0068	0.0069	-0.0001	0.343	-0.256	-0.269	0.02	0.006	-0.082	12
8	0.0017	0.0017	0	0.264	-0.052	-0.022	0.001	0.019	0.016	11
9	0.0075	0.0075	0	0.304	-0.085	-0.055	0	0.021	0.007	8
10	0.0012	0.001	0.0002	0.442	0.285	0.475	0.135	0.095	0.272	13
11	0.0038	0.0042	-0.0004	0.232	-0.769	-0.743	0.096	0.576	-0.175	10
12	0.0077	0.0075	0.0001	0.349	0.246	0.338	0.053	0.02	0.16	9
13	0.0025	0.0019	0.0006	0.25	1.028	0.863	0.053	0.073	0.134	47
14	0.0043	0.0041	0.0002	0.345	0.384	0.189	0.011	0.006	-0.073	46
15	0.0048	0.0046	0.0003	0.433	0.482	0.273	0.005	0.016	-0.051	44
16	0.003	0.0027	0.0003	0.197	0.459	0.301	0.001	0.016	-0.019	48
17	0.0008	0.0004	0.0004	0.346	0.655	0.491	0.004	0.017	0.041	49
18	0.0007	0.0004	0.0002	0.4	0.392	0.175	0.015	0.005	-0.09	45
19	0.0012	0.0013	-0.0001	0.267	-0.154	-0.204	0.019	0	-0.084	14
20	0.0014	0.0011	0.0003	0.234	0.489	0.497	0.043	0.04	0.113	17
21	0.0002	0.0002	0.0001	0.269	0.093	0.071	0	0.021	-0.002	18
22	0.0015	0.0015	0	0.474	-0.027	-0.123	0.017	0.008	-0.102	19
23	0.0008	0.0008	1.99E-06	0.257	0.003	-0.029	0.003	0.015	-0.032	15
24	0.0001	0	0.0002	0.38	0.286	0.324	0.022	0.002	0.104	16
25	0.0011	0.0011	2.99E-06	0.427	0.005	-0.059	0.007	0.013	-0.063	35
26	0.0054	0.0067	-0.0012	0.461	-2.112	-1.755	0.027	0.012	-0.131	36
27	0.0047	0.0057	-0.001	0.332	-1.715	-1.166	0.039	0.02	0.119	33
28	-0.0009	0.0006	-0.0015	0.324	-2.549	-2.445	0.183	0.591	-0.309	34
29	0.0018	0.0027	-0.0009	0.225	-1.533	-1.04	0.05	0.118	0.114	37
30	0.0022	0.0033	-0.0012	0.282	-1.97	-1.541	0	0.021	-0.01	1
31	0.0006	0.0006	0	0.462	-0.078	-0.026	0	0.02	0.012	4
32	0.0002	0.0003	-0.0001	0.596	-0.157	-0.119	0.003	0.019	-0.044	5
33	0.0003	0.0004	-0.0001	0.413	-0.301	-0.229	0.013	0.007	-0.079	6
34	0.0005	0.0005	-0.0001	0.605	-0.13	-0.084	0.001	0.021	-0.022	3
35	0.0007	0.0006	0.0001	0.554	0.288	0.419	0.137	0.032	0.28	7
36	0.0002	0.0003	-0.0001	0.454	-0.243	-0.184	0.008	0.013	-0.064	2
37	0.009	0.0084	0.0006	0.447	1.331	0.646	0	0.02	-0.014	31
38	0.0089	0.008	0.0009	0.471	2.02	1.344	0.165	0.201	0.312	32
39	0.0018	0.0012	0.0006	0.706	1.399	0.64	0	0.021	-0.006	30
40	0.007	0.0066	0.0005	0.355	1.112	0.484	0.013	0.004	-0.073	27
41	0.0099	0.0095	0.0004	0.517	1.047	0.314	0.073	0.003	-0.196	26
42	0.0014	0.0007	0.0007	0.704	1.6	1.011	0.108	0.001	0.268	29
43	0.0031	0.0026	0.0005	0.526	1.253	0.531	0.011	0.012	-0.076	28
44	0.0004	0.0007	-0.0003	0.254	-0.455	-0.348	0.001	0.02	-0.015	39
45	0.0006	0.0008	-0.0002	0.495	-0.33	-0.167	0.007	0.015	0.065	40
46	0	0.0001	-0.0001	0.406	-0.207	-0.036	0.024	0.002	0.112	41
47	0.0003	0.0006	-0.0003	0.271	-0.508	-0.404	0.003	0.015	-0.032	42
48	0.0005	0.0007	-0.0002	0.263	-0.399	-0.291	0	0.021	0.001	38
49	0.0003	0.0006	-0.0003	0.434	-0.494	-0.41	0.006	0.015	-0.057	43
50	0	0.0002	-0.0003	0.356	-0.481	-0.385	0.003	0.017	-0.037	50

CMz										
Run Order	Actual Value	Predicted Value	Residual	Leverage	Internally Studentized Residuals	Externally Studentized Residuals	Cook's Distance	Cook's Random Distance	Influence on Fitted Value DFFITS	Standard Order
1	-0.0033	-0.0034	0.0001	0.215	0.112	0.114	0.002	0.012	0.039	25
2	-0.0045	-0.0042	-0.0003	0.272	-0.397	-0.348	0.008	0.006	-0.088	23
3	-0.0014	-0.0015	0	0.347	0.064	0.096	0.003	0.013	0.055	20
4	-0.0033	-0.0035	0.0002	0.364	0.25	0.298	0.018	0.004	0.139	21
5	-0.0013	-0.0012	-0.0001	0.217	-0.111	-0.081	0	0.017	-0.006	22
6	-0.0023	-0.002	-0.0003	0.218	-0.41	-0.341	0.006	0.005	-0.069	24
7	-0.0082	-0.0062	-0.002	0.202	-2.781	-2.732	0.144	0.639	-0.331	12
8	-0.0029	-0.0023	-0.0006	0.174	-0.915	-0.53	0.021	0.059	0.112	11
9	-0.0065	-0.0053	-0.0012	0.271	-1.79	-1.33	0.003	0.018	-0.054	8
10	-0.0026	-0.0019	-0.0006	0.303	-0.882	-0.341	0.073	0.136	0.249	13
11	-0.0045	-0.0032	-0.0012	0.258	-1.783	-1.338	0.003	0.019	-0.054	10
12	-0.0066	-0.0053	-0.0013	0.216	-1.84	-1.393	0.004	0.015	-0.055	9
13	-0.0039	-0.0036	-0.0003	0.183	-0.442	-0.363	0.007	0.006	-0.063	47
14	-0.0045	-0.0051	0.0006	0.29	0.89	0.872	0.077	0.158	0.288	46
15	-0.0063	-0.0063	0	0.336	0.048	0.081	0.002	0.014	0.05	44
16	-0.0033	-0.0032	-0.0001	0.177	-0.103	-0.071	0	0.018	-0.002	48
17	-0.0016	-0.0012	-0.0005	0.337	-0.723	-0.702	0.058	0.015	-0.24	49
18	-0.0013	-0.0011	-0.0001	0.384	-0.227	-0.201	0.003	0.014	-0.06	45
19	-0.0026	-0.0022	-0.0004	0.199	-0.573	-0.462	0.01	0.001	-0.08	14
20	-0.0016	-0.0014	-0.0002	0.159	-0.357	-0.272	0.002	0.012	-0.031	17
21	-0.0007	-0.0004	-0.0002	0.314	-0.366	-0.31	0.006	0.011	-0.075	18
22	-0.0017	-0.0016	-0.0001	0.382	-0.203	-0.149	0	0.017	-0.023	19
23	-0.0012	-0.0014	0.0002	0.213	0.282	0.273	0.011	0.001	0.086	15
24	-0.0005	-0.0007	0.0002	0.379	0.374	0.466	0.052	0.002	0.231	16
25	-0.0029	-0.0028	-0.0001	0.46	-0.202	-0.15	0.001	0.018	-0.029	35
26	-0.0074	-0.0079	0.0005	0.459	0.779	0.15	0.069	0.023	-0.304	36
27	-0.0034	-0.0046	0.0013	0.287	1.909	1.59	0.062	0.062	0.242	33
28	-0.0012	-0.0023	0.0011	0.353	1.643	1.195	0.018	0.009	0.146	34
29	-0.0029	-0.0036	0.0008	0.254	1.136	0.705	0.001	0.014	-0.031	37
30	-0.0041	-0.005	0.0008	0.385	1.272	0.778	0	0.017	-0.008	1
31	-0.0003	-0.0007	0.0004	0.294	0.805	0.489	0.022	0.004	0.154	4
32	-0.0003	-0.0001	-0.0001	0.495	-0.308	-0.213	0.008	0.012	-0.099	5
33	-0.0002	-0.0001	-0.0001	0.367	-0.23	-0.135	0.002	0.016	-0.044	6
34	-0.0003	0.0001	-0.0003	0.578	-0.835	-0.685	0.112	0.006	-0.393	3
35	-0.0002	-0.0003	0.0002	0.479	0.378	0.301	0.02	0.007	0.159	7
36	-0.0002	-0.0001	-0.0001	0.387	-0.215	-0.129	0.002	0.017	-0.044	2
37	-0.0036	-0.004	0.0004	0.377	0.968	0.405	0	0.018	0.018	31
38	-0.0057	-0.0063	0.0006	0.345	1.319	0.615	0.007	0.007	0.088	32
39	-0.0031	-0.0038	0.0007	0.578	1.744	0.935	0.091	0.009	0.344	30
40	-0.0041	-0.0043	0.0002	0.244	0.406	0.106	0.005	0.005	-0.065	27
41	-0.0045	-0.0055	0.001	0.502	2.303	1.412	0.209	0.166	0.532	26
42	-0.0024	-0.0022	-0.0002	0.571	-0.545	-0.938	0.552	0.94	-0.76	29
43	-0.0037	-0.004	0.0003	0.305	0.625	0.207	0.002	0.013	-0.049	28
44	-0.001	-0.0012	0.0002	0.3	0.297	0.254	0.002	0.015	0.046	39
45	-0.0011	-0.0006	-0.0005	0.366	-0.789	-0.964	0.18	0.339	-0.43	40
46	-0.0004	-0.0006	0.0003	0.28	0.359	0.318	0.005	0.011	0.064	41
47	-0.0006	-0.0006	0.0001	0.174	0.085	0.049	0	0.017	-0.012	42
48	-0.0009	-0.0012	0.0003	0.208	0.439	0.382	0.006	0.007	0.063	38
49	-0.0011	-0.0017	0.0006	0.289	0.813	0.795	0.056	0.028	0.219	43
50	-0.0002	-0.0001	-0.0001	0.286	-0.076	-0.129	0.007	0.009	-0.075	50

Residual Diagnostics for 5-Blade Experiment

CFx										
Run Order	Actual Value	Predicted Value	Residual	Leverage	Internally Studentized Residuals	Externally Studentized Residuals	Cook's Distance	Cook's Random Distance	Influence on Fitted Value DFFITS	Standard Order
1	0.1563	0.1576	-0.0012	0.224	-0.63	-0.305	0.012	0.028	0.13	48
2	0.158	0.1595	-0.0015	0.596	-0.906	-0.119	0.036	0.001	0.358	50
3	0.1548	0.1545	0.0003	0.223	0.157	0.437	0.105	0.92	0.336	47
4	0.1545	0.1593	-0.0048	0.505	-2.675	-2.825	0.307	0.489	-1.078	49
5	0.1552	0.1576	-0.0025	0.664	-1.454	-0.806	0.003	0.018	-0.102	46
6	0.1539	0.1566	-0.0027	0.448	-1.517	-1.05	0.005	0.017	-0.127	45
7	0.1643	0.1695	-0.0052	0.383	-2.759	-3.004	0.251	0.7	-0.9	51
8	0.1589	0.1575	0.0014	0.664	0.9	0.173	0.017	0.009	-0.24	36
9	0.1567	0.1526	0.0041	0.207	2.166	1.84	0.034	0.102	0.259	35
10	0.1612	0.1591	0.0021	0.574	1.264	0.789	0.006	0.017	0.137	32
11	0.1554	0.1549	0.0005	0.26	0.263	-0.014	0.019	0.024	-0.184	33
12	0.1568	0.154	0.0028	0.329	1.509	1.173	0.016	0.012	0.192	37
13	0.1556	0.1539	0.0018	0.22	0.929	0.621	0	0.016	-0.007	34
14	0.1537	0.1524	0.0013	0.244	0.68	0.375	0.002	0.01	-0.069	31
15	0.1512	0.1525	-0.0013	0.26	-0.648	-0.54	0.004	0.014	-0.083	23
16	0.1454	0.1453	0.0002	0.283	0.088	0.192	0.008	0.004	0.132	20
17	0.1455	0.1451	0.0004	0.35	0.226	0.394	0.025	0.001	0.244	21
18	0.1478	0.1494	-0.0016	0.264	-0.837	-0.713	0.008	0.003	-0.131	17
19	0.1536	0.1548	-0.0012	0.462	-0.675	-0.591	0.011	0.009	-0.18	22
20	0.1451	0.1456	-0.0005	0.342	-0.287	-0.155	0	0.016	0.033	18
21	0.152	0.1533	-0.0013	0.316	-0.68	-0.581	0.006	0.014	-0.117	19
22	0.1564	0.1549	0.0014	0.321	0.976	0.498	0.001	0.017	0.037	15
23	0.1564	0.1568	-0.0004	0.446	-0.257	-0.499	0.056	0.035	-0.391	14
24	0.1571	0.1554	0.0018	0.511	1.352	0.77	0.017	0.016	0.218	12
25	0.1638	0.1621	0.0018	0.524	1.333	0.774	0.019	0.023	0.23	9
26	0.1554	0.1557	-0.0003	0.532	-0.244	-0.613	0.088	0.029	-0.519	16
27	0.1738	0.1724	0.0015	0.302	1.007	0.528	0.001	0.017	0.044	13
28	0.158	0.1558	0.0022	0.601	1.783	1.113	0.07	0.003	0.467	11
29	0.1912	0.189	0.0022	0.751	2.066	1.395	0.227	0.022	0.818	10
30	0.1549	0.1541	0.0008	0.36	0.442	0.338	0.001	0.015	0.059	56
31	0.1469	0.1467	0.0002	0.319	0.109	0.01	0.002	0.014	-0.061	58
32	0.1406	0.1399	0.0007	0.17	0.381	0.288	0	0.016	0.017	55
33	0.1349	0.1346	0.0003	0.588	0.179	-0.029	0.005	0.013	-0.121	54
34	0.1456	0.1459	-0.0003	0.217	-0.167	-0.212	0.006	0.004	-0.096	53
35	0.1549	0.1535	0.0014	0.355	0.778	0.681	0.013	0.004	0.186	52
36	0.1538	0.1529	0.001	0.188	0.489	0.382	0.001	0.014	0.038	57
37	0.088	0.0867	0.0012	0.828[1]	1.231	1.634	0.72	0.111	1.354	6
38	0.1405	0.1386	0.0019	0.442	1.44	1.086	0.082	0.066	0.478	3
39	0.1372	0.137	0.0002	0.525	0.121	0.072	0	0.016	0.025	5
40	0.1507	0.1508	-0.0001	0.692	-0.084	-0.135	0.004	0.015	-0.11	8
41	0.1182	0.1174	0.0008	0.309	0.582	0.387	0.006	0.007	0.114	4
42	0.1528	0.1535	-0.0008	0.656	-0.644	-0.687	0.078	0.001	-0.478	2
43	0.1318	0.1332	-0.0014	0.437	-1.013	-0.788	0.048	0.012	-0.362	1
44	0.1153	0.1165	-0.0012	0.723	-1.109	-1.238	0.272	0.052	-0.916	7
45	0.1105	0.1105	5.71E-06	0.409	0.003	-0.14	0.007	0.009	-0.142	28
46	0.1037	0.104	-0.0003	0.157	-0.147	-0.172	0.003	0.005	-0.063	29
47	0.1282	0.1279	0.0003	0.276	0.169	0.088	0	0.016	-0.031	27
48	0.137	0.1367	0.0003	0.206	0.145	0.081	0	0.015	-0.026	24
49	0.1502	0.1483	0.0019	0.371	1.005	0.996	0.039	0.005	0.324	30
50	0.1064	0.1047	0.0017	0.444	0.905	0.932	0.042	0.002	0.356	26
51	0.1508	0.1507	0.0001	0.282	0.064	-0.023	0.002	0.012	-0.068	25
52	0.154	0.1555	-0.0015	0.541	-0.888	-0.618	0.007	0.015	-0.145	39
53	0.1476	0.1482	-0.0006	0.204	-0.312	-0.155	0.002	0.01	0.057	41
54	0.1296	0.1301	-0.0005	0.267	-0.265	-0.08	0.004	0.007	0.092	43
55	0.1225	0.1221	0.0004	0.254	0.205	0.345	0.025	0.032	0.211	44
56	0.1473	0.1491	-0.0018	0.385	-1.025	-0.797	0.011	0.009	-0.167	38
57	0.0984	0.1018	-0.0034	0.479	-1.96	-1.979	0.184	0.232	-0.795	40
58	0.1232	0.1245	-0.0014	0.196	-0.719	-0.512	0	0.017	-0.021	42

CFy										
Run Order	Actual Value	Predicted Value	Residual	Leverage	Internally Studentized Residuals	Externally Studentized Residuals	Cook's Distance	Cook's Random Distance	Influence on Fitted Value DFFITS	Standard Order
1	0	-3.33E-06	0	0.11	0.037	0.025	0	0.013	-0.003	48
2	0.0003	0.0001	0.0001	0.321	0.152	0.137	0.001	0.012	0.031	50
3	-0.0007	-0.0012	0.0005	0.171	0.54	0.486	0.021	0	0.086	47
4	0.0018	0.0008	0.001	0.212	1.009	0.973	0.107	0.179	0.223	49
5	-0.0003	0	-0.0003	0.389	-0.356	-0.467	0.063	0	-0.222	46
6	0.0002	0.0005	-0.0002	0.252	-0.26	-0.268	0.009	0.003	-0.083	45
7	0	0.0006	-0.0007	0.196	-0.684	-0.657	0.052	0.045	-0.154	51
8	-0.0023	-0.0008	-0.0015	0.331	-1.536	-1.236	0.012	0.009	-0.096	36
9	-0.0017	2.56E-06	-0.0017	0.102	-1.677	-1.379	0.005	0.004	-0.042	35
10	-0.0009	0.001	-0.0019	0.277	-1.979	-1.779	0.079	0.04	-0.235	32
11	-0.0002	-0.0001	-0.0002	0.177	-0.167	0.083	0.113	0.552	0.208	33
12	-0.0011	-0.0001	-0.001	0.183	-1.044	-0.751	0.005	0.006	0.046	37
13	-0.0013	-5.35E-06	-0.0013	0.149	-1.311	-1.031	0	0.013	-0.007	34
14	-0.0024	-0.0008	-0.0016	0.182	-1.588	-1.291	0.007	0.006	-0.059	31
15	0.0006	-0.0006	0.0012	0.129	1.282	0.972	0	0.013	0.01	23
16	0.0017	0.0001	0.0016	0.171	1.646	1.302	0.01	0.003	0.073	20
17	0.0019	0.0007	0.0013	0.202	1.327	1.001	0.001	0.013	0.024	21
18	0.0009	0.0003	0.0005	0.163	0.566	0.309	0.024	0.028	-0.103	17
19	0.0016	0.0009	0.0008	0.247	0.794	0.45	0.026	0.006	-0.117	22
20	0.0011	-0.0004	0.0015	0.202	1.626	1.287	0.013	0.003	0.085	18
21	0.0006	-0.0009	0.0015	0.164	1.543	1.22	0.008	0.007	0.057	19
22	-0.0009	-0.0012	0.0003	0.216	0.453	0.27	0.002	0.009	0.035	15
23	-0.0001	-0.0002	0.0002	0.135	0.221	0.118	0	0.013	0	14
24	-0.0008	-0.0003	-0.0004	0.263	-0.592	-0.47	0.048	0.017	-0.164	12
25	0.0013	0.0005	0.0007	0.309	1.02	0.717	0.065	0.018	0.199	9
26	-0.0008	-0.0014	0.0006	0.34	0.774	0.532	0.029	0	0.146	16
27	0.0017	0.0017	-0.0001	0.239	-0.077	-0.091	0.005	0.007	-0.051	13
28	-0.0015	-0.001	-0.0004	0.37	-0.593	-0.539	0.083	0.028	-0.249	11
29	0.0031	0.0026	0.0005	0.463[1]	0.67	0.511	0.043	0.001	0.192	10
30	-0.0009	-0.0006	-0.0003	0.203	-0.333	-0.264	0.001	0.012	-0.02	56
31	0.0013	0.0007	0.0006	0.116	0.67	0.603	0.027	0.11	0.1	58
32	-0.0005	0.0002	-0.0008	0.133	-0.782	-0.661	0.015	0.002	-0.072	55
33	0.0004	0.0003	0.0001	0.31	0.121	0.22	0.027	0.001	0.134	54
34	-0.0015	-0.0007	-0.0007	0.135	-0.775	-0.651	0.012	0.002	-0.07	53
35	-0.0003	-5.51E-06	-0.0003	0.173	-0.27	-0.205	0	0.013	-0.006	52
36	0.0002	0.0005	-0.0003	0.13	-0.342	-0.269	0	0.012	-0.013	57
37	0.0008	0.0007	0.0001	0.512[1]	0.146	-0.129	0.047	0.002	-0.2	6
38	1.68E-06	-0.0001	0.0001	0.266	0.075	-0.039	0.01	0.003	-0.08	3
39	0.0025	0.0021	0.0004	0.206	0.485	0.275	0	0.013	0.005	5
40	0.0011	0.0002	0.0009	0.436	1.216	0.932	0.113	0.02	0.31	8
41	0.0015	0.0013	0.0002	0.208	0.222	0.087	0.003	0.008	-0.036	4
42	0.0014	0.0011	0.0003	0.331	0.44	0.227	0	0.013	-0.008	2
43	0.0012	0.0005	0.0008	0.143	0.977	0.611	0.006	0.001	0.054	1
44	0.0019	0.0017	0.0002	0.41	0.269	0.059	0.008	0.008	-0.079	7
45	-0.0006	0.0007	-0.0013	0.205	-1.365	-1.073	0.005	0.009	-0.052	28
46	0.0001	0.0006	-0.0004	0.156	-0.454	-0.234	0.023	0.034	0.102	29
47	0.0013	0.0019	-0.0007	0.215	-0.694	-0.41	0.019	0.003	0.099	27
48	-0.0004	0.0009	-0.0013	0.095	-1.352	-1.063	0.001	0.009	-0.022	24
49	0.0002	0.0018	-0.0015	0.297	-1.615	-1.364	0.043	0.004	-0.172	30
50	-0.0008	0.0002	-0.001	0.197	-1.075	-0.791	0	0.012	0.01	26
51	-0.0017	-0.0001	-0.0015	0.171	-1.587	-1.31	0.019	0.005	-0.088	25
52	0.0028	0.0017	0.0011	0.327	1.075	0.931	0.015	0.007	0.104	39
53	0.0009	9.25E-08	0.0009	0.136	0.909	0.747	0	0.013	0.013	41
54	0.0011	-0.0001	0.0011	0.112	1.106	0.937	0.003	0.007	0.034	43
55	0.0014	0.0008	0.0006	0.158	0.607	0.448	0.004	0.006	-0.037	44
56	0.0005	-0.0003	0.0008	0.222	0.849	0.675	0	0.013	0.005	38
57	0.0017	0.0004	0.0013	0.209	1.26	1.11	0.019	0.002	0.103	40
58	0.0004	0.0003	0.0002	0.133	0.185	0.059	0.022	0.028	-0.088	42

CFz										
Run Order	Actual Value	Predicted Value	Residual	Leverage	Internally Studentized Residuals	Externally Studentized Residuals	Cook's Distance	Cook's Random Distance	Influence on Fitted Value DFFITS	Standard Order
1	-0.0099	-0.0108	0.0009	0.156	0.825	0.638	0.004	0.002	0.053	48
2	-0.0146	-0.0149	0.0002	0.404	0.201	0.002	0.013	0.005	-0.129	50
3	-0.0048	-0.0055	0.0007	0.238	0.621	0.48	0.003	0.012	0.045	47
4	-0.0104	-0.011	0.0006	0.29	0.518	0.378	0.001	0.014	0.022	49
5	-0.0026	-0.0028	0.0003	0.498	0.254	-0.011	0.024	0.005	-0.17	46
6	-0.0106	-0.0115	0.0009	0.254	0.874	0.704	0.011	0	0.104	45
7	-0.0162	-0.0162	2.63E-06	0.233	0.002	-0.106	0.016	0.001	-0.108	51
8	-0.0045	-0.0022	-0.0024	0.473	-2.447	-2.022	0.19	0.147	-0.52	36
9	-0.0119	-0.0097	-0.0022	0.152	-2.104	-1.51	0.01	0.009	-0.082	35
10	-0.0183	-0.0157	-0.0026	0.41	-2.611	-2.305	0.234	0.363	-0.561	32
11	-0.0049	-0.0041	-0.0008	0.255	-0.795	-0.315	0.046	0.075	0.177	33
12	-0.0024	-0.0013	-0.0011	0.254	-1.097	-0.588	0.013	0.006	0.101	37
13	-0.0133	-0.0121	-0.0012	0.182	-1.167	-0.697	0.006	0.007	0.054	34
14	-0.0064	-0.0056	-0.0009	0.263	-0.871	-0.388	0.027	0.022	0.156	31
15	-0.0047	-0.0054	0.0007	0.131	0.639	0.364	0.013	0.036	-0.078	23
16	-0.0109	-0.013	0.0021	0.223	1.944	1.527	0.023	0.013	0.141	20
17	-0.0088	-0.0108	0.002	0.271	1.872	1.491	0.03	0.012	0.164	21
18	-0.0074	-0.0087	0.0013	0.28	1.261	0.836	0	0.013	-0.021	17
19	-0.0001	-0.0007	0.0005	0.329	0.505	0.02	0.104	0.192	-0.307	22
20	-0.0099	-0.0115	0.0016	0.243	1.486	1.068	0.002	0.013	0.04	18
21	-0.0001	-0.0021	0.002	0.16	1.85	1.449	0.015	0.012	0.089	19
22	-0.0055	-0.0052	-0.0002	0.275	-0.322	-0.159	0.001	0.013	-0.025	15
23	-0.0112	-0.01	-0.0013	0.214	-1.717	-0.93	0.045	0.244	-0.19	14
24	-0.008	-0.0078	-0.0001	0.456	-0.22	-0.1	0	0.014	-0.016	12
25	-0.0154	-0.0154	-0.0001	0.456	-0.125	-0.031	0	0.014	0.017	9
26	-0.0037	-0.0041	0.0004	0.52	0.604	0.537	0.082	0.008	0.317	16
27	-0.0146	-0.0148	0.0002	0.377	0.26	0.209	0.011	0.004	0.106	13
28	-0.0055	-0.0054	-0.0002	0.513	-0.251	-0.119	0.001	0.014	-0.027	11
29	-0.0162	-0.0165	0.0003	0.623[1]	0.536	0.601	0.129	0.006	0.418	10
30	-0.0019	-0.0015	-0.0004	0.334	-0.367	-0.287	0.003	0.012	-0.05	56
31	-0.004	-0.0034	-0.0005	0.151	-0.52	-0.394	0.002	0.006	-0.04	58
32	-0.0061	-0.0053	-0.0008	0.145	-0.739	-0.576	0.009	0	-0.068	55
33	-0.0064	-0.0065	0.0002	0.404	0.167	0.294	0.032	0.001	0.19	54
34	-0.0039	-0.0041	0.0002	0.151	0.16	0.162	0.005	0.002	0.052	53
35	-0.0011	-0.0006	-0.0005	0.179	-0.483	-0.37	0.003	0.007	-0.043	52
36	-0.001	-0.0012	0.0002	0.202	0.176	0.193	0.008	0.001	0.075	57
37	0.0016	0.0015	0.0001	0.723[1]	0.136	-0.317	0.096	0.001	-0.357	6
38	0.0006	0.0005	0.0001	0.447	0.139	-0.06	0.011	0.007	-0.11	3
39	0.0012	0.001	0.0002	0.324	0.244	0.05	0.002	0.011	-0.046	5
40	0.0017	0.0013	0.0004	0.640[1]	0.728	0.338	0.008	0.012	0.105	8
41	0.0016	0.0015	0.0001	0.297	0.212	0.038	0.002	0.01	-0.046	4
42	0.0013	0.001	0.0003	0.536	0.418	0.102	0.002	0.013	-0.043	2
43	0.0019	0.001	0.0009	0.23	1.267	0.626	0.013	0.001	0.102	1
44	0.0014	0.0007	0.0006	0.613	1.032	0.602	0.052	0.002	0.263	7
45	-0.0015	-0.0009	-0.0007	0.25	-0.624	-0.435	0	0.014	0.009	28
46	-0.0014	-0.001	-0.0004	0.189	-0.343	-0.19	0.005	0.004	0.058	29
47	-0.0002	-0.0002	0	0.229	-0.043	0.115	0.028	0.02	0.146	27
48	-0.0017	-0.0004	-0.0013	0.118	-1.173	-0.934	0.006	0.001	-0.058	24
49	-0.0009	-0.0002	-0.0008	0.327	-0.713	-0.517	0	0.014	-0.019	30
50	-0.0023	-0.0014	-0.0009	0.243	-0.864	-0.677	0.004	0.01	-0.055	26
51	-0.0011	-0.0001	-0.0011	0.188	-0.975	-0.787	0.008	0.005	-0.066	25
52	0.0014	0.0005	0.0009	0.463	0.923	0.885	0.092	0.01	0.331	39
53	-0.001	-0.0013	0.0003	0.183	0.275	0.165	0	0.013	-0.016	41
54	-0.0022	-0.0027	0.0005	0.178	0.449	0.307	0	0.014	0.012	43
55	-0.003	-0.0027	-0.0003	0.248	-0.302	-0.356	0.035	0.023	-0.162	44
56	-0.0006	-0.0012	0.0006	0.321	0.606	0.459	0.006	0.008	0.076	38
57	-0.0038	-0.0045	0.0007	0.411	0.677	0.546	0.014	0.006	0.133	40
58	-0.0025	-0.0026	0.0001	0.162	0.135	0.056	0.002	0.008	-0.033	42

CMx										
Run Order	Actual Value	Predicted Value	Residual	Leverage	Internally Studentized Residuals	Externally Studentized Residuals	Cook's Distance	Cook's Random Distance	Influence on Fitted Value DFFITS	Standard Order
1	-0.0117	-0.0118	0.0001	0.185	0.468	0.148	0.043	0.187	-0.196	48
2	-0.0118	-0.012	0.0002	0.45	1.792	1.187	0.004	0.013	0.092	50
3	-0.0115	-0.0115	0	0.161	0.167	-0.118	0.09	0.613	-0.24	47
4	-0.0116	-0.012	0.0004	0.421	3.41	3.569	0.484	0.798	1.114	49
5	-0.0115	-0.0116	0.0001	0.487[1]	0.58	-0.33	0.221	0.202	-0.673	46
6	-0.0116	-0.0119	0.0002	0.362	1.891	1.424	0.012	0.018	0.151	45
7	-0.012	-0.0125	0.0005	0.268	3.682	4.314[2]	0.430[3]	1.689[3]	0.93	51
8	-0.0117	-0.0117	-0.0001	0.376	-0.608	-0.611	0.016	0.005	-0.179	36
9	-0.0119	-0.0117	-0.0001	0.129	-1.032	-1.012	0.017	0.005	-0.119	35
10	-0.0122	-0.0122	0	0.241	-0.116	-0.058	0.001	0.013	0.033	32
11	-0.0116	-0.0116	0.0001	0.146	0.379	0.418	0.011	0.002	0.1	33
12	-0.0116	-0.0115	-0.0001	0.187	-0.497	-0.471	0.003	0.011	-0.061	37
13	-0.0118	-0.0118	0	0.107	0.266	0.287	0.005	0.003	0.058	34
14	-0.0116	-0.0116	0	0.138	-0.194	-0.159	0	0.013	0.004	31
15	-0.0115	-0.0116	0.0001	0.097	0.592	0.561	0.002	0.011	0.036	23
16	-0.0118	-0.0117	-0.0001	0.102	-0.474	-0.499	0.011	0.014	-0.086	20
17	-0.0117	-0.0117	0	0.161	-0.285	-0.349	0.012	0.001	-0.106	21
18	-0.0116	-0.0116	0.0001	0.116	0.551	0.514	0.002	0.009	0.034	17
19	-0.0114	-0.0115	0.0001	0.252	0.874	0.877	0.021	0	0.179	22
20	-0.0117	-0.0116	0	0.146	-0.318	-0.369	0.009	0	-0.098	18
21	-0.0114	-0.0115	0.0002	0.099	1.29	1.29	0.021	0.028	0.117	19
22	-0.0116	-0.0115	-0.0002	0.191	-1.257	-0.928	0.001	0.014	-0.029	15
23	-0.0117	-0.0117	-0.0001	0.241	-0.419	-0.125	0.019	0.014	0.161	14
24	-0.0117	-0.0116	-0.0001	0.321	-0.829	-0.436	0.007	0.009	0.105	12
25	-0.0125	-0.0122	-0.0002	0.253	-1.897	-1.622	0.042	0.047	-0.237	9
26	-0.0116	-0.0115	-0.0001	0.327	-0.653	-0.258	0.014	0.003	0.163	16
27	-0.0129	-0.0126	-0.0003	0.173	-2.045	-1.71	0.025	0.026	-0.169	13
28	-0.0117	-0.0116	-0.0001	0.344	-1.039	-0.632	0.001	0.012	0.038	11
29	-0.0136	-0.0134	-0.0002	0.531[1]	-1.846	-1.426	0.079	0.006	-0.418	10
30	-0.0117	-0.0116	-0.0001	0.151	-0.55	-0.465	0	0.013	0.004	56
31	-0.0117	-0.0116	-0.0001	0.146	-0.443	-0.357	0	0.012	0.021	58
32	-0.0117	-0.0115	-0.0002	0.065	-1.374	-1.315	0.007	0.006	-0.06	55
33	-0.0115	-0.0114	-0.0001	0.279	-0.811	-0.727	0.005	0.017	-0.084	54
34	-0.0117	-0.0116	-0.0001	0.082	-0.932	-0.87	0.002	0.009	-0.034	53
35	-0.0116	-0.0116	0	0.12	-0.223	-0.146	0.003	0.006	0.046	52
36	-0.0116	-0.0116	0	0.087	-0.143	-0.086	0.002	0.005	0.04	57
37	-0.0096	-0.0095	-0.0001	0.553[1]	-0.493	-0.96	0.222	0.027	-0.691	6
38	-0.0116	-0.0116	0	0.28	0.28	0.179	0	0.013	-0.015	3
39	-0.0114	-0.0115	0	0.369	0.412	0.297	0.001	0.014	0.03	5
40	-0.0116	-0.0117	0.0001	0.473	0.805	0.717	0.028	0.004	0.248	8
41	-0.0108	-0.0108	0	0.176	0.188	0.116	0	0.012	-0.023	4
42	-0.0116	-0.0116	0	0.302	0.334	0.229	0	0.013	0.001	2
43	-0.0113	-0.0114	0.0001	0.254	1.051	0.947	0.028	0	0.197	1
44	-0.0107	-0.0108	0	0.485[1]	0.414	0.278	0.001	0.014	0.037	7
45	-0.0109	-0.0109	0	0.378	0.201	0.29	0.013	0.007	0.154	28
46	-0.0105	-0.0105	0	0.14	0.266	0.265	0.003	0.006	0.055	29
47	-0.0112	-0.0113	0.0001	0.238	0.529	0.568	0.02	0	0.171	27
48	-0.0115	-0.0115	0	0.164	-0.271	-0.238	0.001	0.013	-0.026	24
49	-0.0117	-0.0116	-0.0001	0.313	-0.925	-0.952	0.05	0.007	-0.294	30
50	-0.0105	-0.0105	0	0.276	-0.359	-0.341	0.004	0.011	-0.078	26
51	-0.0117	-0.0117	-0.0001	0.202	-0.401	-0.377	0.004	0.009	-0.065	25
52	-0.0116	-0.0115	0	0.449	-0.364	-0.433	0.018	0.006	-0.195	39
53	-0.0117	-0.0116	0	0.113	-0.191	-0.179	0	0.012	-0.018	41
54	-0.0115	-0.0114	0	0.218	-0.296	-0.293	0.003	0.01	-0.062	43
55	-0.0111	-0.0111	0	0.155	0.107	0.114	0.001	0.012	0.026	44
56	-0.0117	-0.0117	-0.0001	0.227	-0.439	-0.453	0.009	0.005	-0.107	38
57	-0.0103	-0.0104	0.0001	0.222	1.082	1.153	0.067	0.077	0.294	40
58	-0.0112	-0.0112	0	0.123	-0.242	-0.23	0.001	0.011	-0.027	42

CMy										
Run Order	Actual Value	Predicted Value	Residual	Leverage	Internally Studentized Residuals	Externally Studentized Residuals	Cook's Distance	Cook's Random Distance	Influence on Fitted Value DFFITS	Standard Order
1	0.0082	0.0077	0.0005	0.162	0.966	0.771	0.004	0.008	0.05	48
2	0.0106	0.0106	0	0.447	-0.04	-0.438	0.105	0.029	-0.412	50
3	0.0042	0.0042	0	0.127	-0.088	-0.159	0.022	0.039	-0.095	47
4	0.0095	0.0088	0.0007	0.362	1.449	1.384	0.11	0.035	0.364	49
5	0.0023	0.0018	0.0005	0.491	1.022	0.886	0.037	0.005	0.232	46
6	0.0084	0.0079	0.0004	0.273	0.907	0.715	0.005	0.01	0.069	45
7	0.0115	0.0111	0.0004	0.175	0.794	0.613	0.001	0.013	0.024	51
8	0.0001	0.001	-0.0009	0.401	-1.931	-1.564	0.028	0.005	-0.197	36
9	0.005	0.0063	-0.0013	0.149	-2.557	-2.321	0.047	0.15	-0.181	35
10	0.0074	0.008	-0.0007	0.355	-1.324	-0.843	0.008	0.008	0.097	32
11	0.0027	0.0033	-0.0005	0.192	-1.064	-0.716	0.013	0.011	0.09	33
12	0.0009	0.0015	-0.0006	0.204	-1.221	-0.864	0.006	0.008	0.062	37
13	0.0066	0.0074	-0.0008	0.082	-1.59	-1.295	0	0.015	-0.011	34
14	0.0032	0.0039	-0.0007	0.154	-1.363	-1.036	0.001	0.011	0.019	31
15	0.0042	0.0038	0.0003	0.113	0.632	0.414	0.008	0.01	-0.059	23
16	0.0074	0.0066	0.0008	0.205	1.692	1.38	0.013	0.009	0.107	20
17	0.0067	0.0059	0.0008	0.24	1.583	1.273	0.011	0.011	0.101	21
18	0.0066	0.0058	0.0007	0.178	1.494	1.174	0.004	0.009	0.055	17
19	0.0017	0.0016	0.0001	0.276	0.265	-0.105	0.091	0.152	-0.291	22
20	0.0074	0.0067	0.0007	0.194	1.348	1.024	0.001	0.013	0.029	18
21	0.0026	0.0017	0.0009	0.13	1.764	1.463	0.012	0.011	0.081	19
22	0.0028	0.0033	-0.0005	0.2	-1.277	-0.857	0.027	0.023	-0.148	15
23	0.0082	0.0082	-8.93E-06	0.206	-0.022	0.026	0.002	0.009	0.038	14
24	0.005	0.0053	-0.0003	0.406	-0.793	-0.584	0.031	0.001	-0.189	12
25	0.0119	0.0118	0.0001	0.367	0.244	0.303	0.034	0.005	0.18	9
26	0.0023	0.0017	0.0006	0.376	1.621	1.449	0.28	0.936	0.611	16
27	0.0122	0.0121	0.0001	0.251	0.301	0.271	0.013	0.001	0.11	13
28	0.0034	0.0038	-0.0005	0.406	-1.21	-0.906	0.074	0.02	-0.312	11
29	0.0126	0.0131	-0.0005	0.606[1]	-1.369	-1.284	0.309	0.112	-0.699	10
30	0.0009	0.0009	0	0.269	0.052	0.04	0	0.014	0.002	56
31	0.003	0.0028	0.0002	0.214	0.37	0.341	0.005	0.005	0.071	58
32	0.0035	0.0036	-0.0001	0.102	-0.111	-0.1	0	0.012	-0.015	55
33	0.0043	0.0044	-0.0001	0.34	-0.138	-0.175	0.005	0.012	-0.078	54
34	0.0027	0.0025	0.0002	0.109	0.379	0.326	0.003	0.005	0.036	53
35	0.0009	0.0011	-0.0002	0.131	-0.412	-0.369	0.006	0.001	-0.058	52
36	0.0017	0.0016	0.0001	0.13	0.19	0.161	0	0.012	0.018	57
37	0.0007	0.0004	0.0004	0.625[1]	0.996	0.9	0.136	0.001	0.448	6
38	0.0002	0.0003	-0.0001	0.329	-0.146	-0.25	0.027	0	-0.17	3
39	0.0004	0.0005	0	0.412	-0.076	-0.251	0.037	0.002	-0.211	5
40	0.0006	0.0003	0.0003	0.565[1]	0.697	0.462	0.012	0.009	0.135	8
41	0.0006	0.0004	0.0002	0.165	0.538	0.33	0	0.013	0.014	4
42	0.0004	0.0003	0.0001	0.408	0.356	0.148	0.001	0.013	-0.039	2
43	0.0007	0.0003	0.0004	0.212	0.902	0.604	0.008	0.003	0.08	1
44	0.0005	0.0003	0.0002	0.548[1]	0.579	0.344	0.003	0.013	0.067	7
45	0.0007	0.001	-0.0003	0.3	-0.513	-0.315	0.003	0.01	0.053	28
46	0.0009	0.0011	-0.0002	0.141	-0.337	-0.213	0.003	0.005	0.043	29
47	0.0013	0.0012	0.0001	0.188	0.274	0.383	0.044	0.093	0.18	27
48	0.0005	0.001	-0.0005	0.139	-1.015	-0.83	0.004	0.005	-0.051	24
49	0.0004	0.0008	-0.0005	0.245	-0.95	-0.781	0.007	0.008	-0.079	30
50	0.0005	0.0012	-0.0006	0.162	-1.225	-1.043	0.015	0.002	-0.098	26
51	0	0.0005	-0.0005	0.162	-1.013	-0.846	0.007	0.006	-0.065	25
52	0.0012	0.0008	0.0004	0.422	0.854	1.051	0.133	0.04	0.434	39
53	0.0013	0.0012	0.0001	0.071	0.214	0.183	0	0.013	0.006	41
54	0.0016	0.0015	0.0001	0.208	0.122	0.091	0	0.014	-0.004	43
55	0.002	0.0021	-0.0001	0.17	-0.211	-0.238	0.007	0.003	-0.068	44
56	0.001	0.0007	0.0003	0.219	0.595	0.589	0.018	0	0.118	38
57	0.0016	0.0019	-0.0003	0.246	-0.617	-0.703	0.056	0.04	-0.224	40
58	0.0019	0.0019	0.0001	0.069	0.113	0.092	0	0.014	-0.002	42

CMz										
Run Order	Actual Value	Predicted Value	Residual	Leverage	Internally Studentized Residuals	Externally Studentized Residuals	Cook's Distance	Cook's Random Distance	Influence on Fitted Value DFFITS	Standard Order
1	-0.0079	-0.0078	0	0.228	-0.096	0.062	0.015	0.008	0.128	48
2	-0.0096	-0.0093	-0.0004	0.551	-1.143	-0.997	0.041	0	-0.325	50
3	-0.0047	-0.0049	0.0001	0.271	0.378	0.573	0.107	0.391	0.322	47
4	-0.0099	-0.0093	-0.0006	0.462	-1.868	-2.041	0.275	0.636	-0.796	49
5	-0.0031	-0.0027	-0.0004	0.611	-1.05	-0.984	0.063	0.002	-0.384	46
6	-0.0077	-0.0075	-0.0002	0.425	-0.454	-0.178	0.006	0.01	0.11	45
7	-0.0113	-0.0111	-0.0003	0.321	-0.744	-0.547	0.001	0.017	-0.041	51
8	-0.0018	-0.0021	0.0003	0.619	0.96	0.449	0.001	0.016	-0.054	36
9	-0.0072	-0.0077	0.0005	0.2	1.442	1.08	0.01	0.007	0.103	35
10	-0.0104	-0.0107	0.0003	0.51	0.869	0.415	0.003	0.014	-0.076	32
11	-0.0041	-0.0041	0	0.298	-0.042	-0.32	0.061	0.151	-0.293	33
12	-0.0017	-0.0023	0.0006	0.299	1.807	1.488	0.054	0.058	0.287	37
13	-0.0081	-0.0083	0.0002	0.319	0.683	0.341	0.006	0.009	-0.087	34
14	-0.0044	-0.0048	0.0004	0.301	1.221	0.863	0.005	0.012	0.085	31
15	-0.005	-0.0046	-0.0004	0.216	-1.108	-0.878	0.007	0.007	-0.089	23
16	-0.0089	-0.0085	-0.0004	0.254	-0.984	-0.749	0.003	0.011	-0.069	20
17	-0.0082	-0.0081	-0.0001	0.368	-0.334	-0.043	0.019	0.003	0.176	21
18	-0.0065	-0.0064	-0.0001	0.346	-0.182	0.097	0.028	0.01	0.216	17
19	-0.0025	-0.0025	-0.0001	0.427	-0.145	0.245	0.063	0.026	0.336	22
20	-0.0077	-0.0075	-0.0002	0.324	-0.612	-0.367	0.001	0.015	0.041	18
21	-0.0029	-0.0022	-0.0007	0.266	-1.905	-1.767	0.088	0.341	-0.364	19
22	-0.004	-0.0042	0.0002	0.368	0.905	0.492	0.008	0.006	0.116	15
23	-0.0083	-0.0082	-0.0001	0.392	-0.464	-0.434	0.035	0.008	-0.244	14
24	-0.0054	-0.0055	0.0001	0.513	0.507	0.218	0	0.017	0.025	12
25	-0.0099	-0.01	0.0001	0.519	0.534	0.239	0.001	0.017	0.037	9
26	-0.0033	-0.0032	-0.0001	0.514	-0.473	-0.548	0.065	0.012	-0.37	16
27	-0.0109	-0.0111	0.0002	0.358	0.902	0.492	0.008	0.006	0.114	13
28	-0.0041	-0.0044	0.0002	0.659	1.105	0.788	0.082	0.001	0.421	11
29	-0.0118	-0.012	0.0002	0.726	0.875	0.556	0.04	0.006	0.293	10
30	-0.0013	-0.0015	0.0001	0.355	0.424	0.219	0.001	0.014	-0.051	56
31	-0.0037	-0.0038	0.0001	0.306	0.251	0.07	0.005	0.007	-0.093	58
32	-0.004	-0.0043	0.0003	0.193	0.803	0.602	0.002	0.011	0.05	55
33	-0.0047	-0.0049	0.0002	0.545	0.561	0.309	0	0.017	-0.012	54
34	-0.0027	-0.0031	0.0004	0.199	1.144	0.915	0.013	0.003	0.12	53
35	-0.0012	-0.0014	0.0002	0.256	0.606	0.42	0	0.017	0.017	52
36	-0.0021	-0.0021	0.0001	0.259	0.199	0.042	0.006	0.005	-0.089	57
37	-0.0003	-0.0004	4.51E-06	0.810[1]	0.024	0.647	0.216	0.004	0.641	6
38	-0.0001	0	-0.0001	0.471	-0.417	-0.154	0	0.017	0.003	3
39	-0.0011	-0.0011	0	0.501	-0.106	0.087	0.009	0.009	0.127	5
40	-0.0006	-0.0005	-0.0001	0.715	-0.459	-0.113	0	0.017	0.022	8
41	-0.0007	-0.0006	-0.0001	0.428	-0.444	-0.182	0	0.017	-0.01	4
42	-0.0007	-0.0004	-0.0002	0.642	-1.185	-0.851	0.102	0.002	-0.463	2
43	-0.0007	-0.0005	-0.0002	0.428	-0.913	-0.507	0.013	0.006	-0.151	1
44	-0.0009	-0.0008	0	0.692	-0.174	0.163	0.022	0.009	0.215	7
45	-0.001	-0.0014	0.0004	0.424	1.068	0.744	0.001	0.018	0.035	28
46	-0.0014	-0.0014	0.0001	0.209	0.146	-0.068	0.024	0.078	-0.171	29
47	-0.0016	-0.0017	0.0001	0.309	0.262	-0.071	0.04	0.045	-0.251	27
48	-0.0009	-0.0014	0.0006	0.222	1.526	1.256	0.014	0.003	0.132	24
49	-0.0008	-0.0014	0.0005	0.392	1.459	1.23	0.028	0.004	0.232	30
50	-0.0011	-0.0015	0.0005	0.364	1.249	0.989	0.009	0.013	0.123	26
51	0	-0.0005	0.0006	0.252	1.545	1.322	0.024	0.01	0.173	25
52	-0.0019	-0.0014	-0.0004	0.562	-1.279	-0.766	0.002	0.017	-0.059	39
53	-0.0018	-0.0013	-0.0005	0.217	-1.438	-1.031	0.004	0.011	-0.068	41
54	-0.0026	-0.0021	-0.0005	0.293	-1.364	-0.939	0.003	0.014	-0.065	43
55	-0.0029	-0.0025	-0.0004	0.257	-1.274	-0.872	0.001	0.017	-0.039	44
56	-0.0014	-0.001	-0.0004	0.4	-1.213	-0.767	0	0.017	-0.026	38
57	-0.0036	-0.0032	-0.0004	0.465	-1.179	-0.686	0	0.017	0.003	40
58	-0.0026	-0.0023	-0.0002	0.212	-0.696	-0.371	0.006	0.005	0.081	42

Residual Diagnostics for 6-Blade Experiment

CFx										
Run Order	Actual Value	Predicted Value	Residual	Leverage	Internally Studentized Residuals	Externally Studentized Residuals	Cook's Distance	Cook's Random Distance	Influence on Fitted Value DFFITS	Standard Order
1	0.1485	0.1472	0.0014	0.304	1.09	1.094	0.017	0.001	0.332	52
2	0.14	0.1392	0.0008	0.57	0.794	0.789	0.028	0.003	0.45	55
3	0.1712	0.1719	-0.0008	0.62	-0.818	-0.813	0.036	0.002	-0.504	57
4	0.0687	0.069	-0.0003	0.812	-0.479	-0.472	0.033	0.011	-0.383	53
5	0.1063	0.1057	0.0006	0.378	0.539	0.533	0.006	0.01	0.201	54
6	0.1709	0.1707	0.0003	0.428	0.223	0.219	0.001	0.017	0.094	58
7	0.1289	0.1289	0	0.469	0.019	0.019	0	0.019	0.009	56
8	0.1888	0.1882	0.0006	0.411	0.549	0.542	0.007	0.009	0.223	16
9	0.1906	0.1897	0.0009	0.832	1.49	1.525	0.367	0.029	1.269	12
10	0.1916	0.1917	-0.0001	0.775	-0.076	-0.074	0.001	0.019	-0.058	9
11	0.1749	0.1757	-0.0008	0.647	-0.911	-0.908	0.051	0.001	-0.588	15
12	0.2308	0.231	-0.0002	0.826	-0.262	-0.257	0.011	0.017	-0.212	10
13	0.1778	0.1789	-0.0011	0.59	-1.134	-1.14	0.062	0.002	-0.673	13
14	0.1772	0.1763	0.0008	0.569	0.864	0.86	0.033	0.001	0.489	14
15	0.2145	0.214	0.0005	0.492	0.467	0.46	0.007	0.012	0.226	11
16	0.1216	0.1223	-0.0008	0.594	-0.808	-0.802	0.032	0.002	-0.477	18
17	0.1332	0.1327	0.0005	0.473	0.43	0.424	0.006	0.013	0.2	17
18	0.173	0.1709	0.0021	0.255	1.641	1.724	0.047	0.153	0.495	22
19	0.1699	0.1723	-0.0024	0.435	-2.136	-2.292	0.117	0.244	-0.997	19
20	0.1559	0.1568	-0.0008	0.387	-0.719	-0.713	0.011	0.004	-0.276	23
21	0.1569	0.1572	-0.0003	0.313	-0.267	-0.262	0.001	0.017	-0.082	21
22	0.1697	0.1704	-0.0006	0.601	-0.664	-0.657	0.022	0.006	-0.395	20
23	0.1663	0.1666	-0.0003	0.277	-0.225	-0.221	0.001	0.017	-0.061	40
24	0.1765	0.1779	-0.0014	0.279	-1.108	-1.113	0.016	0.001	-0.311	41
25	0.1731	0.1715	0.0016	0.33	1.309	1.327	0.028	0.01	0.438	42
26	0.1714	0.1693	0.0021	0.515	1.979	2.096	0.139	0.164	1.08	44
27	0.1785	0.1796	-0.001	0.409	-0.91	-0.908	0.019	0.001	-0.371	43
28	0.1696	0.1683	0.0013	0.263	1.005	1.005	0.012	0	0.265	39
29	0.1796	0.1791	0.0005	0.581	0.513	0.506	0.012	0.01	0.294	38
30	0.1765	0.1761	0.0004	0.549	0.372	0.367	0.006	0.014	0.201	7
31	0.1808	0.1812	-0.0004	0.582	-0.399	-0.393	0.007	0.014	-0.228	2
32	0.1793	0.1798	-0.0005	0.299	-0.419	-0.413	0.002	0.013	-0.123	8
33	0.1732	0.172	0.0012	0.414	1.047	1.049	0.026	0	0.435	3
34	0.1764	0.1776	-0.0012	0.653	-1.323	-1.342	0.11	0.011	-0.876	1
35	0.1769	0.1771	-0.0002	0.27	-0.165	-0.162	0	0.018	-0.044	4
36	0.1749	0.1751	-0.0002	0.473	-0.187	-0.183	0.001	0.018	-0.087	6
37	0.176	0.1754	0.0006	0.289	0.482	0.475	0.003	0.011	0.137	5
38	0.1777	0.1774	0.0003	0.625	0.291	0.287	0.005	0.016	0.179	46
39	0.178	0.1773	0.0007	0.603	0.729	0.723	0.027	0.004	0.436	47
40	0.1797	0.1782	0.0015	0.564	1.491	1.526	0.096	0.029	0.861	49
41	0.1821	0.1829	-0.0008	0.349	-0.665	-0.658	0.008	0.006	-0.23	48
42	0.176	0.1759	0.0001	0.873	0.175	0.172	0.007	0.018	0.15	45
43	0.1836	0.1865	-0.0029	0.415	-2.59	-2.917	0.159	0.626	-1.211	51
44	0.1787	0.179	-0.0003	0.621	-0.291	-0.286	0.005	0.016	-0.178	50
45	0.1535	0.1514	0.0021	0.355	1.771	1.846	0.057	0.088	0.654	27
46	0.174	0.1733	0.0007	0.517	0.648	0.641	0.015	0.006	0.332	25
47	0.145	0.1459	-0.0009	0.31	-0.69	-0.683	0.007	0.005	-0.212	29
48	0.1212	0.1226	-0.0014	0.501	-1.301	-1.318	0.057	0.009	-0.66	26
49	0.1612	0.1616	-0.0005	0.334	-0.395	-0.389	0.003	0.014	-0.13	30
50	0.1768	0.176	0.0008	0.538	0.791	0.786	0.024	0.003	0.423	24
51	0.1366	0.1378	-0.0012	0.54	-1.222	-1.233	0.058	0.005	-0.666	28
52	0.0975	0.0964	0.0011	0.764	1.571	1.686	0.302	0.075	1.306	36
53	0.1532	0.1533	-0.0001	0.505	-0.116	-0.114	0	0.019	-0.058	37
54	0.1626	0.162	0.0007	0.884	1.282	1.298	0.417	0.008	1.147	33
55	0.1626	0.1632	-0.0006	0.638	-0.671	-0.665	0.027	0.006	-0.424	31
56	0.1764	0.1768	-0.0004	0.9	-0.857	-0.853	0.219	0.001	-0.767	34
57	0.1273	0.1288	-0.0016	0.475	-1.459	-1.49	0.064	0.024	-0.708	35
58	0.1186	0.1186	2.13E-07	0.727	0	0	0	0.019	0	32

CFy										
Run Order	Actual Value	Predicted Value	Residual	Leverage	Internally Studentized Residuals	Externally Studentized Residuals	Cook's Distance	Cook's Random Distance	Influence on Fitted Value DFFITS	Standard Order
1	0.0004	0.0003	0.0001	0.133	0.139	0.172	0.004	0.003	0.065	52
2	0.0001	0.0002	-0.0001	0.477	-0.143	0.062	0.008	0.009	0.147	55
3	-0.0003	-0.0002	-0.0001	0.328	-0.168	-0.043	0.002	0.011	0.071	57
4	0.0009	0.001	-0.0001	0.574	-0.141	0.134	0.016	0.008	0.211	53
5	0.0001	0.0012	-0.0011	0.219	-1.264	-1.197	0.043	0.021	-0.236	54
6	-0.0005	0	-0.0005	0.274	-0.546	-0.437	0.001	0.013	-0.053	58
7	0.0006	0.0011	-0.0006	0.287	-0.637	-0.556	0.006	0.01	-0.099	56
8	-0.0013	0.0001	-0.0013	0.356	-1.803	-1.554	0.132	0.228	-0.549	16
9	-0.0028	-0.0021	-0.0008	0.567	-1.196	-1.217	0.179	0.031	-0.683	12
10	0.0023	0.0025	-0.0002	0.313	-0.234	-0.155	0	0.014	-0.026	9
11	-0.001	-0.0008	-0.0002	0.403	-0.249	-0.172	0.001	0.014	-0.042	15
12	0.0083	0.0088	-0.0005	0.659[1]	-0.842	-0.786	0.078	0.003	-0.468	10
13	-0.0006	-0.0011	0.0005	0.485	0.7	0.78	0.088	0.023	0.444	13
14	-0.0004	-0.0009	0.0005	0.245	0.608	0.508	0.014	0	0.151	14
15	0.0063	0.0052	0.0011	0.366	1.569	1.362	0.102	0.204	0.518	11
16	0.0014	0.0011	0.0003	0.334	0.392	0.204	0.002	0.012	-0.063	18
17	0.0005	0.0002	0.0003	0.286	0.325	0.159	0.002	0.01	-0.067	17
18	-0.0016	-0.0017	0.0001	0.186	0.089	-0.019	0.006	0.005	-0.086	22
19	-0.0007	-0.0012	0.0006	0.207	0.612	0.483	0	0.014	0.02	19
20	0.0005	-0.0009	0.0014	0.146	1.538	1.342	0.012	0.02	0.144	23
21	-0.0003	-0.0006	0.0002	0.179	0.27	0.157	0.002	0.009	-0.049	21
22	-0.001	-0.0018	0.0008	0.379	0.955	0.796	0.011	0.007	0.168	20
23	0.0004	-0.0003	0.0007	0.174	0.797	0.734	0.012	0	0.117	40
24	-0.0007	-0.0013	0.0006	0.148	0.644	0.561	0.003	0.005	0.068	41
25	-0.0015	-0.0011	-0.0004	0.253	-0.502	-0.55	0.02	0.004	-0.188	42
26	-0.001	-0.0007	-0.0003	0.295	-0.293	-0.359	0.012	0.003	-0.154	44
27	-0.002	-0.0021	0.0001	0.248	0.116	0.067	0	0.014	-0.017	43
28	-0.0005	-0.0005	2.20E-06	0.165	0.002	-0.028	0.001	0.012	-0.03	39
29	-0.0019	-0.0024	0.0005	0.437	0.641	0.652	0.025	0.003	0.249	38
30	0.001	0.0029	-0.0019	0.352	-2.156	-1.862	0.041	0.019	-0.307	7
31	-0.0001	0.0006	-0.0007	0.282	-0.793	-0.359	0.027	0.036	0.212	2
32	-0.0021	-0.0015	-0.0006	0.238	-0.614	-0.241	0.031	0.064	0.213	8
33	-0.0046	-0.0024	-0.0022	0.235	-2.426	-2.243	0.047	0.07	-0.288	3
34	-0.0024	-0.0016	-0.0008	0.396	-0.899	-0.302	0.038	0.027	0.294	1
35	-0.0031	-0.0013	-0.0018	0.141	-1.934	-1.663	0.006	0.015	-0.084	4
36	-0.004	-0.0024	-0.0015	0.223	-1.673	-1.347	0.003	0.017	-0.065	6
37	-0.0035	-0.0017	-0.0018	0.148	-1.883	-1.61	0.006	0.017	-0.081	5
38	-0.0022	-0.0017	-0.0006	0.328	-0.653	-0.997	0.138	0.412	-0.55	46
39	-0.0008	-0.0016	0.0008	0.449	0.999	0.708	0.003	0.016	0.085	47
40	-0.0014	-0.002	0.0006	0.18	0.687	0.489	0	0.013	-0.02	49
41	0.0016	0.0006	0.001	0.171	1.069	0.879	0.003	0.014	0.055	48
42	-0.0032	-0.0043	0.0011	0.553	1.37	1.142	0.049	0.009	0.371	45
43	-5.97E-06	-0.0013	0.0013	0.263	1.444	1.261	0.023	0.008	0.198	51
44	-0.001	-0.0023	0.0013	0.356	1.558	1.377	0.042	0.012	0.311	50
45	0.0005	0.0003	0.0002	0.115	0.259	0.18	0.001	0.009	-0.031	27
46	-5.89E-06	-0.0004	0.0004	0.234	0.465	0.336	0	0.014	-0.021	25
47	0.0011	-0.0001	0.0013	0.111	1.34	1.24	0.012	0.008	0.1	29
48	0.0016	0.0003	0.0013	0.263	1.448	1.428	0.05	0.022	0.295	26
49	-0.0001	0	-0.0001	0.218	-0.113	-0.25	0.018	0.009	-0.163	30
50	0	-0.0002	0.0002	0.24	0.254	0.114	0.004	0.008	-0.08	24
51	0.0007	0.0002	0.0005	0.348	0.526	0.36	0	0.014	-0.015	28
52	0.0007	0.0017	-0.0011	0.426	-1.468	-1.324	0.116	0.069	-0.54	36
53	0.0008	0.0014	-0.0006	0.291	-0.761	-0.601	0.013	0.002	-0.151	37
54	0.0015	0.0019	-0.0004	0.769[1]	-0.762	-0.727	0.084	0.007	-0.477	33
55	0.0014	0.0015	-0.0001	0.288	-0.097	-0.029	0	0.014	0.029	31
56	0.0013	0.0015	-0.0001	0.754[1]	-0.247	-0.062	0	0.014	0.02	34
57	0.0016	0.0013	0.0003	0.291	0.439	0.43	0.016	0.001	0.172	35
58	0.0025	0.0017	0.0007	0.311	0.972	0.906	0.058	0.049	0.34	32

CFz										
Run Order	Actual Value	Predicted Value	Residual	Leverage	Internally Studentized Residuals	Externally Studentized Residuals	Cook's Distance	Cook's Random Distance	Influence on Fitted Value DFFITS	Standard Order
1	-0.0012	-0.0021	0.001	0.25	1.215	1.247	0.025	0.134	0.336	52
2	-0.0026	-0.0027	0.0001	0.566	0.223	0.221	0.002	0.015	0.123	55
3	-0.0013	-0.0006	-0.0007	0.538	-1.106	-1.049	0.04	0.002	-0.515	57
4	-0.0049	-0.0055	0.0006	0.825	1.496	1.242	0.167	0.018	0.922	53
5	-0.0035	-0.0024	-0.0011	0.276	-1.446	-1.479	0.034	0.072	-0.418	54
6	-0.0012	-0.0014	0.0002	0.413	0.265	0.255	0.002	0.014	0.098	58
7	-0.0016	-0.001	-0.0006	0.43	-0.824	-0.815	0.019	0.003	-0.343	56
8	-0.0185	-0.017	-0.0014	0.419	-2.072	-2.18	0.115	0.181	-0.906	16
9	-0.0224	-0.0217	-0.0007	0.792	-1.716	-1.767	0.424	0.068	-1.396	12
10	-0.0174	-0.0172	-0.0002	0.788	-0.468	-0.394	0.017	0.014	-0.287	9
11	-0.0077	-0.0072	-0.0005	0.521	-0.807	-0.809	0.028	0.01	-0.422	15
12	-0.0223	-0.0225	0.0002	0.817	0.532	0.521	0.039	0.015	0.416	10
13	-0.0045	-0.0044	0	0.571	-0.039	-0.021	0	0.017	-0.004	13
14	-0.0098	-0.0102	0.0003	0.569	0.568	0.579	0.018	0.023	0.335	14
15	-0.0183	-0.0192	0.0009	0.446	1.28	1.261	0.045	0.018	0.538	11
16	-0.0152	-0.0156	0.0003	0.507	0.525	0.519	0.011	0.009	0.26	18
17	-0.0133	-0.0138	0.0005	0.451	0.734	0.701	0.013	0.007	0.288	17
18	-0.0041	-0.0035	-0.0006	0.193	-0.703	-0.695	0.004	0.006	-0.133	22
19	-0.0051	-0.005	-0.0002	0.381	-0.251	-0.246	0.001	0.015	-0.092	19
20	-0.0066	-0.0063	-0.0003	0.306	-0.362	-0.35	0.002	0.014	-0.099	23
21	-0.0078	-0.0077	-0.0001	0.233	-0.065	-0.063	0	0.017	-0.014	21
22	-0.0029	-0.0029	0.0001	0.574	0.087	0.086	0	0.017	0.048	20
23	-0.0111	-0.0132	0.0021	0.332	2.839	3.197	0.147	0.838	1.033	40
24	-0.007	-0.0065	-0.0005	0.25	-0.637	-0.632	0.006	0.017	-0.159	41
25	-0.0136	-0.0129	-0.0007	0.268	-0.951	-0.962	0.015	0.06	-0.27	42
26	-0.0163	-0.0166	0.0003	0.413	0.478	0.47	0.006	0.019	0.187	44
27	-0.0044	-0.0047	0.0003	0.322	0.365	0.361	0.002	0.016	0.115	43
28	-0.0167	-0.0162	-0.0006	0.19	-0.724	-0.722	0.006	0.026	-0.143	39
29	-0.0044	-0.0044	0.0001	0.541	0.089	0.079	0	0.017	0.038	38
30	-0.0272	-0.0253	-0.0019	0.527	-3.091	-3.41	0.323[1]	1.003[1]	-1.666	7
31	-0.0223	-0.0224	0.0001	0.403	0.111	0.131	0.001	0.019	0.066	2
32	-0.004	-0.0048	0.0007	0.333	0.95	1.011	0.032	0.358	0.384	8
33	-0.0111	-0.0109	-0.0002	0.362	-0.259	-0.24	0.001	0.022	-0.075	3
34	-0.0167	-0.017	0.0003	0.526	0.412	0.48	0.014	0.087	0.287	1
35	-0.0122	-0.0111	-0.0011	0.315	-1.477	-1.504	0.038	0.03	-0.466	4
36	-0.0062	-0.0058	-0.0004	0.374	-0.542	-0.513	0.005	0.017	-0.171	6
37	-0.0103	-0.0103	0	0.232	-0.026	-0.017	0	0.017	0.003	5
38	-0.0047	-0.0039	-0.0007	0.538	-1.152	-1.231	0.079	0.451	-0.69	46
39	-0.0048	-0.0052	0.0004	0.534	0.716	0.707	0.022	0.012	0.374	47
40	-0.0075	-0.008	0.0005	0.424	0.775	0.73	0.013	0.012	0.277	49
41	-0.0153	-0.0158	0.0005	0.297	0.609	0.612	0.006	0.015	0.182	48
42	-0.0071	-0.0073	0.0003	0.871	0.797	0.615	0.063	0.015	0.493	45
43	-0.0188	-0.0201	0.0013	0.315	1.716	1.767	0.05	0.068	0.543	51
44	-0.0158	-0.0164	0.0006	0.499	0.992	0.965	0.033	0.008	0.46	50
45	-0.0034	-0.003	-0.0004	0.287	-0.47	-0.472	0.004	0.02	-0.141	27
46	-0.0015	-0.0022	0.0007	0.462	1.081	1.027	0.028	0.003	0.422	25
47	-0.0026	-0.0025	-0.0001	0.264	-0.094	-0.095	0	0.017	-0.026	29
48	-0.0044	-0.0051	0.0006	0.351	0.884	0.869	0.015	0.002	0.296	26
49	-0.0002	0.0002	-0.0004	0.324	-0.518	-0.517	0.006	0.029	-0.169	30
50	-0.0007	-0.0005	-0.0001	0.54	-0.226	-0.226	0.002	0.017	-0.12	24
51	-0.0037	-0.0042	0.0005	0.495	0.785	0.748	0.018	0.007	0.338	28
52	0	-0.0002	0.0002	0.649	0.358	0.354	0.009	0.013	0.229	36
53	-0.0001	-0.0011	0.001	0.452	1.498	1.512	0.067	0.027	0.673	37
54	-0.0006	-0.0009	0.0003	0.888	0.867	0.768	0.137	0.009	0.66	33
55	-0.0016	-0.0018	0.0002	0.647	0.371	0.369	0.01	0.015	0.238	31
56	-0.0016	-0.0013	-0.0003	0.899	-1.209	-1.091	0.309	0.008	-0.954	34
57	-0.0017	-0.001	-0.0007	0.373	-0.962	-0.956	0.021	0	-0.355	35
58	-0.0023	-0.0016	-0.0007	0.713	-1.348	-1.34	0.159	0.011	-0.942	32

CMx										
Run Order	Actual Value	Predicted Value	Residual	Leverage	Internally Studentized Residuals	Externally Studentized Residuals	Cook's Distance	Cook's Random Distance	Influence on Fitted Value DFFITS	Standard Order
1	-0.0138	-0.0138	0	0.228	0.263	0.259	0.001	0.014	0.059	52
2	-0.0133	-0.0133	0	0.509	0.154	0.152	0.001	0.015	0.077	55
3	-0.0141	-0.0141	0.0001	0.481	0.407	0.402	0.006	0.011	0.193	57
4	-0.0094	-0.0097	0.0003	0.728	3.42	4.173[1]	1.322[2]	1.821[2]	3.044[2]	53
5	-0.0121	-0.012	-0.0001	0.255	-0.608	-0.602	0.005	0.006	-0.154	54
6	-0.0141	-0.0139	-0.0002	0.355	-1.103	-1.107	0.028	0.001	-0.393	58
7	-0.0129	-0.013	0.0001	0.376	0.633	0.628	0.01	0.006	0.236	56
8	-0.0154	-0.0151	-0.0003	0.342	-1.957	-2.047	0.083	0.125	-0.7	16
9	-0.0158	-0.0157	-0.0001	0.742	-0.948	-0.947	0.108	0	-0.702	12
10	-0.0154	-0.0155	0.0001	0.673	1.186	1.194	0.121	0.003	0.803	9
11	-0.0143	-0.0144	0.0001	0.496	0.593	0.587	0.014	0.007	0.292	15
12	-0.018	-0.0181	0	0.76	0.549	0.543	0.04	0.008	0.412	10
13	-0.0141	-0.0141	0.0001	0.531	0.479	0.474	0.011	0.009	0.252	13
14	-0.0143	-0.0144	0.0001	0.467	0.795	0.79	0.023	0.002	0.369	14
15	-0.0168	-0.0167	-0.0001	0.382	-0.678	-0.672	0.012	0.005	-0.257	11
16	-0.0131	-0.0131	-2.97E-06	0.431	-0.022	-0.022	0	0.016	-0.009	18
17	-0.0138	-0.0135	-0.0003	0.324	-1.855	-1.928	0.069	0.093	-0.625	17
18	-0.0144	-0.0145	4.46E-06	0.217	0.028	0.028	0	0.016	0.006	22
19	-0.0142	-0.0143	0.0001	0.344	0.618	0.613	0.008	0.006	0.211	19
20	-0.0144	-0.0144	4.10E-06	0.246	0.026	0.026	0	0.016	0.006	23
21	-0.0141	-0.0141	0.0001	0.211	0.426	0.421	0.002	0.01	0.089	21
22	-0.0143	-0.0145	0.0002	0.452	1.188	1.196	0.049	0.003	0.54	20
23	-0.0145	-0.0146	0.0001	0.213	0.619	0.613	0.004	0.006	0.13	40
24	-0.0142	-0.0143	0.0001	0.186	0.52	0.515	0.003	0.008	0.096	41
25	-0.0143	-0.0143	0	0.281	-0.111	-0.11	0	0.015	-0.031	42
26	-0.0145	-0.0144	-0.0001	0.36	-0.665	-0.659	0.01	0.005	-0.238	44
27	-0.0141	-0.0142	0.0001	0.299	0.736	0.731	0.01	0.003	0.219	43
28	-0.0146	-0.0145	-0.0001	0.179	-0.584	-0.578	0.003	0.007	-0.103	39
29	-0.0141	-0.0143	0.0002	0.475	1.61	1.651	0.098	0.04	0.784	38
30	-0.0153	-0.0152	-0.0001	0.406	-0.45	-0.445	0.006	0.01	-0.18	7
31	-0.0149	-0.015	0.0001	0.378	1.061	1.075	0.031	0.014	0.417	2
32	-0.0142	-0.0141	0	0.233	-0.242	-0.239	0.001	0.014	-0.056	8
33	-0.0146	-0.0144	-0.0001	0.278	-0.946	-0.944	0.014	0	-0.262	3
34	-0.0145	-0.0144	-0.0001	0.497	-0.462	-0.457	0.009	0.01	-0.227	1
35	-0.0144	-0.0143	-0.0001	0.22	-0.866	-0.863	0.009	0.001	-0.19	4
36	-0.0142	-0.0142	1.14E-06	0.289	0.008	0.007	0	0.016	0.002	6
37	-0.0143	-0.0143	-0.0001	0.167	-0.472	-0.467	0.002	0.009	-0.078	5
38	-0.014	-0.014	-0.0001	0.533	-0.523	-0.517	0.013	0.008	-0.275	46
39	-0.014	-0.014	-0.0001	0.552	-0.514	-0.509	0.014	0.008	-0.281	47
40	-0.0143	-0.0141	-0.0002	0.389	-1.37	-1.388	0.05	0.012	-0.54	49
41	-0.0146	-0.0147	0.0001	0.329	0.761	0.756	0.012	0.003	0.249	48
42	-0.0143	-0.0142	-0.0001	0.785	-0.661	-0.655	0.066	0.005	-0.514	45
43	-0.0147	-0.0149	0.0002	0.362	1.716	1.769	0.07	0.059	0.641	51
44	-0.0145	-0.0146	0.0002	0.493	1.401	1.422	0.08	0.014	0.701	50
45	-0.014	-0.0138	-0.0002	0.259	-1.363	-1.381	0.027	0.012	-0.358	27
46	-0.0143	-0.0142	-0.0001	0.361	-0.817	-0.813	0.016	0.002	-0.293	25
47	-0.0139	-0.014	0.0001	0.265	0.814	0.81	0.01	0.002	0.214	29
48	-0.0128	-0.013	0.0002	0.336	1.151	1.157	0.028	0.002	0.389	26
49	-0.0144	-0.0143	0	0.264	-0.326	-0.322	0.002	0.012	-0.085	30
50	-0.0142	-0.014	-0.0002	0.399	-1.396	-1.417	0.054	0.014	-0.565	24
51	-0.0133	-0.0133	1.73E-06	0.436	0.013	0.013	0	0.016	0.006	28
52	-0.0114	-0.011	-0.0004	0.616	-3.616	-4.536[1]	0.879[2]	2.303[2]	-2.798[2]	36
53	-0.0141	-0.0142	0.0001	0.424	0.378	0.373	0.004	0.011	0.158	37
54	-0.0143	-0.0142	0	0.813	-0.543	-0.537	0.053	0.008	-0.436	33
55	-0.0139	-0.0139	-3.08E-06	0.552	-0.026	-0.025	0	0.016	-0.014	31
56	-0.0139	-0.0141	0.0001	0.823	1.928	2.012	0.718	0.115	1.655	34
57	-0.0128	-0.013	0.0002	0.354	1.484	1.512	0.05	0.023	0.535	35
58	-0.0126	-0.0126	0	0.645	-0.36	-0.356	0.01	0.012	-0.23	32

CMy										
Run Order	Actual Value	Predicted Value	Residual	Leverage	Internally Studentized Residuals	Externally Studentized Residuals	Cook's Distance	Cook's Random Distance	Influence on Fitted Value DFFITS	Standard Order
1	0.0009	0.0006	0.0003	0.247	0.631	0.699	0.03	0.048	0.25	52
2	0.0007	0.0008	-0.0002	0.463	-0.488	-0.412	0.004	0.016	-0.115	55
3	-0.0001	0.0004	-0.0005	0.358	-1.245	-1.237	0.05	0.027	-0.399	57
4	0.0002	-0.0001	0.0003	0.625	0.685	1.386	0.284	0.177	1.032	53
5	0.0002	0.0009	-0.0007	0.243	-1.722	-1.707	0.072	0.29	-0.407	54
6	0.0001	0.0001	0	0.239	-0.024	0.047	0.002	0.012	0.064	58
7	0.0011	0.0011	-1.22E-06	0.347	-0.003	0.114	0.005	0.01	0.116	56
8	0.0122	0.0126	-0.0005	0.378	-1.411	-0.849	0.01	0.012	-0.18	16
9	0.0129	0.0135	-0.0006	0.788	-2.454	-2.241	0.765	0.234	-1.585	12
10	0.0111	0.0114	-0.0003	0.673	-1.176	-0.471	0.003	0.017	-0.099	9
11	0.0071	0.0072	-0.0001	0.452	-0.336	0.049	0.012	0.008	0.194	15
12	0.0153	0.0156	-0.0002	0.758	-1.018	-0.195	0.002	0.017	0.077	10
13	0.0034	0.0034	-0.0001	0.56	-0.202	0.317	0.051	0.049	0.393	13
14	0.007	0.0075	-0.0005	0.447	-1.469	-0.907	0.019	0.014	-0.247	14
15	0.0154	0.0155	-0.0001	0.38	-0.343	-0.023	0.005	0.009	0.135	11
16	0.0028	0.0026	0.0002	0.51	0.47	0.376	0.004	0.016	0.116	18
17	0.0022	0.0023	0	0.346	-0.12	-0.221	0.007	0.006	-0.145	17
18	0.0018	0.0017	0.0002	0.196	0.364	0.277	0	0.017	0.019	22
19	0.0031	0.0028	0.0003	0.353	0.7	0.611	0.01	0.005	0.165	19
20	0.0023	0.0023	-1.12E-06	0.245	-0.003	-0.068	0.002	0.011	-0.066	23
21	0.004	0.0038	0.0001	0.24	0.321	0.234	0	0.017	0.012	21
22	0.0011	0.0009	0.0002	0.526	0.531	0.432	0.006	0.015	0.145	20
23	0.0055	0.0046	0.0008	0.317	1.978	2.171	0.197[1]	1.370[1]	0.752	40
24	0.0028	0.003	-0.0002	0.216	-0.522	-0.489	0.006	0.002	-0.117	41
25	0.0061	0.0064	-0.0002	0.258	-0.51	-0.499	0.009	0.002	-0.144	42
26	0.0069	0.007	0	0.375	-0.097	-0.109	0.001	0.016	-0.047	44
27	0.0003	0.0002	0.0001	0.319	0.206	0.206	0.002	0.015	0.068	43
28	0.0057	0.006	-0.0003	0.189	-0.791	-0.74	0.013	0.004	-0.157	39
29	0.0003	0.0004	0	0.501	-0.072	-0.104	0.001	0.017	-0.062	38
30	0.0059	0.0066	-0.0007	0.454	-1.915	-1.591	0.061	0.017	-0.469	7
31	0.008	0.0082	-0.0001	0.422	-0.288	0.171	0.038	0.027	0.337	2
32	0.001	0.001	0	0.309	0.099	0.392	0.045	0.088	0.33	8
33	0.0014	0.0022	-0.0008	0.295	-2.028	-1.735	0.041	0.052	-0.342	3
34	0.0075	0.0079	-0.0004	0.501	-1.201	-0.768	0.004	0.018	-0.109	1
35	0.0054	0.0058	-0.0004	0.273	-0.965	-0.647	0	0.018	-0.008	4
36	0.0006	0.0011	-0.0005	0.335	-1.198	-0.837	0.002	0.018	-0.08	6
37	0.0036	0.004	-0.0004	0.233	-1.051	-0.748	0	0.019	-0.03	5
38	0.0014	0.001	0.0004	0.488	0.987	0.334	0.017	0.015	-0.231	46
39	0.0025	0.002	0.0005	0.427	1.3	0.79	0	0.017	-0.004	47
40	0.0041	0.004	0.0002	0.352	0.412	-0.067	0.036	0.057	-0.328	49
41	0.0102	0.0097	0.0005	0.29	1.232	0.865	0	0.017	0.005	48
42	0.0013	0.0008	0.0006	0.742	1.671	0.874	0.011	0.019	0.193	45
43	0.0117	0.011	0.0007	0.247	1.61	1.292	0.007	0.028	0.116	51
44	0.01	0.0088	0.0012	0.397	3.014	3.083	0.193	0.661	0.909	50
45	0.002	0.0021	-0.0002	0.254	-0.416	-0.44	0.011	0.002	-0.163	27
46	0.001	0.001	0	0.346	0.044	-0.041	0.002	0.015	-0.069	25
47	0.0019	0.0018	0.0001	0.229	0.232	0.159	0	0.017	0.001	29
48	0.0021	0.0018	0.0003	0.407	0.792	0.74	0.023	0.001	0.264	26
49	0.0017	0.0014	0.0003	0.281	0.799	0.697	0.011	0.002	0.166	30
50	0.0006	0.0006	0	0.473	-0.081	-0.223	0.009	0.009	-0.178	24
51	0.0024	0.0022	0.0002	0.45	0.459	0.377	0.004	0.015	0.114	28
52	0.0001	0.0002	-0.0001	0.682	-0.466	-0.576	0.057	0.003	-0.431	36
53	0	-0.0001	0.0001	0.368	0.232	0.151	0.001	0.017	0.043	37
54	-0.0002	-0.0003	0.0001	0.81	0.268	0.206	0.007	0.015	0.146	33
55	-0.0005	-0.0005	-7.56E-06	0.607	-0.028	-0.077	0.001	0.016	-0.067	31
56	-0.0005	-0.0006	0.0001	0.851[2]	0.605	0.683	0.128	0.004	0.566	34
57	-0.0004	-0.0004	0.0001	0.369	0.187	0.118	0	0.017	0.031	35
58	-0.0004	-0.0004	7.30E-06	0.661	0.029	-0.035	0.001	0.017	-0.044	32

CMz										
Run Order	Actual Value	Predicted Value	Residual	Leverage	Internally Studentized Residuals	Externally Studentized Residuals	Cook's Distance	Cook's Random Distance	Influence on Fitted Value DFFITS	Standard Order
1	-0.0015	-0.0015	0.0001	0.151	0.131	0.06	0.001	0.009	-0.04	52
2	-0.0015	-0.0015	0.0001	0.27	0.177	0.058	0.003	0.01	-0.068	55
3	-0.0005	-0.0007	0.0003	0.211	0.709	0.602	0.004	0.01	0.071	57
4	-0.0023	-0.0023	0	0.393	-0.065	-0.27	0.023	0.005	-0.229	53
5	-0.0017	-0.0021	0.0004	0.155	1.145	1.008	0.01	0.002	0.118	54
6	-0.0005	-0.0009	0.0003	0.128	0.885	0.767	0.004	0.006	0.065	58
7	-0.0017	-0.0017	0.0001	0.217	0.141	0.045	0.002	0.009	-0.058	56
8	-0.0112	-0.0118	0.0006	0.197	2.06	1.357	0.018	0.021	0.188	16
9	-0.0098	-0.0101	0.0003	0.629[1]	1.208	0.593	0.012	0.016	0.169	12
10	-0.0123	-0.0126	0.0003	0.361	0.917	0.472	0	0.014	0.031	9
11	-0.0073	-0.0074	0.0001	0.306	0.507	0.198	0.002	0.01	-0.061	15
12	-0.017	-0.0172	0.0002	0.579[1]	0.806	0.234	0.002	0.013	-0.066	10
13	-0.0039	-0.0041	0.0002	0.497	0.619	0.152	0.005	0.012	-0.109	13
14	-0.0076	-0.0074	-0.0002	0.308	-0.674	-0.676	0.066	0.12	-0.342	14
15	-0.0148	-0.0153	0.0005	0.249	1.716	1.083	0.014	0	0.169	11
16	-0.0087	-0.0085	-0.0002	0.38	-0.506	-0.424	0.005	0.012	-0.108	18
17	-0.0075	-0.0074	-0.0001	0.199	-0.202	-0.135	0	0.013	0.007	17
18	-0.0024	-0.0026	0.0002	0.111	0.604	0.539	0.007	0.006	0.086	22
19	-0.0034	-0.0033	0	0.222	-0.111	-0.049	0.001	0.013	0.029	19
20	-0.0047	-0.0042	-0.0005	0.19	-1.312	-1.152	0.025	0.019	-0.198	23
21	-0.0051	-0.0053	0.0002	0.121	0.529	0.48	0.006	0.001	0.085	21
22	-0.0019	-0.0015	-0.0004	0.327	-1.015	-0.947	0.038	0.002	-0.276	20
23	-0.0079	-0.0078	-0.0002	0.236	-0.472	-0.492	0.015	0.001	-0.156	40
24	-0.0049	-0.0044	-0.0005	0.142	-1.382	-1.26	0.041	0.254	-0.216	41
25	-0.0074	-0.0076	0.0002	0.149	0.432	0.366	0.001	0.011	0.04	42
26	-0.0088	-0.0093	0.0005	0.223	1.399	1.308	0.051	0.069	0.287	44
27	-0.002	-0.0019	-0.0001	0.205	-0.274	-0.289	0.005	0.005	-0.091	43
28	-0.0092	-0.0096	0.0005	0.115	1.204	1.052	0.012	0.019	0.117	39
29	-0.002	-0.0021	0.0001	0.247	0.386	0.326	0.002	0.011	0.055	38
30	-0.0138	-0.0137	-0.0001	0.257	-0.306	-0.458	0.036	0.025	-0.254	7
31	-0.0126	-0.0128	0.0002	0.266	0.595	0.356	0.001	0.012	-0.037	2
32	-0.0025	-0.0026	0.0001	0.203	0.236	0.07	0.006	0.006	-0.093	8
33	-0.004	-0.0045	0.0005	0.183	1.336	1.067	0.008	0.008	0.109	3
34	-0.0088	-0.0089	0.0001	0.332	0.152	-0.112	0.023	0.008	-0.207	1
35	-0.0065	-0.0071	0.0006	0.193	1.687	1.421	0.024	0.02	0.188	4
36	-0.0023	-0.0026	0.0002	0.214	0.66	0.443	0	0.013	-0.012	6
37	-0.0053	-0.006	0.0007	0.131	1.979	1.673	0.021	0.057	0.16	5
38	-0.003	-0.0025	-0.0005	0.395	-1.471	-1.031	0.004	0.016	-0.099	46
39	-0.0039	-0.0035	-0.0004	0.138	-1.019	-0.744	0	0.012	0.017	47
40	-0.0052	-0.0054	0.0001	0.206	0.364	0.561	0.069	0.466	0.309	49
41	-0.0119	-0.0111	-0.0008	0.201	-2.011	-1.804	0.033	0.069	-0.211	48
42	-0.003	-0.0027	-0.0003	0.567[1]	-0.982	-0.215	0.034	0.011	0.294	45
43	-0.0118	-0.011	-0.0008	0.138	-2.114	-1.876	0.021	0.061	-0.151	51
44	-0.0095	-0.0087	-0.0008	0.221	-2.197	-1.936	0.037	0.058	-0.253	50
45	-0.0026	-0.0023	-0.0003	0.19	-0.875	-0.706	0.005	0.005	-0.088	27
46	-0.0014	-0.0013	-0.0001	0.205	-0.35	-0.235	0	0.013	0.007	25
47	-0.003	-0.0027	-0.0003	0.165	-0.937	-0.766	0.006	0.003	-0.088	29
48	-0.0039	-0.0036	-0.0003	0.191	-0.808	-0.654	0.004	0.008	-0.08	26
49	-0.0014	-0.0014	-9.32E-06	0.238	-0.026	0.068	0.005	0.007	0.086	30
50	-0.0009	-0.001	0.0001	0.308	0.213	0.327	0.018	0.004	0.191	24
51	-0.0031	-0.003	-0.0001	0.384	-0.248	-0.082	0.002	0.011	0.068	28
52	-0.0003	-0.0004	0.0001	0.640[1]	0.551	0.642	0.088	0.002	0.456	36
53	-0.0004	-0.0007	0.0002	0.238	0.808	0.581	0.011	0	0.153	37
54	-0.0006	-0.0004	-0.0002	0.631[1]	-0.959	-0.82	0.096	0	-0.494	33
55	-0.0006	-0.0004	-0.0002	0.368	-0.689	-0.494	0.012	0.004	-0.166	31
56	-0.0005	-0.0003	-0.0002	0.667[1]	-0.994	-0.902	0.137	0.001	-0.584	34
57	-0.0006	-0.0006	0	0.273	-0.124	-0.069	0	0.014	-0.005	35
58	-0.0008	-0.0009	0.0001	0.396	0.211	0.196	0.004	0.01	0.099	32

G.1: RESIDUAL DIAGNOSTICS FOR HIGH-SPEED EXPERIMENT

CFx										
Run Order	Actual Value	Predicted Value	Residual	Leverage	Internally Studentized Residuals	Externally Studentized Residuals	Cook's Distance	Cook's Random Distance	Influence on Fitted Value DFFITS	Standard Order
1	0.1012	0.0998	0.0014	0.385	1.215	1.267	0.042	0.033	0.509	29
2	0.1444	0.1446	-0.0002	0.695	-0.266	-0.445	0.02	0.014	-0.353	28
3	0.0508	0.0509	-0.0001	0.227	-0.067	-0.086	0	0.017	-0.039	30
4	0.0505	0.0507	-0.0002	0.225	-0.169	-0.183	0.001	0.014	-0.063	59
5	0.0396	0.0382	0.0014	0.36	1.165	1.156	0.025	0.041	0.379	44
6	0.0631	0.0625	0.0006	0.667	0.712	0.39	0.003	0.02	0.128	45
7	0.111	0.1102	0.0008	0.641	0.834	0.572	0.009	0.023	0.246	43
8	0.0493	0.0492	0	0.565	0.039	0.254	0.009	0.036	0.236	51
9	0.0657	0.0669	-0.0011	0.428	-1.023	-0.998	0.025	0.009	-0.41	50
10	0.0191	0.0195	-0.0003	0.534	-0.329	-0.205	0	0.018	-0.048	49
11	0.0747	0.0755	-0.0008	0.397	-0.726	-0.512	0.001	0.027	-0.078	25
12	0.0339	0.0344	-0.0005	0.531	-0.536	-0.163	0.001	0.018	0.091	27
13	0.1432	0.1456	-0.0024	0.576	-2.423	-2.69	0.243	0.526	-1.466	26
14	0.0926	0.0922	0.0004	0.527	0.413	0.627	0.028	0.047	0.428	39
15	0.066	0.0676	-0.0016	0.66	-1.754	-1.958	0.23	0.252	-1.276	38
16	0.038	0.0382	-0.0003	0.254	-0.21	-0.144	0	0.021	-0.001	37
17	0.0379	0.0381	-0.0003	0.254	-0.209	-0.144	0	0.021	-0.001	58
18	0.0262	0.0255	0.0007	0.891	1.148	0.287	0.002	0.022	0.097	10
19	0.1274	0.1269	0.0004	0.574	0.441	0.034	0.004	0.029	-0.158	9
20	0.0291	0.0282	0.0009	0.573	0.882	0.59	0.006	0.034	0.199	11
21	0.1163	0.1142	0.002	0.398	1.801	1.753	0.057	0.115	0.623	12
22	0.0111	0.0116	-0.0005	0.572	-0.514	-0.091	0.003	0.027	0.144	46
23	0.0922	0.0932	-0.001	0.581	-0.991	-0.752	0.015	0.05	-0.301	47
24	0.0975	0.0988	-0.0013	0.241	-1.028	-0.87	0.003	0.034	-0.123	48
25	0.0973	0.099	-0.0016	0.251	-1.316	-1.163	0.008	0.035	-0.207	60
26	0.0939	0.0924	0.0015	0.627	1.554	1.953	0.223	0.207	1.272	16
27	0.0766	0.0759	0.0007	0.3	0.547	0.547	0.005	0.007	0.169	15
28	-0.0013	-0.0005	-0.0008	0.772	-0.989	-1.57	0.295	0.167	-1.279	14
29	0.0003	0.0011	-0.0008	0.588	-0.785	-1.185	0.114	0.191	-0.831	13
30	0.0766	0.076	0.0006	0.425	0.519	0.522	0.007	0.012	0.218	31
31	0.0057	0.0043	0.0014	0.635	1.495	1.7	0.155	0.091	1.087	33
32	0.039	0.0402	-0.0013	0.481	-1.176	-1.403	0.08	0.155	-0.766	32
33	0.1272	0.1262	0.001	0.587	1.177	0.857	0.021	0.072	0.399	40
34	0.0505	0.0505	0	0.537	-0.034	-0.367	0.018	0.098	-0.353	41
35	0.0016	-0.0001	0.0017	0.679	2.248	1.892	0.172	0.094	1.162	42
36	0.0527	0.0527	0	0.675	0.062	0.358	0.018	0.032	0.339	4
37	0.1059	0.1072	-0.0013	0.526	-1.372	-1.164	0.04	0.031	-0.555	3
38	-0.0027	-0.0023	-0.0004	0.588	-0.521	-0.288	0.001	0.023	-0.09	2
39	0.0424	0.0427	-0.0003	0.607	-0.349	-0.116	0	0.022	0.011	1
40	-0.0071	-0.0066	-0.0005	0.696	-0.668	-0.606	0.025	0.019	-0.41	5
41	0.1134	0.1128	0.0007	0.51	0.717	0.71	0.02	0.001	0.388	8
42	0.1009	0.1009	0.0001	0.832	0.12	0.212	0.007	0.017	0.191	7
43	0.0259	0.0266	-0.0007	0.609	-0.828	-0.729	0.025	0.005	-0.43	6
44	0.1377	0.1365	0.0011	0.727	1.559	1.109	0.075	0.042	0.684	20
45	0.0191	0.0199	-0.0007	0.71	-1.014	-1.63	0.269	0.94	-1.336	17
46	0.0779	0.0762	0.0017	0.521	1.805	1.45	0.051	0.045	0.645	19
47	0.1119	0.1107	0.0012	0.72	1.604	1.224	0.095	0.067	0.771	18
48	0.0631	0.0624	0.0007	0.571	0.813	0.979	0.058	0.062	0.655	34
49	0.0879	0.0907	-0.0028	0.5	-2.907	-2.952	0.209	0.964	-1.435	36
50	0.01	0.01	0	0.371	-0.014	0.08	0.001	0.018	0.088	35
51	0.0101	0.01	0.0001	0.372	0.105	0.181	0.002	0.013	0.125	61
52	0.0078	0.0061	0.0017	0.73	2.051	2.457	0.411	0.551	1.751	52
53	0.0882	0.0878	0.0005	0.427	0.403	0.324	0.001	0.019	0.094	53
54	0.0419	0.0427	-0.0008	0.364	-0.629	-0.819	0.036	0.22	-0.425	54
55	0.0459	0.046	-0.0001	0.334	-0.069	0.03	0.001	0.018	0.076	56
56	0.1069	0.1081	-0.0012	0.549	-1.104	-1.215	0.072	0.005	-0.668	57
57	0.0073	0.0078	-0.0005	0.469	-0.513	-0.355	0.001	0.02	-0.086	55
58	0.0074	0.0076	-0.0002	0.471	-0.197	-0.052	0	0.023	0.051	62
59	0.0145	0.0149	-0.0004	0.516	-0.355	-0.499	0.017	0.036	-0.324	24
60	0.1004	0.1003	0.0002	0.607	0.169	0.085	0	0.019	0.015	23
61	0.0859	0.0848	0.0012	0.603	1.233	1.258	0.072	0.014	0.734	21
62	0.0311	0.0312	-0.0001	0.4	-0.057	-0.113	0.001	0.017	-0.08	22

CFy										
Run Order	Actual Value	Predicted Value	Residual	Leverage	Internally Studentized Residuals	Externally Studentized Residuals	Cook's Distance	Cook's Random Distance	Influence on Fitted Value DFFITS	Standard Order
1	0.0004	0.0006	-0.0002	0.252	-0.463	-0.552	0.025	0.052	-0.236	29
2	0.0005	-0.0001	0.0005	0.233	1.638	1.438	0.025	0.059	0.301	28
3	0.0005	0.0004	0.0001	0.157	0.242	0.16	0	0.014	-0.015	30
4	0.0006	0.0004	0.0001	0.155	0.364	0.266	0	0.015	0.003	59
5	0.0003	0.0002	0.0001	0.154	0.386	0.323	0	0.014	0.02	44
6	0.0007	0.0006	0.0002	0.39	0.508	0.432	0.003	0.013	0.108	45
7	-0.0001	-0.0002	0.0001	0.273	0.298	0.216	0	0.013	0.003	43
8	0	-0.0003	0.0003	0.402	1.011	0.618	0	0.015	0.024	51
9	0.0002	-0.0003	0.0005	0.358	1.662	1.504	0.045	0.112	0.402	50
10	0.0005	0.0001	0.0004	0.232	1.118	0.832	0.001	0.022	0.059	49
11	0.0012	0.0012	-0.0001	0.261	-0.177	-0.237	0.005	0.01	-0.118	25
12	0.0016	0.0014	0.0002	0.405	0.784	0.731	0.018	0.001	0.272	27
13	-0.0002	-0.0003	0.0001	0.269	0.29	0.217	0	0.014	0.025	26
14	0	-0.0002	0.0002	0.372	0.652	0.446	0.001	0.016	0.05	39
15	0.0006	0.0002	0.0003	0.349	1.054	0.825	0.009	0.005	0.182	38
16	-0.0001	-0.0003	0.0002	0.146	0.612	0.456	0	0.016	0.016	37
17	-0.0002	-0.0003	0.0001	0.146	0.371	0.248	0	0.013	-0.018	58
18	0.0025	0.0022	0.0003	0.538	1.09	1.466	0.185	0.269	0.923	10
19	0.0003	0.0008	-0.0004	0.28	-1.331	-1.12	0.017	0.004	-0.258	9
20	0.0013	0.0015	-0.0002	0.22	-0.678	-0.541	0.002	0.014	-0.071	11
21	-0.0001	0.0001	-0.0003	0.346	-0.9	-0.802	0.018	0.007	-0.226	12
22	0.0005	0.0003	0.0002	0.164	0.692	0.488	0.001	0.012	-0.04	46
23	0.0005	0.0001	0.0004	0.341	1.208	0.941	0.004	0.022	0.113	47
24	0.0005	0.0001	0.0004	0.167	1.149	0.929	0.001	0.021	0.043	48
25	0.0007	0.0001	0.0006	0.17	1.672	1.46	0.008	0.032	0.143	60
26	-0.0001	0	-0.0001	0.161	-0.297	-0.145	0.003	0.017	0.081	16
27	-0.0002	0	-0.0001	0.133	-0.398	-0.259	0.001	0.012	0.05	15
28	0.0003	0.0005	-0.0002	0.273	-0.636	-0.404	0.001	0.012	0.046	14
29	-0.0002	0.0006	-0.0009	0.245	-2.575	-2.58	0.092	0.466	-0.551	13
30	-0.0002	-0.0001	-0.0001	0.214	-0.382	-0.318	0.001	0.014	-0.049	31
31	-0.0003	-0.0001	-0.0003	0.394	-0.945	-0.944	0.035	0.005	-0.369	33
32	-0.0004	-0.0006	0.0002	0.488	0.57	0.84	0.072	0.007	0.529	32
33	0.0001	0.0003	-0.0002	0.452	-0.85	-0.52	0.004	0.023	-0.137	40
34	0	0.0004	-0.0003	0.696[x]	-1.636	-1.367	0.187	0.027	-0.86	41
35	-0.0004	-0.0004	3.23E-06	0.631	0.015	0.412	0.038	0.005	0.407	42
36	-0.0015	-0.0016	0.0001	0.746[x]	0.497	0.185	0.001	0.015	0.056	4
37	-0.0005	-0.0005	-0.0001	0.431	-0.254	-0.33	0.011	0.004	-0.214	3
38	-0.0011	-0.0016	0.0005	0.339	1.847	1.395	0.04	0.055	0.432	2
39	-0.0008	-0.0007	-0.0001	0.463	-0.404	-0.475	0.022	0.006	-0.299	1
40	-0.0011	-0.0009	-0.0002	0.593	-0.82	-0.615	0.026	0.005	-0.322	5
41	-0.0006	-0.0005	-0.0001	0.411	-0.588	-0.402	0.004	0.015	-0.129	8
42	-0.0004	-0.0003	-0.0001	0.675	-0.719	-0.469	0.016	0.01	-0.256	7
43	-0.0006	-0.0008	0.0002	0.372	0.673	0.574	0.014	0	0.256	6
44	-0.0015	-0.001	-0.0005	0.501	-2.083	-1.602	0.109	0.064	-0.702	20
45	0.0014	0.0011	0.0002	0.483	1.023	1.125	0.119	0.229	0.689	17
46	-0.0012	-0.001	-0.0002	0.279	-0.597	-0.345	0	0.016	-0.026	19
47	-0.0029	-0.0027	-0.0003	0.780[x]	-1.463	-1.073	0.166	0.014	-0.724	18
48	0.0004	0.0005	-0.0001	0.750[x]	-0.509	-1.083	0.29	0.115	-0.951	34
49	0.0002	0.0001	0.0001	0.313	0.341	0.185	0	0.016	0.009	36
50	0.0017	0.0014	0.0003	0.31	1.089	0.755	0.008	0.003	0.189	35
51	0.0015	0.0014	0.0001	0.313	0.499	0.303	0	0.016	0.047	61
52	-0.0003	0.0003	-0.0005	0.292	-1.679	-1.466	0.024	0.02	-0.326	52
53	-0.0008	-0.0003	-0.0004	0.246	-1.353	-1.149	0.01	0.017	-0.194	53
54	0.0002	0.0001	0.0001	0.24	0.33	0.543	0.055	0.471	0.32	54
55	0.0001	0.0004	-0.0003	0.237	-0.954	-0.954	0.027	0.008	-0.239	56
56	-0.0003	-0.0002	-0.0001	0.145	-0.358	-0.311	0.001	0.013	-0.032	57
57	0.0005	0.0004	0.0001	0.222	0.445	0.461	0.006	0.001	0.141	55
58	0.0004	0.0004	0	0.222	0.049	0.085	0.001	0.012	0.05	62
59	-0.0001	0.0001	-0.0003	0.418	-0.873	-0.662	0.007	0.022	-0.149	24
60	-0.001	-0.0013	0.0003	0.37	0.843	1.086	0.09	0.265	0.579	23
61	-0.0013	-0.0012	-0.0002	0.217	-0.475	-0.304	0	0.013	0.02	21
62	-0.0005	0.0003	-0.0008	0.285	-2.46	-2.304	0.103	0.472	-0.605	22

CFz										
Run Order	Actual Value	Predicted Value	Residual	Leverage	Internally Studentized Residuals	Externally Studentized Residuals	Cook's Distance	Cook's Random Distance	Influence on Fitted Value DFFITS	Standard Order
1	-0.0049	-0.0045	-0.0004	0.37	-1.433	-1.301	0.052	0.02	-0.368	29
2	-0.0038	-0.0033	-0.0004	0.742	-1.663	-2.149	0.418	0.253	-1.385	28
3	-0.0051	-0.0049	-0.0001	0.36	-0.497	-0.152	0.005	0.005	0.145	30
4	-0.0051	-0.005	-0.0001	0.355	-0.421	-0.084	0.006	0.002	0.168	59
5	-0.0044	-0.0047	0.0003	0.303	0.876	0.391	0.018	0.131	-0.204	44
6	-0.0037	-0.0042	0.0006	0.536	1.895	1.92	0.108	0.093	0.716	45
7	-0.0018	-0.0023	0.0005	0.719	1.82	1.877	0.226	0.091	0.992	43
8	-0.0069	-0.007	0.0001	0.531	0.372	0.296	0.002	0.028	0.098	51
9	-0.0045	-0.0047	0.0002	0.654	0.677	0.842	0.056	0.001	0.521	50
10	-0.0092	-0.0092	0	0.52	-0.127	-0.469	0.043	0.037	-0.4	49
11	-0.0098	-0.0101	0.0003	0.431	1.062	0.726	0.003	0.036	0.094	25
12	-0.0118	-0.0119	0.0001	0.704	0.447	-0.844	0.229	0.451	-1.044	27
13	-0.0053	-0.0058	0.0005	0.602	1.932	2.133	0.202	0.37	1.071	26
14	-0.0006	-0.0003	-0.0003	0.729	-1.231	-0.082	0.049	0.02	0.437	39
15	-0.0015	-0.0011	-0.0004	0.659	-1.732	-1.133	0.02	0.024	-0.305	38
16	-0.0017	-0.0012	-0.0005	0.224	-1.591	-1.133	0.003	0.043	-0.082	37
17	-0.0016	-0.0012	-0.0004	0.225	-1.426	-0.973	0.001	0.043	-0.042	58
18	-0.014	-0.0137	-0.0003	0.678	-1.224	-1.259	0.083	0.024	-0.672	10
19	-0.0069	-0.0068	-0.0001	0.696	-0.371	0.182	0.032	0.01	0.345	9
20	-0.0132	-0.0133	0.0001	0.497	0.407	1.007	0.165	0.843	0.78	11
21	-0.0072	-0.0068	-0.0004	0.721	-1.379	-3.397	1.921[t]	3.635[t]	-2.754[t]	12
22	-0.0065	-0.0062	-0.0003	0.506	-0.982	-1.084	0.066	0.004	-0.467	46
23	-0.0033	-0.0032	-0.0001	0.682	-0.48	0.06	0.024	0.013	0.298	47
24	-0.0035	-0.0034	-0.0001	0.316	-0.275	-0.073	0.003	0.009	0.114	48
25	-0.0037	-0.0034	-0.0003	0.322	-0.876	-0.717	0.003	0.023	-0.114	60
26	-0.003	-0.0026	-0.0003	0.41	-1.152	-1.07	0.024	0.007	-0.296	16
27	-0.0034	-0.0032	-0.0001	0.416	-0.472	-0.159	0.007	0.013	0.149	15
28	-0.0061	-0.0059	-0.0002	0.894	-0.793	-0.189	0.001	0.031	0.044	14
29	-0.0068	-0.0066	-0.0002	0.497	-0.735	-0.498	0.001	0.032	-0.042	13
30	-0.0004	-0.0007	0.0003	0.426	1.015	0.585	0	0.025	-0.013	31
31	-0.0012	-0.0017	0.0005	0.681	1.902	2.382	0.375	0.372	1.416	33
32	-0.0008	-0.001	0.0002	0.761	0.915	-0.258	0.1	0.016	-0.617	32
33	-0.0006	-0.0006	0	0.925	0.178	-0.355	0.085	0.015	-0.378	40
34	-0.001	-0.001	0	0.806	-0.189	-0.913	0.242	0.136	-0.87	41
35	-0.0011	-0.0012	0.0002	0.914	1.075	2.098	1.179[t]	0.539[t]	1.91	42
36	-0.0014	-0.0013	-0.0001	0.848	-0.618	-0.169	0.001	0.031	-0.042	4
37	-0.0006	-0.0005	-0.0002	0.812	-0.971	-0.746	0.072	0.022	-0.514	3
38	-0.0013	-0.0012	-0.0001	0.765	-0.63	-0.24	0.001	0.033	-0.074	2
39	-0.0009	-0.0008	-0.0001	0.817	-0.347	0.212	0.022	0.02	0.293	1
40	-0.0006	-0.0007	0	0.95	0.276	-2.256	2.530[t]	0.736[t]	-2.291	5
41	-0.0003	-0.0005	0.0002	0.858	1.693	2.627	1.994[t]	0.678[t]	2.303	8
42	-0.0001	-0.0002	0.0001	0.926	1.078	0.303	0.01	0.03	0.154	7
43	-0.0006	-0.0007	0.0001	0.872	0.964	0.233	0.001	0.036	0.059	6
44	-0.0033	-0.0033	2.58E-06	0.966	0.02	-1.133	1.059[t]	0.027[t]	-1.135	20
45	-0.011	-0.0111	0	0.938	0.341	0.113	0.003	0.032	0.068	17
46	-0.007	-0.0073	0.0002	0.634	1.187	1.157	0.139	0.123	0.754	19
47	-0.0042	-0.0041	-0.0001	0.851	-0.536	-1.415	0.461	0.236	-1.297	18
48	-0.0064	-0.0063	-0.0001	0.876	-0.683	-0.259	0.007	0.031	-0.132	34
49	-0.0047	-0.0046	-0.0002	0.721	-0.926	-0.678	0.041	0.029	-0.407	36
50	-0.0104	-0.0104	0	0.431	-0.198	0.006	0.001	0.027	0.083	35
51	-0.0105	-0.0104	-0.0001	0.432	-0.525	-0.222	0	0.035	-0.017	61
52	-0.005	-0.0052	0.0002	0.896	0.826	1.055	0.268	0	0.823	52
53	-0.0018	-0.0021	0.0003	0.48	0.926	0.871	0.023	0.015	0.321	53
54	-0.0042	-0.0042	0	0.313	0.161	-0.071	0.014	0.024	-0.176	54
55	-0.0048	-0.0048	0	0.528	-0.151	-0.648	0.091	0.148	-0.558	56
56	-0.0025	-0.0028	0.0002	0.316	0.737	0.746	0.021	0	0.222	57
57	-0.0067	-0.0067	0	0.375	0.164	0.042	0.001	0.029	-0.065	55
58	-0.0065	-0.0067	0.0002	0.376	0.578	0.494	0.003	0.017	0.116	62
59	-0.0097	-0.0096	-0.0001	0.513	-0.39	-0.082	0.005	0.018	0.129	24
60	-0.0029	-0.0027	-0.0003	0.855	-1.152	-1.378	0.194	0.025	-0.953	23
61	-0.0038	-0.0037	-0.0001	0.485	-0.37	-0.093	0.003	0.023	0.11	21
62	-0.0079	-0.0077	-0.0002	0.555	-0.63	-0.43	0.003	0.03	-0.101	22

CMx										
Run Order	Actual Value	Predicted Value	Residual	Leverage	Internally Studentized Residuals	Externally Studentized Residuals	Cook's Distance	Cook's Random Distance	Influence on Fitted Value DFFITS	Standard Order
1	-0.0115	-0.0115	0	0.446	-0.596	-1.011	0.357[t]	3.777[t]	-0.648	29
2	-0.0137	-0.0137	6.88E-06	0.9	0.124	1.079	0.951	0.01	1.041	28
3	-0.0075	-0.0075	0	0.373	0.291	0.277	0.005	0.011	0.102	30
4	-0.0075	-0.0075	0	0.369	0.318	0.303	0.005	0.005	0.112	59
5	-0.0054	-0.0053	-0.0001	0.55	-1.156	-1.342	0.304	0.059	-0.65	44
6	-0.0073	-0.0073	-0.0001	0.842	-0.969	0.849	0.873	0.148	1.274	45
7	-0.0096	-0.0096	-0.0001	0.888	-1.284	-3.994	6.297[t]	1.835[t]	-3.449[t]	43
8	-0.0059	-0.0059	-0.0001	0.708	-0.925	-0.497	0.001	0.048	-0.051	51
9	-0.0068	-0.0067	-0.0001	0.834	-0.998	-1.125	0.281	0.625	-0.725	50
10	-0.0033	-0.0033	-0.0001	0.792	-0.965	-0.722	0.103	0.048	-0.37	49
11	-0.0094	-0.0094	-1.29E-06	0.665	-0.023	0.378	0.09	0.009	0.389	25
12	-0.0059	-0.0059	0	0.81	-0.311	-0.983	0.281	0.032	-0.841	27
13	-0.0134	-0.0134	-1.87E-06	0.826	-0.034	0.51	0.146	0.027	0.524	26
14	-0.0081	-0.0081	-0.0001	0.828	-0.961	-1.291	0.363	0.173	-0.865	39
15	-0.0072	-0.0071	0	0.838	-0.823	-0.372	0.001	0.044	-0.035	38
16	-0.0052	-0.0051	0	0.297	-0.802	-0.503	0	0.082	-0.013	37
17	-0.0051	-0.0051	0	0.297	-0.671	-0.379	0.001	0.061	0.029	58
18	-0.0048	-0.0048	-3.01E-06	1.003	-0.058	-2.553	3.858[t]	1.033[t]	-2.535	10
19	-0.0128	-0.0128	0	0.737	0.331	1.003	0.345	0.2	0.843	9
20	-0.0052	-0.0052	0	0.763	0.29	1.322	0.831	0.287	1.194	11
21	-0.0119	-0.0119	-8.03E-06	0.797	-0.147	-2.179	1.942[t]	2.557[t]	-2.109	12
22	-0.0034	-0.0033	-0.0001	0.703	-2.408	-4.834[z]	1.919[t]	4.134[t]	-2.863[t]	46
23	-0.0102	-0.01	-0.0001	0.667	-2.132	-1.72	0.132	0.199	-0.493	47
24	-0.0103	-0.0102	-0.0001	0.373	-1.761	-1.061	0.005	0.007	0.104	48
25	-0.0103	-0.0102	-0.0001	0.395	-2.019	-1.339	0	0.084	0	60
26	-0.009	-0.0091	0	0.79	0.547	-0.259	0.147	0.008	-0.534	16
27	-0.008	-0.0081	0	0.575	0.74	0.787	0.053	0.079	0.31	15
28	-0.0017	-0.0017	0	0.955	0.67	0.479	0.722	0.025	0.386	14
29	-0.0018	-0.0018	0	0.789	0.687	0.706	0.122	0.042	0.408	13
30	-0.0076	-0.0076	0	0.651	0.559	1.121	0.4	0.203	0.84	31
31	-0.0022	-0.0022	0	0.882	0.225	-2.031	2.487[t]	0.887[t]	-2.115	33
32	-0.005	-0.0051	0	0.837	0.4	0.288	0.016	0.043	0.149	32
33	-0.0119	-0.0119	4.81E-06	0.948	0.153	-1.414	1.573[t]	0.311[t]	-1.44	40
34	-0.0072	-0.0072	5.79E-06	0.841	0.172	-0.582	0.237	0.072	-0.621	41
35	-0.0025	-0.0025	0	0.945	0.736	3.057	2.787[t]	3.002[t]	2.872[t]	42
36	-0.0065	-0.0065	5.60E-06	0.921	0.173	-1.831	2.671[t]	0.497[t]	-1.864	4
37	-0.0094	-0.0095	0	0.938	0.773	2.727	3.798[t]	1.229[t]	2.563	3
38	-0.0015	-0.0016	0	0.939	0.717	2.773	5.130[t]	1.017[t]	2.638[t]	2
39	-0.0055	-0.0055	3.68E-06	0.96	0.117	-2.189	2.991[t]	0.737[t]	-2.212	1
40	-0.002	-0.002	0	0.957	-0.401	-2.294	2.426[t]	1.491[t]	-2.217	5
41	-0.012	-0.012	-1.39E-06	0.898	-0.047	-0.144	0.03	0.034	-0.138	8
42	-0.0118	-0.0118	3.70E-06	0.958	0.134	0.678	0.303	0.018	0.657	7
43	-0.0054	-0.0054	5.24E-06	0.91	0.184	0.601	0.168	0.002	0.565	6
44	-0.0117	-0.0117	5.06E-06	0.983	0.164	-3.13	8.394[t]	1.891[t]	-3.156[t]	20
45	-0.004	-0.004	0	0.934	0.588	1.486	1.265[t]	0.178[t]	1.373	17
46	-0.0084	-0.0084	0	0.817	0.504	0.455	0.049	0.012	0.324	19
47	-0.0105	-0.0105	3.99E-06	0.882	0.123	-0.633	0.237	0.057	-0.661	18
48	-0.0071	-0.0071	0	0.94	0.624	1.246	1.050[t]	0.033[t]	1.136	34
49	-0.0087	-0.0087	0	0.908	0.495	0.872	1.313[t]	0.074[t]	0.812	36
50	-0.0029	-0.0029	9.97E-06	0.469	0.271	0.056	0.001	0.077	-0.036	35
51	-0.0029	-0.0029	0	0.473	0.297	0.072	0	0.079	-0.028	61
52	-0.0021	-0.0021	0	0.927	0.834	0.771	1.007[t]	0.271[t]	0.624	52
53	-0.0079	-0.0079	0	0.681	0.769	0.396	0.001	0.061	-0.035	53
54	-0.0053	-0.0053	0.0001	0.43	0.87	0.72	0.018	0.061	0.158	54
55	-0.0064	-0.0065	0.0001	0.608	1.328	-0.116	0.505[t]	2.947[t]	-0.89	56
56	-0.0107	-0.0108	0.0001	0.629	1.954	2.94	1.089[t]	1.363[t]	1.595	57
57	-0.0029	-0.003	0.0001	0.437	1.749	1.217	0.001	0.072	0.049	55
58	-0.0029	-0.003	0.0001	0.438	1.771	1.246	0.002	0.066	0.062	62
59	-0.003	-0.0031	0	0.699	0.599	0.833	0.215	0.022	0.564	24
60	-0.0083	-0.0083	0	0.989	0.68	2.369	3.342[t]	0.565[t]	2.164	23
61	-0.0078	-0.0078	0	0.861	0.336	-2.649	4.485[t]	1.997[t]	-2.782[t]	21
62	-0.0042	-0.0043	0	0.785	0.491	0.177	0.001	0.052	-0.04	22

CMy										
Run Order	Actual Value	Predicted Value	Residual	Leverage	Internally Studentized Residuals	Externally Studentized Residuals	Cook's Distance	Cook's Random Distance	Influence on Fitted Value DFFITS	Standard Order
1	0.0001	0.0001	0	0.442	0.183	0.175	0.001	0.02	0.079	29
2	0.0003	0.0004	-0.0001	0.549	-1.133	-1.079	0.045	0.001	-0.586	28
3	0.0005	0.0005	0	0.363	0.376	0.348	0.002	0.013	0.126	30
4	0.0005	0.0004	0	0.362	0.405	0.375	0.003	0.013	0.135	59
5	0.0003	0.0002	0.0002	0.313	1.256	1.28	0.024	0.076	0.397	44
6	0.0001	0.0001	0	0.368	0.269	0.208	0	0.016	0.041	45
7	0.0006	0.0005	0.0001	0.502	0.51	0.438	0.005	0.024	0.185	43
8	0.0004	0.0004	0.0001	0.364	0.439	0.409	0.003	0.023	0.133	51
9	0.0013	0.001	0.0003	0.526	2.39	2.552	0.206	0.363	1.324	50
10	0.0003	0.0004	-0.0001	0.272	-0.792	-0.806	0.014	0.161	-0.264	49
11	0.0011	0.0011	0	0.323	0.108	0.089	0	0.023	0.016	25
12	0.0011	0.0011	0	0.526	0.248	0.224	0.002	0.015	0.107	27
13	0.0016	0.0016	0	0.45	0.263	0.24	0.001	0.014	0.098	26
14	-0.0004	-0.0005	0.0001	0.48	1.24	1.32	0.069	0.459	0.685	39
15	-0.0007	-0.0004	-0.0003	0.465	-2.712	-2.874	0.173	0.557	-1.254	38
16	-0.0007	-0.0006	-0.0001	0.226	-0.751	-0.729	0.005	0.074	-0.154	37
17	-0.0006	-0.0006	-0.0001	0.226	-0.591	-0.558	0.003	0.049	-0.11	58
18	0.0004	0.0005	-0.0002	0.509	-1.489	-1.416	0.057	0.019	-0.665	10
19	0.0012	0.0011	0.0001	0.442	0.903	0.942	0.03	0.054	0.45	9
20	0.0008	0.0009	-0.0001	0.297	-0.657	-0.633	0.006	0.006	-0.185	11
21	0.002	0.0019	0.0001	0.606	0.635	0.742	0.039	0.074	0.494	12
22	0.0001	-3.06E-06	0.0001	0.302	0.41	0.442	0.005	0.043	0.166	46
23	0.0001	0.0003	-0.0002	0.473	-1.388	-1.418	0.063	0.019	-0.677	47
24	0.0004	0.0004	0	0.325	0.197	0.211	0.001	0.014	0.083	48
25	0.0003	0.0004	0	0.329	-0.31	-0.276	0.001	0.016	-0.074	60
26	0.0002	0.0003	-0.0001	0.347	-0.726	-0.707	0.009	0.046	-0.235	16
27	0.0004	0.0003	0	0.399	0.271	0.367	0.008	0.073	0.211	15
28	0.0001	0.0002	0	0.945	-1.237	-0.593	0.075	0.017	-0.483	14
29	-0.0003	-0.0002	-0.0002	0.379	-1.35	-1.34	0.034	0.065	-0.49	13
30	-0.0002	-0.0005	0.0002	0.284	1.562	1.688	0.038	0.157	0.487	31
31	-0.0004	-0.0006	0.0002	0.369	1.477	1.511	0.041	0.143	0.544	33
32	-0.0003	-0.0002	-0.0001	0.517	-0.603	-0.806	0.042	0.34	-0.524	32
33	-0.0004	-0.0004	0	0.629	0.18	0.171	0.002	0.018	0.107	40
34	-0.0004	-0.0005	0	0.703	0.39	0.365	0.01	0.013	0.252	41
35	-0.0003	-0.0002	0	0.746	-0.638	-0.616	0.036	0.011	-0.459	42
36	-0.0005	-0.0005	0	0.54	0.174	0.165	0.001	0.018	0.089	4
37	-0.0003	-0.0004	0.0001	0.559	1.034	0.981	0.04	0.008	0.545	3
38	-0.0004	-0.0004	0	0.461	-0.111	-0.101	0	0.018	-0.045	2
39	-0.0003	-0.0002	-0.0001	0.528	-1.053	-1.001	0.036	0	-0.527	1
40	-0.0002	-0.0002	-4.82E-06	0.865	-0.088	-0.087	0.002	0.019	-0.076	5
41	-0.0003	-0.0002	-0.0001	0.648	-1.152	-1.113	0.074	0.006	-0.72	8
42	-0.0005	-0.0005	0	0.674	0.296	0.28	0.005	0.015	0.187	7
43	-0.0004	-0.0004	0.0001	0.558	0.822	0.771	0.023	0.002	0.42	6
44	0.0021	0.0022	-0.0001	0.626	-0.749	-0.702	0.026	0.004	-0.431	20
45	0.0011	0.0011	0	0.789	0.249	0.25	0.008	0.022	0.198	17
46	0.0016	0.0017	-0.0001	0.635	-0.686	-0.652	0.024	0.01	-0.408	19
47	0.0018	0.0017	0.0001	0.603	1.203	1.158	0.067	0.015	0.698	18
48	0.0013	0.0014	-0.0001	0.546	-0.998	-0.955	0.035	0.002	-0.521	34
49	0.001	0.0011	-0.0001	0.481	-1.221	-1.166	0.039	0.005	-0.556	36
50	0.0006	0.0005	0.0001	0.347	1.014	0.954	0.015	0.002	0.331	35
51	0.0006	0.0005	0.0001	0.348	0.908	0.853	0.012	0.003	0.296	61
52	0.002	0.0019	0.0001	0.887	2.381	2.398	1.132[t]	0.284[t]	2.099[t]	52
53	0.0012	0.0015	-0.0003	0.556	-2.898	-3.026	0.327[t]	1.287[t]	-1.696	53
54	0.0015	0.0014	0.0002	0.538	1.664	1.617	0.103	0.201	0.881	54
55	0.0004	0.0004	0	0.416	0.23	0.199	0.001	0.016	0.067	56
56	0.0004	0.0003	0.0001	0.268	0.912	0.895	0.01	0.002	0.233	57
57	-0.0002	-0.0001	0	0.313	-0.312	-0.317	0.002	0.012	-0.111	55
58	-0.0001	-0.0001	9.67E-06	0.313	0.076	0.052	0	0.017	0.002	62
59	0.0002	0.0002	0	0.36	-0.143	-0.086	0	0.018	0.003	24
60	0.0011	0.0011	0	0.6	-0.406	-0.278	0.002	0.018	-0.111	23
61	0.0009	0.0008	0.0001	0.334	0.458	0.467	0.005	0.009	0.172	21
62	0.0007	0.0009	-0.0002	0.387	-1.844	-1.942	0.075	0.158	-0.756	22

CMz										
Run Order	Actual Value	Predicted Value	Residual	Leverage	Internally Studentized Residuals	Externally Studentized Residuals	Cook's Distance	Cook's Random Distance	Influence on Fitted Value DFFITS	Standard Order
1	-0.0024	-0.0023	-0.0001	0.426	-0.749	0.05	0.261[t]	1.903[t]	0.474	29
2	-0.002	-0.0017	-0.0003	0.798	-1.59	-2.031	0.58	0.371	-1.192	28
3	-0.0026	-0.0024	-0.0002	0.364	-1.342	-0.862	0.001	0.049	-0.036	30
4	-0.0026	-0.0024	-0.0002	0.358	-1.474	-1	0.004	0.019	-0.088	59
5	-0.002	-0.0019	0	0.524	-0.223	0.175	0.069	0.005	0.319	44
6	-0.002	-0.0019	-0.0001	0.749	-0.524	-1.019	0.239	0.022	-0.725	45
7	-0.0012	-0.0012	-0.0001	0.803	-0.407	-0.387	0.019	0.037	-0.188	43
8	-0.0031	-0.003	-0.0001	0.693	-0.671	-0.075	0.034	0.015	0.273	51
9	-0.0029	-0.0027	-0.0002	0.794	-0.998	-1.379	0.342	0.046	-0.894	50
10	-0.0037	-0.0036	-0.0001	0.667	-0.77	-0.401	0	0.041	-0.004	49
11	-0.0049	-0.0047	-0.0002	0.599	-0.965	-1.086	0.171	0.025	-0.551	25
12	-0.0051	-0.005	-0.0001	0.79	-0.816	-0.565	0.015	0.053	-0.183	27
13	-0.0028	-0.0028	-0.0001	0.665	-0.564	0.018	0.042	0.004	0.319	26
14	-0.0003	-0.0001	-0.0002	0.755	-1.477	-0.744	0	0.051	-0.008	39
15	-0.0006	-0.0004	-0.0002	0.76	-1.478	-0.74	0	0.05	0.003	38
16	-0.0004	-0.0002	-0.0003	0.252	-1.564	-1.018	0.002	0.046	-0.044	37
17	-0.0004	-0.0002	-0.0002	0.252	-1.397	-0.861	0	0.054	0	58
18	-0.0064	-0.0067	0.0003	0.956	1.755	2.595	1.430[t]	1.074[t]	1.853	10
19	-0.0035	-0.0037	0.0002	0.684	1.053	-0.397	0.496[t]	1.443[t]	-0.928	9
20	-0.0053	-0.0055	0.0002	0.75	1.451	0.812	0.022	0.063	0.177	11
21	-0.0035	-0.0038	0.0003	0.792	1.697	2.5	1.391[t]	0.498[t]	1.679	12
22	-0.0027	-0.0027	-0.0001	0.646	-0.32	0.906	0.707[t]	1.127[t]	1.097	46
23	-0.0021	-0.002	-0.0001	0.658	-0.58	-0.265	0.003	0.044	0.072	47
24	-0.0022	-0.0021	-0.0001	0.375	-0.551	-0.357	0	0.049	0.015	48
25	-0.0023	-0.0021	-0.0002	0.393	-1.007	-0.899	0.018	0.024	-0.204	60
26	-0.0015	-0.0016	0.0002	0.672	0.937	0.503	0.003	0.04	-0.078	16
27	-0.0016	-0.0018	0.0002	0.463	0.853	0.47	0.008	0.025	-0.108	15
28	-0.0021	-0.0023	0.0002	0.893	1.094	1.294	0.503	0.01	0.847	14
29	-0.0023	-0.0025	0.0002	0.64	1.147	1.243	0.134	0.034	0.511	13
30	-0.0001	-0.0002	0.0001	0.478	0.481	0.146	0.011	0.015	-0.132	31
31	-0.0003	-0.0004	0.0001	0.74	0.848	1.036	0.14	0.011	0.595	33
32	-0.0002	-0.0003	0.0001	0.799	0.627	0.224	0.002	0.045	-0.052	32
33	-0.0004	-0.0005	0.0001	0.948	1.206	2.246	3.235[t]	0.387[t]	2.03	40
34	-0.0005	-0.0006	0.0001	0.824	1.138	1.099	0.362	0.013	0.812	41
35	-0.0003	-0.0003	0	0.917	0.509	-1.468	1.129[t]	0.730[t]	-1.59	42
36	0.0001	0.0002	0	0.904	-0.489	0.377	0.182	0.01	0.474	4
37	-0.0001	-0.0001	0	0.826	-0.473	0.05	0.015	0.033	0.177	3
38	-0.0001	8.38E-06	-0.0001	0.915	-0.886	-1.3	0.703	0.057	-1.098	2
39	-0.0001	-0.0001	-0.0001	0.89	-0.592	-0.127	0	0.051	0.014	1
40	-0.0001	-0.0003	0.0001	0.957	1.676	2.29	2.440[t]	0.767[t]	1.979	5
41	-0.0003	-0.0004	0.0001	0.882	1.429	1.552	1.636[t]	0.086[t]	1.303	8
42	-0.0005	-0.0006	0.0001	0.944	1.426	0.697	0.131	0.021	0.44	7
43	-0.0002	-0.0003	0.0001	0.874	0.708	-0.917	0.543	0.533	-1.083	6
44	-0.0019	-0.002	0.0001	0.981	1.201	3.083	9.152[t]	1.103[t]	2.899[t]	20
45	-0.0048	-0.0049	0.0001	0.932	0.688	-1.22	1.391[t]	0.115[t]	-1.354	17
46	-0.0032	-0.0033	0.0001	0.769	0.712	-0.023	0.025	0.015	-0.223	19
47	-0.0019	-0.002	0.0001	0.855	1.196	0.959	0.218	0.008	0.653	18
48	-0.0032	-0.0031	-0.0001	0.918	-0.669	-0.442	0.069	0.041	-0.306	34
49	-0.0029	-0.0028	0	0.764	-0.297	0.297	0.075	0.001	0.383	36
50	-0.0046	-0.0045	-0.0001	0.435	-0.94	-0.438	0.006	0.01	-0.115	35
51	-0.0045	-0.0045	0	0.437	-0.356	-0.077	0.001	0.042	0.045	61
52	-0.0016	-0.0019	0.0002	0.905	1.544	-0.257	0.48	0.016	-0.805	52
53	-0.0013	-0.0016	0.0003	0.58	1.809	1.482	0.052	0.009	0.353	53
54	-0.0015	-0.0017	0.0003	0.417	1.519	1.012	0.001	0.056	0.027	54
55	-0.0022	-0.0023	0	0.582	0.112	0.952	0.372[t]	1.119[t]	0.874	56
56	-0.0018	-0.0017	-0.0001	0.617	-0.642	-1.771	0.982	0.853	-1.342	57
57	-0.003	-0.0029	-0.0001	0.43	-0.54	-0.475	0.005	0.018	-0.111	55
58	-0.003	-0.003	-0.0001	0.432	-0.337	-0.222	0	0.055	0.004	62
59	-0.0039	-0.0038	0	0.65	-0.266	-0.653	0.149	0.036	-0.511	24
60	-0.0017	-0.0017	0	0.965	-0.214	-1.095	0.527	0.052	-1.013	23
61	-0.002	-0.002	0	0.787	0.08	0.595	0.17	0.033	0.559	21
62	-0.003	-0.003	0	0.652	0.17	0.59	0.133	0.011	0.498	22

H: LOW-SPEED REGRESSION MODELS (NATURAL UNITS)

3-Blade Regression Model

CFx	CFy	CFz	CMx	CMy	CMz
1.67E-01 Intercept	-1.10E-02 Intercept	-1.28E-01 Intercept	-1.09E-02 Intercept	-4.15E-03 Intercept	-3.03E-03 Intercept
-2.81E-02 Velocity	3.54E-03 Velocity	7.39E-04 Velocity	4.77E-04 Velocity	3.85E-03 Velocity	-8.90E-05 Velocity
-2.05E-03 AOI	1.27E-04 AOI	-2.80E-05 AOI	5.80E-05 AOI	-7.95E-06 AOI	-6.20E-05 AOI
-1.10E-05 RPM	4.29E-06 RPM	1.11E-04 RPM	1.41E-06 RPM	4.07E-07 RPM	2.23E-06 RPM
2.79E-04 Velocity * AOI	1.10E-05 Velocity * AOI	-6.90E-05 Velocity * AOI	-1.20E-05 Velocity * AOI	1.06E-06 Velocity * AOI	-2.60E-05 Velocity * AOI
7.03E-06 Velocity * RPM	-1.28E-06 Velocity * RPM	5.65E-07 Velocity * RPM	-2.88E-07 Velocity * RPM	-4.94E-07 Velocity * RPM	1.86E-08 Velocity * RPM
3.63E-07 AOI * RPM	-5.64E-08 AOI * RPM	4.68E-08 AOI * RPM	-1.85E-08 AOI * RPM	6.35E-09 AOI * RPM	5.80E-09 AOI * RPM
1.36E-03 Velocity^2	-2.62E-04 Velocity^2	-2.26E-04 Velocity^2	4.40E-05 Velocity^2	-7.04E-04 Velocity^2	3.48E-06 Velocity^2
3.60E-05 AOI^2	-8.65E-07 AOI^2	-2.19E-06 AOI^2	-4.49E-07 AOI^2	-1.71E-07 AOI^2	2.67E-06 AOI^2
4.83E-10 RPM^2	-4.23E-10 RPM^2	-3.47E-08 RPM^2	-1.50E-10 RPM^2	4.10E-11 RPM^2	-4.98E-10 RPM^2
-7.34E-08 Velocity * AOI * RPM	-4.23E-09 Velocity * AOI * RPM	8.68E-09 Velocity * AOI * RPM	4.11E-09 Velocity * AOI * RPM	-1.99E-09 Velocity * AOI * RPM	4.62E-09 Velocity * AOI * RPM
-2.37E-06 Velocity^2 * AOI	1.61E-06 Velocity^2 * AOI	4.34E-07 Velocity * AOI^2	-5.71E-07 Velocity^2 * AOI	1.27E-06 Velocity^2 * AOI	2.59E-07 Velocity^2 * AOI
-2.68E-07 Velocity^2 * RPM	7.92E-08 Velocity^2 * RPM	-1.19E-10 Velocity * RPM^2	-5.61E-09 Velocity^2 * RPM	1.09E-07 Velocity^2 * RPM	-6.29E-08 Velocity * AOI^2
2.96E-07 Velocity * AOI^2	-2.76E-07 Velocity * AOI^2	3.57E-10 AOI^2 * RPM	1.03E-07 Velocity * AOI^2	3.15E-08 Velocity * AOI^2	-1.86E-12 Velocity * RPM^2
-3.77E-10 Velocity * RPM^2	1.26E-10 Velocity * RPM^2	-7.37E-12 AOI * RPM^2	3.07E-11 Velocity * RPM^2	-1.59E-11 Velocity * RPM^2	-4.70E-13 AOI * RPM^2
-6.06E-09 AOI^2 * RPM	4.49E-10 AOI^2 * RPM	1.20E-05 Velocity^3	4.55E-11 AOI^2 * RPM	3.40E-05 Velocity^3	-4.49E-08 AOI^3
-4.92E-12 AOI * RPM^2	6.18E-12 AOI * RPM^2	4.67E-12 RPM^3	1.50E-12 AOI * RPM^2	1.83E-10 Velocity^2 * AOI * RPM	3.53E-14 RPM^3
-6.50E-05 Velocity^3	3.14E-06 Velocity^3	-6.12E-11 Velocity * AOI^2 * RPM	1.44E-09 AOI^3	-1.22E-07 Velocity^3 * AOI	-2.91E-13 Velocity * AOI * RPM^2
-1.97E-07 AOI^3	-2.97E-09 AOI^3	6.66E-15 Velocity * RPM^3	7.35E-11 Velocity^2 * AOI * RPM	-5.26E-09 Velocity^3 * RPM	6.83E-10 Velocity * AOI^3
5.55E-08 Velocity^2 * AOI^2	1.97E-10 Velocity^2 * AOI * RPM	-2.29E-16 RPM^4	-7.86E-12 Velocity * AOI^2 * RPM		2.23E-10 AOI^4
4.94E-12 Velocity * AOI * RPM^2	-7.81E-12 Velocity^2 * RPM^2		-3.48E-13 Velocity * AOI * RPM^2		
1.18E-08 Velocity^3 * RPM	-4.00E-14 AOI^2 * RPM^2		-4.85E-10 Velocity * AOI^3		
-6.53E-09 Velocity * AOI^3	-1.14E-07 Velocity^3 * AOI				
3.48E-11 AOI^3 * RPM	2.28E-09 Velocity * AOI^3				

4-Blade Regression Model

CFx	CFy	CFz	CMx	CMy	CMz
-4.55E-02 Intercept	1.07E-01 Intercept	1.81E-04 Intercept	4.49E-03 Intercept	9.19E-02 Intercept	-4.52E-03 Intercept
1.15E-02 Velocity	-1.59E-02 Velocity	-2.41E-04 Velocity	-2.06E-03 Velocity	-1.39E-02 Velocity	3.13E-03 Velocity
8.34E-04 AOI	4.50E-05 AOI	-1.24E-03 AOI	2.99E-06 AOI	-7.20E-05 AOI	-5.10E-05 AOI
9.30E-05 RPM	-6.20E-05 RPM	1.39E-06 RPM	-7.60E-06 RPM	-5.30E-05 RPM	2.56E-06 RPM
-4.10E-05 Velocity * AOI	6.95E-06 Velocity * AOI	-1.70E-05 Velocity * AOI	1.18E-06 Velocity * AOI	-7.57E-06 Velocity * AOI	-1.85E-06 Velocity * AOI
-5.56E-06 Velocity * RPM	9.55E-06 Velocity * RPM	5.10E-08 Velocity * RPM	7.30E-07 Velocity * RPM	8.30E-06 Velocity * RPM	-1.55E-06 Velocity * RPM
-3.28E-07 AOI * RPM	6.07E-08 AOI * RPM	7.67E-07 AOI * RPM	1.99E-09 AOI * RPM	1.60E-08 AOI * RPM	4.76E-09 AOI * RPM
-1.92E-03 Velocity^2	-1.64E-04 Velocity^2	-1.20E-05 AOI^2	1.97E-04 Velocity^2	-8.40E-05 Velocity^2	-2.82E-04 Velocity^2
-7.24E-08 AOI^2	-1.10E-05 AOI^2	-4.48E-10 RPM^2	-3.64E-07 AOI^2	6.34E-07 AOI^2	8.63E-07 AOI^2
-1.50E-08 RPM^2	1.15E-08 RPM^2	8.62E-10 Velocity * AOI * RPM	1.33E-09 RPM^2	1.02E-08 RPM^2	-3.09E-10 RPM^2
1.44E-08 Velocity * AOI * RPM	-9.65E-09 Velocity * AOI * RPM	-1.44E-07 Velocity * AOI^2	-5.22E-10 Velocity * AOI * RPM	-8.09E-10 Velocity * AOI * RPM	1.28E-07 Velocity^2 * RPM
-4.10E-07 Velocity^2 * AOI	4.26E-06 Velocity^2 * AOI	2.03E-09 AOI^2 * RPM	-5.69E-07 Velocity^2 * AOI	2.69E-06 Velocity^2 * AOI	-2.26E-07 Velocity * AOI^2
6.64E-07 Velocity^2 * RPM	8.37E-09 Velocity^2 * RPM	-1.45E-10 AOI * RPM^2	-6.59E-08 Velocity^2 * RPM	4.61E-08 Velocity * AOI^2	1.70E-10 Velocity * RPM^2
1.99E-06 Velocity * AOI^2	-2.04E-07 Velocity * AOI^2	9.35E-08 AOI^3	3.97E-08 Velocity * AOI^2	-1.56E-09 Velocity * RPM^2	-8.29E-09 AOI^3
5.38E-10 Velocity * RPM^2	-1.79E-09 Velocity * RPM^2	3.45E-14 RPM^3	-6.47E-11 Velocity * RPM^2	-1.15E-10 AOI^2 * RPM	-1.34E-11 Velocity^2 * RPM^2
5.60E-10 AOI^2 * RPM	1.96E-09 AOI^2 * RPM	1.41E-09 Velocity * AOI^3	2.66E-09 AOI^3	3.67E-06 Velocity^3	2.21E-09 Velocity * AOI^3
2.46E-11 AOI * RPM^2	-1.15E-11 AOI * RPM^2	-1.60E-11 AOI^3 * RPM	-7.68E-14 RPM^3	-6.46E-13 RPM^3	
-6.44E-06 Velocity^3	5.85E-06 Velocity^3	8.56E-15 AOI * RPM^3	8.73E-11 Velocity^2 * AOI * RPM	-1.31E-07 Velocity^3 * AOI	
-2.27E-08 AOI^3	8.21E-08 AOI^3		5.64E-12 Velocity^2 * RPM^2	9.73E-14 Velocity * RPM^3	
7.99E-13 RPM^3	-6.95E-13 RPM^3		-2.77E-10 Velocity * AOI^3		
-1.29E-09 Velocity^2 * AOI * RPM	-1.05E-10 Velocity^2 * AOI * RPM				
-5.63E-11 Velocity^2 * RPM^2	9.06E-13 Velocity * AOI * RPM^2				
-1.67E-10 Velocity * AOI^2 * RPM	-1.59E-07 Velocity^3 * AOI				
4.82E-07 Velocity^3 * AOI	1.78E-09 Velocity * AOI^3				
-8.18E-09 Velocity * AOI^3	1.09E-13 Velocity * RPM^3				
	-1.38E-11 AOI^3 * RPM				

5-Blade Regression Model

CFx	CFy	CFz	CMx	CMy	CMz
2.78E-01 Intercept	1.46E-02 Intercept	4.71E-03 Intercept	-9.85E-03 Intercept	2.21E-03 Intercept	-6.98E-03 Intercept
-8.19E-02 Velocity	-7.88E-04 Velocity	-1.56E-03 Velocity	-4.21E-04 Velocity	-5.36E-04 Velocity	2.15E-03 Velocity
2.26E-03 AOI	-5.00E-05 AOI	-2.83E-04 AOI	-6.90E-05 AOI	-2.31E-04 AOI	-2.52E-04 AOI
-5.10E-05 RPM	-6.25E-06 RPM	-1.45E-07 RPM	-6.07E-07 RPM	-3.57E-07 RPM	1.78E-06 RPM
-2.19E-04 Velocity * AOI	9.12E-06 Velocity * AOI	-2.60E-05 Velocity * AOI	1.50E-05 Velocity * AOI	6.80E-05 Velocity * AOI	-7.30E-05 Velocity * AOI
3.20E-05 Velocity * RPM	-5.12E-08 Velocity * RPM	-3.56E-08 Velocity * RPM	5.80E-08 Velocity * RPM	1.04E-07 Velocity * RPM	-1.19E-07 Velocity * RPM
-6.93E-07 AOI * RPM	1.37E-09 AOI * RPM	4.34E-08 AOI * RPM	2.18E-08 AOI * RPM	4.60E-08 AOI * RPM	1.39E-07 AOI * RPM
4.96E-03 $Velocity^2$	1.59E-04 $Velocity^2$	2.69E-04 $Velocity^2$	6.90E-05 $Velocity^2$	3.30E-05 $Velocity^2$	-4.14E-04 $Velocity^2$
-1.10E-05 AOI^2	1.74E-07 AOI^2	2.59E-06 AOI^2	5.82E-11 RPM^2	9.13E-07 AOI^2	4.66E-06 AOI^2
5.37E-09 RPM^2	7.76E-10 RPM^2	5.87E-09 Velocity * AOI * RPM	-2.61E-09 Velocity * AOI * RPM	-1.16E-08 Velocity * AOI * RPM	-1.77E-10 RPM^2
4.89E-08 Velocity * AOI * RPM	-1.67E-09 Velocity * AOI * RPM	-3.35E-06 $Velocity^2$ * AOI	-1.78E-06 $Velocity^2$ * AOI	-4.25E-06 $Velocity^2$ * AOI	1.25E-08 Velocity * AOI * RPM
1.70E-05 $Velocity^2$ * AOI	1.44E-08 Velocity * AOI^2	2.64E-07 Velocity * AOI^2	-1.02E-08 $Velocity^2$ * RPM	-6.47E-09 $Velocity^2$ * RPM	2.63E-06 $Velocity^2$ * AOI
-2.14E-06 $Velocity^2$ * RPM	-7.15E-06 $Velocity^3$	-3.67E-10 AOI^2 * RPM	-1.66E-12 AOI * RPM^2	4.95E-08 Velocity * AOI^2	6.83E-09 $Velocity^2$ * RPM
2.49E-06 Velocity * AOI^2		-1.20E-05 $Velocity^3$	2.97E-10 $Velocity^2$ * AOI * RPM	-2.17E-10 AOI^2 * RPM	7.94E-08 Velocity * AOI^2
-3.11E-09 Velocity * RPM^2		-6.83E-09 AOI^3		7.99E-10 $Velocity^2$ * AOI * RPM	-1.95E-09 AOI^2 * RPM
1.87E-09 AOI^2 * RPM		-5.60E-11 Velocity * AOI^2 * RPM			-1.79E-11 AOI * RPM^2
4.42E-11 AOI * RPM^2		1.47E-07 $Velocity^3$ * AOI			3.70E-05 $Velocity^3$
2.14E-08 AOI^3		7.74E-10 Velocity * AOI^3			-4.52E-09 AOI^3
5.21E-08 $Velocity^2$ * AOI^2					-4.55E-10 $Velocity^2$ * AOI * RPM
-3.62E-09 $Velocity^2$ * AOI * RPM					-4.73E-11 Velocity * AOI^2 * RPM
2.21E-10 $Velocity^2$ * RPM^2					2.24E-13 AOI^2 * RPM^2
-3.17E-10 Velocity * AOI^2 * RPM					1.34E-09 Velocity * AOI^3
-1.13E-08 Velocity * AOI^3					-1.25E-06 $Velocity^4$

6-Blade Regression Model

CFx	CFy	CFz	CMx	CMy	CMz
1.01E-01 Intercept	-1.97E-01 Intercept	-5.43E-01 Intercept	3.63E-03 Intercept	-1.71E-01 Intercept	3.98E-04 Intercept
-4.18E-02 Velocity	-2.64E-03 Velocity	-2.69E-03 Velocity	1.55E-03 Velocity	-1.48E-03 Velocity	-5.84E-04 Velocity
3.03E-03 AOI	-5.49E-04 AOI	-1.32E-03 AOI	-2.35E-04 AOI	4.05E-06 AOI	6.29E-06 AOI
4.20E-05 RPM	2.10E-04 RPM	5.47E-04 RPM	-1.50E-05 RPM	1.67E-04 RPM	-1.38E-07 RPM
1.44E-04 Velocity * AOI	6.40E-05 Velocity * AOI	-2.20E-05 Velocity * AOI	-2.70E-05 Velocity * AOI	1.40E-05 Velocity * AOI	-2.40E-05 Velocity * AOI
2.10E-05 Velocity * RPM	1.31E-06 Velocity * RPM	1.56E-06 Velocity * RPM	-8.72E-07 Velocity * RPM	6.78E-07 Velocity * RPM	1.09E-07 Velocity * RPM
-2.19E-06 AOI * RPM	2.19E-07 AOI * RPM	1.18E-06 AOI * RPM	2.06E-07 AOI * RPM	4.07E-08 AOI * RPM	-6.49E-09 AOI * RPM
4.40E-05 $Velocity^2$	-6.41E-07 AOI^2	-1.35E-04 $Velocity^2$	1.02E-04 $Velocity^2$	1.00E-05 $Velocity^2$	4.40E-05 $Velocity^2$
9.88E-06 AOI^2	-8.06E-08 RPM^2	-1.80E-05 AOI^2	-1.33E-06 AOI^2	-3.96E-06 AOI^2	1.06E-06 AOI^2
-5.50E-09 RPM^2	-3.11E-08 Velocity * AOI * RPM	-2.03E-07 RPM^2	3.96E-09 RPM^2	-5.97E-08 RPM^2	3.38E-09 Velocity * AOI * RPM
-6.22E-08 Velocity * AOI * RPM	3.14E-07 Velocity * AOI^2	-9.28E-09 Velocity * AOI * RPM	1.36E-08 Velocity * AOI * RPM	1.56E-09 Velocity * AOI * RPM	-5.85E-08 $Velocity^2$ * AOI
8.72E-06 $Velocity^2$ * AOI	-1.56E-10 Velocity * RPM^2	1.03E-06 $Velocity^2$ * AOI	-1.62E-06 $Velocity^2$ * AOI	-3.00E-06 $Velocity^2$ * AOI	-8.41E-09 $Velocity^2$ * RPM
3.43E-07 $Velocity^2$ * RPM	3.23E-10 AOI^2 * RPM	4.22E-08 $Velocity^2$ * RPM	-1.60E-08 $Velocity^2$ * RPM	-1.47E-09 $Velocity^2$ * RPM	-2.61E-07 Velocity * AOI^2
2.04E-06 Velocity * AOI^2	-2.62E-11 AOI * RPM^2	1.49E-07 Velocity * AOI^2	7.20E-08 Velocity * AOI^2	4.19E-07 Velocity * AOI^2	-8.38E-09 AOI^3
-4.62E-09 Velocity * RPM^2	1.32E-11 RPM^3	-2.40E-10 Velocity * RPM^2	1.04E-10 Velocity * RPM^2	-7.65E-11 Velocity * RPM^2	5.83E-09 $Velocity^2$ * AOI^2
7.78E-10 AOI^2 * RPM	-7.64E-11 Velocity * AOI^2 * RPM	2.99E-09 AOI^2 * RPM	6.94E-11 AOI^2 * RPM	1.91E-10 AOI^2 * RPM	1.89E-09 Velocity * AOI^3
4.88E-10 AOI * RPM^2	3.84E-12 Velocity * AOI * RPM^2	-2.81E-10 AOI * RPM^2	-5.50E-11 AOI * RPM^2	-5.45E-12 AOI * RPM^2	
-1.06E-04 $Velocity^3$	-7.91E-16 RPM^4	1.30E-07 AOI^3	2.09E-08 AOI^3	2.39E-08 AOI^3	
-2.22E-07 AOI^3		3.28E-11 RPM^3	-3.37E-13 RPM^3	9.23E-12 RPM^3	
5.90E-14 RPM^3		3.33E-08 $Velocity^2$ * AOI^2	2.47E-10 $Velocity^2$ * AOI * RPM	1.18E-08 $Velocity^2$ * AOI^2	
8.30E-08 $Velocity^2$ * AOI^2		-1.01E-09 $Velocity^2$ * AOI * RPM	-1.75E-11 Velocity * AOI^2 * RPM	3.26E-10 $Velocity^2$ * AOI * RPM	
-2.44E-09 $Velocity^2$ * AOI * RPM		-1.14E-10 Velocity * AOI^2 * RPM	-1.45E-12 Velocity * AOI * RPM^2	-7.63E-11 Velocity * AOI^2 * RPM	
-9.23E-11 $Velocity^2$ * RPM^2		3.95E-12 Velocity * AOI * RPM^2	4.58E-15 AOI * RPM^3	-1.28E-09 Velocity * AOI^3	
-2.19E-10 Velocity * AOI^2 * RPM		-2.00E-11 AOI^3 * RPM	-1.13E-10 AOI^4	-5.23E-16 RPM^4	
8.28E-12 Velocity * AOI * RPM^2		1.95E-14 AOI * RPM^3			
2.54E-08 $Velocity^3$ * RPM		-1.94E-15 RPM^4			
-1.42E-08 Velocity * AOI^3					
4.12E-13 Velocity * RPM^3					
-3.70E-14 AOI * RPM^3					
1.21E-09 AOI^4					

H.1: LOW-SPEED REGRESSION MODELS (CODED)

3-Blade Regression Model

CFx		CFy		CFz		CMx		CMy		CMz	
1.13E-01	Intercept	-1.20E-03	Intercept	-4.90E-03	Intercept	-8.20E-03	Intercept	2.30E-03	Intercept	-3.30E-03	Intercept
-5.40E-03	Velocity	0.00E+00	Velocity	-4.70E-03	Velocity	-1.00E-04	Velocity	1.00E-03	Velocity	-2.00E-03	Velocity
1.73E-02	AOI	-1.80E-03	AOI	-5.50E-03	AOI	-1.00E-04	AOI	1.50E-03	AOI	-3.50E-03	AOI
7.90E-03	RPM	-1.20E-03	RPM	9.00E-04	RPM	-1.00E-04	RPM	-4.00E-04	RPM	1.10E-03	RPM
1.62E-02	Velocity * AOI	0.00E+00	Velocity * AOI	-3.10E-03	Velocity * AOI	-1.00E-04	Velocity * AOI	1.70E-03	Velocity * AOI	-2.00E-03	Velocity * AOI
6.00E-04	Velocity * RPM	-7.00E-04	Velocity * RPM	6.00E-04	Velocity * RPM	6.02E-06	Velocity * RPM	1.10E-03	Velocity * RPM	8.00E-04	Velocity * RPM
-1.94E-02	AOI * RPM	-9.00E-04	AOI * RPM	2.50E-03	AOI * RPM	3.00E-04	AOI * RPM	0.00E+00	AOI * RPM	1.30E-03	AOI * RPM
-2.10E-03	Velocity^2	3.00E-04	Velocity^2	3.00E-04	Velocity^2	2.00E-04	Velocity^2	-3.00E-04	Velocity^2	4.00E-04	Velocity^2
1.00E-03	AOI^2	1.00E-03	AOI^2	1.40E-03	AOI^2	-2.00E-04	AOI^2	1.00E-04	AOI^2	-1.10E-03	AOI^2
-2.40E-03	RPM^2	1.00E-03	RPM^2	1.00E-03	RPM^2	1.00E-04	RPM^2	-3.00E-04	RPM^2	-4.00E-04	RPM^2
-1.16E-02	Velocity * AOI * RPM	-7.00E-04	Velocity * AOI * RPM	6.00E-04	Velocity * AOI * RPM	4.00E-04	Velocity * AOI * RPM	1.00E-04	Velocity * AOI * RPM	8.00E-04	Velocity * AOI * RPM
3.90E-03	Velocity^2 * AOI	2.00E-04	Velocity^2 * AOI	1.80E-03	Velocity * AOI^2	-3.00E-04	Velocity^2 * AOI	-4.00E-04	Velocity^2 * AOI	3.00E-04	Velocity^2 * AOI
-9.00E-04	Velocity^2 * RPM	5.00E-04	Velocity^2 * RPM	-8.00E-04	Velocity * RPM^2	-1.00E-04	Velocity^2 * RPM	4.00E-04	Velocity^2 * RPM	5.00E-04	Velocity * AOI^2
1.10E-03	Velocity * AOI^2	7.00E-04	Velocity * AOI^2	-1.00E-03	AOI^2 * RPM	-1.00E-04	Velocity * AOI^2	4.00E-04	Velocity * AOI^2	-3.00E-04	Velocity * RPM^2
-2.20E-03	Velocity * RPM^2	4.00E-04	Velocity * RPM^2	-1.10E-03	AOI * RPM^2	2.00E-04	Velocity * RPM^2	-5.00E-04	Velocity * RPM^2	-5.00E-04	AOI * RPM^2
-3.70E-03	AOI^2 * RPM	3.00E-04	AOI^2 * RPM	1.20E-03	Velocity^3	-1.00E-04	AOI^2 * RPM	2.00E-04	Velocity^3	6.00E-04	AOI^3
5.30E-03	AOI * RPM^2	4.00E-04	AOI * RPM^2	8.00E-04	RPM^3	-2.00E-04	AOI * RPM^2	6.00E-04	Velocity^2 * AOI * RPM	2.00E-04	RPM^3
-8.00E-04	Velocity^3	-3.00E-04	Velocity^3	-1.40E-03	Velocity * AOI^2 * RPM	-2.00E-04	AOI^3	-7.00E-04	Velocity^3 * AOI	-3.00E-04	Velocity * AOI * RPM^2
-9.10E-03	AOI^3	1.60E-03	AOI^3	1.40E-03	Velocity * RPM^3	2.00E-04	Velocity^2 * AOI * RPM	-1.10E-03	Velocity^3 * RPM	5.00E-04	Velocity * AOI^3
3.20E-03	Velocity^2 * AOI^2	4.00E-04	Velocity^2 * AOI * RPM	-2.20E-03	RPM^4	-2.00E-04	Velocity * AOI^2 * RPM			1.40E-03	AOI^4
4.40E-03	Velocity * AOI * RPM^2	-6.00E-04	Velocity^2 * RPM^2			-3.00E-04	Velocity * AOI * RPM^2				
2.80E-03	Velocity^3 * RPM	-5.00E-04	AOI^2 * RPM^2			-3.00E-04	Velocity * AOI^3				
-4.60E-03	Velocity * AOI^3	-6.00E-04	Velocity^3 * AOI								
8.30E-03	AOI^3 * RPM	1.20E-03	Velocity * AOI^3								

4-Blade Regression Model

CFx		CFy		CFz		CMx		CMy		CMz	
1.32E-01	Intercept	-1.80E-03	Intercept	-6.30E-03	Intercept	-1.00E-02	Intercept	2.20E-03	Intercept	-3.50E-03	Intercept
-8.20E-03	Velocity	2.00E-04	Velocity	-4.00E-03	Velocity	-1.00E-04	Velocity	1.70E-03	Velocity	-1.90E-03	Velocity
1.56E-02	AOI	-3.00E-03	AOI	-7.50E-03	AOI	-3.00E-04	AOI	2.60E-03	AOI	-2.80E-03	AOI
2.50E-03	RPM	0.00E+00	RPM	6.00E-04	RPM	2.00E-04	RPM	0.00E+00	RPM	9.00E-04	RPM
1.39E-02	Velocity * AOI	2.00E-04	Velocity * AOI	-4.40E-03	Velocity * AOI	-3.00E-04	Velocity * AOI	2.60E-03	Velocity * AOI	-1.80E-03	Velocity * AOI
2.90E-03	Velocity * RPM	-9.00E-04	Velocity * RPM	5.00E-04	Velocity * RPM	-1.00E-04	Velocity * RPM	-4.00E-04	Velocity * RPM	4.00E-04	Velocity * RPM
-6.10E-03	AOI * RPM	1.00E-03	AOI * RPM	1.20E-03	AOI * RPM	2.00E-04	AOI * RPM	-2.00E-04	AOI * RPM	6.00E-04	AOI * RPM
6.00E-04	Velocity^2	4.00E-04	Velocity^2	2.00E-03	AOI^2	0.00E+00	Velocity^2	-3.00E-04	Velocity^2	8.00E-04	Velocity^2
-3.30E-03	AOI^2	2.00E-03	AOI^2	-3.00E-04	RPM^2	1.00E-04	AOI^2	9.00E-04	AOI^2	8.00E-04	AOI^2
-4.00E-04	RPM^2	9.23E-06	RPM^2	5.00E-04	Velocity * AOI * RPM	-1.00E-04	RPM^2	-1.00E-04	RPM^2	3.00E-04	RPM^2
-6.50E-03	Velocity * AOI * RPM	-4.00E-04	Velocity * AOI * RPM	9.00E-04	Velocity * AOI^2	2.00E-04	Velocity * AOI * RPM	-2.00E-04	Velocity * AOI * RPM	-3.00E-04	Velocity^2 * RPM
3.60E-03	Velocity^2 * AOI	4.00E-04	Velocity^2 * AOI	-1.10E-03	AOI^2 * RPM	-2.00E-04	Velocity^2 * AOI	-2.00E-04	Velocity^2 * AOI	1.30E-03	Velocity * AOI^2
2.00E-04	Velocity^2 * RPM	0.00E+00	Velocity^2 * RPM	-4.00E-04	AOI * RPM^2	-1.00E-04	Velocity^2 * RPM	6.00E-04	Velocity * AOI^2	-1.00E-04	Velocity * RPM^2
-1.40E-03	Velocity * AOI^2	8.00E-04	Velocity * AOI^2	2.70E-03	AOI^3	0.00E+00	Velocity * AOI^2	0.00E+00	Velocity * RPM^2	8.00E-04	AOI^3
-2.30E-03	Velocity * RPM^2	2.00E-04	Velocity * RPM^2	1.00E-03	RPM^3	1.00E-04	Velocity * RPM^2	-3.00E-04	AOI^2 * RPM	-8.00E-04	Velocity^2 * RPM^2
-1.90E-03	AOI^2 * RPM	-3.00E-04	AOI^2 * RPM	1.10E-03	Velocity * AOI^3	1.00E-04	AOI^3	-1.00E-04	Velocity^3	1.20E-03	Velocity * AOI^3
2.00E-03	AOI * RPM^2	0.00E+00	AOI * RPM^2	-1.30E-03	AOI^3 * RPM	-2.00E-04	RPM^3	1.05E-06	RPM^3		
2.00E-03	Velocity^3	-2.00E-04	Velocity^3	9.00E-04	AOI * RPM^3	1.00E-04	Velocity^2 * AOI * RPM	-6.00E-04	Velocity^3 * AOI		
-1.00E-02	AOI^3	3.10E-03	AOI^3			3.00E-04	Velocity^2 * RPM^2	5.00E-04	Velocity * RPM^3		
2.10E-03	RPM^3	-1.00E-04	RPM^3			-2.00E-04	Velocity * AOI^3				
-2.00E-03	Velocity^2 * AOI * RPM	-4.00E-04	Velocity^2 * AOI * RPM								
-2.30E-03	Velocity^2 * RPM^2	8.00E-04	Velocity * AOI * RPM^2								
-2.20E-03	Velocity * AOI^2 * RPM	-7.00E-04	Velocity^3 * AOI								
2.50E-03	Velocity^3 * AOI	1.20E-03	Velocity * AOI^3								
-4.80E-03	Velocity * AOI^3	7.00E-04	Velocity * RPM^3								
		-1.40E-03	AOI^3 * RPM								

5-Blade Regression Model

CFx		CFy		CFz		CMx		CMy		CMz	
1.48E-01	Intercept	-5.00E-04	Intercept	-5.70E-03	Intercept	-1.16E-02	Intercept	3.70E-03	Intercept	-4.60E-03	Intercept
-8.90E-03	Velocity	9.00E-04	Velocity	-4.30E-03	Velocity	1.00E-04	Velocity	2.10E-03	Velocity	-2.80E-03	Velocity
1.77E-02	AOI	-5.00E-04	AOI	-5.30E-03	AOI	-1.00E-04	AOI	3.80E-03	AOI	-4.40E-03	AOI
4.20E-03	RPM	4.00E-04	RPM	1.40E-03	RPM	0.00E+00	RPM	-3.00E-04	RPM	6.00E-04	RPM
2.38E-02	Velocity * AOI	5.00E-04	Velocity * AOI	-5.40E-03	Velocity * AOI	-6.00E-04	Velocity * AOI	2.80E-03	Velocity * AOI	-2.70E-03	Velocity * AOI
2.50E-03	Velocity * RPM	-6.00E-04	Velocity * RPM	6.00E-04	Velocity * RPM	0.00E+00	Velocity * RPM	-1.00E-04	Velocity * RPM	7.00E-04	Velocity * RPM
-5.80E-03	AOI * RPM	-6.00E-04	AOI * RPM	2.00E-04	AOI * RPM	1.00E-04	AOI * RPM	-8.00E-04	AOI * RPM	1.00E-03	AOI * RPM
-3.30E-03	Velocity^2	0.00E+00	Velocity^2	0.00E+00	Velocity^2	1.00E-04	Velocity^2	-4.00E-04	Velocity^2	1.20E-03	Velocity^2
-2.30E-03	AOI^2	6.00E-04	AOI^2	1.30E-03	AOI^2	0.00E+00	RPM^2	4.00E-04	AOI^2	3.00E-04	AOI^2
-2.30E-03	RPM^2	8.00E-04	RPM^2	1.00E-04	Velocity * AOI * RPM	3.00E-04	Velocity * AOI * RPM	-1.00E-04	Velocity * AOI * RPM	-5.00E-04	RPM^2
-7.30E-03	Velocity * AOI * RPM	-3.00E-04	Velocity * AOI * RPM	-2.00E-04	Velocity^2 * AOI	-4.00E-04	Velocity^2 * AOI	-4.00E-04	Velocity^2 * AOI	3.00E-04	Velocity * AOI * RPM
5.50E-03	Velocity^2 * AOI	5.00E-04	Velocity * AOI^2	1.60E-03	Velocity * AOI^2	0.00E+00	Velocity^2 * RPM	5.00E-04	Velocity^2 * RPM	5.00E-04	Velocity^2 * AOI
-2.40E-03	Velocity^2 * RPM	-9.00E-04	Velocity^3	-1.40E-03	AOI^2 * RPM	-1.00E-04	AOI * RPM^2	7.00E-04	Velocity * AOI^2	-1.00E-04	Velocity^2 * RPM
-4.00E-04	Velocity * AOI^2			-4.00E-04	Velocity^3	2.00E-04	Velocity^2 * AOI * RPM	-4.00E-04	AOI^2 * RPM	5.00E-04	Velocity * AOI^2
-1.00E-04	Velocity * RPM^2			-2.00E-04	AOI^3			7.00E-04	Velocity^2 * AOI * RPM	-1.00E-04	AOI^2 * RPM
-4.00E-04	AOI^2 * RPM			-8.00E-04	Velocity * AOI^2 * RPM					3.00E-04	AOI * RPM^2
2.60E-03	AOI * RPM^2			1.20E-03	Velocity^3 * AOI					2.00E-04	Velocity^3
-6.70E-03	AOI^3			1.20E-03	Velocity * AOI^3					7.00E-04	AOI^3
3.50E-03	Velocity^2 * AOI^2									-4.00E-04	Velocity^2 * AOI * RPM
-2.90E-03	Velocity^2 * AOI * RPM									-5.00E-04	Velocity * AOI^2 * RPM
4.30E-03	Velocity^2 * RPM^2									7.00E-04	AOI^2 * RPM^2
-3.50E-03	Velocity * AOI^2 * RPM									7.00E-04	Velocity * AOI^3
-8.00E-03	Velocity * AOI^3									-7.00E-04	Velocity^4

6-Blade Regression Model

CFx		CFy		CFz		CMx		CMy		CMz	
1.67E-01	Intercept	-1.40E-03	Intercept	-9.00E-03	Intercept	-1.44E-02	Intercept	3.80E-03	Intercept	-5.70E-03	Intercept
-1.17E-02	Velocity	8.00E-04	Velocity	-6.00E-03	Velocity	1.00E-04	Velocity	2.40E-03	Velocity	-3.70E-03	Velocity
2.63E-02	AOI	-8.00E-04	AOI	-1.10E-02	AOI	-2.00E-04	AOI	3.60E-03	AOI	-5.20E-03	AOI
7.90E-03	RPM	-1.00E-04	RPM	2.10E-03	RPM	2.00E-04	RPM	-4.00E-04	RPM	1.40E-03	RPM
3.16E-02	Velocity * AOI	1.00E-04	Velocity * AOI	-5.60E-03	Velocity * AOI	-1.00E-03	Velocity * AOI	3.80E-03	Velocity * AOI	-3.60E-03	Velocity * AOI
-1.70E-03	Velocity * RPM	-7.00E-04	Velocity * RPM	2.10E-03	Velocity * RPM	-1.00E-04	Velocity * RPM	8.00E-04	Velocity * RPM	1.00E-03	Velocity * RPM
-1.14E-02	AOI * RPM	-9.00E-04	AOI * RPM	3.00E-03	AOI * RPM	2.00E-04	AOI * RPM	-1.00E-03	AOI * RPM	1.10E-03	AOI * RPM
1.00E-04	Velocity^2	1.60E-03	AOI^2	-9.00E-04	Velocity^2	1.00E-04	Velocity^2	-1.10E-03	Velocity^2	4.00E-04	Velocity^2
-1.24E-02	AOI^2	2.80E-03	RPM^2	1.40E-03	AOI^2	1.00E-03	AOI^2	9.00E-04	AOI^2	6.00E-04	AOI^2
-1.80E-03	RPM^2	-1.90E-03	Velocity * AOI * RPM	3.60E-03	RPM^2	1.00E-04	RPM^2	1.20E-03	RPM^2	1.10E-03	Velocity * AOI * RPM
-1.50E-02	Velocity * AOI * RPM	-2.00E-04	Velocity * AOI^2	-4.00E-04	Velocity * AOI * RPM	9.00E-04	Velocity * AOI * RPM	-5.00E-04	Velocity * AOI * RPM	7.00E-04	Velocity^2 * AOI
8.30E-03	Velocity^2 * AOI	6.00E-04	Velocity * RPM^2	1.00E-04	Velocity^2 * AOI	-7.00E-04	Velocity^2 * AOI	-6.00E-04	Velocity^2 * AOI	-3.00E-04	Velocity^2 * RPM
-9.00E-04	Velocity^2 * RPM	-7.00E-04	AOI^2 * RPM	-3.00E-04	Velocity^2 * RPM	-1.00E-04	Velocity^2 * RPM	5.00E-04	Velocity^2 * RPM	1.20E-03	Velocity * AOI^2
1.70E-03	Velocity * AOI^2	1.00E-04	AOI * RPM^2	1.60E-03	Velocity * AOI^2	0.00E+00	Velocity * AOI^2	9.00E-04	Velocity * AOI^2	7.00E-04	AOI^3
-1.90E-03	Velocity * RPM^2	-5.00E-04	RPM^3	-3.00E-04	Velocity * RPM^2	2.00E-04	Velocity * RPM^2	-4.00E-04	Velocity * RPM^2	5.00E-04	Velocity^2 * AOI^2
-2.40E-03	AOI^2 * RPM	-1.30E-03	Velocity * AOI^2 * RPM	-2.50E-03	AOI^2 * RPM	-2.00E-04	AOI^2 * RPM	-1.10E-03	AOI^2 * RPM	1.20E-03	Velocity * AOI^3
5.80E-03	AOI * RPM^2	1.70E-03	Velocity * AOI * RPM^2	-3.00E-04	AOI * RPM^2	-5.00E-04	AOI * RPM^2	-4.00E-04	AOI * RPM^2		
3.00E-04	Velocity^3	-2.50E-03	RPM^4	5.60E-03	AOI^3	-2.00E-04	AOI^3	1.70E-03	AOI^3		
-9.80E-03	AOI^3			1.30E-03	RPM^3	-2.00E-04	RPM^3	5.00E-04	RPM^3		
2.10E-03	RPM^3			2.10E-03	Velocity^2 * AOI^2	4.00E-04	Velocity^2 * AOI * RPM	6.00E-04	Velocity^2 * AOI^2		
5.20E-03	Velocity^2 * AOI^2			-1.60E-03	Velocity^2 * AOI * RPM	-3.00E-04	Velocity * AOI^2 * RPM	7.00E-04	Velocity^2 * AOI * RPM		
-3.80E-03	Velocity^2 * AOI * RPM			-1.80E-03	Velocity * AOI^2 * RPM	-6.00E-04	Velocity * AOI * RPM^2	-1.30E-03	Velocity * AOI^2 * RPM		
-3.60E-03	Velocity^2 * RPM^2			1.50E-03	Velocity * AOI * RPM^2	4.00E-04	AOI * RPM^3	-8.00E-04	Velocity * AOI^3		
-3.40E-03	Velocity * AOI^2 * RPM			-3.10E-03	AOI^3 * RPM	-7.00E-04	AOI^4	-1.80E-03	RPM^4		
3.20E-03	Velocity * AOI * RPM^2			1.90E-03	AOI * RPM^3						
4.00E-03	Velocity^3 * RPM			-4.80E-03	RPM^4						
-8.90E-03	Velocity * AOI^3										
4.00E-03	Velocity * RPM^3										
-3.60E-03	AOI * RPM^3										
7.60E-03	AOI^4										

H.2: HIGH-SPEED REGRESSION MODELS (CODED)

Key:
A - Velocity b - AOI
C - RPM d - Blades

CFx	CFy	CFz	CMx	CMy	CMz
4.61E-02	3.00E-04	-5.00E-03	-6.30E-03	4.00E-04	-2.10E-03
-7.73E-02 A	4.00E-04 A	-2.70E-03 A	6.50E-03 A	-1.00E-04 A	-6.00E-04 A
7.20E-03 b	4.00E-04 b	-3.70E-03 b	-5.00E-04 b	7.00E-04 b	-1.80E-03 b
3.37E-02 C	-4.00E-04 C	1.90E-03 C	-3.00E-03 C	4.00E-04 C	6.00E-04 C
-7.10E-03 d[1]	-1.00E-04 d[1]	6.00E-04 d[1]	1.20E-03 d[1]	9.00E-04 d[1]	4.00E-04 d[1]
-7.10E-03 d[2]	-1.00E-04 d[2]	3.00E-04 d[2]	9.00E-04 d[2]	-3.00E-04 d[2]	2.00E-04 d[2]
4.80E-03 d[3]	-2.00E-04 d[3]	-1.00E-04 d[3]	-5.00E-04 d[3]	-3.00E-04 d[3]	-1.00E-04 d[3]
3.40E-03 Ab	7.00E-04 Ab	-2.60E-03 Ab	-4.00E-04 Ab	-3.00E-04 Ab	-9.00E-04 Ab
2.68E-02 AC	-1.00E-04 bC	1.40E-03 AC	-3.60E-03 AC	3.00E-04 AC	1.00E-03 AC
1.73E-02 Ad[1]	-3.00E-04 bd[1]	5.00E-04 Ad[1]	-1.80E-03 Ad[1]	3.00E-04 Ad[1]	3.00E-04 Ad[1]
2.60E-03 Ad[2]	7.00E-04 bd[2]	0.00E+00 Ad[2]	-2.00E-04 Ad[2]	0.00E+00 Ad[2]	1.00E-04 Ad[2]
-7.40E-03 Ad[3]	-1.00E-03 bd[3]	-1.00E-04 Ad[3]	4.00E-04 Ad[3]	-1.00E-04 Ad[3]	-1.00E-04 Ad[3]
-2.10E-03 bC	-1.00E-04 Cd[1]	1.10E-03 bC	1.00E-04 bC	2.00E-04 bC	4.00E-04 bC
-1.80E-03 bd[1]	1.00E-04 Cd[2]	8.00E-04 bd[1]	1.00E-04 bd[1]	-2.00E-04 bd[1]	4.00E-04 bd[1]
-1.90E-03 bd[2]	3.00E-04 Cd[3]	4.00E-04 bd[2]	0.00E+00 bd[2]	-1.00E-04 bd[2]	-1.00E-04 bd[2]
1.50E-03 bd[3]	-6.00E-04 b^2	1.00E-04 bd[3]	1.00E-04 bd[3]	3.00E-04 bd[3]	3.00E-04 bd[3]
-6.30E-03 Cd[1]	3.00E-04 C^2	-1.00E-04 Cd[1]	7.00E-04 Cd[1]	-1.00E-04 Cd[1]	-2.00E-04 Cd[1]
-1.50E-03 Cd[2]	1.00E-04 bCd[1]	-1.00E-04 Cd[2]	1.00E-04 Cd[2]	0.00E+00 Cd[2]	-1.00E-04 Cd[2]
3.40E-03 Cd[3]	-5.00E-04 bCd[2]	-4.00E-04 Cd[3]	-2.00E-04 Cd[3]	-1.00E-04 Cd[3]	-1.00E-04 Cd[3]
-1.23E-02 A^2	8.00E-04 bCd[3]	-6.00E-04 A^2	2.50E-03 A^2	-2.00E-04 A^2	-6.00E-04 A^2
3.60E-03 b^2	3.00E-04 b^2C	4.00E-04 b^2	-3.00E-04 b^2	-1.00E-04 b^2	3.00E-04 b^2
-1.05E-02 C^2		-4.00E-04 C^2	1.30E-03 C^2	-2.00E-04 A^2b	-5.00E-04 C^2
-5.20E-03 ACd[1]		9.00E-04 AbC	1.00E-04 AbC	3.00E-04 A^2d[1]	3.00E-04 AbC
5.00E-04 ACd[2]		2.00E-04 Abd[1]	3.00E-04 Abd[1]	1.00E-04 A^2d[2]	2.00E-04 Abd[1]
2.90E-03 ACd[3]		3.00E-04 Abd[2]	-2.00E-04 Abd[2]	0.00E+00 A^2d[3]	1.00E-04 Abd[2]
4.90E-03 A^2C		-2.00E-04 Abd[3]	-1.00E-04 Abd[3]	-1.20E-03 b^2d[1]	-2.00E-04 Abd[3]
-8.60E-03 AC^2		-5.00E-04 ACd[1]	8.00E-04 ACd[1]	2.00E-04 b^2d[2]	-2.00E-04 ACd[1]
-1.50E-03 b^2C		1.00E-04 ACd[2]	-2.00E-04 ACd[2]	5.00E-04 b^2d[3]	0.00E+00 ACd[2]
2.30E-03 C^2d[1]		-1.00E-04 ACd[3]	0.00E+00 ACd[3]	-3.00E-04 A^3	-1.00E-04 ACd[3]
1.00E-04 C^2d[2]		0.00E+00 bCd[1]	-1.00E-04 bCd[1]		0.00E+00 bCd[1]
-1.90E-03 C^2d[3]		-4.00E-04 bCd[2]	3.00E-04 bCd[2]		0.00E+00 bCd[2]
2.50E-03 C^3		2.00E-04 bCd[3]	-2.00E-04 bCd[3]		-2.00E-04 bCd[3]
		-8.00E-04 A^2b	3.00E-04 A^2b		-2.00E-04 A^2b
		3.00E-04 A^2d[1]	-1.10E-03 A^2C		9.00E-04 A^2C
		-1.00E-04 A^2d[2]	-4.00E-04 A^2d[1]		2.00E-04 A^2d[1]
		5.00E-04 A^2d[3]	2.00E-04 A^2d[2]		-2.00E-04 A^2d[2]
		-5.00E-04 b^2C	-1.00E-04 A^2d[3]		1.00E-04 A^2d[3]
		-6.00E-04 A^3	-4.00E-04 Ab^2		-3.00E-04 AC^2
			1.00E-03 AC^2		-2.00E-04 b^2C
			4.00E-04 b^2C		0.00E+00 C^2d[1]
			-2.00E-04 bC^2		2.00E-04 C^2d[2]
			-2.00E-04 C^2d[1]		1.00E-04 C^2d[3]
			-1.00E-04 C^2d[2]		-7.00E-04 A^3
			-1.00E-04 C^2d[3]		
			4.00E-04 A^3		
			-1.00E-04 C^3		

I: MATLAB PREDICTION TOOL CODE

Table of Contents


```
% Simulation Database Prediction Tool for Propeller Characterization
% Michael Stratton
% Spring 2021
%
 ************************************************************************
% ***** Excel data folders MUST be in same folder as program file!!
 *****
%
 ************************************************************************
% Program will overwrite old data in Excel file but if new input range
 is
% smaller than previous range the old output will still show up;
 delete
% prior to running program if desired
%
 ************************************************************************

clear, clc
close all
format shortG

% Adding Excel sub-files to .m filepath
currentFile = mfilename('fullpath');
[filepath,name,ext] = fileparts(currentFile);
addpath(fullfile(filepath,'Model Data'))

filename_3X = '3-Blade X.xlsx';
filename_4X = '4-Blade X.xlsx';
filename_5X = '5-Blade X.xlsx';
filename_6X = '6-Blade X.xlsx';
filename_HSX = 'High-Speed X.xlsx';
filename_B = 'Regression Models.xlsx';
filename_FI = 'Factor Input.xlsx';

% Low-Speed Data
```

3-Blade

Importing desired low-speed data points

```
x3 = readmatrix(filename_FI,'Sheet','Input LS','Range','A3');
```

```
% Desired data points in natural units
x_13 = x3(:,1); % Velocity
x_23 = x3(:,2); % AoA
x_33 = x3(:,3); % RPM

% Transforming to coded variables
x1c3 = (x_13 - (2 + 12)/2)/((12 - 2)/2);
x2c2 = (x_23 - (0 + 100)/2)/((100 - 0)/2);
x3c3 = (x_33 - (3000 + 6800)/2)/((6800 - 3000)/2);

xc3 = [ones(length(x_13),1) x1c3 x2c2 x3c3 x1c3.*x2c2 x1c3.*x3c3
 x2c2.*x3c3 x1c3.^2 x2c2.^2 x3c3.^2 x1c3.*x2c2.*x3c3 x1c3.^2.*x2c2
 x1c3.^2.*x3c3 x1c3.*x2c2.^2 ...
    x1c3.*x3c3.^2 x2c2.^2.*x3c3 x2c2.*x3c3.^2 x1c3.^3 x2c2.^3
 x3c3.^3 x1c3.^2.*x2c2.^2 x1c3.^2.*x2c2.*x3c3 x1c3.^2.*x3c3.^2
 x1c3.*x2c2.^2.*x3c3 ...
    x1c3.*x2c2.*x3c3.^2 x2c2.^2.*x3c3.^2 x1c3.^3.*x2c2 x1c3.^3.*x3c3
 x1c3.*x2c2.^3 x1c3.*x3c3.^3 x2c2.^3.*x3c3 x2c2.*x3c3.^3 x1c3.^4
 x2c2.^4 x3c3.^4];

% 3-Blade quartic Model
% Importing regression coefficients
b1_3 = readmatrix(filename_B,'Sheet','3 Blade','Range','B3:B37')';
b2_3 = readmatrix(filename_B,'Sheet','3 Blade','Range','C3:C37')';
b3_3 = readmatrix(filename_B,'Sheet','3 Blade','Range','D3:D37')';
b4_3 = readmatrix(filename_B,'Sheet','3 Blade','Range','E3:E37')';
b5_3 = readmatrix(filename_B,'Sheet','3 Blade','Range','F3:F37')';
b6_3 = readmatrix(filename_B,'Sheet','3 Blade','Range','G3:G37')';
b_3 = {b1_3 b2_3 b3_3 b4_3 b5_3 b6_3};

% Regression equation
y1_3 = b1_3.*xc3;
y2_3 = b2_3.*xc3;
y3_3 = b3_3.*xc3;
y4_3 = b4_3.*xc3;
y5_3 = b5_3.*xc3;
y6_3 = b6_3.*xc3;

% Adding terms in regression equation
CFx_3 = sum(y1_3');
CFy_3 = sum(y2_3');
CFz_3 = sum(y3_3');
CMx_3 = sum(y4_3');
CMy_3 = sum(y5_3');
CMz_3 = sum(y6_3');
C_3 = [CFx_3' CFy_3' CFz_3' CMx_3' CMy_3' CMz_3'];
```

4-Blade

Importing desired low-speed data points

```
x4 = readmatrix(filename_FI,'Sheet','Input LS','Range','D3');
% Desired data points in natural units
```

```
x_14 = x4(:,1); % Velocity
x_24 = x4(:,2); % AoA
x_34 = x4(:,3); % RPM

% Transforming to coded variables
x1c4 = (x_14 - (2 + 12)/2)/((12 - 2)/2);
x2c4 = (x_24 - (0 + 100)/2)/((100 - 0)/2);
x3c4 = (x_34 - (4000 + 6500)/2)/((6500 - 4000)/2);

xc4 = [ones(length(x_14),1) x1c4 x2c4 x3c4 x1c4.*x2c4 x1c4.*x3c4
 x2c4.*x3c4 x1c4.^2 x2c4.^2 x3c4.^2 x1c4.*x2c4.*x3c4 x1c4.^2.*x2c4
 x1c4.^2.*x3c4 x1c4.*x2c4.^2 ...
    x1c4.*x3c4.^2 x2c4.^2.*x3c4 x2c4.*x3c4.^2 x1c4.^3 x2c4.^3
 x3c4.^3 x1c4.^2.*x2c4.^2 x1c4.^2.*x2c4.*x3c4 x1c4.^2.*x3c4.^2
 x1c4.*x2c4.^2.*x3c4 ...
    x1c4.*x2c4.*x3c4.^2 x2c4.^2.*x3c4.^2 x1c4.^3.*x2c4 x1c4.^3.*x3c4
 x1c4.*x2c4.^3 x1c4.*x3c4.^3 x2c4.^3.*x3c4 x2c4.*x3c4.^3 x1c4.^4
 x2c4.^4 x3c4.^4];

% 4-Blade quartic model
% Importing regression coefficients
b1_4 = readmatrix(filename_B,'Sheet','4 Blade','Range','B3:B37')';
b2_4 = readmatrix(filename_B,'Sheet','4 Blade','Range','C3:C37')';
b3_4 = readmatrix(filename_B,'Sheet','4 Blade','Range','D3:D37')';
b4_4 = readmatrix(filename_B,'Sheet','4 Blade','Range','E3:E37')';
b5_4 = readmatrix(filename_B,'Sheet','4 Blade','Range','F3:F37')';
b6_4 = readmatrix(filename_B,'Sheet','4 Blade','Range','G3:G37')';
b_4 = {b1_4 b2_4 b3_4 b4_4 b5_4 b6_4};

% Regression equation
y1_4 = b1_4.*xc4;
y2_4 = b2_4.*xc4;
y3_4 = b3_4.*xc4;
y4_4 = b4_4.*xc4;
y5_4 = b5_4.*xc4;
y6_4 = b6_4.*xc4;

% Adding terms in regression equation
CFx_4 = sum(y1_4');
CFy_4 = sum(y2_4');
CFz_4 = sum(y3_4');
CMx_4 = sum(y4_4');
CMy_4 = sum(y5_4');
CMz_4 = sum(y6_4');
C_4 = [CFx_4' CFy_4' CFz_4' CMx_4' CMy_4' CMz_4'];
```

5-Blade

Importing desired low-speed data points

```
x5 = readmatrix(filename_FI,'Sheet','Input LS','Range','G3');
% Desired data points in natural units
x_15 = x5(:,1); % Velocity
```

```
x_25 = x5(:,2); % AoA
x_35 = x5(:,3); % RPM

% Transforming to coded variables
x1c5 = (x_15 - (2 + 12)/2)/((12 - 2)/2);
x2c5 = (x_25 - (0 + 100)/2)/((100 - 0)/2);
x3c5 = (x_35 - (4000 + 5800)/2)/((5800 - 4000)/2);

xc5 = [ones(length(x_15),1) x1c5 x2c5 x3c5 x1c5.*x2c5 x1c5.*x3c5
 x2c5.*x3c5 x1c5.^2 x2c5.^2 x3c5.^2 x1c5.*x2c5.*x3c5 x1c5.^2.*x2c5
 x1c5.^2.*x3c5 x1c5.*x2c5.^2 ...
    x1c5.*x3c5.^2 x2c5.^2.*x3c5 x2c5.*x3c5.^2 x1c5.^3 x2c5.^3
 x3c5.^3 x1c5.^2.*x2c5.^2 x1c5.^2.*x2c5.*x3c5 x1c5.^2.*x3c5.^2
 x1c5.*x2c5.^2.*x3c5 ...
    x1c5.*x2c5.*x3c5.^2 x2c5.^2.*x3c5.^2 x1c5.^3.*x2c5 x1c5.^3.*x3c5
 x1c5.*x2c5.^3 x1c5.*x3c5.^3 x2c5.^3.*x3c5 x2c5.*x3c5.^3 x1c5.^4
 x2c5.^4 x3c5.^4];

% 5-Blade quartic model
% Importing regression coefficients
b1_5 = readmatrix(filename_B,'Sheet','5 Blade','Range','B3:B37')';
b2_5 = readmatrix(filename_B,'Sheet','5 Blade','Range','C3:C37')';
b3_5 = readmatrix(filename_B,'Sheet','5 Blade','Range','D3:D37')';
b4_5 = readmatrix(filename_B,'Sheet','5 Blade','Range','E3:E37')';
b5_5 = readmatrix(filename_B,'Sheet','5 Blade','Range','F3:F37')';
b6_5 = readmatrix(filename_B,'Sheet','5 Blade','Range','G3:G37')';
b_5 = {b1_5 b2_5 b3_5 b4_5 b5_5 b6_5};

% Regression equation
y1_5 = b1_5.*xc5;
y2_5 = b2_5.*xc5;
y3_5 = b3_5.*xc5;
y4_5 = b4_5.*xc5;
y5_5 = b5_5.*xc5;
y6_5 = b6_5.*xc5;

% Adding terms in regression equation
CFx_5 = sum(y1_5');
CFy_5 = sum(y2_5');
CFz_5 = sum(y3_5');
CMx_5 = sum(y4_5');
CMy_5 = sum(y5_5');
CMz_5 = sum(y6_5');
C_5 = [CFx_5' CFy_5' CFz_5' CMx_5' CMy_5' CMz_5'];
```

6-Blade

Importing desired low-speed data points

```
x6 = readmatrix(filename_FI,'Sheet','Input LS','Range','J3');
% Desired data points in natural units
x_16 = x6(:,1); % Velocity
x_26 = x6(:,2); % AoA
```

```
x_36 = x6(:,3); % RPM

% Transforming to coded variables
x1c6 = (x_16 - (2 + 12)/2)/((12 - 2)/2);
x2c6 = (x_26 - (0 + 100)/2)/((100 - 0)/2);
x3c6 = (x_36 - (3000 + 5500)/2)/((5500 - 3000)/2);

xc6 = [ones(length(x_16),1) x1c6 x2c6 x3c6 x1c6.*x2c6 x1c6.*x3c6
 x2c6.*x3c6 x1c6.^2 x2c6.^2 x3c6.^2 x1c6.*x2c6.*x3c6 x1c6.^2.*x2c6
 x1c6.^2.*x3c6 x1c6.*x2c6.^2 ...
    x1c6.*x3c6.^2 x2c6.^2.*x3c6 x2c6.*x3c6.^2 x1c6.^3 x2c6.^3
 x3c6.^3 x1c6.^2.*x2c6.^2 x1c6.^2.*x2c6.*x3c6 x1c6.^2.*x3c6.^2
 x1c6.*x2c6.^2.*x3c6 ...
    x1c6.*x2c6.*x3c6.^2 x2c6.^2.*x3c6.^2 x1c6.^3.*x2c6 x1c6.^3.*x3c6
 x1c6.*x2c6.^3 x1c6.*x3c6.^3 x2c6.^3.*x3c6 x2c6.*x3c6.^3 x1c6.^4
 x2c6.^4 x3c6.^4];

% 6-Blade quartic model
% Importing regression coefficients
b1_6 = readmatrix(filename_B,'Sheet','6 Blade','Range','B3:B37')';
b2_6 = readmatrix(filename_B,'Sheet','6 Blade','Range','C3:C37')';
b3_6 = readmatrix(filename_B,'Sheet','6 Blade','Range','D3:D37')';
b4_6 = readmatrix(filename_B,'Sheet','6 Blade','Range','E3:E37')';
b5_6 = readmatrix(filename_B,'Sheet','6 Blade','Range','F3:F37')';
b6_6 = readmatrix(filename_B,'Sheet','6 Blade','Range','G3:G37')';
b_6 = {b1_6 b2_6 b3_6 b4_6 b5_6 b6_6};

% Regression equation
y1_6 = b1_6.*xc6;
y2_6 = b2_6.*xc6;
y3_6 = b3_6.*xc6;
y4_6 = b4_6.*xc6;
y5_6 = b5_6.*xc6;
y6_6 = b6_6.*xc6;

% Adding terms in regression equation
CFx_6 = sum(y1_6');
CFy_6 = sum(y2_6');
CFz_6 = sum(y3_6');
CMx_6 = sum(y4_6');
CMy_6 = sum(y5_6');
CMz_6 = sum(y6_6');
C_6 = [CFx_6' CFy_6' CFz_6' CMx_6' CMy_6' CMz_6'];

C = {C_3 C_4 C_5 C_6};
C_LS = [C{1}; C{2}; C{3}; C{4}];

% Writing responses to excel file
filelocation = 'E:\Academia\Propeller Characterization\Thesis\MATLAB
\MATLAB Simulation Database Tool\Model Data\Factor Input.xlsx';
writematrix(C_3,filelocation,'Sheet',2,'Range','A3')
writematrix(C_4,filelocation,'Sheet',2,'Range','G3')
writematrix(C_5,filelocation,'Sheet',2,'Range','M3')
writematrix(C_6,filelocation,'Sheet',2,'Range','S3')
```

High-Speed Data

Importing regression coefficients

```
b1_hs = readmatrix(filename_B,'Sheet','High-Speed','Range','B3:B37')';
b2_hs = readmatrix(filename_B,'Sheet','High-Speed','Range','C3:C37')';
b3_hs = readmatrix(filename_B,'Sheet','High-Speed','Range','D3:D37')';
b4_hs = readmatrix(filename_B,'Sheet','High-Speed','Range','E3:E37')';
b5_hs = readmatrix(filename_B,'Sheet','High-Speed','Range','F3:F37')';
b6_hs = readmatrix(filename_B,'Sheet','High-Speed','Range','G3:G37')';
b_hs = {b1_hs b2_hs b3_hs b4_hs b5_hs b6_hs};

% Importing desired data points
x_hs = readmatrix(filename_FI,'Sheet','Input HS','Range','A2');
% Desired data points in natural units
x_1_hs = x_hs(:,1); % Velocity
x_2_hs = x_hs(:,2); % AoA
x_3_hs = x_hs(:,3); % RPM
x_4_hs = x_hs(:,4); % Blades

% Transforming to coded variables
x1c_hs = (x_1_hs - (11 + 30)/2)/((30 - 11)/2);
x2c_hs = (x_2_hs - (0 + 20)/2)/((20 - 0)/2);
x3c_hs = (x_3_hs - (4000 + 6000)/2)/((6000 - 4000)/2);
x4c_hs = (x_4_hs - (3 + 6)/2)/((6 - 3)/2);
xc_hs = [ones(length(x_1_hs),1) x1c_hs x2c_hs x3c_hs x4c_hs
 x1c_hs.*x2c_hs x1c_hs.*x3c_hs x1c_hs.*x4c_hs x2c_hs.*x3c_hs
 x2c_hs.*x4c_hs x3c_hs.*x4c_hs x1c_hs.^2 x2c_hs.^2 x3c_hs.^2
 x4c_hs.^2 ...
    x1c_hs.*x2c_hs.*x3c_hs x1c_hs.*x2c_hs.*x4c_hs
 x1c_hs.*x3c_hs.*x4c_hs x2c_hs.*x3c_hs.*x4c_hs x1c_hs.^2.*x2c_hs
 x1c_hs.^2.*x3c_hs x1c_hs.^2.*x4c_hs x1c_hs.*x2c_hs.^2
 x1c_hs.*x3c_hs.^2 ...
    x1c_hs.*x4c_hs.^2 x2c_hs.^2.*x3c_hs x2c_hs.^2.*x4c_hs
 x2c_hs.*x3c_hs.^2 x2c_hs.*x4c_hs.^2 x3c_hs.^2.*x4c_hs
 x3c_hs.*x4c_hs.^2 x1c_hs.^3 x2c_hs.^3 x3c_hs.^3 x4c_hs.^3];

% Regression equation
y1_hs = b1_hs.*xc_hs;
y2_hs = b2_hs.*xc_hs;
y3_hs = b3_hs.*xc_hs;
y4_hs = b4_hs.*xc_hs;
y5_hs = b5_hs.*xc_hs;
y6_hs = b6_hs.*xc_hs;

% Adding terms in regression equation
CFx_hs = sum(y1_hs');
CFy_hs = sum(y2_hs');
CFz_hs = sum(y3_hs');
CMx_hs = sum(y4_hs');
CMy_hs = sum(y5_hs');
CMz_hs = sum(y6_hs');
C_hs = [CFx_hs' CFy_hs' CFz_hs' CMx_hs' CMy_hs' CMz_hs'];
```

```
filelocation = 'E:\Academia\Propeller Characterization\Thesis\MATLAB
\MATLAB Simulation Database Tool\Model Data\Factor Input.xlsx';
writematrix(x_4_hs,filelocation,'Sheet',4,'Range','A2')
writematrix(C_hs,filelocation,'Sheet',4,'Range','B2')
```

Published with MATLAB® R2020b

VITA

Michael Cristian Stratton was born and raised in Virginia. He earned a Bachelor's Degree in Mechanical Engineering from Old Dominion University in December of 2019. While pursuing his undergraduate degree he contributed to a capstone project that gave Old Dominion University its first fully functioning shock tunnel. In his final year of undergraduate studies, he was encouraged by his advisor Dr. Drew Landman.to continue his education by enrolling in graduate school He left Virginia prior to graduating to join the Flight Dynamics Branch at Naval Air Systems Command in Patuxent River, Maryland.